

**Switzerland**

Swiss Geodetic Commission



**Suisse**

Commission Géodésique Suisse

**Swiss National Report on the  
GEODETIC ACTIVITIES  
in the years 2007 to 2011**

Presented to the XXV General Assembly  
of the International Union of Geodesy and Geophysics  
in Melbourne, Australia, June/July 2011



**Rapport National Suisse sur les  
ACTIVITÉS GÉODÉSIQUES  
exécutées de 2007 à 2011**

Présenté à la vingt-cinquième Assemblée générale  
de l'Union Géodésique et Géophysique Internationale  
tenue à Melbourne, Australie, juin/juillet 2011

**Zürich 2011**



**Switzerland**  
Swiss Geodetic Commission



**Suisse**  
Commission Géodésique Suisse

**Swiss National Report on the  
GEODETIC ACTIVITIES  
in the years 2007 to 2011**

Presented to the XXV General Assembly  
of the International Union of Geodesy and Geophysics  
in Melbourne, Australia, June/July 2011



**Rapport National Suisse sur les  
ACTIVITÉS GÉODÉSIQUES  
exécutées de 2007 à 2011**

Présenté à la vingt-cinquième Assemblée générale  
de l'Union Géodésique et Géophysique Internationale  
tenue à Melbourne, Australie, juin/juillet 2011

**Zürich 2011**

**Swiss Geodetic Commission/Commission Géodésique Suisse**

ETH Zurich  
Schafmattstr. 34  
8093 Zurich  
Switzerland

<http://www.sgc.ethz.ch/publications>

Edited by:

J. Mueller-Gantenbein, Secretary of the SGC

A. Wiget (Commission 1)

U. Marti (Commission 2)

M. Rothacher (Commission 3)

P.-Y. Gilliéron (Commission 4)

In addition to the bibliographies at the end of each section we recommend the following www-sites:

Astronomical Institute of the University of Bern (AIUB): <http://www.aiub.unibe.ch/>

Institute of Geodesy and Photogrammetry,  
Eidgenössische Technische Hochschule, ETH Zurich: <http://www.igp.ethz.ch/>

Federal Office of Topography (swisstopo): <http://www.swisstopo.ch/>

Geodetic Engineering Laboratory,  
École polytechnique fédérale de Lausanne EPFL: <http://topo.epfl.ch/>

Haute Ecole d'Ingénierie et de Gestion du Canton de Vaud: <http://www.heig-vd.ch/>

University of Applied Sciences Northwestern Switzerland,  
Fachhochschule Nordwestschweiz: <http://www.fhnw.ch/>

ISBN 978-3-908440-26-0

Printed by: adag, Zurich

©2011 Swiss Geodetic Commission

## PREFACE

The Swiss Geodetic Commission (SGC) is an organisation within the Swiss Academy of Sciences (SCNAT). It is devoted to research into scientific problems of geodesy including the transfer to practical application in national surveying. Of particular importance is the promotion of international cooperation and national coordination.

For the compilation of the national report covering the scientific activities of the past 4 years it was decided to follow the structure of previous national reports and to divide it into 4 commissions according to the structure of the International Association of Geodesy (IAG):

- 1 Reference Frames
- 2 Gravity Field
- 3 Earth Rotation and Geodynamics
- 4 Positioning & Applications

These main chapters were compiled by an editorial staff consisting of A. Wiget (Commission 1), U. Marti (Commission 2), M. Rothacher (Commission 3), P.-Y. Gilliéron (Commission 4). Our special thanks go to J. Mueller-Gantenbein, secretary of SGC, for the careful editing and preparation of the layout. Without her efforts this report could not have been realized in due time.

The SGC expresses its appreciative thanks to all colleagues who have contributed to this report and who are promoting Geodetic Sciences in Switzerland. Financial support was provided by the SCNAT. Its valuable help is gratefully acknowledged.

On behalf of the Swiss Geodetic Commission, June 2011

Urs Marti  
Vice-President of SGC

Alain Geiger  
President of SGC



# Contents

## Commission 1: Reference Frames

CODE Contributions to the IGS .....	1
<i>by S. Schaer, H. Bock, R. Dach, S. Lutz, M. Meindl, E. Orliac and D. Thaller</i>	
EUREF Activities at CODE .....	3
<i>by S. Schaer, R. Dach, S. Lutz and M. Meindl</i>	
Reprocessing Activities at CODE .....	5
<i>by S. Lutz, P. Steigenberger, R. Dach, S. Schaer, M. Meindl, L. Ostini and K. Sosnica</i>	
GNSS Data Calibration Parameters .....	7
<i>by S. Schaer and R. Dach</i>	
AIUB contribution to the Galileo Reference Terrestrial Frame .....	10
<i>by L. Prange, R. Dach and A. Steinbach</i>	
Combining SLR and GNSS measurements .....	12
<i>by D. Thaller, K. Sosnica, G. Beutler, R. Dach and A. Jäggi</i>	
The Zimmerwald Observatory .....	15
<i>by T. Schildknecht, A. Jäggi, M. Ploner and E. Brockmann</i>	
Satellite Laser Ranging at Zimmerwald .....	18
<i>by A. Jäggi, M. Ploner, J. Utzinger, M. Prohaska, E. Pop, W. Gurtner and E. Brockmann</i>	
New Legislation for Geoinformation and National Survey .....	20
<i>by A. Wiget</i>	
Internet platform and transformation service to support the reference frame change in Switzerland .....	21
<i>by M. Kistler, U. Marti, J. Ray and A. Wiget</i>	
Enhancing the Swiss Permanent GPS Network (AGNES) for GLONASS .....	24
<i>by E. Brockmann and U. Wild</i>	
Analysis of Permanent GNSS Networks at swisstopo (PNAC) .....	25
<i>by E. Brockmann, D. Ineichen and S. Schaer</i>	
Densification and validation of the LV95 reference frame with the campaign CHTRF2010 .....	27
<i>by E. Brockmann and A. Schlatter</i>	
Measurements for the National Height System .....	29
<i>by A. Schlatter</i>	
GNSS Clock Modelling and Estimation .....	30
<i>by K. Wang and M. Rothacher</i>	
Bibliography Commission 1 .....	34

## Commission 2: Gravity Field

Phase center modeling and its impact on LEO Precise Orbit Determination .....	43
<i>by A. Jäggi, H. Bock, U. Meyer, L. Prange, G. Beutler and R. Dach</i>	
Global Gravity Field Determination based on the GRACE-Mission .....	45
<i>by A. Jäggi, G. Beutler, U. Meyer, L. Prange and L. Mervart</i>	
Global gravity field determination based on CHAMP-GPS-data .....	47
<i>by L. Prange, A. Jäggi and G. Beutler</i>	
Processing Facility for ESA's GOCE Gravity Field Explorer Mission .....	49
<i>by H. Bock, A. Jäggi, U. Meyer, R. Dach and G. Beutler</i>	
Absolute and Relative Gravity Measurements .....	51
<i>by U. Marti, H. Baumann, B. Bürki and S. Guillaume</i>	
Gravity measurements for the Vertical network .....	53
<i>by U. Marti and A. Schlatter</i>	
The Earth Tide Observatory in Zimmerwald .....	54
<i>by U. Marti and B. Bürki</i>	
Ultra precise geoid determination for a new generation of future linear collider: A feasibility study at CERN .....	55
<i>by S. Guillaume, M. Jones, B. Bürki and A. Geiger</i>	
GeoHALO: Geoscientific Research with the New German “High Altitude and Long Range Research Aircraft” (HALO) .....	57
<i>by A. Geiger, M. Müller, M. Rothacher and M. Scheinert</i>	
Sea Surface Topography and Marine Geoid by Airborne Laser Altimetry and Shipborne Ultrasound Altimetry .....	58
<i>by P. Limpach, H.-G. Kahle and A. Geiger</i>	
Geoid Modeling in the Aegean Sea .....	60
<i>by P. Limpach, H.-G. Kahle and A. Geiger</i>	
Astrogeodetic geoid and isostatic considerations in the North Aegean sea, Greece .....	62
<i>by A. E. Somieski, B. Bürki and H.-G. Kahle</i>	
Bibliography Commission 2 .....	63



## Commission 3: Earth Rotation and Geodynamics

CODE Contributions to Earth Rotation Monitoring .....	65
<i>by S. Schaer, R. Dach, S. Lutz, M. Meindl, D. Thaller and G. Beutler</i>	
Subdaily variations in the Earth rotation .....	67
<i>by N. Panafidina and M. Rothacher</i>	
Recent Crustal Vertical Movements from leveling .....	69
and GNSS permanent networks	
<i>by E. Brockmann and A. Schlatter</i>	
Combined multi-annual GNSS solutions from .....	70
permanent networks and campaigns	
<i>by E. Brockmann</i>	
SWISS-4D II: Geodetic analysis of geodynamic deformations in Switzerland .....	71
<i>by A. Villiger, A. Geiger, A. Wiget and U. Marti</i>	
COGEAR Coupled seismogenic Geohazards in Alpine Regions (COGEAR) .....	72
<i>by A. Geiger, A. Villiger and D. Fäh</i>	
Crustal deformation field in Greece determined from GPS measurements .....	74
<i>by M.D. Müller, Ch. Hollenstein, A. Geiger and H.-G. Kahle</i>	
Analysis of long-term GPS observations in Greece and geodynamic implications .....	76
<i>by M.D. Müller, A. Geiger and H.-G. Kahle</i>	
GNSS Seismology .....	78
<i>by S. Häberling and M. Rothacher</i>	
Influence of Atmospheric Pressure Loading on GNSS Analysis .....	79
<i>by R. Dach, S. Lutz, J. Böhm and P. Steigenberger</i>	
Bibliography Commission 3 .....	82

## Commission 4: Positioning and Applications

Real-Time Airborne Mapping .....	85
<i>by J. Skaloud, P. Schaer, P. Tomé and Y. Stebler</i>	
Quality Control in Airborne Laser Scanning .....	86
<i>by J. Skaloud, P. Schaer, P. Tomé, Y. Stebler and K. Legat</i>	
Calibration Procedures in Mobile Mapping .....	87
<i>by J. Skaloud, P. Schaer and K. Legat</i>	
Integrated Sensor Orientation .....	88
<i>by J. Skaloud, D. Rouzaud and F. Bayoud</i>	
GNSS/MEMS-IMU Integration for Positioning and Orientation .....	89
<i>by A. Waegli, J. Skaloud, S. Guerrier, V. Constantin and H. Fournier</i>	
Positioning in dynamic applications .....	90
<i>by J. Skaloud, A. Waegli, S. Guerrier and P. Tomé</i>	
Indoor Positioning and Map Matching .....	91
<i>by P.-Y. Gilliéron, B. Merminod, V. Renaudin, P. Tomé, O. Yalak and F. Tappero</i>	
Terrestrial Laser Scanning for Natural Hazards .....	92
<i>by J. Wu, P.-Y. Gilliéron and B. Merminod</i>	
Bernese Software .....	93
<i>by R. Dach, H. Bock, U. Hugentobler, A. Jäggi, S. Lutz, M. Meindl, L. Mervart, U. Meyer, E. Orliac, L. Ostini, L. Prange, M. Rothacher, S. Schaer, K. Sosnica, A. Steinbach, D. Thaller, P. Walser and G. Beutler</i>	
Multi-GNSS Ambiguity Resolution Algorithms .....	95
<i>by S. Schaer and M. Meindl</i>	
Analysis and Reassessment of Coordinate Time Series Using FODITS .....	97
<i>by L. Ostini, R. Dach, M. Meindl, U. Hugentobler, S. Schaer and G. Beutler</i>	
CODE Contribution to Global Ionosphere Monitoring .....	100
<i>by S. Schaer and S. Lutz</i>	
Geodetic monitoring with 3D adjustment software Trinet+ .....	102
<i>by P.-H. Cattin and C. Muller</i>	
Near real-time monitoring with low-cost GPS equipments .....	103
<i>by P.-H. Cattin and J. Brahier</i>	
Points cloud phenomenon: ghosts in the scan .....	104
<i>by V. Barras, N. Ferreira and T. Dobers</i>	
The Swiss Positioning Service (swipos) .....	105
<i>by U. Wild, D. Andrey and Ch. Misslin</i>	
Control Point Data Service (FPDS) .....	108
<i>by M. Burkard</i>	
GIS System for the National border of Switzerland .....	109
<i>by B. Vogel</i>	
Contributions of swisstopo to GNSS Meteorology .....	111
<i>by E. Brockmann, D. Ineichen and S. Schaer</i>	

National Surveying Contributions to the AlpTransit Gotthard Base Tunnel .....	113
<i>by A. Wiget, U. Marti and A. Schlatter</i>	
Geodetic Reference System and Break-Through-Results in the Gotthard-Basetunnel .....	116
<i>by R. Stengele and I. Schätti-Stählin</i>	
Renaissance of hydro-electric power in Switzerland: Geodetic base networks for new underground pumped storage facility in the Alps .....	119
<i>by M. Kistler and E. Brockmann</i>	
GBAS Activities .....	120
<i>by M. Scaramuzza and P. Truffer</i>	
GPS performance analysis for ADS-B applications .....	121
<i>by M. Troller, P. Truffer and M. Scaramuzza</i>	
EGNOS for civil aviation applications .....	122
<i>by M. Troller and M. Scaramuzza</i>	
Real-time change of Swiss reference frames with swipos GIS/GEO and RTCM Coordinate Transformation Messages .....	123
<i>by B. Sievers and M. Saner</i>	
Comparative baseline computation with Bernese GPS Software and Leica Geo Office as well as 3D computation of a slipping region with TRINET+ .....	125
<i>by B. Sievers, S. Kaiser and M. Schratner</i>	
International Conference on Indoor Positioning and Indoor Navigation (IPIN) .....	128
<i>by R. Mautz and H. Ingensand</i>	
CLIPS – A Camera and Laser-Based Indoor Positioning System .....	130
<i>by S. Tilch and R. Mautz</i>	
Glacier Monitoring .....	131
<i>by R. Mautz and D.E. Grimm</i>	
Streambed Topography Measurement using Range Imaging .....	132
<i>by T.K. Kohoutek and M. Nitsche</i>	
Range Imaging for Indoor Positioning .....	133
<i>by T.K. Kohoutek, A. Donaubaauer and R. Mautz</i>	
Sensor Fusion for Digital Elevation and Object Modelling in Rome .....	134
<i>by T.K. Kohoutek and P. Theiler</i>	
Unmanned aerial vehicle in cadastral applications .....	135
<i>by Henri Eisenbeiss, Madeleine Manyoky and Pascal Theiler</i>	
Positioning methods of Unmanned Aerial Vehicles (UAVs) .....	136
<i>by H. Eisenbeiss</i>	
GNSS Orientation Finding .....	137
<i>by D.E. Grimm</i>	
GPS-Tomography and Assimilation in Numerical Weather Models (GANUWE) .....	138
<i>by D. Perler and A. Geiger</i>	
Geodetic contribution to the process understanding and prediction of hydrological extremes and complex hazards (APUNCH) .....	140
<i>by F. Hurter and A. Geiger</i>	
X-Sense: Monitoring Alpine Mass Movements at Multiple Scales .....	141
<i>by P. Limpach, F. Neyer and A. Geiger</i>	

GPS-Gyro .....	143
<i>by S. Häberling and A. Geiger</i>	
Geodetic aspects of GNSS assisted approach and landing, Radar surveillance and multilateration .....	144
<i>by M. Manyoky, C. Iosifescu, A. Villiger, St. Rutzer and A. Geiger</i>	
Analysis and corrections of non-hydrostatic effects on GNSS observations and antenna errors for accurate GPS and Galileo IWV estimates .....	146
<i>by F. Scirè Scappuzzo, B. Bürki, A. Geiger and H.-G. Kahle</i>	
Geodetic Project Course 2008 in Greece .....	147
<i>by B. Bürki, H.-G. Kahle, S. Guillaume, Ph. Kehl and M. Müller</i>	
Geodetic Project Course 2010 at CERN .....	151
<i>by S. Guillaume and B. Bürki</i>	
Determination of Atmospheric Water Vapor Abundance using Solar Lunar Spectrometry .....	152
<i>by St. Münch, B. Bürki, M. Rothacher, H.-G. Kahle, P. Sorber, H. Becker-Ross, St. Florek, M. Okruss and R. Tischendorf</i>	
DAEDALUS: A Versatile Digital Clip-on Measuring System for Total Stations .....	153
<i>by B. Bürki, S. Guillaume, P. Sorber and H.-P. Oesch</i>	
Automotive RTK Precision Positioning Approach .....	157
<i>by H.-J. Euler</i>	
First Galileo Data Processing .....	159
<i>by C. Rösli, M. Rothacher, P. Sorber</i>	
Bibliography Commission 4 .....	161

# 1 Reference Frames

## CODE Contributions to the IGS

by S. Schaer<sup>1</sup>, H. Bock<sup>2</sup>, R. Dach<sup>2</sup>, S. Lutz<sup>2</sup>, M. Meindl<sup>2</sup>, E. Orlicac<sup>2</sup> and D. Thaller<sup>2</sup>

<sup>1</sup>Federal Office of Topography, swisstopo

<sup>2</sup>Astronomical Institute University of Bern

The Center of Orbit Determination in Europe (CODE) is a consortium of four institutions, namely the Astronomical Institute of University of Bern (AIUB, Switzerland), the Swiss Federal Office of Topography (swisstopo, Switzerland), the Federal Agency of Cartography and Geodesy (BKG, Germany), and the Institut für Astronomische und Physikalische Geodäsie at Technische Universität München (IAPG/TUM, Germany). CODE is an Analysis Center (AC) of the International GNSS Service (IGS, GNSS standing for Global Navigation Satellite System). CODE started to be operational in 1992 and has been generating series of products since then. A list of all CODE products is available from [ftp://ftp.unibe.ch/aiub/BSWUSER50/TXT/AIUB\\_AFTP.README](ftp://ftp.unibe.ch/aiub/BSWUSER50/TXT/AIUB_AFTP.README). All the data processing is carried out with the development version of the Bernese Software (BSW, [Dach et al., 2007]). The main products delivered by CODE to the IGS are GNSS orbits, Earth orientation parameters, station coordinates, model parameters describing the troposphere and ionosphere, global ionosphere maps, phase-consistent satellite and receiver clock corrections (with a special high-rate GPS product with a resolution of 5 seconds) [Bock et al., 2009], and differential code biases (DCBs). Please refer to [Schaer et al., 2011] for further information on CODE's effort towards the modelling of DCBs and antenna phase center variation (PCVs).

As an AC of the IGS, CODE aims to produce and provide the IGS with the best possible products, i.e. with the best possible accuracy, and this, for all flying GNSS satellites (with freely available data), even satellites flagged as unhealthy by their operators, or satellites with repositioning events (manoeuvres), see Figure 1.1.

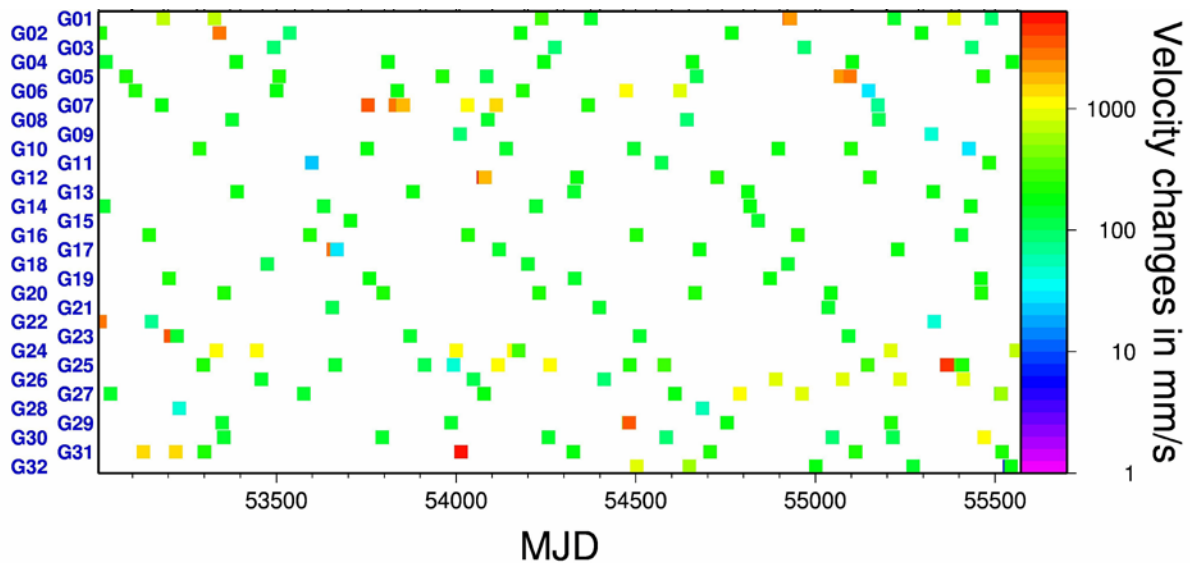


Figure 1.1: Manoeuvres as detected by CODE for GPS satellites between 2004 and 2010.

Since May 2003, all CODE products are based on a rigorous GNSS (GPS + GLONASS at writing time) combined analysis [Dach et al., 2010A] that applies to all contributions CODE contributions: ultra-rapid, rapid, and final. A description of CODE multi-GNSS processing is offered in [Dach et al., 2009]. CODE IGS routine processing is carried out on the basis of the data publicly available from the IGS. Figure 1.2 shows e.g. the ground networks used for the final analysis.

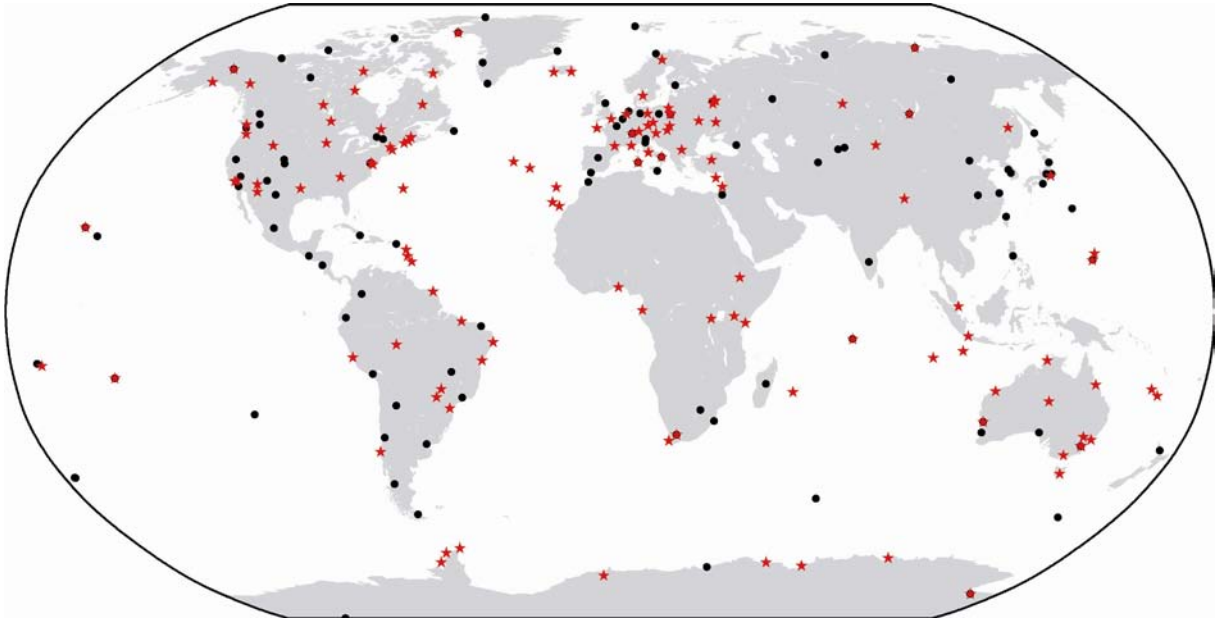


Figure 1.2: Network used by CODE for its contribution to the IGS final products in February 2011 (black dots: GPS stations, red stars: GPS/GLONASS stations).

As the driving motivation of CODE is to propose products of the highest quality possible, permanent improvements are brought either to the BSW itself or to the data processing strategy. Below is given a summary of the major changes or enhancements made by CODE within the last years that directly affected the products delivered to the IGS:

- Handling of the L2C quarter cycle shift issue.
- Improvement of phase pre-processing for short baselines, with decision criteria now depending on the baseline length to guarantee the cleaning of the original L1 and L2 data for the shortest baselines.
- Handling of satellite manoeuvres was extended to GLONASS, with arc splitting decision criteria being GNSS specific.
- Change of antenna z-offset for GLONASS satellite R23 [IGSMail-5978].
- Provision of high-rate (5 sec) GPS satellite clock correction (GPS week 1477).
- Earth Orientation Parameters resolution increased from 2 hours to 1 hour (GPS week 1486).
- Activation of a refined version of the module computing the local site displacements due to ocean tidal loading (hardisp.f) following the International Earth Rotation Service (IERS) 2003 Conventions, following [IGSMail-5300].
- Activation of the VMF1 [Boehm et al., 2007] troposphere modelling in the final products on GPS week 1604 [IGSMail-6287].
- Activation of three higher order ionosphere (HOI) correction terms (2nd order, 3rd order, and ray curvature) [Schaer and Lutz, 2011] in the final products on GPS week 1604; HOI were activated in the rapid products on the 25th and 26th February, 2010, see [IGSMail-6287].
- P2C2 code bias retrieval started on 22nd June 2010 [Schaer and Dach, 2010].
- First processing of data from a Block IIF satellite (PRN25/SVN62 on 7th June, 2010)

In order to improve its robustness in product delivery, CODE has setup a “backup server” for the ultra-rapid and rapid processing. That way, when the primary server behaves abnormally or is being maintained, the generation and delivery of the ultra-rapid products shall be conducted from the backup server.

It is also worth mentioning that CODE is actively participating in the IGS reprocessing effort; for more information on this topic, please refer to [Lutz et al., 2011].

## EUREF Activities at CODE

by S. Schaer<sup>1</sup>, R. Dach<sup>2</sup>, S. Lutz<sup>2</sup> and M. Meindl<sup>2</sup>

<sup>1</sup> Federal Office of Topography, swisstopo

<sup>2</sup> Astronomical Institute University of Bern

EUREF is an integrated component of the Subcommittee 1.3, Regional Reference Frames, of the IAG (International Association of Geodesy). A key component is the EUREF Permanent Network (EPN, Bruyninx et al., 2001), consisting of 245 GNSS tracking stations (status as of 04. February 2011). The data is analyzed in a distributed processing scheme between 17 local analysis centers (LAC). It is worth mentioning that 14 of them are using the Bernese Software (Dach et al, 2007) developed at AIUB.

CODE, the Center for Orbit Determination in Europe, is one of the EUREF-LAC. It is a joint venture between the Astronomical Institute of the University of Bern (AIUB, Switzerland), the Swiss Federal Office of Topography (swisstopo, Wabern, Switzerland), the Federal Agency for Cartography and Geodesy (BKG, Frankfurt am Main, Germany), and the Institut für Astronomische und Physikalische Geodäsie at Technische Universität München (IAPG, TUM, Munich, Germany).

CODE generates a combined GPS/GLONASS solution for weekly station coordinates since 2003. The network of EPN-stations processed by CODE covers all parts of Europe and the bounding areas (see Figure 1.3). The weekly solution contains currently about 60 stations where 35 of them track GPS and GLONASS. The development of GPS-only and combined GPS/GLONASS tracking sites in the EPN subnetwork processed at CODE is shown in Figure 1.4.

This environment is well suited to evaluate different solution strategies. Among others, the impact on station coordinates using satellites orbits from the International GNSS Service (IGS, Dow et al., 2009) and from the CODE analysis center may be investigated. GPS-only and combined GPS/GLONASS solutions (using different combination strategies) are also computed and evaluated. Additional series are generated to compare the impact of different receiver/satellite antenna phase center models on the results.

One example for such comparisons of series is provided in Figure 1.5. It shows the repeatability for daily solutions considering only the GLONASS- (grey bars) and only the GPS-measurements (green bars). In addition, two solutions are displayed with different assumptions for the internal receiver clock regarding the observations from the different systems: (1) to have only an offset (one constant inter-system bias) between the two clocks (red bars) or (2) to have fully independent receiver clocks for each system (blue bars).

The diagram reveals at first the high quality standard of the solution (for most of the stations on the 1 to 2 mm level for the horizontal and 5 mm for the vertical components). It is furthermore remarkable that the repeatability of the GLONASS-only solution is comparable to the performance of the GPS and the combined solutions – even if there are only about two third of the number of satellites available with respect to GPS. The differences between the two combined multi-GNSS solutions are small. They are discussed in detail in the study on the stability of the inter-system bias presented in Dach et al., 2010B.

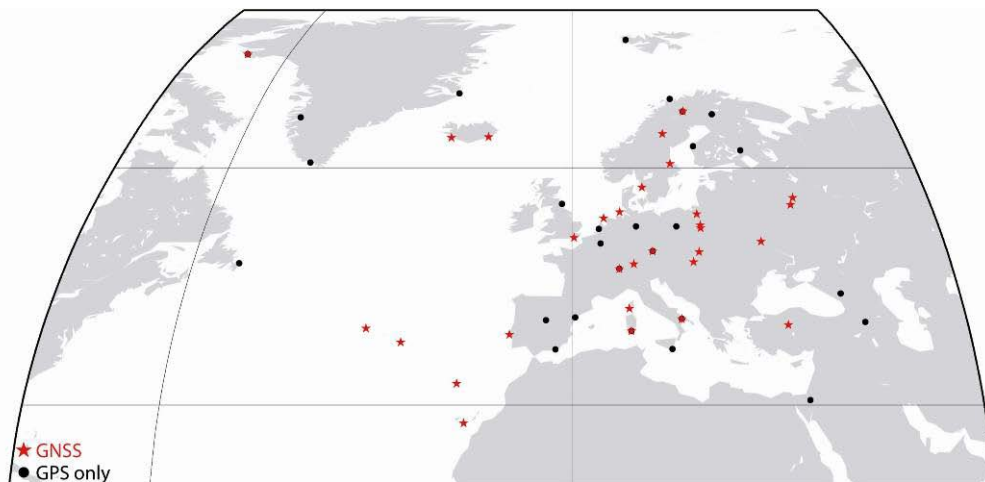


Figure 1.3: Stations in the contribution of CODE to the EPN solution.

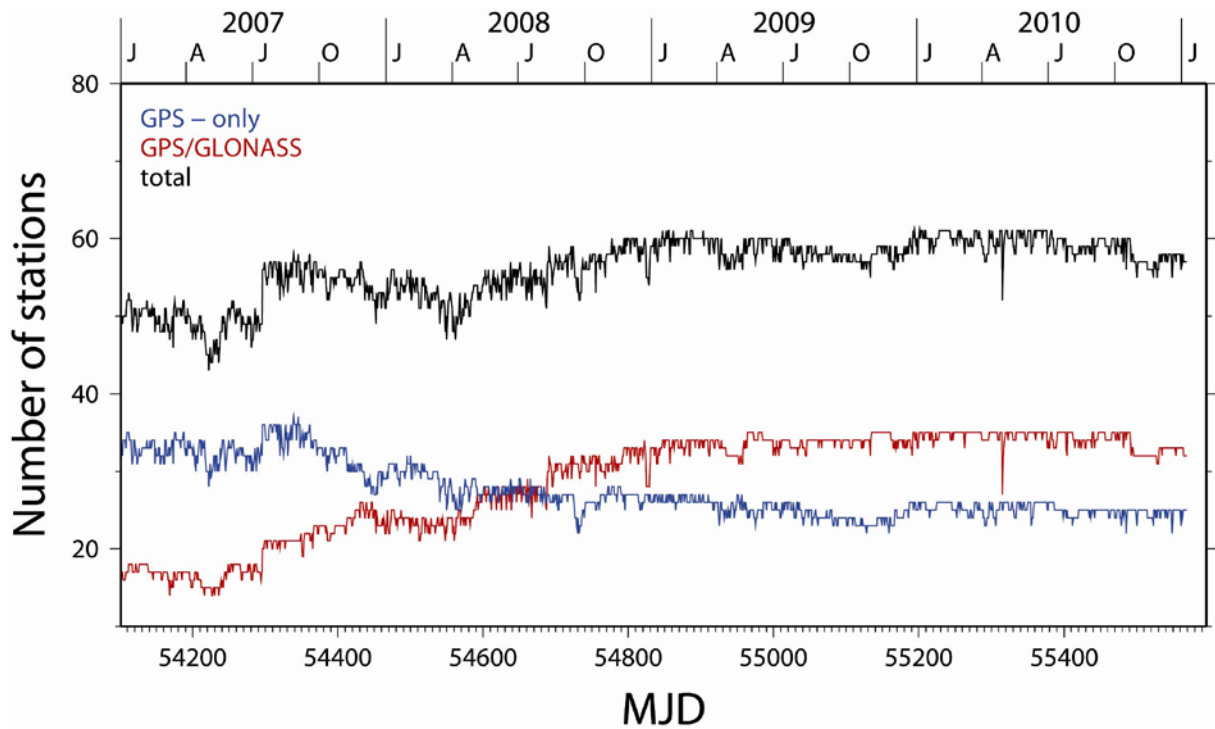


Figure 1.4: Development of the GPS-only and combined GPS/GLONASS tracking receivers in the EPN subnetwork processed at CODE.

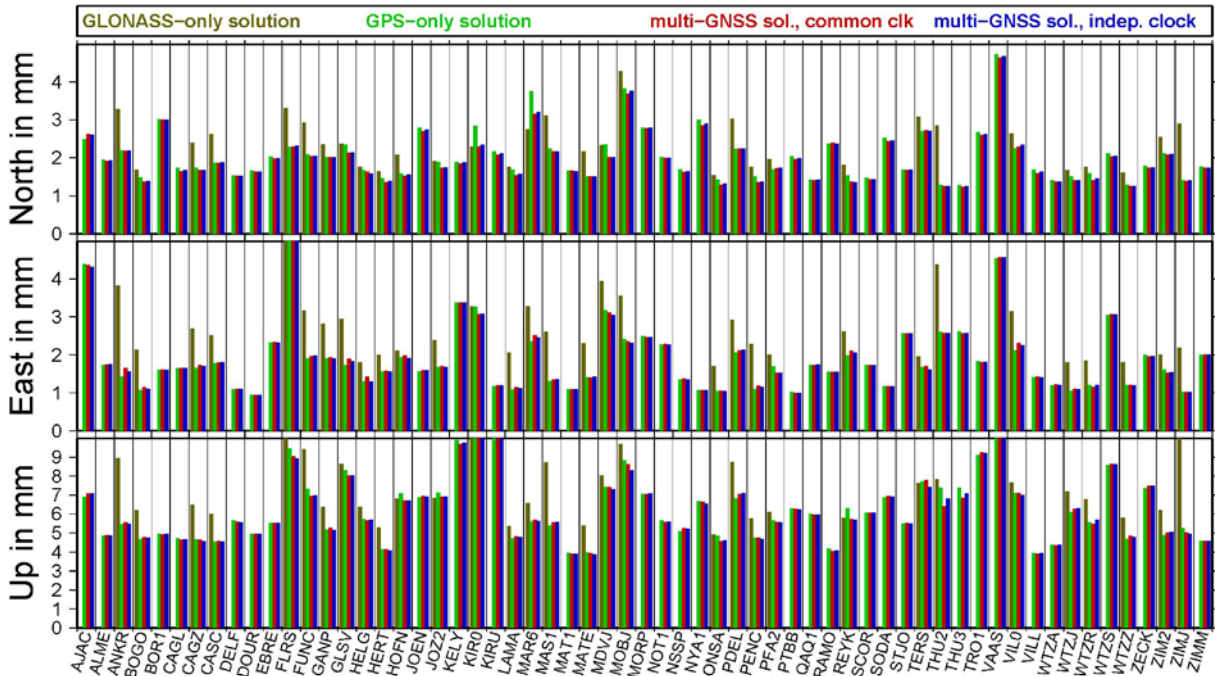


Figure 1.5: Repeatability of daily coordinate results computed as single and multi-GNSS solutions.



## Reprocessing Activities at CODE

by S. Lutz<sup>1</sup>, P. Steigenberger<sup>2</sup>, R. Dach<sup>1</sup>, S. Schaer<sup>1</sup>, M. Meindl<sup>1</sup>, L. Ostini<sup>1</sup> and K. Sosnica<sup>1</sup>

<sup>1</sup>Astronomical Institute University of Bern

<sup>2</sup>Institut für Astronomische und Physikalische Geodäsie, Technische Universität München, Munich, Germany

CODE, the Center for Orbit Determination in Europe, is a joint venture of the Astronomical Institute of the University of Bern (AIUB, Bern, Switzerland), the Swiss Federal Office of Topography (swisstopo, Wabern, Switzerland), the Federal Agency for Cartography and Geodesy (BKG, Frankfurt am Main, Germany), and the Institut für Astronomische und Physikalische Geodäsie of the Technische Universität München (IAPG/TUM, Munich, Germany). CODE has been one of the global analysis centers of the IGS (International GNSS Service, a voluntary federation of more than 200 worldwide agencies that pool resources and permanent GPS and GLONASS station data to generate precise GPS and GLONASS products) since the start of IGS test campaign operations on June 21, 1992. All operational computations are performed at the AIUB using the development version of the Bernese Software (Dach et al. 2007). Since May 2003, CODE has been analyzing GNSS (GPS and GLONASS) data in a combined analysis to achieve the best possible consistency of the GPS and GLONASS orbit products. This strategy is not only applied to the CODE contributions to the IGS final products, but also to its rapid and ultra-rapid products.

In the past, interpreting GNSS-derived long time series was difficult due to inconsistencies caused by changes in the processing strategies by, e.g., model updates and/or a more sophisticated parameterization. This problem can only be overcome by a complete and homogeneous reprocessing starting with the original (RINEX) observation data and using of course the latest available models and analysis strategies. In February 2008, the Analysis Centers of the IGS started the process of reanalyzing the full history of GPS data collected by the global network of the IGS since 1994 in a fully consistent way using the latest models and methodology. For the CODE contribution to the IGS reprocessing, all relevant parameters of a global GPS solution were estimated based on 15 years of GPS observation data from 244 different tracking stations.

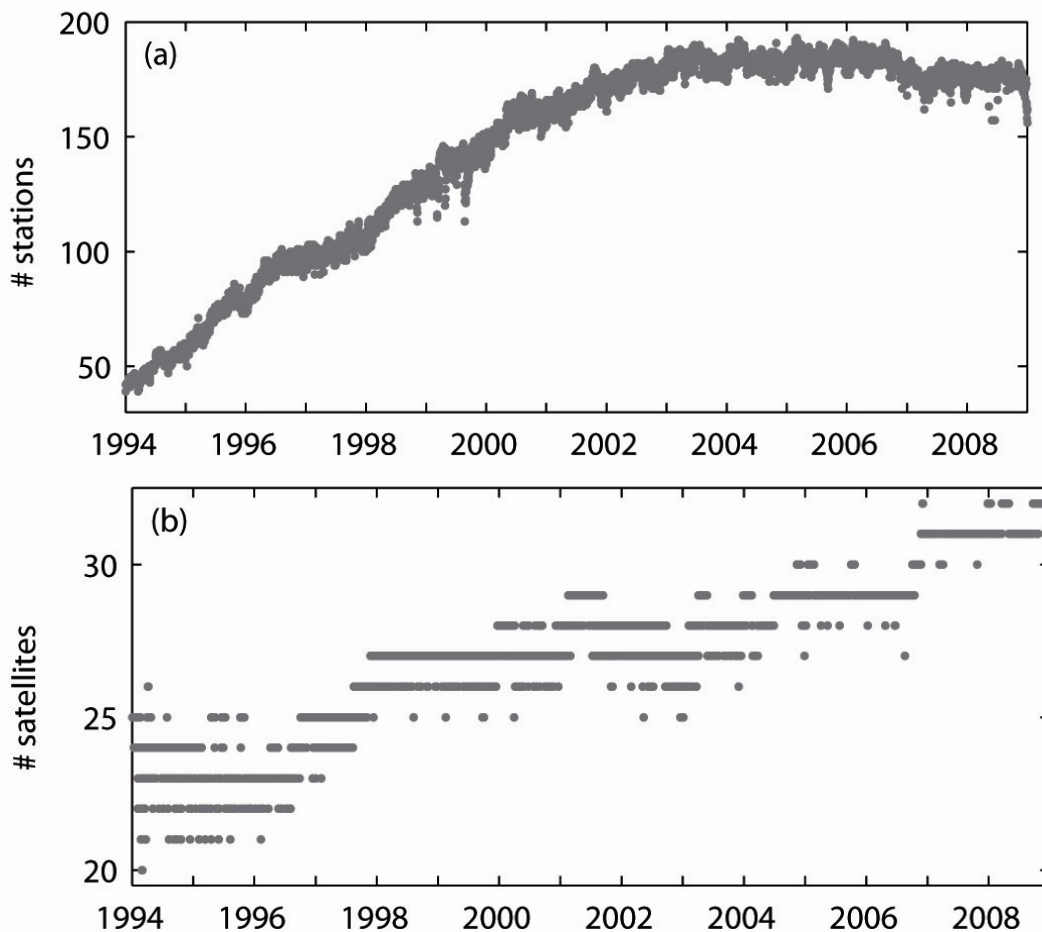


Figure 1.6: Number of active tracking stations (a) at one epoch and total number of GPS satellites (b) considered in the first IGS reprocessing campaign computed at CODE.

The quality and homogeneity of all types of parameters estimated within the reprocessing campaign could be significantly improved compared to the official solutions, particularly in the early years.

In addition to the GPS-only contribution to the IGS reprocessing, a GLONASS extension of the reprocessing was performed to provide fully consistent and also reprocessed GLONASS orbits for the time interval between May 2003 and December 2008 to the users.

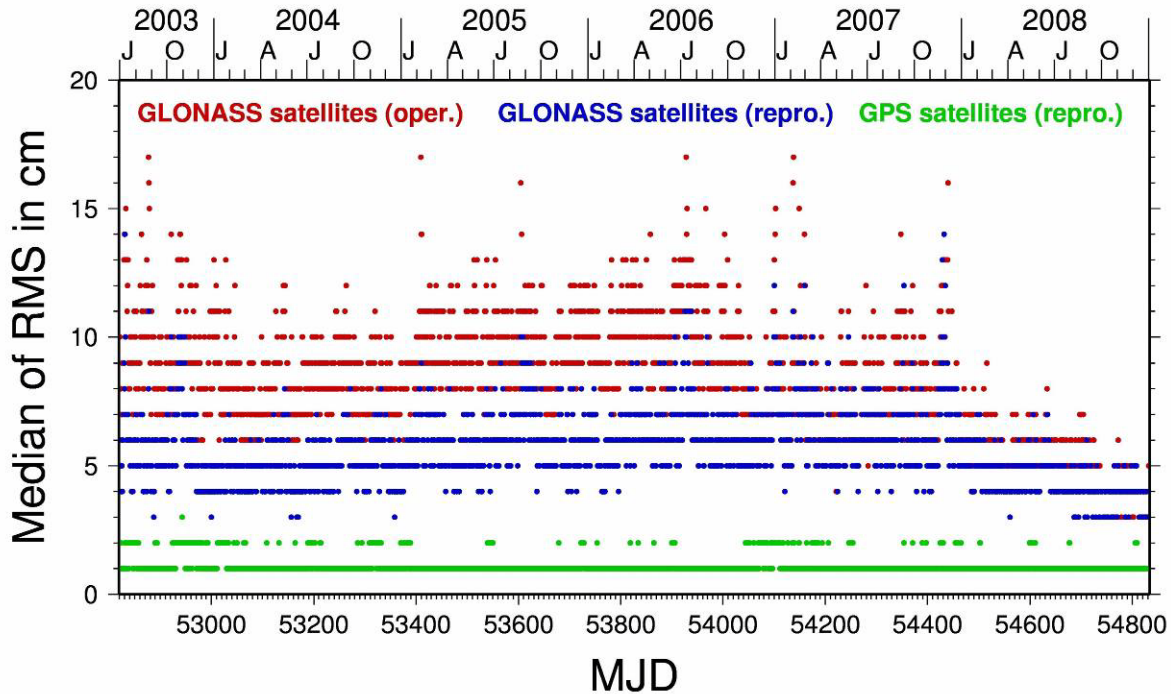


Figure 1.7: Median of the RMS for the fit of a three-day arc through the daily independent orbit solutions for the GLONASS satellites obtained in the CODE reprocessing (blue) and the operational CODE final solutions (red). For comparison the analogue values for the GPS satellites from the operational solution are added (green).

The time series of combined GPS/GLONASS solutions were used as the basis to update the antenna phase center model. With a limited set of GLONASS calibrations, it is possible to assess the impact of GNSS-specific receiver antenna corrections that have been ignored within the IGS so far. The updated GLONASS antenna phase center model helps to improve the orbit quality. GLONASS-only rapid-static or kinematic solutions benefit mostly from the updated satellite antenna corrections and the reference frame of combined GPS/GLONASS solutions will not be degraded (Springer et al. 2010). The new coefficients will be provided as a contribution to the next generation of standard IGS antenna phase center corrections.

The reprocessing activities will be continued using the series of homogeneously preprocessed observation files for specific studies (see e.g., Dach et al., 2011A). In the frame of a DFG/SNF (the German and Swiss science foundations) project it is planned to extend the reprocessing with SLR (Satellite Laser Ranging) measurements (see, Thaller et al., 2011). This project, a collaboration with research groups from the Universities of Technology in Dresden and Munich (TUD and TUM, both Germany) and ETHZ (Swiss Federal Institute of Technology, Zurich, Switzerland), intends to combine reprocessed GNSS (including both GPS and GLONASS) and SLR observations.

# GNSS Data Calibration Parameters

by S. Schaer<sup>1</sup> and R. Dach<sup>2</sup>

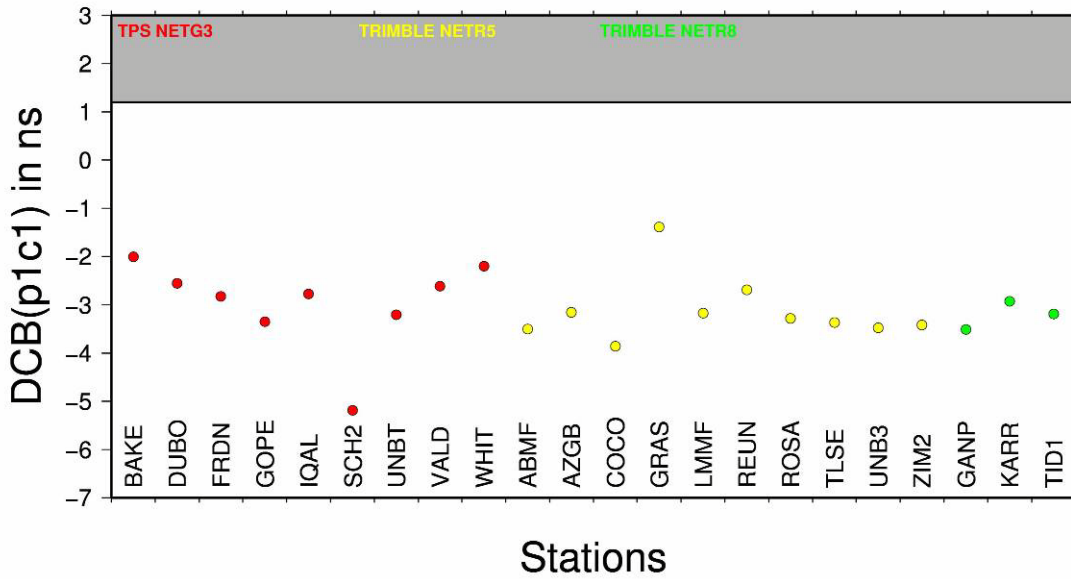
<sup>1</sup> Federal Office of Topography, swisstopo

<sup>2</sup> Astronomical Institute University of Bern

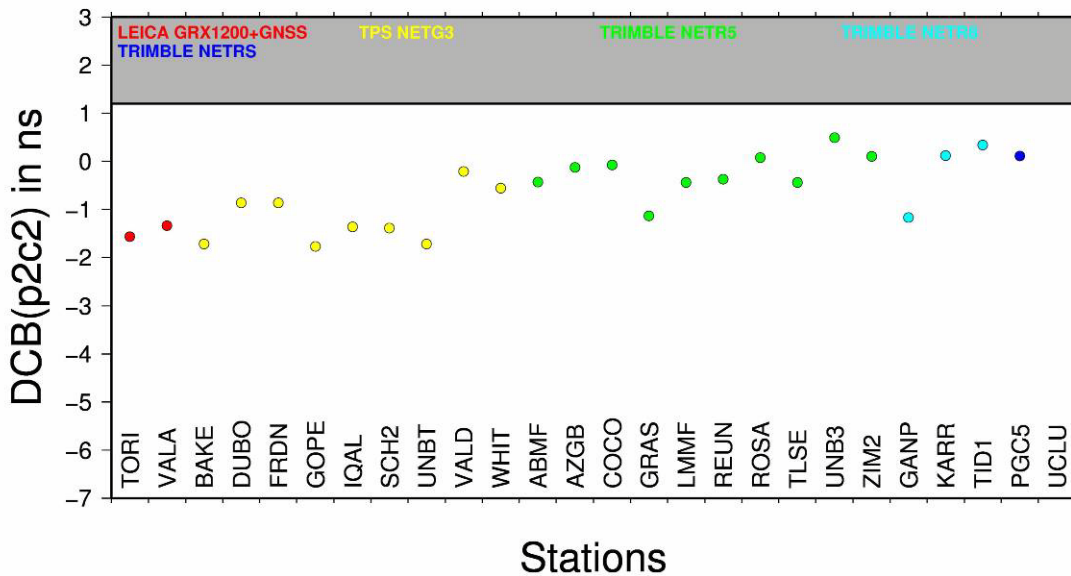
## a) Differential Code Biases

Traditionally, the Differential Code Biases (DCB) have directly been derived during the GNSS data processing at CODE. Station- and satellite-specific values for GPS/GLONASS P1-P2 as well as satellite-specific corrections for GPS P1-C1 are provided as monthly mean values (<http://www.aiub.unibe.ch/download/CODE/>).

Recently, GNSS DCB values are also directly extracted from RINEX observation files (occasionally containing P1 and C1 or P2 and C2 measurements at the same time). This allows us to provide P1-C1 and P2-C2 DCB receiver/satellite corrections for GPS and GLONASS measurements.



(a) P1-C1 receiver DCB for GLONASS



(b) P2-C2 receiver DCB for GPS

Figure 1.8: Receiver DCB values directly derived from RINEX observation files containing pairs of corresponding (P1/C1, or P2/C2) observations at the same time.

## b) Biases in the GPS/GLONASS processing

In case of the GPS/GLONASS clock estimation, we have to consider the following types of code biases:

- Differential code bias (DCB: P1-C1/P2-C2) exists not only for GPS but also for GLONASS.
- Intersystem bias (ISB) responds to the difference between the GPS and GLONASS receiver time frame.
- Inter-frequency bias (IFB) appears for GLONASS because each satellite uses its own frequency for signal transmission. The antipodal satellites share the same frequencies.

In GNSS data processing, only the sum of these three biases can be assessed, e.g., by estimating one bias per GLONASS satellite with respect to all GPS satellites for each GPS/GLONASS tracking station.

The reference for the ISB estimates may be arbitrarily chosen because it depends on the assumptions for the IFB and DCB concerning GLONASS. Nevertheless, the results in Figure 1.9 show that the ISB dominate the bias budget. One bias parameter for each satellite/station combination has been computed from 30 days in September 2010. The variation between the ISB of different receiver types is visible. It is also worth mentioning that the six “exceptional” values for the TRIMBLE NETR5 receiver type are related to latest receiver firmware version (4.15 or higher).

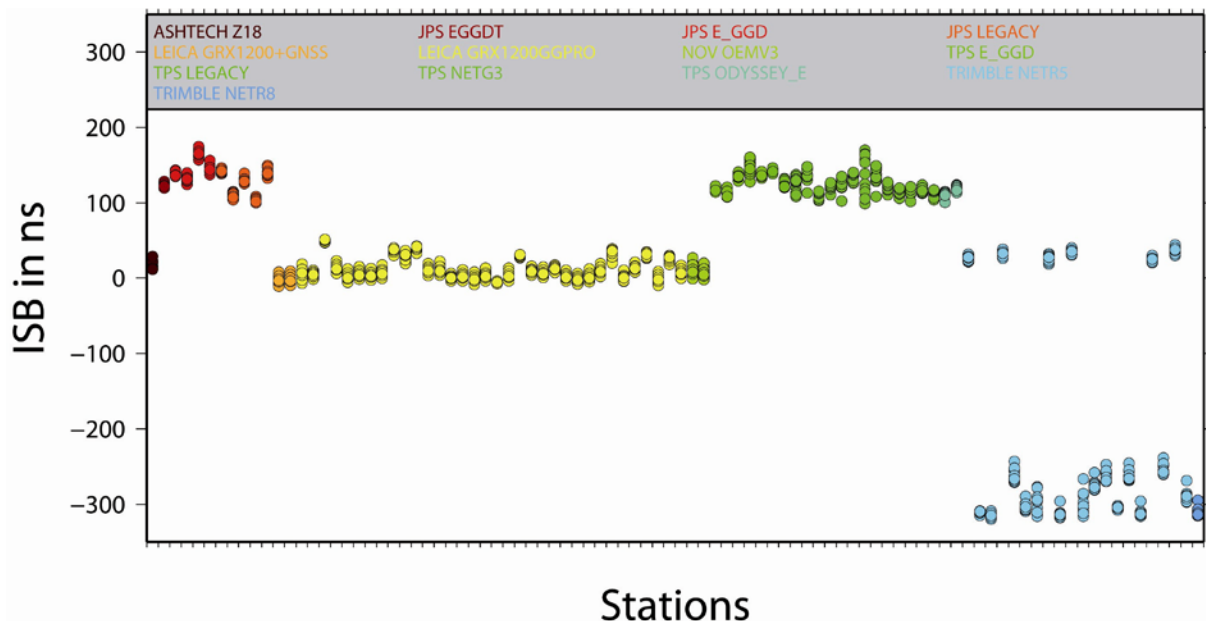
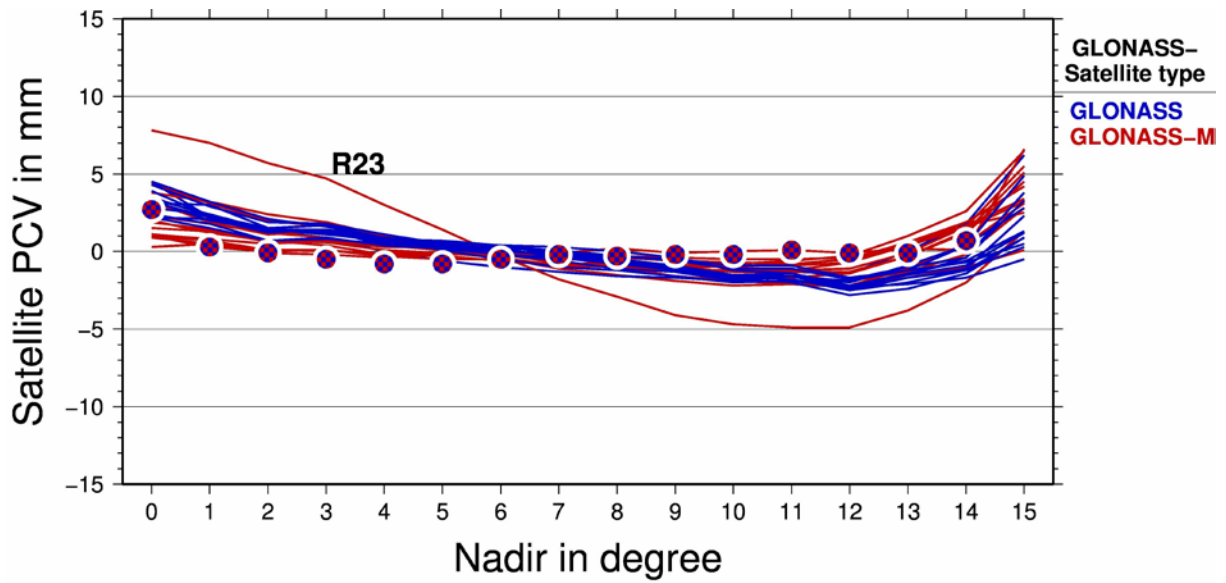


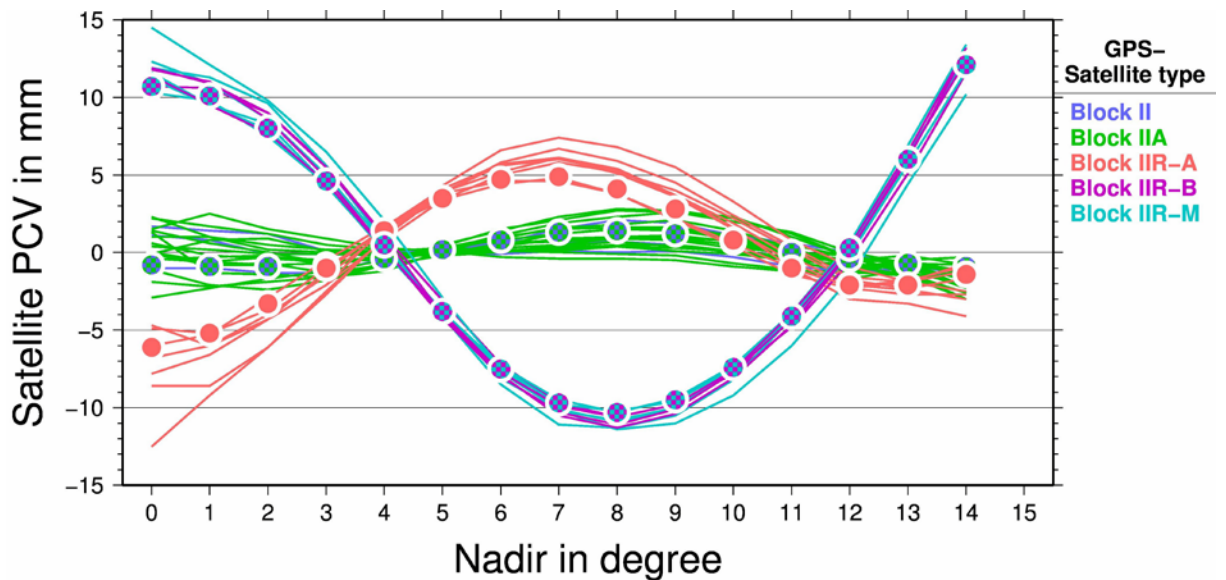
Figure 1.9: ISB values for a selected number of GPS/GLONASS tracking stations computed from 30 days in September 2010.

## c) Antenna calibration update

The GLONASS satellite antenna corrections for the igs05.atx dataset have been computed at the beginning of 2006 with a very limited GLONASS tracking network. At that time, just few months of tracking data were available with respect to the first GLONASS-M satellite generation. In the meantime, the complete GLONASS satellite constellation has been exchanged. The data from the GLONASS extension of the CODE reprocessing (see Lutz et al, 2011) has been used to update the GLONASS satellite antenna corrections. Yearly solutions did show a very high consistency and suggest that the differences between the corrections for individual satellites are significant. The nadir-dependent component for all active satellites in the period of this solution (2003 to 2008) is shown in Figure 1.10. All details for the solution are presented and discussed in Dach et al., 2011B. In this paper, it is also discussed to use system-specific antenna corrections for the multi-GNSS receivers.



(a) PCV for the GPS satellites



(b) PCV for the GLONASS satellites

Figure 1.10: Nadir-dependent satellite antenna phase center variation (PCV) corrections for all satellites observed for more than 90 days during the GLONASS extension of the CODE reprocessing. The colors indicate the different satellite types, the dots illustrate the corresponding igs05.atx corrections.

The GLONASS satellite antenna correction model has been compared with an independent solution generated at ESOC's analysis center in Dilssner et al., 2010. Both solutions are in general agreement and form the basis for the GLONASS satellite part of the new igs08.atx GNSS PCV model.



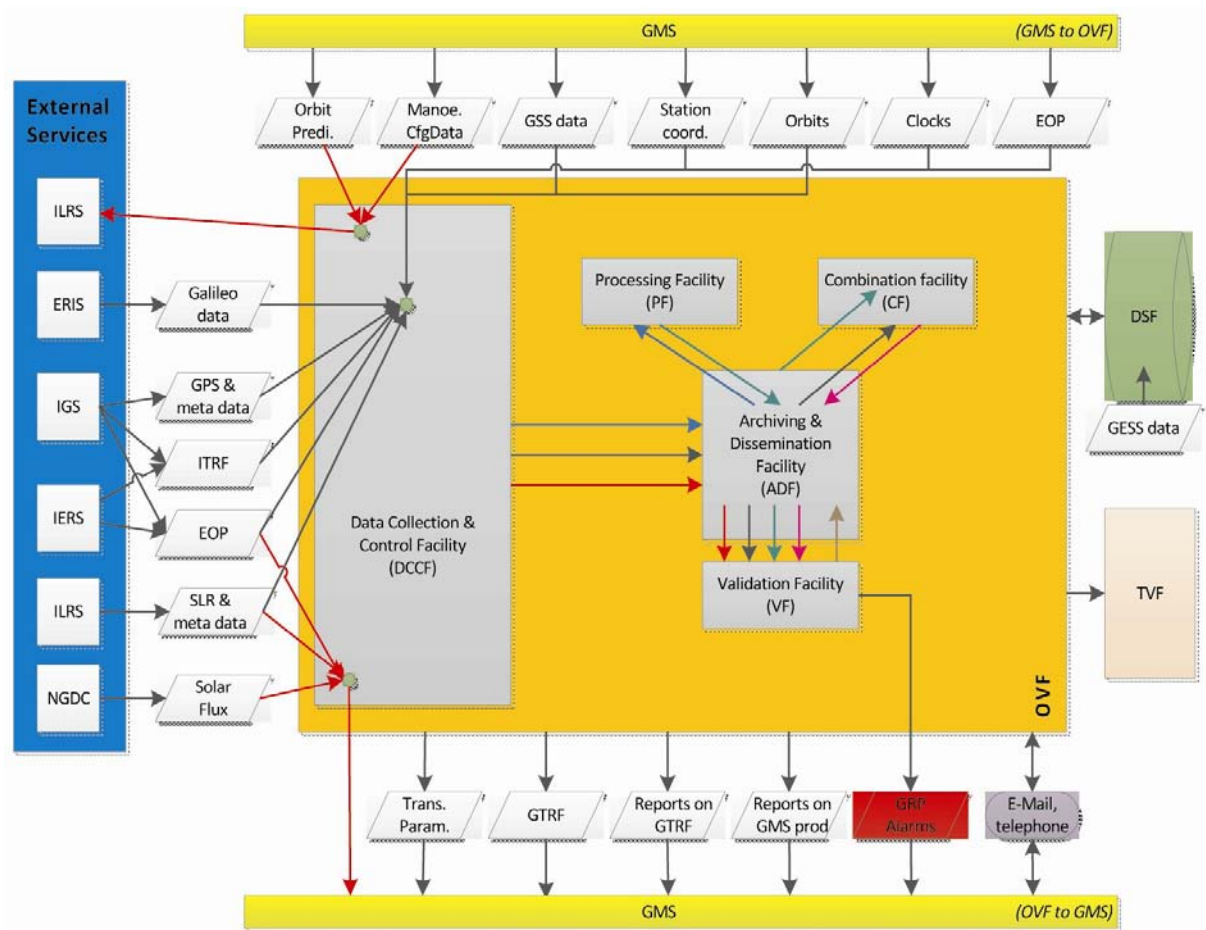


Figure 1.12: TGVF OVF Architecture – Overview

## Combining SLR and GNSS measurements

by D. Thaller, K. Sosnica, G. Beutler, R. Dach and A. Jäggi

*Astronomical Institute University of Bern*

The activities at AIUB related to the analysis of SLR data can be grouped in three major topics:

1. Analysis of LAGEOS data;
2. Statistics on SLR range residuals to GNSS orbits based on microwave data;
3. Combined analysis of microwave and SLR range data to GNSS satellites.

The Bernese Software (Dach et al. 2007) recently has been extended for the capability of analysing SLR observations to spherical geodetic satellites, e.g. LAGEOS and ETALON (see Thaller et al. 2008). Since July 2010, the contribution of BKG (Bundesamt für Kartographie und Geodäsie, Frankfurt am Main, Germany) (one of the partners within the CODE (Center for Orbit Determination in Europe (see Schaer et al. 2011) consortium) to the International Laser Ranging Service (ILRS)) is based on the SLR development version of the Bernese Software. Seven-day solutions based on LAGEOS data are delivered on a routine basis to the ILRS. Estimated parameters are station coordinates, polar motion, LOD, range biases (for a few stations only) and satellite orbits. The ILRS has two product lines: the so-called "DAILY" product is due just one day after the data (i.e. covering the time span from "today - 8 days" until "today - 1 day"). The so-called "WEEKLY" product covers the time span from Sunday to Saturday and is due on Tuesday evening.

The comparison of SLR range data with GNSS orbits based on microwave data allows to validate the GNSS orbits. On the other hand, the SLR measurements can be calibrated, too. CODE, as an Associated Analysis Center (AAC) of the ILRS, provides daily comparisons of SLR tracking data with CODE orbits for GPS and GLONASS satellites in form of quick-look reports. These reports are distributed via e-mail to the SLR-report mail exploder every day, giving rapid feedback on the SLR data quality to the ILRS community.

Besides the pure SLR residual analysis, a combined analysis of microwave and SLR range measurements to GPS and GLONASS satellites has been performed at AIUB (see Thaller et al. 2010). In such an analysis the GNSS satellites can be used as co-location point instead (or in addition) to the co-located ground stations. Using satellite co-locations implies that one common set of orbit parameters is estimated based on microwave and SLR range observations together.

The common orbit parameters allow it to transfer the absolute scale information provided by the SLR range observations directly to the GNSS part. This is of particular interest because the GNSS-derived scale is contaminated by uncertainties in modeling the phase center of the transmitting and receiving antennas. Other studies already revealed that the satellite antenna offsets (SAO) of the GNSS microwave antenna w.r.t the center of mass (COM) of the satellite officially adopted within the IGS (given by igs05.atx, see Schmid et al. 2007) might be wrong by several centimeters. Therefore, we estimated the SAO from a combined analysis of GNSS microwave and SLR range data. Four years of data have been considered (2006-2009). The estimated corrections for the SAO in nadir direction are shown in Figure 1.13. The mean correction for the GPS satellites clearly differ from the mean correction for the GLONASS satellites, i.e., 76.4 mm and -47.7 mm, respectively.

When estimating the SAO parameters, the GNSS part has a rank deficiency regarding the scale, so that the GNSS sub-network in the combined analysis will fully adapt the scale provided by the SLR data. We see a difference of 0.59 ppb for the GNSS sub-network between the solution with estimated SAO parameters and a solution with SAO fixed to the IGS05 values, whereas the scale of the SLR sub-network does not change. This behaviour clearly demonstrates that SLR provides the scale in the combined solution (although there is only a very few amount of SLR data available compared to the amount of microwave data). Furthermore, it becomes clear that the SAO values provided by IGS05 does not fit to the scale of SLR.

On the SLR side, the uncertainties in the offsets of the laser retro-reflector arrays (LRA) w.r.t. COM of the GNSS satellites and the presence of range biases have to be handled. We set-up one bias parameter per SLR station and GNSS satellite. Figure 1.14 shows the resulting bias parameters for two satellites.



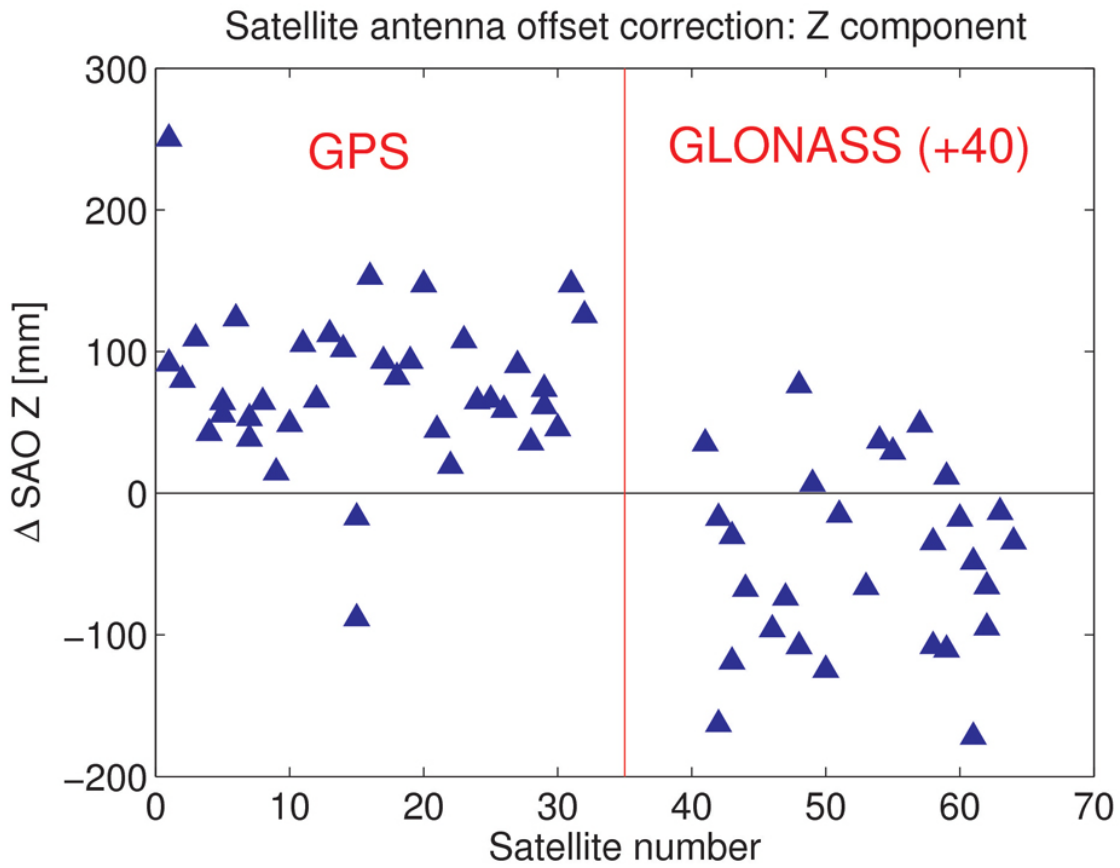
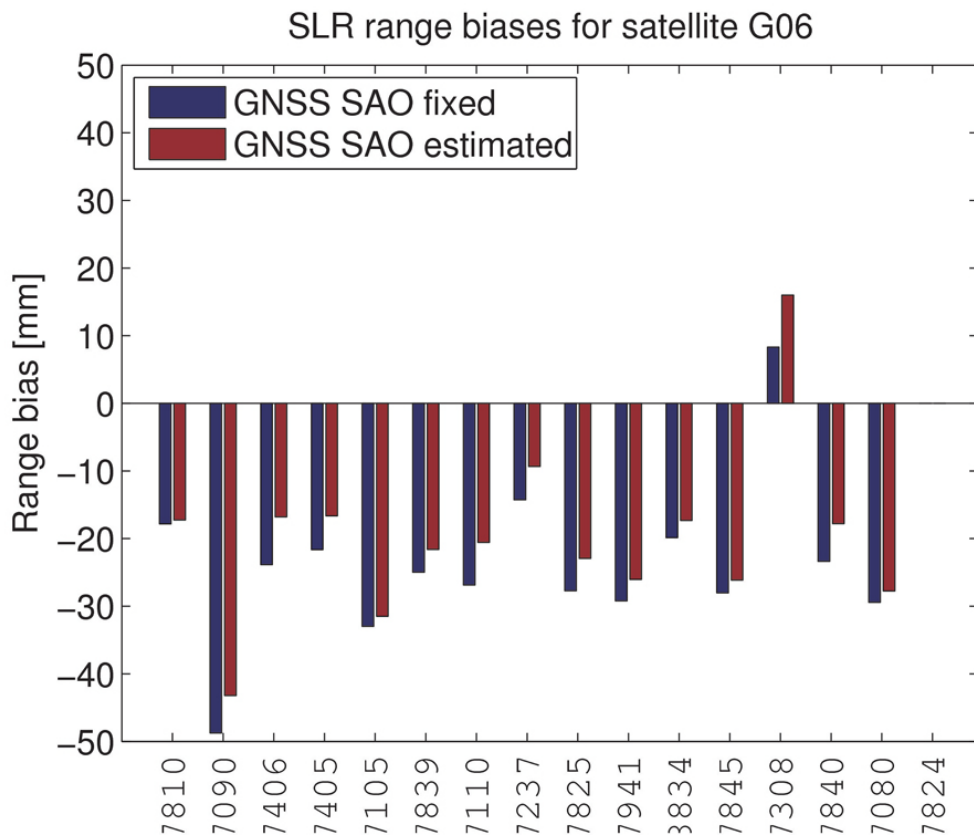


Figure 1.13: Estimated corrections for the GNSS SAO (z-component) w.r.t. the official values given in the file *igs05.atx*.



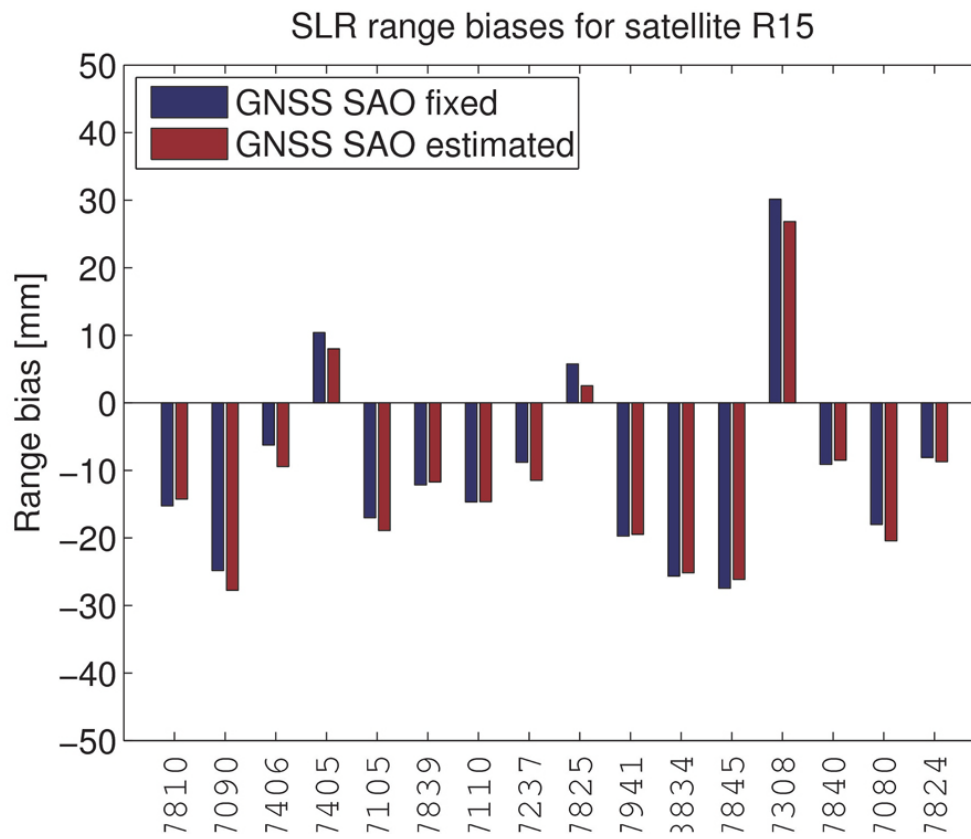


Figure 1.14: Bias parameters estimated for each SLR station in order to account for discrepancies between GNSS and SLR. a) GPS PRN 06, b) GLONASS PRN 15.

## **The Zimmerwald Observatory**

by T. Schildknecht<sup>1</sup>, A. Jäggi<sup>1</sup>, M. Ploner<sup>1</sup> and E. Brockmann<sup>2</sup>

<sup>1</sup> *Astronomical Institute University of Bern*

<sup>2</sup> *Federal Office of Topography, swisstopo*

The main activities at the Zimmerwald Observatory are:

### **Satellite Laser Ranging (SLR):**

The Zimmerwald observatory is a station of the global tracking network of the International Laser Ranging Service (ILRS). The SLR observations acquired with the monostatic 1-m Zimmerwald Laser and Astrometric Telescope (ZIMLAT, see Figure 1.15) are delivered in near real-time to the global ILRS data centers. The SLR activities at Zimmerwald are performed by the Astronomical Institute of the University of Bern (AIUB) and the Swiss Federal Office of Topography (swisstopo). Detailed descriptions of the activities of the last four years may be found in (Jäggi et al., 2011A).

### **Astrometric Observations:**

Direction observations of satellites, space-debris, and near-Earth asteroids using charge-coupled device (CCD) cameras are performed at the Zimmerwald observatory. The astrometric observations acquired with the 1-m ZIMLAT telescope are predominantly used to build-up and maintain orbit catalogues of small-size space debris in high-altitude orbits, and of large objects in the geostationary ring. The project shares the 1-m ZIMLAT telescope with the SLR project during night-time. The CCD activities are performed by AIUB.

### **Global Navigation Satellite Systems (GNSS):**

GNSS receivers are operated at Zimmerwald by swisstopo and AIUB. In the second half of 2007 the additional GNSS receiver ZIM2 was installed in the frame of enhancing the Automated GNSS Network for Switzerland (AGNES) with GLONASS. The data of the new station, which is mounted on a 9-meter mast similar to the main station ZIMM (see Figure 1.15), is delivered to the data centers of IGS and EUREF starting with week 1458 (December 16, 2007). Figure 1.16 (top, left and right) shows that 4 additional GLONASS satellites per epoch were observed on average with the combined GNSS receiver in the beginning of 2008. Due to the evolution of the GLONASS system more than 10 additional satellites could be collected in the beginning of 2011 as compared to the GPS receiver with a maximum number of 12 channels (Figure 1.16, bottom, left and right).

### **Gravimetry:**

A permanent Earth tide gravimeter is operated at Zimmerwald by ETH Zurich. The instrument of the type ET-25 (LaCoste & Romberg) collected, with the exception of some short time periods, a continuous data set (Marti and Bürki, 2011). Additionally twice a year, absolute gravity measurements using a FG5 (Micro-g LaCoste) instrument were performed by swisstopo in collaboration with the Federal Office of Metrology (METAS).

### **Local ties between geodetic markers:**

According to a 5-year cycle the local ties in Zimmerwald were re-observed in July 2008 by swisstopo. Compared to the previous determination of the local ties a more robust network geometry and improvements concerning the physical realization of the GNSS antenna reference points of ZIMM and ZIM2 were introduced without removing the antenna. The results of the surveys are shown in Figure 1.17 as a function of time for the local tie between SLR and GPS. A relative difference in the horizontal position of about 7 mm (5 mm in each component) and 5 mm in height is visible since 1995.



Figure 1.15: The Zimmerwald Observatory with the monostatic 1-m laser and astrometric Telescope ZIMLAT (foreground), the 9-meter masts of the GPS-only station ZIMM (left) and the GPS/GLONASS station ZIM2 (right).

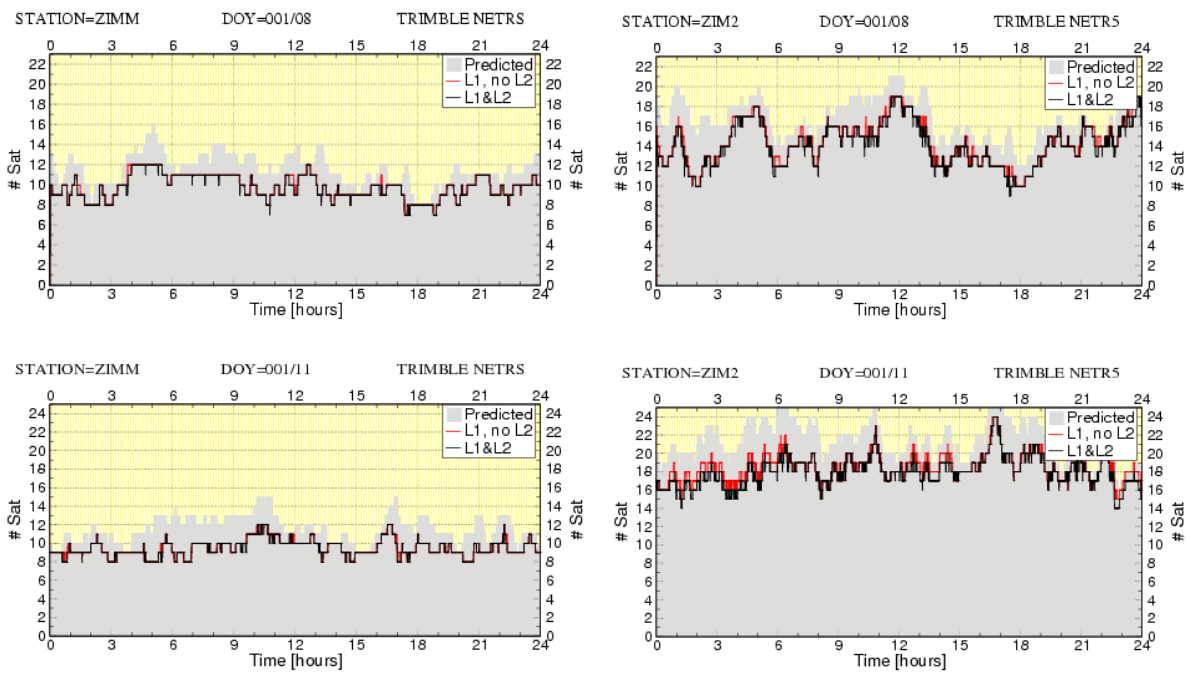


Figure 1.16: GNSS observations on January 1, 2008 (top) and January 1, 2011 (bottom) of the station ZIMM (12 channel GPS-only receiver, left) and station ZIM2 (GPS/GLONASS receiver, right).

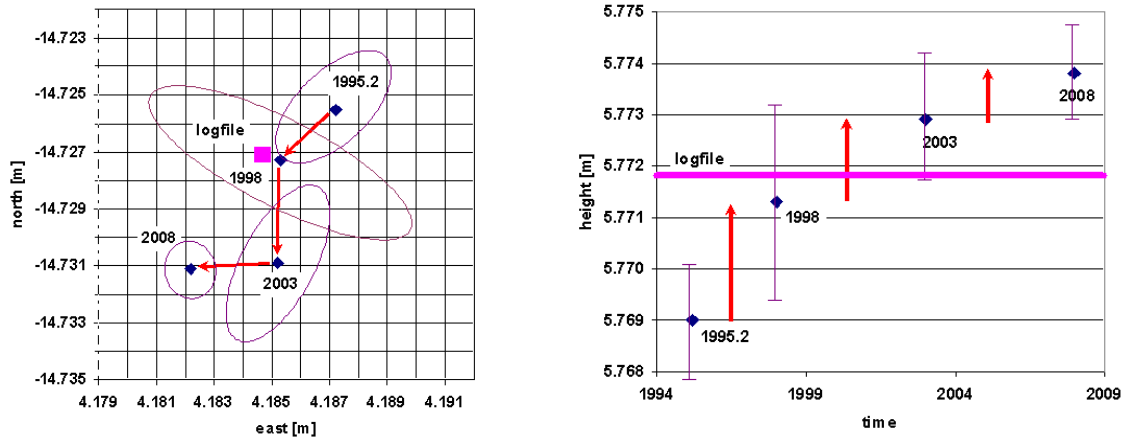


Figure 1.17: Local tie between the SLR reference point (physical reference point) and the GPS antenna reference point (ZIMM 14001M004) for the horizontal (left) and vertical component (right). The error bars represent the 95% confidence interval. The value of the ZIMM logfile is displayed for comparison.

## Satellite Laser Ranging at Zimmerwald

by A. Jäggi<sup>1</sup>, M. Ploner<sup>1</sup>, J. Utzinger<sup>1</sup>, M. Prohaska<sup>1</sup>, E. Pop<sup>1</sup>, W. Gurtner<sup>1</sup> and E. Brockmann<sup>2</sup>

<sup>1</sup> Astronomical Institute University of Bern

<sup>2</sup> Federal Office of Topography, swisstopo

In spring 2008 the Titanium-Sapphire laser was replaced by a new 100 Hz Nd:YAG system (Gurtner et al., 2009). The design of the new system enables a high flexibility in the selection of the actual firing rate and epochs, which also allows for synchronous operation in one-way laser ranging experiments to spaceborne optical transponders such as the Lunar Reconnaissance Orbiter (LRO). Firing order and range-gate generation are controlled by a PC card with a field-programmable gate array provided by the Technical University of Graz. The protection of the receiver from backscatter in the monostatic 1-m Zimmerwald Laser and Astrometric Telescope (ZIMLAT) is realized with a synchronized rotating shutter.

Figure 1.18 (left) shows the number of measured single-shot ranges per month since 1997. The pronounced increase in spring 2008 reflects the upgrade from the 10 Hz Titanium-Sapphire laser to the new 100 Hz Nd:YAG system. Figure 1.18 (right) illustrates that not just the number of single-shot measurements has increased, the data yield in terms of collected normal points is steadily growing as well. Weeks with a top performance, e.g., between 6th and 12th September 2009 with a total of 396 observed satellite passes, demonstrate the impressive outcome under optimal conditions. Zimmerwald is among the most productive stations of the International Laser Ranging Service (ILRS).

During the last four years Zimmerwald significantly contributed to new and advanced concepts and procedures within the ILRS, e.g.,

- one-way ranging to the LRO satellite (only the ILRS stations NGSLR, Herstmonceux, and Zimmerwald are able to perform synchronous measurements, see Figure 1.19)
- tracking of an increased number of satellites at high orbital altitudes, e.g., additional GLONASS satellites
- tracking of satellites at very low orbital altitudes, e.g., the GOCE satellite (Jäggi et al., 2011)
- tracking of vulnerable satellites, e.g., the ICESAT satellite
- test and integration of the consolidated laser ranging data format

The maintenance and operation of the satellite laser ranging facility are supported by the Swiss Federal Office of Topography (swisstopo), the Swiss National Science Foundation (SNF), and the Swiss Academy of Sciences (scnat).

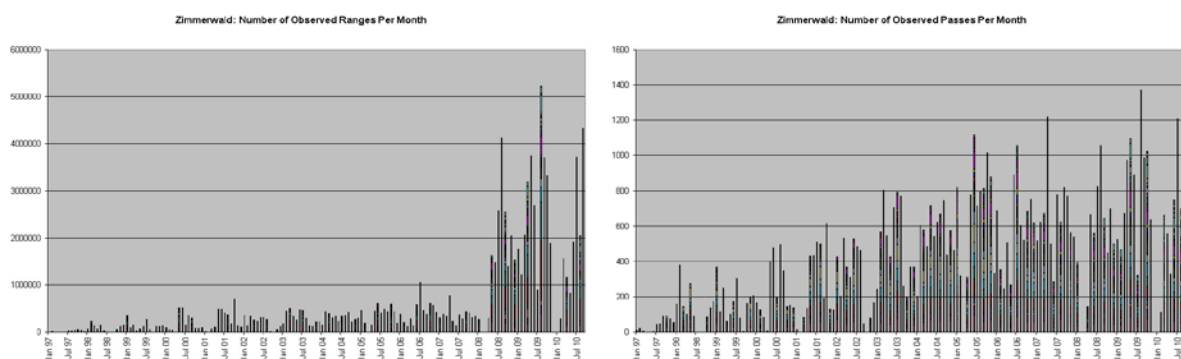


Figure 1.18: Number of observed single-shot ranges per month since 1997 (left) and number of observed normal points per month (right).

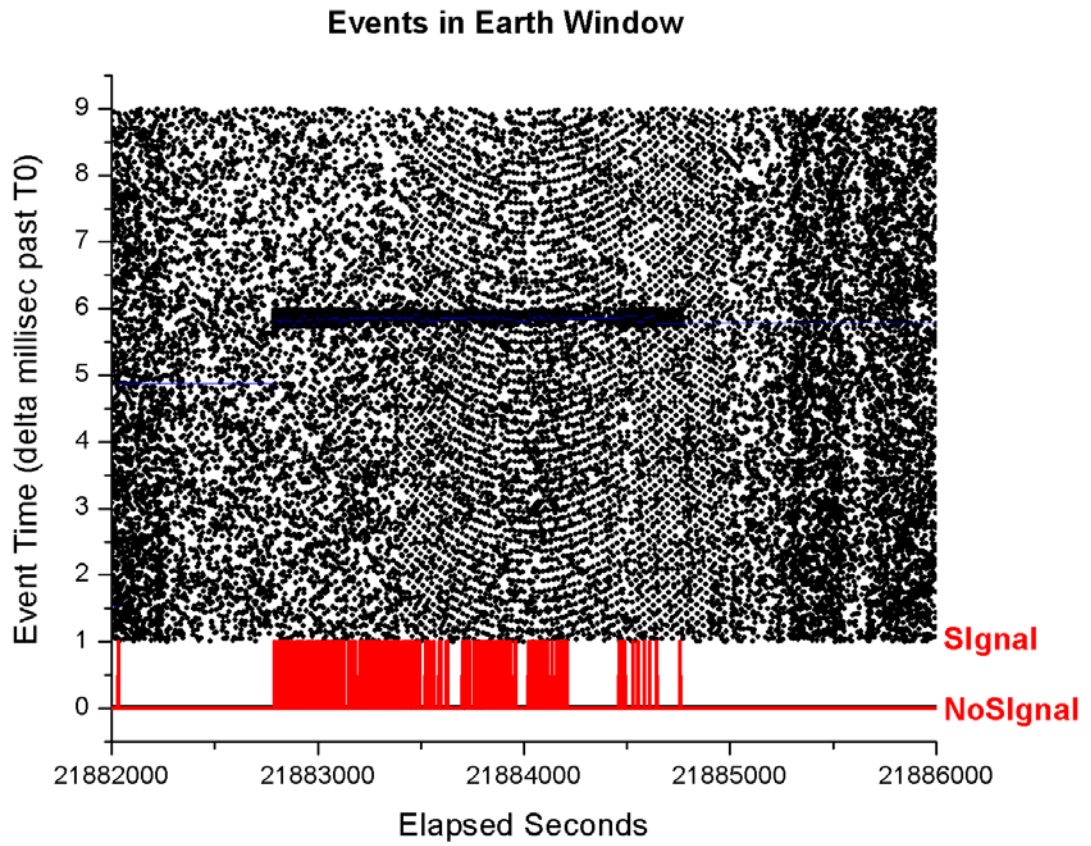


Figure 1.19: Events in the laser altimeter Earth window registered during simultaneous LRO tracking from Grasse (curves) and Zimmerwald (straight line).

## **New Legislation for Geoinformation and National Survey**

*by A. Wiget*

*Federal Office of Topography, swisstopo*

On July 1st, 2008, the Federal Act on Geoinformation (Geoinformation Act, GeoIA, SR510.62) entered into force ([http://www.admin.ch/ch/e/rs/c510\\_62.html](http://www.admin.ch/ch/e/rs/c510_62.html)). This legislation assures the rapid, smooth and sustainable availability of up-to-date geographical data over the entire territory of the Swiss Confederation. Furthermore, the GeoIA sets the legal basis for Cadastral Surveying and the Swiss Geological Survey. The purpose is to provide geoinformation for the federal, cantonal and municipal authorities, as well as for the private sector, the general population and scientific circles. Geodata shall be made easily accessible in the required quality and at reasonable costs, so that the data can be used in a broad variety of applications. To support this goal, a new platform ([www.geo.admin.ch](http://www.geo.admin.ch)) was established where users are able to directly access federal geoinformation, geodata, geo-services and metadata.

In successive ordinances to the GeoIA, regulations concerning further details such as the qualitative and technical requirements for official geodata are issued. Of special interest in this context are the 'Geoinformation Ordinance' (GeoIO, SR 510.620) and the 'National Survey Ordinance' (NSO, SR 510.626).

The GeoIO specifies regulations valid for all official geodata under federal legislation. A catalogue of these geodata is an appendix to the GeoIO. The official geodetic reference system and reference frame are stated and the Federal Office of Topography swisstopo is entitled to specify the definitions and technical details (see GeoIO-swisstopo and NSO). Furthermore the GeoIO issues regulations on the relevant geodata models and presentation models; data collection, updating, management and archiving; data quality, availability, access, use and exchange; geospatial metadata; geodata services (geoservices) as well as fees for the access to and use of geodata and geoservices of the Confederation.

The NSO regulates the National Survey in more detail. The National Survey shall make the geospatial reference data of the Confederation available for civil and military purposes. This task includes in particular

- the definition of the geodetic reference system and the establishment, updating and management of the reference framework;
- the monumentation and survey of national borders;
- the collection, updating and management of topographic information for the national landscape models;
- the preparation of the National Map series.

For these tasks, the NSO governs the responsibilities and entitles the Federal Office of Topography swisstopo to specify further details (e.g. regarding fundamental stations, permanent GNSS stations and analysis center, national gravity network and geoid model).

Based on these legal regulations swisstopo published in 2010 the concept for data collection, updating and management of the geodetic survey in Switzerland [Wiget et al. 2010A] as well as the quality standards to be observed [Wiget et al. 2010B].



# Internet platform and transformation service to support the reference frame change in Switzerland

by M. Kistler, U. Marti, J. Ray and A. Wiget

Federal Office of Topography, swisstopo

Based on the 'Geoinformation Ordinance' (GeoIO, SR 510.620; Art. 4 and Art. 53) Switzerland is introducing a new reference system (CH1903+) and reference frame (LV95) for the horizontal coordinates of all official geodata. The transition period has to be completed by Dec. 31, 2016 for reference data and by Dec. 31, 2020 for all the other official geodata under federal legislation. Despite the fact that also a new national vertical reference frame has been defined and calculated (LHN95) the official height system will not be changed.

Switzerland is introducing new "absolute" reference frame LV95 with an accuracy of about 1 cm in position and 3 cm in height. To transform geodatasets from the old Swiss coordinate system LV03 to the new one, the Swiss Federal Institute of Technology developed in the nineties the so called Fineltra algorithm, a linear transformation by finite elements. 2006 in collaboration with the cantons, the finite elements in form of the national triangular network have been completed finally (c.f. Swiss National Report on the geodetic activities in the years 2003 to 2007). The Fineltra algorithm provides a very high accurate transformation, but doesn't keep geometric properties, such as isometry. So, other approaches keeping the geometric properties have been demanded. For this purpose, swisstopo developed 2009 a framework with different transformation / interpolation methods according to accuracy and geometric requirements:

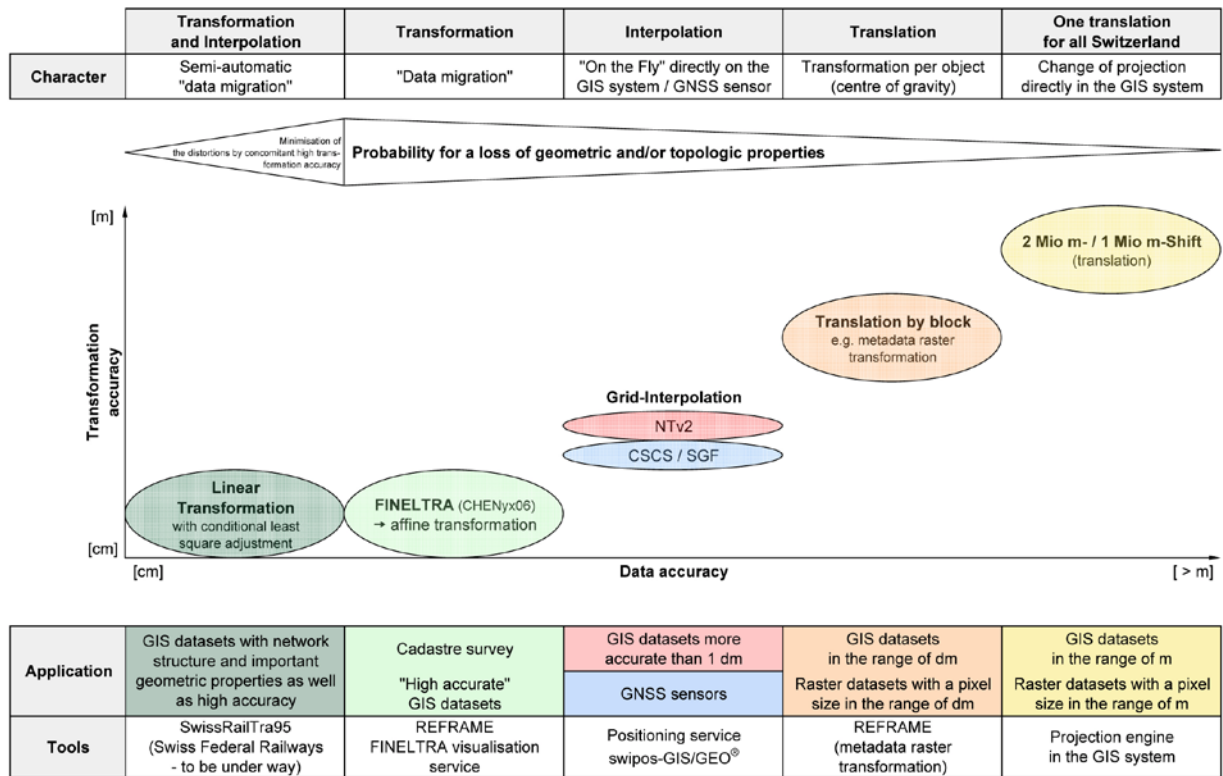


Figure 1.20: Variants of realisation for the reference frame change LV03 - LV95 in Switzerland as a function of data-set accuracy and with indication of the probability of a loss of geometric or topologic properties

While the national surveying and mapping agency of Switzerland, swisstopo, already provides (and updates) all the base datasets in LV95, the cadastral authorities decided to make full use of the transition period and introduce the new reference frame by canton over a period of about 10 years, the latest until end of 2016. As a consequence, two reference frames have to be supported, as well as the transformation between them over a long period.

Due to the fact, that every geodata producer as well as every user in Switzerland is concerned of the reference frame change, swisstopo developed an Internet platform under [www.swisstopo.ch/lv95](http://www.swisstopo.ch/lv95). Under this URL information about the new coordinates can be found and a download service for the official transformation dataset as

well as for the dynamic-link library DLL with the official algorithm for software developers is provided. Furthermore, a transformation service and a visualisation service which indicates the empiric accuracy of the transformation all over Switzerland have been released.

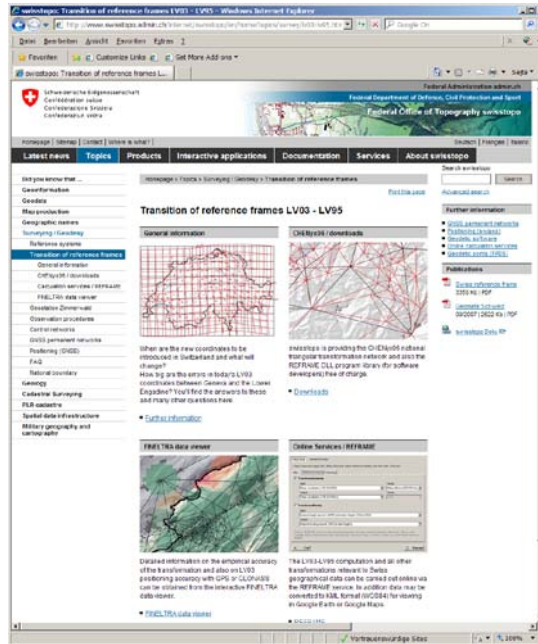


Figure 1.21: Start page of the internet platform concerning the reference frame change with the following subject areas:

- General information
- Download services
- Transformation service "REFRAME"
- Visualisation service "FINELTRA data-viewer"

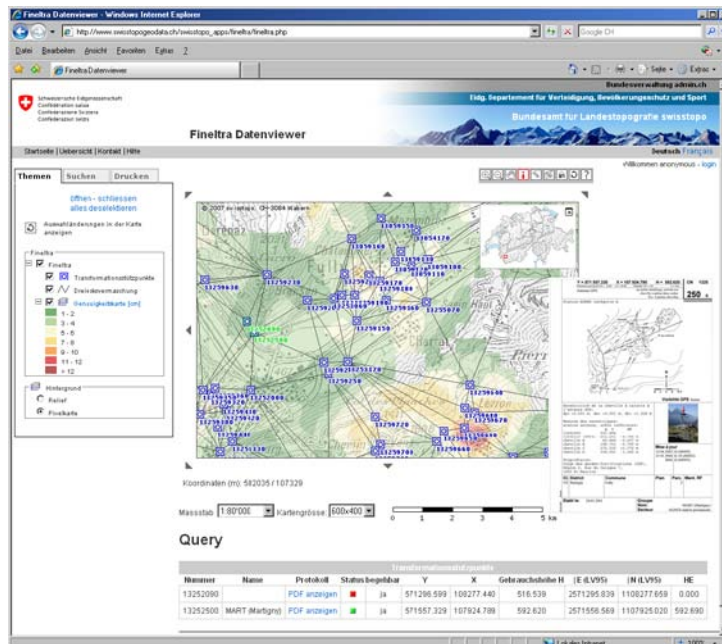


Figure 1.22: Visualisation service "FINELTRA data-viewer" with the national triangulation network, all the control points of the finite element transformation as well as the empiric transformation accuracy. There is also a direct access to all the national and cantonal geodetic benchmarks.

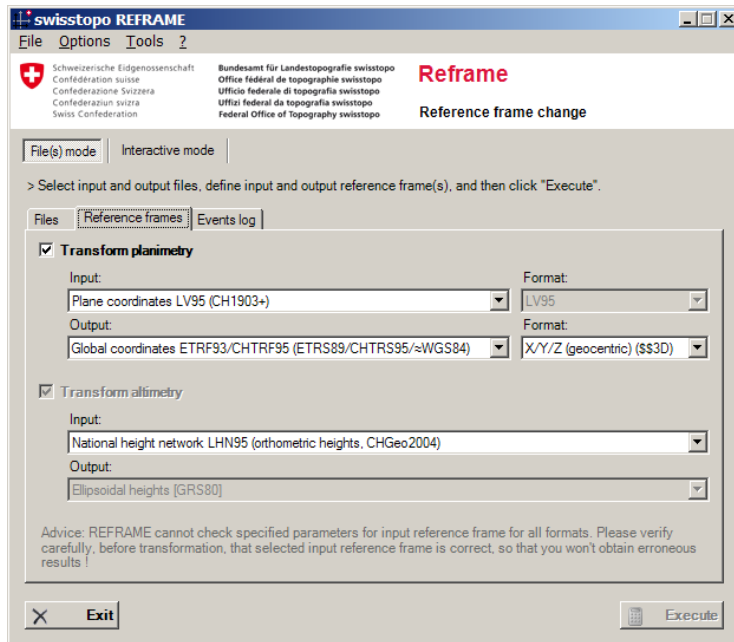


Figure 1.23: Graphic user interface of the new transformation software REFRAME for all the official coordinate transformations in Switzerland and to global reference frames.

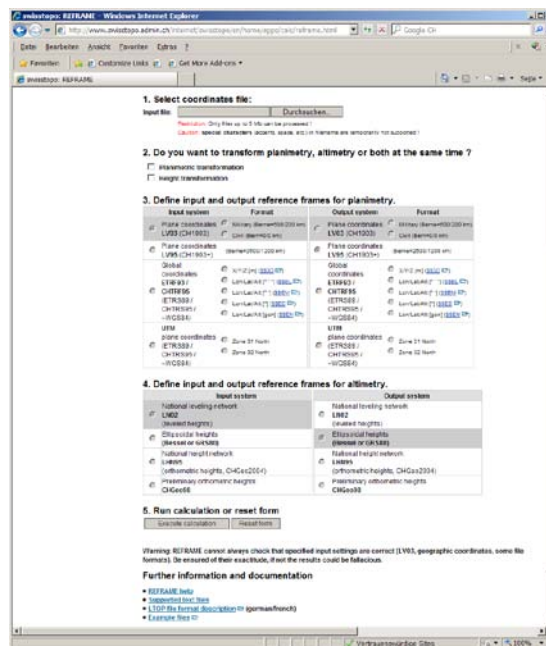


Figure 1.24: Graphic user interface of the Internet transformation service REFRAME.

## Enhancing the Swiss Permanent GPS Network (AGNES) for GLONASS

by E. Brockmann and U. Wild

Federal Office of Topography, swisstopo

All major manufacturers of geodetic GNSS receivers have been designing combined receivers for both GPS and GLONASS since 2006. In order to keep step with this development, swisstopo adapted its CORS network AGNES, consisting of 31 continuously operating stations, to the new technical demands. Since AGNES is a multifunctional reference network not only for applications in national surveying but also for scientific studies and positioning services, swisstopo had to find a compromise between the continuity of the observations and the rapid alignment to the demands and developments of the surveying market.

To assure continuity, conventional GPS receivers operate simultaneously with new GPS/GLONASS receivers on ten AGNES stations. The rest of the 21 AGNES stations were converted during summer 2007. To guarantee highest precision, all of the new GNSS antennas were calibrated by the specialized firm Geo++ in Germany. Absolute azimuth- and elevation-depending antenna phase center variations were derived for GPS (individual corrections for each antenna) and for GLONASS (one group correction).

In the years 2008 and 2009, local tie surveys were carried out at the double stations. Furthermore, antennas were changed in 2009 at some of the double stations. Comparisons between GNSS-derived coordinates and the local ties allow detailed conclusions concerning the quality of antenna calibrations and possible biases when using different processing options in the GNSS analysis.

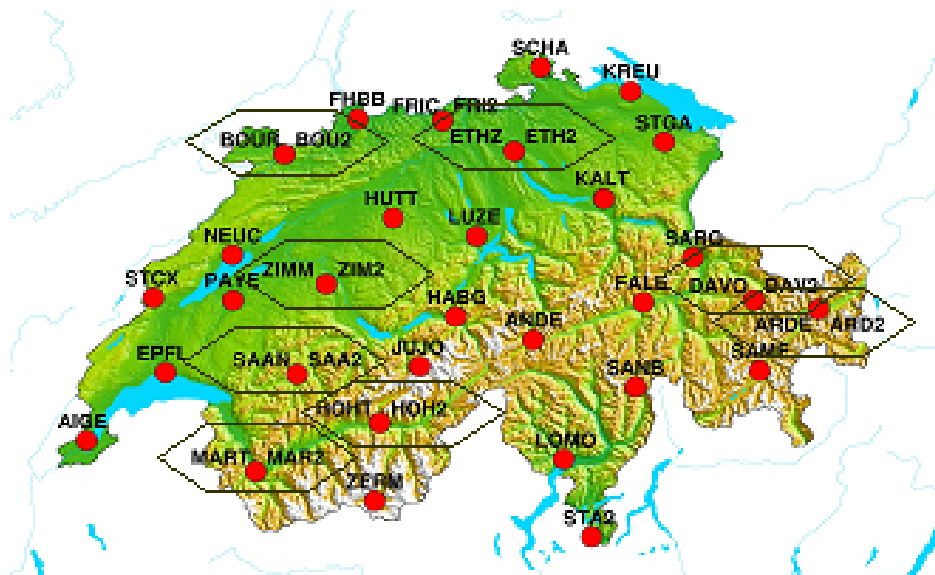


Figure 1.25: Double stations of the GNSS permanent network AGNES (network status January 2011).

## Analysis of Permanent GNSS Networks at swisstopo (PNAC)

by E. Brockmann, D. Ineichen and S. Schaer

Federal Office of Topography, swisstopo

The Automated GNSS Network of Switzerland (AGNES) is a multi-purpose reference network for national first order surveying, scientific research such as geodynamics and GNSS meteorology and serves as a base for the Swiss positioning service (swipos). AGNES was set up beginning in 1998 and reached its designated configuration of 29 stations by the end of 2001. After the enhancement of the network by GPS/GLONASS mid of 2007, totally 41 receivers are operating continuously to serve the various applications.

The characteristics of the permanent GNSS-networks analyzed at swisstopo are shown in Table 1.1. The routine operation of the Permanent Network Analysis Center (PNAC) is divided into 3 sub-network solutions, which are generated on an hourly and daily basis. All analyses are done with the Bernese Software BSW5.0. The use of synergies with the global analyses of the permanent network of the International GNSS Service (IGS) performed at the Astronomical Institute of the University of Bern (AIUB) which operates the Center for Orbit Determination in Europe (CODE) could be realized by several software modules which are absolutely identical at AIUB and swisstopo. Furthermore, improvements of the BSW5.0 were developed (e.g. GLONASS ambiguity resolution) which will be included in future updates of the BSW.

The number of analyzed sites has continuously been increased including foreign stations close to the Swiss national border (partly delivering also data in real-time for the positioning service), third-party stations, and new EPN stations.

The main processing products are continuously derived coordinates for reference frame maintenance and zenith total delay estimates for numerical weather prediction. From solution 1 of Table 1.1, swisstopo contributes, as one of several European processing centers of the European Permanent Network EPN, weekly coordinates and troposphere parameters. Solution 2 and 3 of Table 1.1 are used for monitoring the Swiss reference frame in near real-time and generating products used in federal surveying (see contribution concerning LV95) and for scientific applications (GNSS meteorology, see section 4 and geodynamics, see section 3).

Network solution	Stations (2007 -> 2010)	Processing interval	Delay
1: EUREF (EPN) sub-network	31 -> 50	daily observations	14-21 days
2: AGNES + sub-net EUREF	89 -> 118 (41 AGNES)	daily observations	14-21 days
3: AGNES + sub-net EUREF	80 -> 115 (41 AGNES)	hourly observations	1:45 hour

Table 1.1: Network analyses of permanent GNSS data at swisstopo

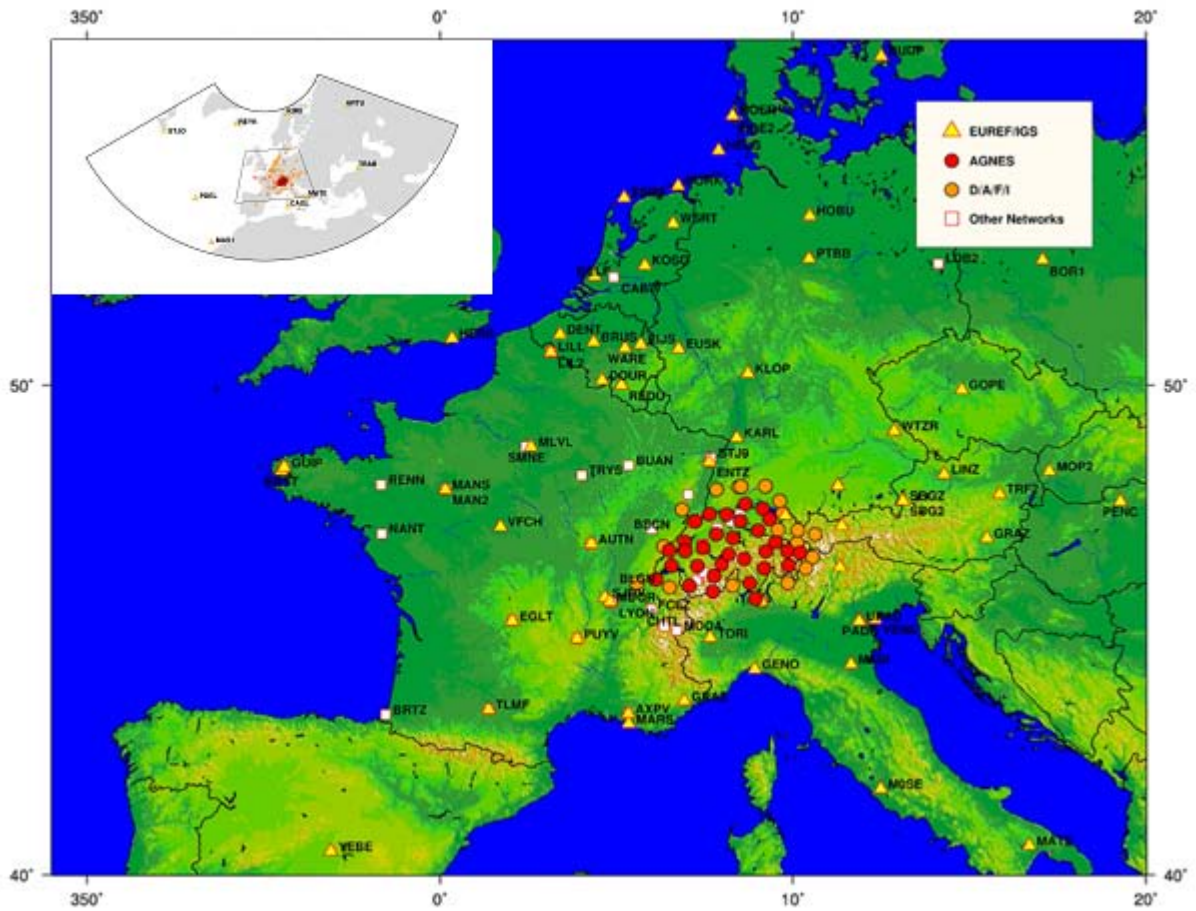


Figure 1.26: The processed networks in Europe and Switzerland.

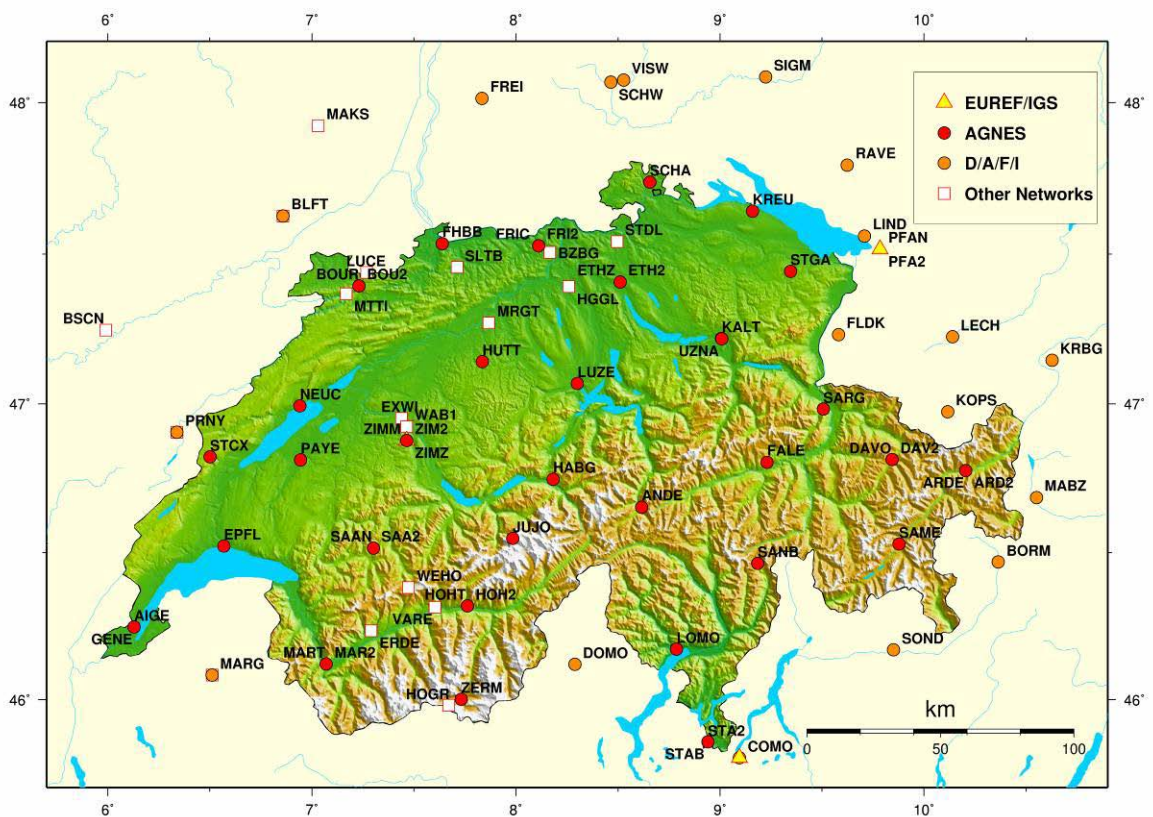


Figure 1.27: Overview of the permanent GNSS stations processed at swisstopo.

# Densification and validation of the LV95 reference frame with the campaign CHTRF2010

by E. Brockmann and A. Schlatter

Federal Office of Topography, swisstopo

Between 1988 and 1995, the Federal Office of Topography (swisstopo) installed the Swiss Reference Network LV95 as the first national network completely determined with GPS observations. Together with the permanent stations of AGNES, this network represents the backbone of the Swiss terrestrial reference frames LV95 and CHTRF95. As a quality check and for studying the stability of the reference frame, a fourth independent coordinate estimation was realized for all reference points in 2010 (see Figure 1.28). During each of the 15 observation weeks (April – October), 2 operators occupied about 16 points using totally 8 GPS receivers and measuring about 40 hours (double as much as in the previous validation campaigns) on each of the 221 points.

The comparison of the horizontal coordinates proved the stability of the reference frame on the cm level (see Figure 1.29). It was therefore not necessary to change any of the published horizontal LV95 coordinates which are rounded to the cm.

Conclusions concerning possible tectonic movements are given in section 3.

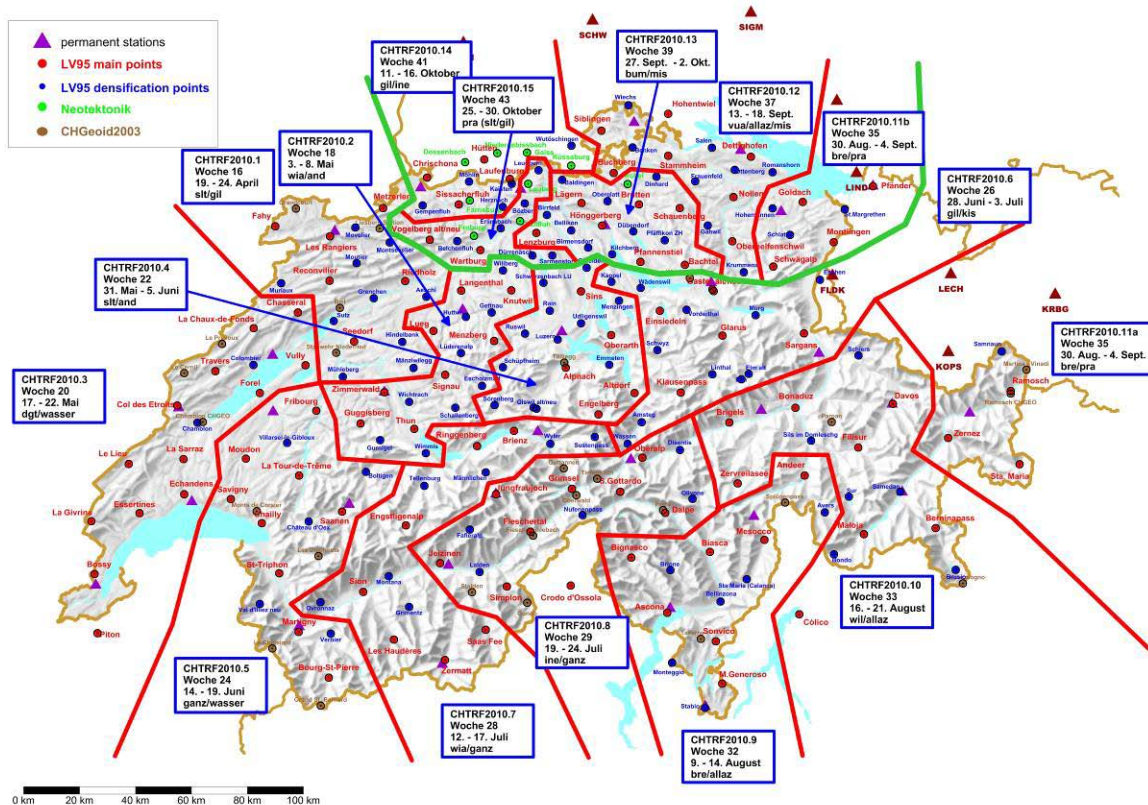


Figure 1.28: Diagram showing the planning of the re-observation of the LV95 reference points.

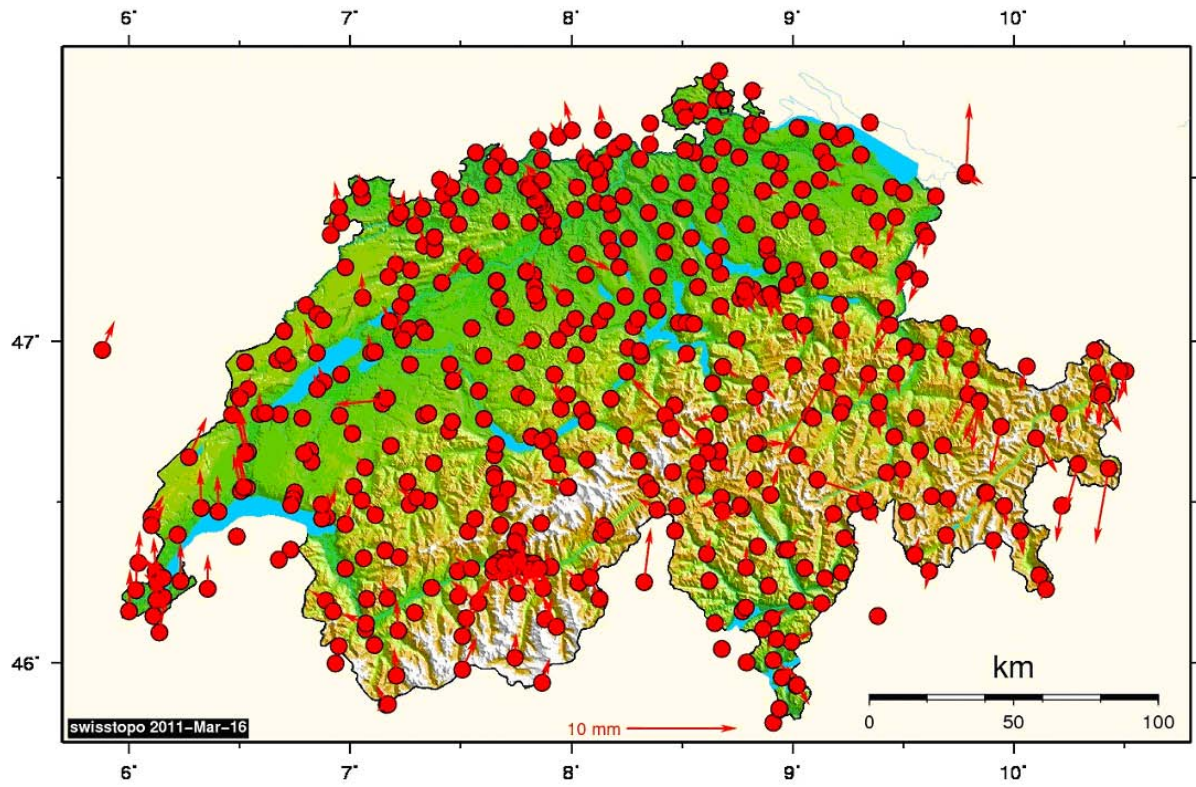


Figure 1.29: Horizontal differences between a coordinate set derived from 1988-2004 and coordinates derived from 1988-2010.



## Measurements for the National Height System

by A. Schlatter

Federal Office of Topography, swisstopo

Between 2007 and 2010 a total of 520 km (around 130 km per year) of leveling observations have been performed for the National Height Network (LHN) (see red lines in Figure 1.30). Usually, these observations were carried out on lines that were leveled for the last time 40 to 50 years ago. In late 2006 a new connection through the 35 km long Lötschberg Base Tunnel could be integrated into the LHN. Further, we integrated a 76 km line of precise leveling measured by the Landesvermessungsamt Baden-Württemberg between Waldshut/Koblentz through Eglisau/Schaffhausen to Thayngen/Bietingen. These measurements for the modernization of the German Main Height Reference System (Haupthöhenetz) follow the Swiss 1st order lines (see green lines in Figure 1.30). In addition to the works for the LHN, further special measurements for the cantons, the hydrological service and the monitoring of tunnels have been performed (see yellow lines in Figure 1.30).

Besides of these line measurements, which principally serve for the realization of the two national vertical reference frames (LN02 and LHN95), geoid determination and the investigation of recent crustal movements, regular local maintenance work is performed. The national height network contains today around 4'500 km of leveling lines with approximately 8'500 benchmarks.

The works for the establishment of the new orthometric height system LHN95, as well as the transformation to the old system (LN02, still official in cadastral surveying) and the European height systems have been documented in 2007. LHN95 served as the basis for the two new base tunnels crossing the Alps at the Gotthard (57 km) and the Lötschberg (35 km). The very good vertical cut-through-errors at both tunnels proved the high quality of LHN95 and the corresponding gravity field models (see as well contributions in Commission 4).

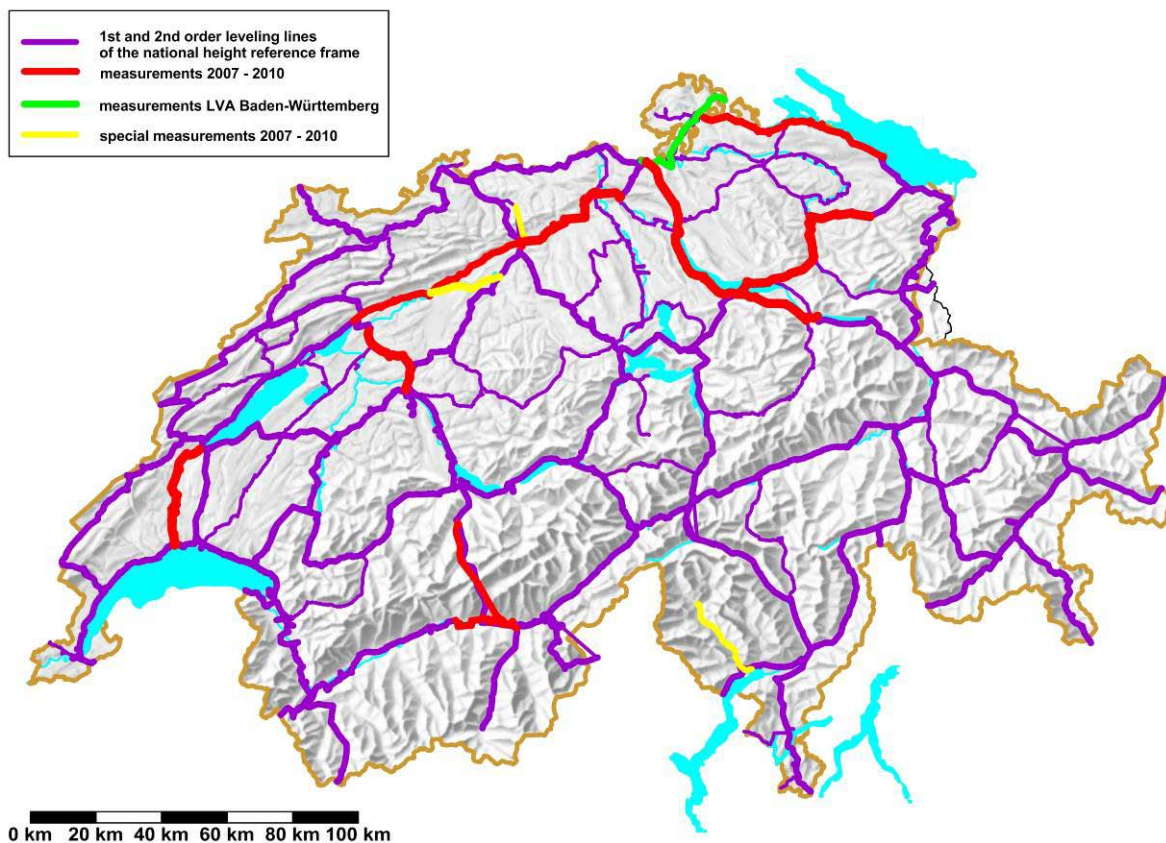


Figure 1.30: Measurements for the National Height System 2007 – 2010.

## GNSS Clock Modelling and Estimation

by K. Wang and M. Rothacher

Geodesy and Geodynamics Lab, Institute of Geodesy and Photogrammetry, ETH Zurich

The synchronization of the receiver clock with the satellite clock is always an important part of the positioning task. In order to exploit a high phase measurement precision the satellite and receiver clock corrections have to be determined for every epoch. However, the clocks do not jump arbitrarily. Modelling of clocks over a longer time interval should reduce the number of estimated parameters and improve the solutions.

For that reason, different sets of clock RINEX files are unified in the IGS Timescale. The performance of the high-performance clocks in the IGS network is analysed and compared with the theoretical characteristics for the corresponding type of clocks.

The IGS Timescale (IGST) is an internally realized frequency ensemble with improved stability which was developed by K. Senior as IGS clock reference, IGST. It is in short term more stable than GPST without losing a link to GPST in the long term.

Figure 1.31 shows that after re-referencing the CODE clock data against IGST the day jumps are much smaller. No detrending has been performed in this graphic.

The characteristics of some high performance clocks are compared with the theoretical ones that are simulated with a Matlab-tool.

1.33(a) shows the comparison of the Modified Allan Deviation (MDEV) for a selected set of station clocks and the theoretical clock behaviour. The theoretical clocks are simulated with different kinds of noises (Flicker frequency noise, Flicker phase noise, white frequency noise, random walk frequency noise, ... ) for one day with a sampling rate of 30 s. The MDEVs are extended to 86400 s by the simulation. Day jumps have not been removed from the raw data.

Figure 1.32 (b) illustrates the day-boundary clock jumps for some receiver clocks with H-masers during December 2008. A separate quadratic polynomial has been removed over the entire plotting interval from each series. The red lines are the residuals after removing the day jumps. At midnight between two adjacent days, the day-to-day offset (e.g. for the station USNO) may amount to 0.4 ns.

Some ESTRACK GNSS receivers are connected to an external clock and are also included in the IGS network. These clocks are specially analysed for a chosen day in December 2008. The list of the ESA clocks with their actual status is shown in Table 1.2.

ESA clock	Clock status
CEBR	H-Maser
KOUR	H-Maser
PERT	Caesium
MAS1	Caesium
KIRU	Caesium - to be decommissioned and exchanged for a slaved crystal associated to a GPS receiver
NNOR	H-Maser in a different building (high noise introduced in the signal in the transmission)
FAA1	Internal clock, Topcon receiver
REDU	Internal clock, Ashtech receiver
VILL	Internal clock, Ashtech receiver
MAL2	Internal clock, Topcon receiver

Table 1.2: ESA clocks in the IGS network.

The modified Allan deviations for these ESA clocks are shown in Figure 1.33 (a). The H-Maser clock of the station KOUR has an MDEV of  $2 \cdot 10^{-15}$  at about 8 hours, and the caesium clock PERT reaches only  $10^{-13}$  at the same averaging time. The internal clocks show generally a higher MDEV especially for short averaging time. It is interesting that the slope for the caesium clock MAS1 is quite flat for short averaging time intervals.

Similarly, the autocorrelation for the ESA clocks are calculated and plotted for 01.12.2008 (see Figure 1.33 (b)). A quadratic polynomial is removed for each time series. The autocorrelations for the internal clocks FAA1, VILL and MAL2 drop very quickly because of the strong noise. A high degree of autocorrelation between adjacent and near-adjacent observations exists in the H-Maser clock residuals of the station KOUR.

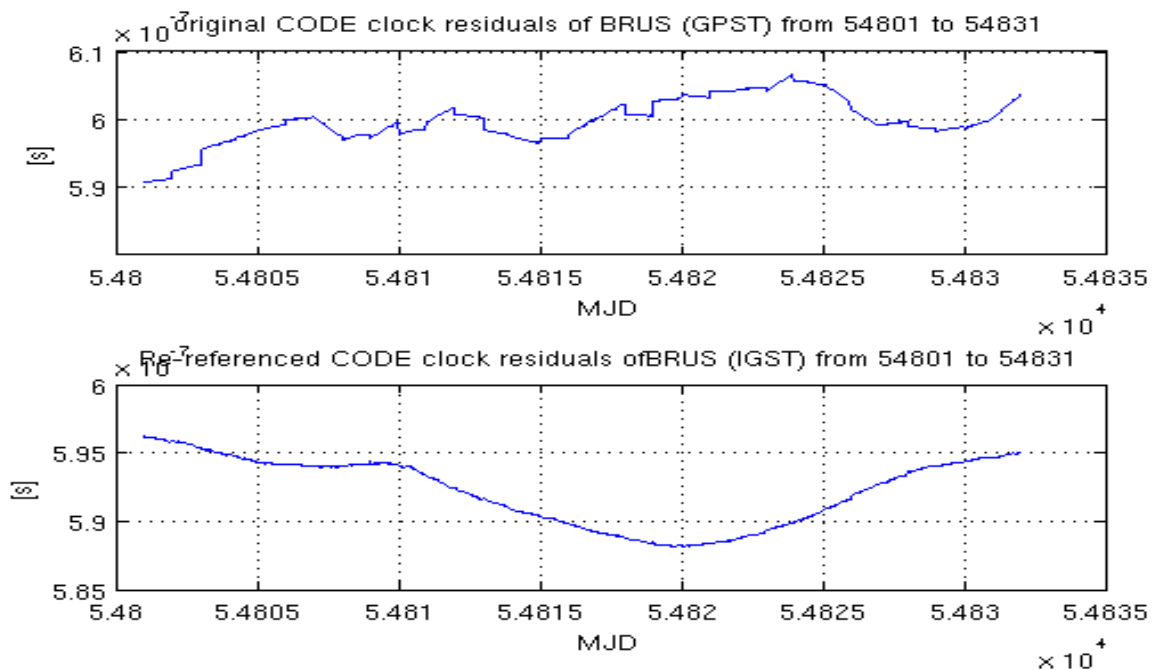


Figure 1.31: Original and re-referenced CODE clocks for BRUS station in December 2008.

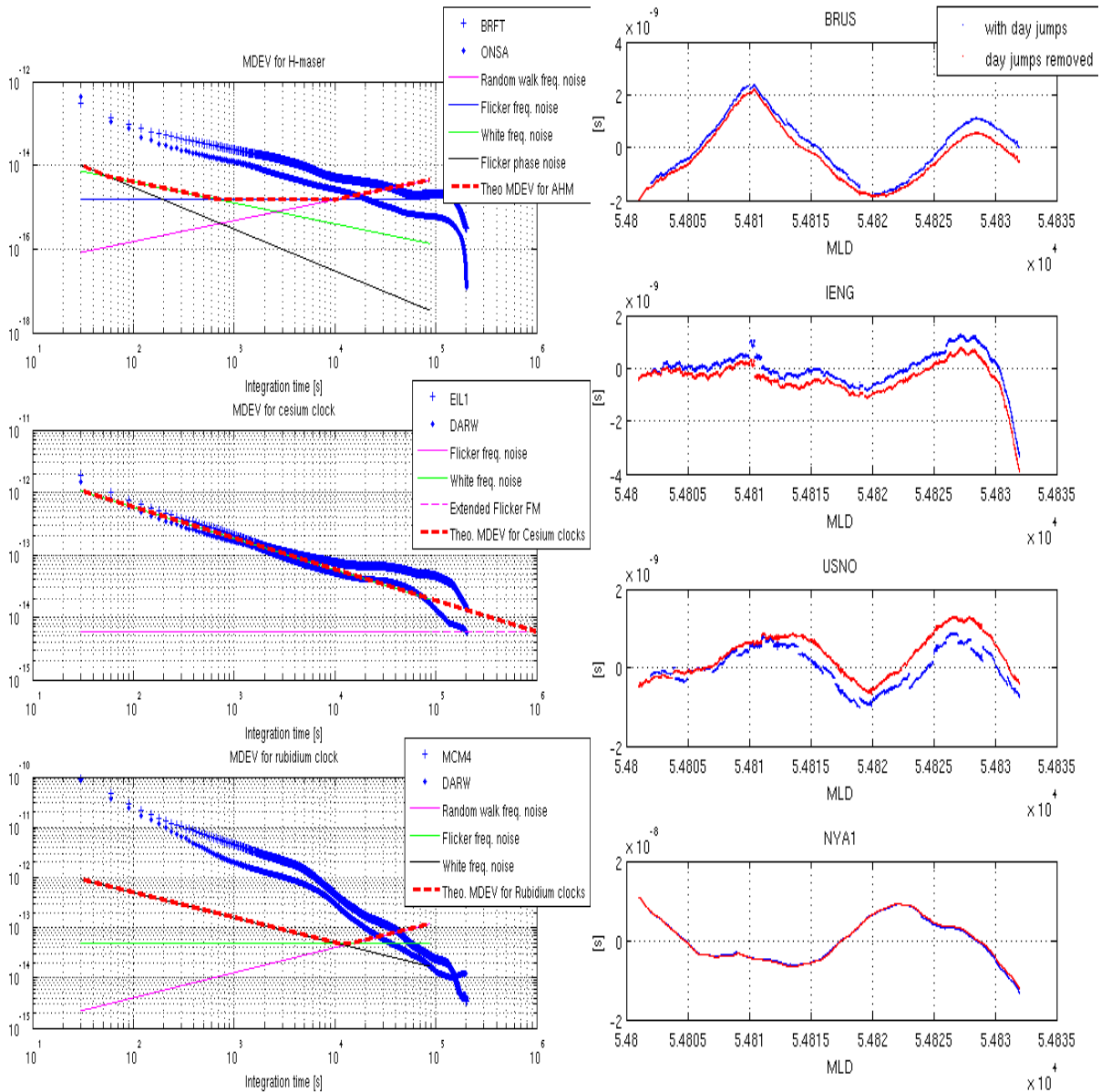


Figure 1.32: (a) Comparison of the MDEVs for the selected station clocks and the theoretical ones. (b) Time series of some H-masers with day jumps during December 2008.

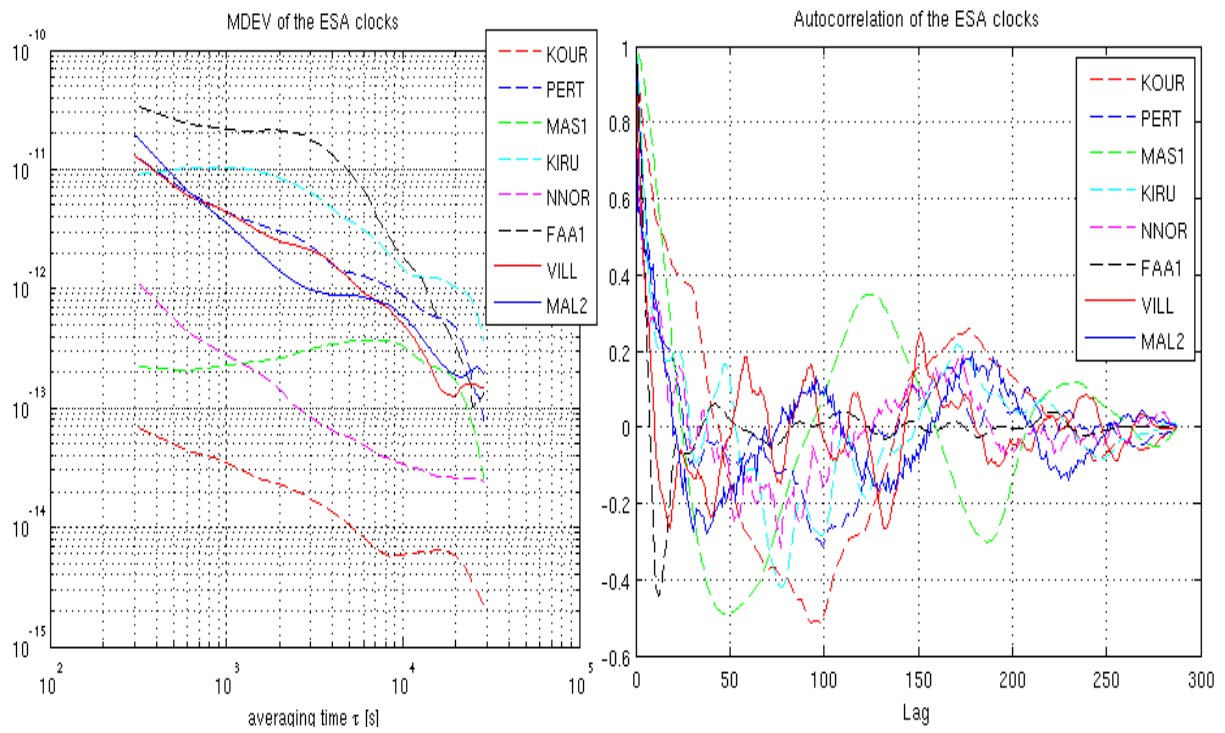


Figure 1.33: (a) MDEV for the ESA clocks on 01.12.2008. (b) Autocorrelations for the ESA clocks on 01.12.2008.

## Bibliography Commission 1

- Abrikosov, O., F. Flechtner, Ch. Förste, U. Meyer, M. Rothacher, R. Schmidt (2007): Contribution of modern satellite tracking data to GOCE-based gravity solutions, 3rd International GOCE User Workshop (Frascati, Italy 2006), ESA Special Publication SP-627, 105-108.
- Bender, M., G. Dick, J. Wickert, T. Schmidt, S. Song, G. Gendt, M. Ge, M. Rothacher (2008): Validation of GPS slant delays using water vapour radiometers and weather models. *Meteorologische Zeitschrift*, Vol. 6, No. 17, 807-812.
- Bender M., G. Dick, J. Wickert, M. Ramatschi, M. Ge, G. Gendt, M. Rothacher, A. Raabe, G. Tetzlaff (2009), Estimates of the information provided by GPS slant data observed in Germany regarding tomographic applications, *J. Geophys. Res.*, 114, D06303, doi:10.1029/2008JD011008.
- Beutler, G., M. Pearlman, H.-P. Plag, R. Neilan, M. Rothacher, R. Rummel (2009): Towards GGOS in 2020. Chapter in: *Global Geodetic Observing System, Meeting the Requirements of a Global Society on a Changing Planet in 2020*, H.-P. Plag and M. Pearlman (eds.), 273-281, DOI 10.1007/978-3-642-02687-4\_3.
- Beutler, G., A. Jäggi, L. Mervart, U. Meyer (2010a): The celestial mechanics approach: theoretical foundations. *Journal of Geodesy*, vol. 84(10), pp. 605-624, DOI 10.1007/s00190-010-0401-7.
- Beutler, G., A. Jäggi, L. Mervart, U. Meyer (2010b): The celestial mechanics approach: application to data of the GRACE mission. *Journal of Geodesy*, vol. 84(11), pp. 661- 681, DOI 10.1007/s00190-010-0402-6.
- Beyerle, G., M. Ramatschi, R. Galas, T. Schmidt, J. Wickert, M. Rothacher (2009): A data archive of GPS navigation messages. *GPS Solutions*, 13, 35–41, DOI 10.1007/s10291-008-0095-y.
- Beyerle, G., L. Grunwaldt, S. Heise, W. Köhler, R. König, G. Michalak, M. Rothacher, T. Schmidt, J. Wickert, B.D. Tapley, B. Giesinger (2010): First results from the GPS atmosphere sounding experiment TOR aboard the TerraSAR-X satellite, *Atmos. Chem. Phys. Discuss.*, 10, 28821-28857, doi:10.5194/acpd-10-28821-2010.
- Blewitt, G., Z. Altamimi, J. Davis, R. Gross, Ch.-J. Kuo, F.G. Lemoine, A.W. Moore, R.E. Neilan, H.-P. Plag, M. Rothacher, C.K. Shum, M.G. Sideris, T. Schöne, P. Tregoning, S. Zerbini (2010): Geodetic Observations and Global Reference Frame Contributions to Understanding Sea-Level Rise and Variability, in "Understanding Sea-Level Rise and Variability", Eds: J.A. Church, Ph.L. Woodworth, Th. Aarup, W.S. Wilson, Wiley-Blackwell, ISBN 978-1-4443-3452-4, pp.256-284 (p.428).
- Bock, H., A. Jäggi, D. Svehla, G. Beutler, U. Hugentobler, P. Visser (2007): Precise Orbit Determination for the GOCE Satellite Using GPS. *Advances in Space Research*, 39(10), 1638-1647, doi:10.1016/j.asr.2007.02.053.
- Bock, H., A. Jäggi, U. Meyer, R. Dach, G. Beutler (2011a): Impact of GPS antenna phase center variations on precise orbits of the GOCE satellite. *Advances in Space Research*, doi:10.1016/j.asr.2011.01.017.
- Bock, H., A. Jäggi, U. Meyer, P. Visser, J. Van den IJssel, T. Van Helleputte, M. Heinze, U. Hugentobler (2011b): GPS-derived orbits for the GOCE satellite. Submitted to *Journal of Geodesy*.
- Boehm, J., R. Heinkelmann, H. Schuh (2007). Short note: a global model of pressure and temperature for geodetic applications. *Journal of Geodesy* 81(10):679–683. doi:10.1007/s00190-007-0135-3.
- Brockmann, E., M. Kistler, U. Marti, A. Schlatter, B. Vogel, A. Wiget, U. Wild (2007): National Report of Switzerland: New Developments in Swiss National Geodetic Surveying. In: Torres, J.A. and H. Hornik (Eds): *Subcommission for the European Reference Frame (EUREF)*. London, June 6-8, 2007, EUREF Publication No 17, pp. 280–286.
- Brockmann, E., D. Ineichen, S. Schaer, U. Wild (2007): GNSS activities within the Automated GPS Network of Switzerland (AGNES). Poster Presentation at the Trimble 2007 GNSS Network Operator Seminar, Barcelona, May 29-30 2007.
- Brockmann, E., D. Ineichen, S. Schaer, U. Wild (2007): GNSS activities within the Automated GPS Network of Switzerland (AGNES). Poster Presentation at the XXIV General Assembly of the International Union of Geodesy and Geophysics in Perugia, Italy, July 2007.

- Brockmann, E., D. Ineichen, M. Kistler, U. Marti, A. Schlatter, B. Vogel, A. Wiget, U. Wild (2008): National Report of Switzerland: New Developments in Swiss National Geodetic Surveying. In: Ihde, J. and H. Hornik (Eds): Subcommission for the European Reference Frame (EUREF), Brussels, 2008, EUREF Publication No 18.
- Brockmann, E., D. Ineichen, M. Kistler, U. Marti, S. Schaer, A. Schlatter, B. Vogel, A. Wiget, U. Wild (2009): National Report of Switzerland: New Developments in Swiss National Geodetic Surveying. In: Ihde, J. and H. Hornik (Eds): Subcommission for the European Reference Frame (EUREF), Firenze, 2009.
- Brockmann, E. (2009): EUREF-TWG Project: Monitoring of official national ETRF coordinates on EPN web. In: Ihde, J. and H. Hornik (Eds): Subcommission for the European Reference Frame (EUREF), Firenze, 2009 (in prep., submitted to BGG).
- Brockmann, E., D. Ineichen, M. Kistler, U. Marti, S. Schaer, A. Schlatter, B. Vogel, A. Wiget, U. Wild (2010): Geodetic activities at swisstopo presented to the EUREF2010 Symposium. In: Ihde, J. and H. Hornik (Eds): Subcommission for the European Reference Frame (EUREF), Gaevele, June 2-4, 2010 (in prep.).
- Brockmann, E., D. Ineichen, S. Schaer, A. Schlatter (2010): Use of double stations in the Swiss Permanent GNSS Network AGNES. In: Ihde, J. and H. Hornik (Eds): Subcommission for the European Reference Frame (EUREF), Gaevele, June 2-4, 2010.
- Brockmann, E. (2010): EUREF-TWG Project: Monitoring of official national ETRF coordinates on EPN web. In: Ihde, J. and H. Hornik (Eds): Subcommission for the European Reference Frame (EUREF), Gaevele, June 2-4, 2010.
- Bruyninx, C., M. Becker, G. Stangl (2001). Regional Densification of the IGS in Europe Using the EUREF Permanent GPS Network (EPN), *Phys. Chem. Earth*, Vol. 26, No 6-8, pp.531-538.
- Dach, R., U. Hugentobler, P. Fridez, M. Meindl, eds. (2007). *Bernese GPS Software, Version 5.0*. Astronomical Institute, University of Bern.
- Dach, R., E. Brockmann, S. Schaer, G. Beutler, M. Meindl, L. Prange, H. Bock, A. Jäggi, L. Ostini (2009). GNSS processing at CODE: status report. *Journal of Geodesy* 83:353-365. DOI 10.1007/s00190-008-0281-2.
- Dach, R., S. Schaer, H. Bock, S. Lutz, G. Beutler (2010): CODE's New Combined GPS/GLONASS Clock Product. IGS Workshop 2010, Newcastle upon Tyne, England, 28 June - 2 July, 2010.
- Dach, R., S. Schaer, S. Lutz, M. Meindl, G. Beutler (2010B). Combining the Observations from Different GNSS. In *Proceedings of EUREF 2010 Symposium*, Gävle, Sweden, June 02-05, 2010.
- Dach, R., S. Schaer, M. Meindl, H. Bock, A. Jäggi, S. Lutz, E. Orliac, L. Ostini, L. Prange, K. Sosnica, A. Steinbach, D. Thaller, P. Walser, G. Beutler (2011). Activities at the CODE Analysis Center. IGS Workshop 2010, Newcastle upon Tyne, England, 28 June - 2 July, 2010.
- Dach, R., S. Lutz, J. Boehm, P. Steigenberger (2011A): Influence of Atmospheric Pressure Loading on GNSS Analysis. *Swiss National Report on the Geodetic Activities in the Years 2007-2011*.
- Dach, R., R. Schmid, M. Schmitz, D. Thaller, S. Schaer, S. Lutz, P. Steigenberger, G. Wübbena, G. Beutler (2011B): Improved antenna phase center models for GLONASS. *GPS Solutions*, vol. 15(1), pp. 49-65, DOI 10.1007/s10291-010-0169-5.
- Dilssner, F., R. Dach, R. Schmid, T. Springer, J. Dow (2010): Update of the IGS antenna phase center model: new GLONASS satellite antenna corrections from CODE and ESOC. IGS Workshop 2010, Newcastle upon Tyne, England, 28 June - 2 July, 2010.
- Dow, J., R. Neilan, C. Rizos (2009): The International GNSS Service in a changing landscape of Global Navigation Satellite Systems. *Journal of Geodesy*, vol. 83(3-4), pp. 191-198, DOI:10.1007/s00190-008-0300-3.
- Drinkwater, M.R., R. Floberghagen, R. Haagmans, D. Muzi, A. Popescu (2003): GOCE: ESA's first Earth Explorer core mission, *Space Science Reviews*, 108(1-2), 419-432, doi:10.1023/A:1026104216284.
- Flechtner, F., Th. Gruber, A. Güntner, M. Mandea, M. Rothacher, T. Schöne, J. Wickert (Eds.) (2010): *System Earth via Geodetic-Geophysical Space Techniques*, ISBN 978-3-642-10227-1, Springer-Verlag Berlin-Heidelberg, p.595.

- Förste, Ch., F. Flechtner, R. Schmidt, R. König, U. Meyer, R. Stubenvoll, M. Rothacher, F. Barthelmes, H. Neumayer, R. Biancale, S. Bruinsma, J.-M. Lemoine, S. Loyer (2007): Global mean gravity field models from combination of satellite mission and altimetry/gravimetry surface data, 3rd International GOCE User Workshop (Frascati, Italy 2006), ESA Special Publication SP-627, 163-167.
- Fritsche, M., R. Dietrich, A. Rülke, M. Rothacher, P. Steigenberger (2009): Low-degree earth deformation from reprocessed GPS observations. *GPS Solutions*, DOI 10.1007/s10291-009-0130-7.
- Ge, M., G. Gendt, M. Rothacher, C. Shi, J. Liu (2008): Resolution of GPS carrier-phase ambiguities in Precise Point Positioning (PPP) with daily observations. *Journal of Geodesy*, 82, 389–399, DOI 10.1007/s00190-007-0187-4.
- Geiger, A., A. Schlatter (2010): Von der Potentialtheorie zu den Senkungen am Gotthardpass. *Geomatik Schweiz* 12/2010: 628-629.
- Gendt, G., Z. Altamimi, R. Dach, W. Söhne, T. Springer, and the GGSP Prototype Team (2010). GGSP: Realisation and maintenance of the Galileo Terrestrial Reference Frame. *Advances in Space Research* DOI 10.1016/j.asr.2010.02.001, in press.
- GGSP homepage: <http://www.ggsp.eu/>
- Gurtner, W., E. Pop, J. Utzinger (2009): The New 100-Hz Laser System in Zimmerwald: Concept, Installation, and First Experiences. In Schillak, S. (Ed.) *Proceedings of the 16th International Workshop on Laser Ranging, SLR – the Next Generation*, pp. 350-357, Space Research Center, Polish Academy of Sciences.
- Heise, S., J. Wickert, G. Beyerle, T. Schmidt, H. Smit, J.P. Cammas, M. Rothacher (2008): Comparison of Water Vapour and Temperature Results From GPS Radio Occultation Aboard CHAMP With MOZAIC Aircraft Measurements. In: *IEEE Transactions on Geoscience and Remote Sensing*, 46, 11, 3406-3411, doi 10.1109/TGRS.2008.920268.
- Helm, A., O. Montenbruck, J. Ashjaee, S. Yudanov, G. Beyerle, R. Stosius, M. Rothacher (2007): GORS - A GNSS Occultation, Reflectometry and Scatterometry Space Receiver, 20th International Technical Meeting of the Satellite Division of The Institute of Navigation - ION GNSS (Fort Worth, Texas, USA 2007), 2011-2021.
- Helm, A., R. Stosius, G. Beyerle, O. Montenbruck, M. Rothacher (2007): Status of GNSS reflectometry related receiver developments and feasibility studies within the German Indonesian Tsunami Early Warning System, *IEEE International Geoscience and Remote Sensing Symposium - IGARSS 2007* (Barcelona, Spain 2007), 5084-5087, DOI 10.1109/IGARSS.2007.4424005.
- Helm, A., H.-U. Wetzell, W. Michajljow, G. Beyerle, Ch. Reigber, M. Rothacher (2007): Natural Hazard Monitoring with reflected GPS signals at Merzbacher Glacier Lake, In: Seyfert, E. (ed.), *Vorträge Dreiländertagung SGPBF, DGPF und OVG*, 19.-21. Juni 2007, Muttentz, Basel, Publikationen der Deutschen Gesellschaft für Photogrammetrie, Fernerkundung und Geoinformation e.V., Band 16, 505-516.
- Ineichen, D., E. Brockmann, S. Schaer (2007): Enhancing the Swiss Permanent GPS Network (AGNES) for GLONASS. In: Torres, J.A. and H. Hornik (Eds): *Subcommission for the European Reference Frame (EUREF)*. London, June 6-8, 2007, EUREF Publication EUREF Publication No 17, pp 139-144.
- Ineichen, D., E. Brockmann, S. Schaer (2008): Processing Combined GPS/GLONASS Data at swisstopo's Local Analysis Center. In: Ihde, J. and H. Hornik (Eds): *Subcommission for the European Reference Frame (EUREF)*, Brussels, 2008, EUREF Publication No 18.
- Jäggi, A., H. Bock, R. Floberghagen (2010): GOCE orbit predictions for SLR tracking. *GPS Solutions*, DOI:10.1007/s10291-010-0176-6.
- Jäggi, A., M. Ploner, J. Utzinger, M. Prohaska, E. Brockmann, E. Pop, W. Gurtner (2011): *Satellite Laser Ranging at Zimmerwald. Swiss National Report on the Geodetic Activities in the Years 2007-2011*.
- Kistler, M., E. Brockmann, U. Marti, C. Métraux, A. Papafitsorou, J. Ray, A. Schlatter, B. Vogel, A. Wiget, U. Wild (2007): Completion of the Swiss national triangular transformation network: Precise transformation between the old reference frame LV03, the new LV95 and global ones like ETRF. In *Proceedings of IUGG XXIV General Assembly (Inter-Association Symposia and Workshop IAG)* July 2-13, 2007 Perugia, Italy.



- Kistler, M., J. Ray (2007): Neue Koordinaten für die Schweiz: Fertigstellung der nationalen Dreiecksvermaschung, neue Transformations-Software REFRAME und Eröffnung des Internet-Portals "Bezugsrahmenwechsel". *Geomatik Schweiz* 9/2007, Seiten 432-437.
- Kistler, M., E. Brockmann, U. Marti, C. Métraux, A. Papafitsorou, J. Ray, A. Schlatter, B. Vogel, A. Wiget, U. Wild (2008): New coordinates for Switzerland: Completion of the Swiss national triangular transformation network for precise transformations between the old reference frame LV03, the new LV95 and global ones like ETRF. Poster presented at the 6th Swiss Geoscience Meeting, Lugano Nov. 22, 2008.
- König, R., M. Rothacher (2007): TanDEM-X Ground Segment Precise Baseline Development Plan 2007, TD-PBD-DP-0001.
- Krügel, M., D. Thaller, V. Tesmer, M. Rothacher, D. Angermann, R. Schmid (2007): Tropospheric parameters: combination studies based on homogeneous VLBI and GPS data, *Journal of Geodesy*, 81, 515–527, DOI 10.1007/s00190-006-0127-8.
- Lutz, S., P. Steigenberger, R. Dach, S. Schaer, M. Meindl, K. Sosnica (2011). *Reprocessing Activities at CODE. This Volume*, p. 5.
- Marti, U. (2007): LSKS 2007: Untersuchung zur Verwendbarkeit der Dreiecksvermaschung Stufe AV (CHENyx07) in Form eines regelmässigen Gitters. *swisstopo-report 07-04*, Bundesamt für Landestopografie, Wabern.
- Marti, U. (2008A): Transformation von Rasterdaten. Wechsel des Bezugsrahmens von LV95 und LV03 von Rasterdaten am Beispiel SWISSIMAGE. *swisstopo-report 08-18*, Bundesamt für Landestopografie, Wabern.
- Marti, U. (2008B): Bezugsrahmenwechsel LV03-LV95. Erzeugung einer NTV2-Datei als Näherungslösung für den Bezugsrahmenwechsel. *swisstopo-report 08-20*, Bundesamt für Landestopografie, Wabern.
- Marti, U., B. Bürki (2011): The Earth Tide Observatory in Zimmerwald, Swiss National Report on the Geodetic Activities in the Years 2007-2011.
- Nothnagel, A., M. Rothacher, D. Angermann, T. Artz, S. Böckmann, W. Bosch, H. Drewes, M. Gerstl, R. Kelm, M. Krügel, D. König, R. König, B. Meisel, H. Müller, B. Richter, N. Panafidina, S. Rudenko, W. Schwegmann, P. Steigenberger, V. Tesmer, D. Thaller (2008): GGOS-D: A German project on the integration of space geodetic techniques. In: Capitaine, N. (eds.) *Proceedings of the "Journées 2007 Systèmes de Référence Spatio-Temporels"*, pp 167-168, Observatoire de Paris, ISBN (Print) 978-2-901057-59-8.
- Nothnagel A., T. Artz, S. Böckmann, N. Panafidina, M. Rothacher, M. Seitz, P. Steigenberger, V. Tesmer, D. Thaller (2010): GGOS-D Consistent and Combined Time Series of Geodetic/Geophysical Parameters, in *System Earth via Geodetic-Geophysical Space Techniques*, Flechtner, F., Gruber Th., Güntner A., Manda M., Rothacher M., Schöne T., Wickert J. (Eds.), ISBN 978-3-642-10227-1, p. 565-576.
- Petrovic, S., R. Schmidt, J. Wunsch, F. Barthelmes, A. Güntner, M. Rothacher (2007): Towards a characterization of temporal gravity field variations in GRACE observations and global hydrology models, *Proceedings of the 1st International Symposium of the International Gravity Field Service 'Gravity field of the earth'*, Harita dergisi : Özel syj?, Special issue 18, (Istanbul 2006), 199-204.
- Plag, H.P., R. Gross, M. Rothacher (2009): Global Geodetic Observing System for geohazards and global change. *Géosciences*, 9, April/May 2009, 96-103.
- Plag, H.P., M. Rothacher, M. Pearlman (2009): The Global Geodetic Observing System – Part 1, the Organization. *Geomatics World*, Jan/Febr 2009, 26-28.
- Plag, H.P., M. Rothacher, M. Pearlman (2009): The Global Geodetic Observing System – Part 2, the System. *Geomatics World*, March/April 2009, 22-25.
- Plag, H.-P., M. Rothacher, M. Pearlman, R. Neilan, C. Ma (2009): The Global Geodetic Observing System. *Advances in Geoscience*, in press.
- Plag H.-P., C. Rizos, M. Rothacher, R. Neilan (2010): The Global Geodetic Observing System (GGOS): Detecting the Fingerprints of Global Change in Geodetic Quantities, in *Advances in Earth Observation of Global Change*, 125-143, DOI: 10.1007/978-90-481-9085-0\_10.

- Ray, J. (2006). New ocean tide loading routine ready. IGSMail-5300, IGS Central Bureau of Information System.
- Ray, J., U. Marti, M. Kistler (2009A): Methoden und Werkzeuge für die Koordinatentransformation zwischen globalen und lokalen Bezugsrahmen und den Datenaustausch mit den Nachbarländern. *Geomatik Schweiz*, 11/2009, Seiten 536-539.
- Ray, J., U. Marti, M. Kistler (2009B): Méthodes et outils pour la transformation de coordonnées entre cadres de référence globaux et locaux et échanges de données avec les pays voisins. *Géomatique Suisse* 11/2009, page 541ff.
- Roh, K.M., H. Luehr, M. Rothacher, S.Y. Park (2009): Investigating suitable orbits for the Swarm constellation mission - The frozen orbit. *Aerospace Science and Technology*, 13 (1), 49-58, doi:10.1016/j.ast.2008.03.001.
- Rothacher, M., D. Thaller, P. Steigenberger (2007): IERS Combination Research Center FESG. In: Wolfgang R. Dick, Bernd Richter (eds.) *IERS Annual Report 2005*, Verlag des Bundesamts für Kartographie und Geodäsie, ISBN (Print) 3-89888-838-X, ISSN 1029-0060.
- Rothacher, M., D. Thaller, P. Steigenberger, R. König (2008): IERS Combination Research Centre GFZ; in: Dick, R.; Richter, B. (eds.) *IERS Annual Report 2006*, pp 134-139, Verlag des Bundesamtes für Kartographie und Geodäsie, ISBN (Print) 3-89888-921-1, ISSN 1029-0060.
- Rothacher, M., D. Thaller, P. Steigenberger, R. König (2008): IERS Combination Research Centre GFZ. In: Dick, R.; Richter, B. (eds.) *IERS Annual Report 2007*, pp 145-150, Verlag des Bundesamts für Kartographie und Geodäsie, ISSN 1029-0060.
- Rothacher, M., G. Beutler, D. Behrend, A. Donnellan, J. Hinderer, C. Ma, C. Noll, J. Oberst, M. Pearlman, H.-P. Plag, B. Richter, T. Schöne, G. Tavernier, P. L. Woodworth (2009): The future Global Geodetic Observing System. Chapter in: *Global Geodetic Observing System, Meeting the Requirements of a Global Society on a Changing Planet in 2020*, H.-P. Plag and M. Pearlman (eds.), 237-272, DOI 10.1007/978-3-642-02687-4\_3.
- Rothacher, M., T. Schöne, J. Schröter, S. Esselborn, D. Sidorenko, V. Ivchenko, H. Reinhardt, F. Richter, S. Rudenko, N. Schön (2009): Sea Level Variations - Prospects from the Past to the Present. *Verbundprojekt im Sonderprogramm Geotechnologien 'Erfassung des Systems Erde aus dem Weltraum'*. *Geotechnologien Schlussbericht*, 34 p.
- Rothacher, M., H. Drewes, A. Nothnagel, B. Richter (2010): Integration of Space Geodetic Techniques as the Basis for a Global geodetic-Geophysical Observation System (GGOS-D): An Overview, in *System Earth via Geodetic-Geophysical Space Techniques*, Flechtner, F., Gruber Th., Güntner A., Manda M., Rothacher M., Schöne T., Wickert J. (Eds.), ISBN 978-3-642-10227-1, p.529-538.
- Rothacher, M., D. Angermann, T. Artz, W. Bosch, H. Drewes, S. Böckmann, M. Gerstl, R. Kelm, D. König, R. König, B. Meisel, H. Müller, A. Nothnagel, N. Panafidina, B. Richter, S. Rudenko, W. Schwegmann, M. Seitz, P. Steigenberger, V. Tesmer, D. Thaller (2011): GGOS-D: Homogeneous Reprocessing and Rigorous Combination of Space Geodetic Observations, *Journal of Geodesy*, doi: 10.1007/s00190-011-0475-x.
- Rülke, A., R. Dietrich, M. Fritsche, M. Rothacher, P. Steigenberger (2008): Realization of the Terrestrial Reference System by a reprocessed global GPS network, *J. Geophys. Res.*, 113, B08403, doi:10.1029/2007JB005231.
- Rummel, R., G. Beutler, V. Dehant, R. Gross, K.H. Ilk, H.-P. Plag, P. Poli, M. Rothacher, S. Stein, R. Thomas, P.L. Woodworth, S. Zerbini, V. Zlotnicki (2009): Understanding a dynamic planet: Earth science requirements for geodesy. Chapter in: *Global Geodetic Observing System, Meeting the Requirements of a Global Society on a Changing Planet in 2020*, H.-P. Plag and M. Pearlman (eds.), 89-133, DOI 10.1007/978-3-642-02687-4\_3.
- Schaer, S., E. Brockmann, D. Ineichen (2007): Inclusion of GLONASS for EPN Analysis at CODE/swisstopo. In: Torres, J.A. and H. Hornik (Eds): *Subcommission for the European Reference Frame (EUREF)*. London, June 6-8, 2007, EUREF Publication No 17, pp. 86-94.
- Schaer, S., E. Brockmann, M. Meindl, G. Beutler (2009): Rapid Static Positioning Using GPS and GLONASS. In: Ihde, J. and H. Hornik (Eds): *Subcommission for the European Reference Frame (EUREF)*, Firenze, 2009.

- Schaer, S., R. Dach (2010). Biases in GNSS Analysis. IGS Workshop 2010, Newcastle upon Tyne, England, 28 June - 2 July, 2010.
- Schaer, S., R. Dach, S. Lutz (2010). CODE analysis model changes (VMF/HOI), IGSMail-6287, IGS Central Bureau Information System.
- Schaer, S., H. Bock, R. Dach, S. Lutz, M. Meindl, E. Orliac, D. Thaller (2011): CODE Contributions to the IGS. This Volume, p. 1.
- Schiller, S., G. M. Tino, P. Gill, C. Salomon, U. Sterr, E. Peik, A. Nevsky, A. Görlitz, D. Svehla, G. Ferrari, N. Poli, L. Lusanna, H. Klein, H. Margolis, P. Lemonde, P. Laurent, G. Santarelli, A. Clairon, W. Ertmer, E. Rasel, J. Müller, L. Iorio, C. Lämmerzahl, H. Dittus, E. Gill, M. Rothacher, F. Flechner, U. Schreiber, V. Flambaum, Wei-Tou Ni, Liang Liu, Xuzong Chen, Jingbiao Chen, Kelin Gao, L. Cacciapuoti, R. Holzwarth, M. P. Heß and W. Schäfer (2009): Einstein Gravity Explorer—a medium-class fundamental physics mission. *Experimental Astronomy*, 23, 2, 573-610, DOI 10.1007/s10686-008-9126-5.
- Schlatter, A., U. Marti (2007): Aufbau der neuen Landesvermessung der Schweiz 'LV95'. Teil 12: Landeshöhennetz 'LHN95': Konzept, Referenzsystem, kinematischen Gesamtausgleichung und Bezug zum Landesnivellement 'LN02'. swisstopo-Doku Nr. 20, Bundesamt für Landestopografie, Wabern.
- Schlatter, A. (2007): Das neue Landeshöhennetz der Schweiz LHN95. Geodätisch-geophysikalische Arbeiten in der Schweiz, Volume 72, Schweizerische Geodätische Kommission.
- Schmid, R., P. Steigenberger, G. Gendt, M. Ge, M. Rothacher (2007): Generation of a consistent absolute phase center correction model for GPS receiver and satellite antennas. *Journal of Geodesy* 81(12):781-798, doi: 10.1007/s00190-007-0148-y.
- Schmidt, R., F. Flechtner, A. Güntner, R. König, U. Meyer, K.-H. Neumayer, Ch. Reigber, M. Rothacher, S. Petrovic, S.Y. Zhu (2007): GRACE Time-Variable Gravity Accuracy Assessment, Dynamic planet : Monitoring and understanding a dynamic planet with geodetic and oceanographic tools; IAG Symposium, Cairns, Australia, 22-26 August, 2005, Springer, 237-243.
- Schneider, D., H. Degen, H.A. Ebener, Th. Klöti, G. Koller, M. Rickenbacher, R. Wullschleger (2007): Ferdinand Rudolf Hassler (1770-1843): Schweizer Pionier für die Vermessung, Kartierung und Masse der USA. F.R. Hassler-Ausstellung 2007. swisstopo-report 06-12, Bundesamt für Landestopografie, Wabern.
- Sobolev, S. V., A.Y. Babeyko, R. Wang, A. Hoechner, R. Galas, M. Rothacher, D.V. Sein, J. Schröter, J. Lauterjung, C. Subarya (2007): Tsunami early warning using GPS-Shield arrays, *Journal of Geophysical Research*, 112, DOI 10.1029/2006JB004640.
- Springer, T., R. Dach (2010): GPS, GLONASS and More. *GPS World*, vol. 21(6), pp. 48-58.
- Steigenberger, P., V. Tesmer, M. Krügel, D. Thaller, R. Schmid, S. Vey, M. Rothacher (2007): Comparisons of homogeneously reprocessed GPS and VLBI long time-series of troposphere zenith delays and gradients, *Journal of Geodesy*, 81, 503–514, DOI 10.1007/s00190-006-0124-y.
- Steigenberger, P., M. Rothacher, V. Tesmer (2007): Comparisons of homogeneously reprocessed GPS and VLBI long time series, in: Proceedings of the IERS Workshop on Combination 2005, IERS Technical Note, Verlag des Bundesamtes für Kartographie und Geodäsie, in press.
- Steigenberger, P., M. Rothacher, R. Schmid, A. Rülke, M. Fritsche, R. Dietrich, V. Tesmer (2009): Effects of different antenna phase center models on GPS-derived reference frames, in: H. Drewes (ed.), *Geodetic Reference Frames*, International Association of Geodesy Symposia 134, 83-88, DOI 10.1007/978-3-642-00860-3\_13.
- Steigenberger, P., M. Rothacher, M. Fritsche, A. Rülke, R. Dietrich (2009): Quality of reprocessed GPS satellite orbits. *J Geod*, 83:241–248, DOI 10.1007/s00190-008-0228-7.
- Tesmer, V., J. Boehm, B. Meisel, M. Rothacher, P. Steigenberger (2008): Atmospheric loading coefficients determined from homogeneously reprocessed GPS and VLBI height time series; in: Finkelstein, A.; Behrend, D. (eds.) *Measuring the Future*, Proceedings of the Fifth IVS General Meeting, pp 307-313, ISBN (Print) 978-5-02-025332-2.
- Tesmer, V., P. Steigenberger, M. Rothacher, J. Boehm, B. Meisel (2009): Annual deformation signals from homogeneously reprocessed VLBI and GPS height time series. *Journal of Geodesy*, DOI 10.1007/s00190-009-0316-3.

- Thaller, D., M. Krügel, M. Rothacher, V. Tesmer, R. Schmid, D. Angermann (2007): Combined Earth orientation parameters based on homogeneous and continuous VLBI and GPS data, *Journal of Geodesy*, 81, 529–541, DOI 10.1007/s00190-006-0115-z.
- Thaller, D., M. Mareyen, R. Dach, G. Beutler, W. Gurtner, B. Richter, J. Ihde (2008): Preparing the Bernese GPS Software for the analysis of SLR observations to geodetic satellites. Proceedings of the 16th International Workshop on Laser Ranging, October 13-17, 2008, Poznan, Poland.
- Thaller, D., M. Rothacher and M. Krügel (2009): Combining One Year of Homogeneously Processed GPS, VLBI and SLR Data. In: H. Drewes (ed.), *Geodetic Reference Frames*, International Association of Geodesy Symposia 134, 17-22, DOI 10.1007/978-3-642-00860-3\_13.
- Thaller, D., K. Sosnica, G. Beutler, R. Dach, A. Jäggi (2011): Combining SLR and GNSS measurements. This Volume, p. 12.
- Thaller, D., R. Dach, M. Seitz, G. Beutler, M. Mareyen, B. Richter (2011): Combination of GNSS and SLR observations using satellite co-locations. Accepted for publication in *Journal of Geodesy*, doi: 10.1007/s00190-010-0433-z.
- Trubitsyn, V., M. K. Kaban, M. Rothacher (2008): Mechanical and thermal effects of floating continents on the global mantle convection, *Phys. Earth Planet. Interiors*, doi:10.1016/j.pepi.2008.03.011, in press.
- Vey S., R. Dietrich, M. Fritsche, A. Rülke, P. Steigenberger, M. Rothacher (2009), On the homogeneity and interpretation of precipitable water time series derived from global GPS observations, *J. Geophys. Res.*, 114, D10101, doi: 10.1029/2008JD010415.
- Vey, S., Dietrich, R., Rülke, A., Fritsche, M., Steigenberger, P., and Rothacher, M. (2009): Validation of Precipitable Water Vapor within the NCEP-DOE Reanalysis using Global GPS Observations from One Decade, *Journal of Climate*, 2009 early online release, doi: 10.1175/2009JCLI2787.1
- Vey, S; Dietrich, R; Rulke, A; Fritsche, M; Steigenberger, P; Rothacher, M (2010): Validation of Precipitable Water Vapor within the NCEP/DOE Reanalysis Using Global GPS Observations from One Decade, *Journal of Climate* 23 (7):1675-1695, ISSN 0894-8755, doi 10.1175/2009JCLI2787.1.
- Visser, P., J. Van den IJssel, T. Van Helleputte, H. Bock, A. Jäggi, G. Beutler, D. Svehla, U. Hugentobler, M. Heinze (2009): Orbit determination for the GOCE satellite. *Advances in Space Research*, 43(5), 760-768, doi:10.1016/j.asr.2008.09.016.
- Vogel, B., M. Burkard, M. Kistler, U. Marti, J. Ray, M. Scherrer, A. Schlatter, A. Wiget (2009): Aufbau der neuen Landesvermessung der Schweiz 'LV95'. Teil 13. Einführung des Bezugsrahmens 'LV95' in die Nationale Geodateninfrastruktur. swisstopo-Doku Nr. 21, Bundesamt für Landestopografie, Wabern.
- Wickert, J., G. Beyerle, C. Falck, F. Flechtner, R. Galas, L. Grunwaldt, S.B. Healy, S. Heise, W. Köhler, R. König, F.-H. Massmann, G. Michalak, D. Offiler, D. Pingel, P. Poli, E. Ozawa, M. Rothacher, T. Schmidt, B. Tapley, W. Wergen (2007): Global atmospheric data from CHAMP and GRACE in near-real time, in: *Observations of the System Earth from Space*, Geotechnologien status seminar, 22-23 November 2007, Bavarian Academy of Sciences and Humanities, Munich; Geotechnologien Science Report, 36-40.
- Wickert, J., G. Michalak, T. Schmidt, G. Beyerle, C.Z. Cheng, S.B. Healy, S. Heise, C.Y. Huang, N. Jakowski, W. Köhler, C. Mayer, D. Offiler, E. Ozawa, A.G. Pavelyev, M. Rothacher, B. Tapley, C. Arras (2009): GPS radio occultation: results from CHAMP, GRACE and FORMOSAT-3/COSMIC. In: *Terrestrial Atmospheric and Oceanic Sciences*, 20, 1, 35-50, doi 10.3319/TAO.2007.12.26.01(F3C).
- Wickert, J., G. Beyerle, C. Falck, S.B. Healy, St. Heise, W. Köhler, G. Michalak, D. Offiler, D. Pingel, M-Ramatschi, M. Rothacher, T. Schmidt (2010): Global Atmosphere Data from CHAMP and GRACE-A: Overview and Results, in *System Earth via Geodetic-Geophysical Space Techniques*, Flechtner, F., Gruber Th., Güntner A., Manda M., Rothacher M., Schöne T., Wickert J. (Eds.), ISBN 978-3-642-10227-1, pp. 433-442.
- Wiget, A. (2008): Das Bezugssystem ETRS89 und nationale Koordinatensysteme der Schweiz. Kurzbericht mit besonderer Berücksichtigung der Lage- und Höhendifferenzen zwischen Deutschland und der Schweiz. swisstopo-report 08-17, Bundesamt für Landestopografie, Wabern.
- Wiget, A., A. Buogo, R. Buser, R. Sonney (2008): The national Spatial Data Infrastructure. Paper presented at the 6th Swiss Geoscience Meeting, Lugano Nov. 22, 2008.

- Wiget, A. (2009A): "Neue Koordinaten für die Schweiz", Einführung in den Bezugsrahmenwechsel LV03 → LV95. Dokumentation zur Informationsveranstaltung "Neue Koordinaten für die Schweiz", Zürich, 30.10.2009.
- Wiget, A. (2009B): "De nouvelles coordonnées pour la Suisse". Introduction dans le thème du changement de cadre de référence. Documents pour la Journée d'information "De nouvelles coordonnées pour la Suisse", Lausanne, 27.11.2009.
- Wiget, A., E. Brockmann, M. Kistler, U. Marti, A. Schlatter, B. Vogel, U. Wild (2010A): Nachführungskonzept für die geodätische Landesvermessung. swisstopo-report 09-14, Bundesamt für Landestopografie, Wabern.
- Wiget, A., D. Andrey, E. Brockmann, D. Ineichen, M. Kistler, U. Marti, A. Schlatter, B. Vogel, U. Wild (2010B): Qualitätsstandards der Landesvermessung. swisstopo-report 10-11, Bundesamt für Landestopografie, Wabern.
- Wiget A., U. Marti, A. Schlatter (2010): Beiträge der Landesvermessung zum AlpTransit Gotthard-Basistunnel. Geomatik Schweiz 12/2010: pp. 575-58.
- Willis P., H. Fagard, P. Ferrage, F. G. Lemoine, C. E. Noll, R. Noomen, M. Otten, J. C. Ries, M. Rothacher, L. Soudarin, G. Tavernier, J.-J. Valette (2010): The International DORIS Service (IDS): Toward maturity, Advances in Space Research, Volume 45, Issue 12, DORIS: Scientific Applications in Geodesy and Geodynamics, p. 1408-1420, ISSN 0273-1177, doi: 10.1016/j.asr.2009.11.018.



## 2 Gravity Field

### Phase center modeling and its impact on LEO Precise Orbit Determination

by A. Jäggi, H. Bock, U. Meyer, L. Prange, G. Beutler and R. Dach

*Astronomical Institute University of Berne*

Precise orbits of low Earth orbiters (LEOs) are a requirement for many scientific satellite missions. Most of the satellites with demanding requirements concerning precise orbit determination (POD) are equipped with dual-frequency on-board receivers to collect the observations from Global Navigation Satellite Systems (GNSS), such as the Global Positioning System (GPS). The precision of LEO POD is nowadays mainly limited by the modeling of the carrier phase observations. The precise location of the GNSS antennas' phase center is in particular a prerequisite for high-precision orbit analyses.

On 5 November 2006, absolute instead of relative values for the phase center location of GNSS receiver and transmitter antennas were adopted in the processing standards of the International GNSS Service (IGS). Absolute phase center modeling is based on robot calibrations for a subset of terrestrial GNSS antennas, whereas compatible antenna models for all other terrestrial receiver antennas are derived by conversion from relative corrections, and by estimation for the GNSS transmitter antennas. Consistent antenna models for LEO missions are available from robot calibrations as well, but they are of limited value because of significant systematic errors in the carrier phase measurements, which are due to the actual spacecraft environment, e.g., near-field multipath or cross-talk with active GPS occultation antennas.

Using the data of the on-board GPS receivers of the twin-satellites of the Gravity Recovery and Climate Experiment (GRACE) mission, different methodologies of empirical phase center modeling were developed and their impact on LEO precise orbit modeling was assessed (Jäggi et al., 2009). Figure 2.1 shows the empirically derived phase center variations for the chokering antennas on-board the two GRACE satellites and reveals patchy structures with typical amplitudes of up to 1cm. The phase center variations are similar for both GRACE antennas, because of an identical near-field multipath environment. The bottom parts of Figure 2.1 (left, right) are different, because of receiver internal cross-talk caused by the active occultation antenna on GRACE-A.

The impact of empirically determined phase center variations on GPS-based POD is significant. The validation of GRACE orbits based on undifferenced GPS data with ultra-precise inter-satellite K-band range measurements confirms an improvement of up to a factor of 1.7 for reduced-dynamic and kinematic solutions, and even millimeter-precise ambiguity-fixed baseline solutions are further improved when empirical phase center variations are taken into account (see Figure 2.2, left). The latter aspect is of particular interest for the analysis of GPS data from the TanDEM-X interferometry mission (launched in June 2010), where baseline vectors between the two satellites have to be determined with millimeter-precision for the generation of highly accurate digital elevation models.

Empirical phase center modeling is, however, not only of interest for POD but also for subsequent applications relying on orbit positions, e.g., for the recovery of the Earth's gravity field (Jäggi et al., 2010). Since kinematic positions are particularly sensitive to a correct modeling of the antenna phase center location, model errors may easily propagate into the recovered gravity field coefficients. Figure 2.2 (right) shows that the quality of the low degree spherical harmonic coefficients derived from GRACE kinematic positions may be significantly improved when empirically determined phase center variations are taken into account for the kinematic orbit determination. Solutions based on GRACE-A kinematic positions benefit in particular because of the more pronounced antenna phase center variations (see Figure 2.1, left).

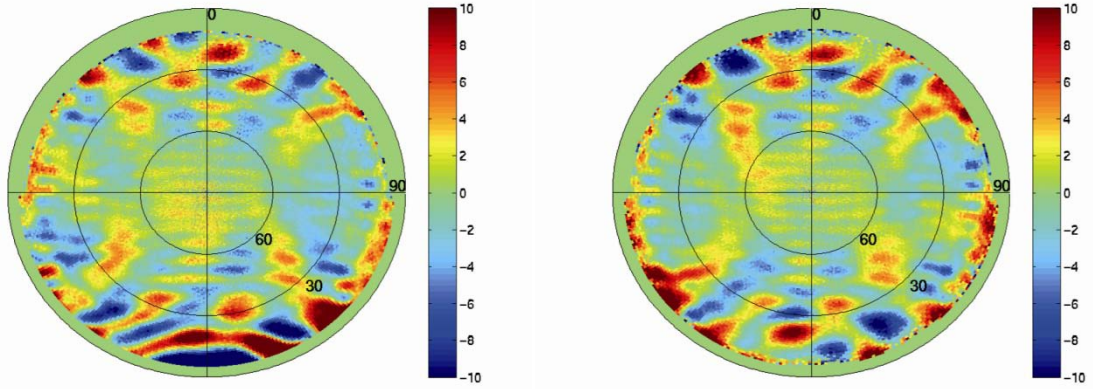


Figure 2.1: Phase center variations in millimeters for the trailing satellite GRACE-A (left) and the leading satellite GRACE-B (right) as a function of azimuth and elevation in the respective antenna-fixed coordinate systems. Azimuth 0 points into the direction of flight.

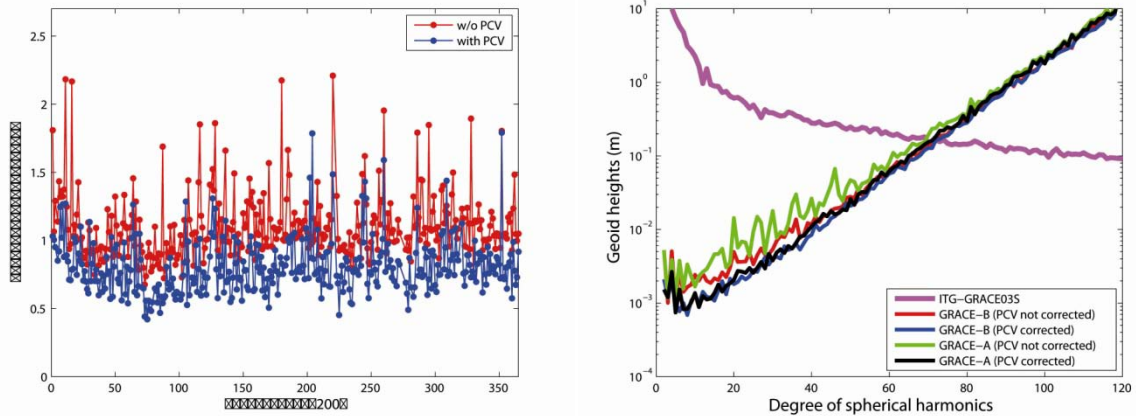


Figure 2.2: Daily K-band range standard deviations for distances between double-difference reduced-dynamic GRACE-A and GRACE-B orbits (left). Square-roots of degree difference variances of annual gravity field recoveries from kinematic GRACE positions with respect to the superior gravity field model ITG-GRACE03S based on K-band data (right).



## Global Gravity Field Determination based on the GRACE-Mission

by A. Jäggi, G. Beutler, U. Meyer, L. Prange and L. Mervart

*Astronomical Institute University of Bern*

Gravity field determination from measurements collected by Global Positioning System (GPS) receivers on-board of Low Earth Orbiters (LEOs) is a generalized orbit determination problem, involving all satellites of the constellation (Beutler et al., 2010a). This fact is exploited by the Celestial Mechanics Approach (CMA), which was developed at the Astronomical Institute of the University of Bern (AIUB). The CMA is highly flexible and has already been applied in single satellite mode to the satellite missions CHAMP (Prange et al., 2009, 2010), GRACE (Jäggi et al., 2009), and GOCE (Jäggi et al., 2010b). In the CMA, GPS-derived kinematic positions of the LEOs are used as pseudo-observations together with their covariance information (Jäggi et al., 2011a). In the case of GRACE, a microwave link (K-band) additionally delivers highly accurate inter-satellite range measurements dedicated to gravity field research. Satellite-only static gravity fields of unprecedented resolution and accuracy may be determined from the combination of GPS and K-band observations. Monthly snapshots reveal seasonal and secular variations in gravity due to, e.g., the hydrological cycle, polar and glacial ice mass change, or global isostatic adjustment.

The sensitivity of the inter-satellite range-rate observable to the gravitational pull of the Earth allows for the determination of a satellite-only static gravity field up to a spherical harmonics degree of about 160, which corresponds to a spatial resolution of about 250 km on the surface of the Earth. The GRACE orbits and partial derivatives w.r.t. all parameters are computed in daily batches. Subsequently, arc- and satellite-specific parameters are pre-eliminated and the reduced normal equations are accumulated to monthly, annual and multi-annual solutions. The first static field AIUB-GRACE01S was presented in Jäggi et al. (2010a). An intermediary solution AIUB-GRACE02S, which is already comparable in quality to the well-established satellite-only gravity fields GGM03S and EIGEN5S, was presented by Jäggi et al. (2011b). At the moment a publication on the new static field AIUB-GRACE03S (Figure 2.3), which includes more than 6 years of GRACE data, is in preparation. The CMA proved to be independent of the a priori gravity field used in the orbit modeling process. The solution of the highly nonlinear problem is found without further iteration. This independence of a priori information is a unique feature of the CMA and becomes very important, when normal equations from different satellite missions are combined (Beutler et al., 2010b).

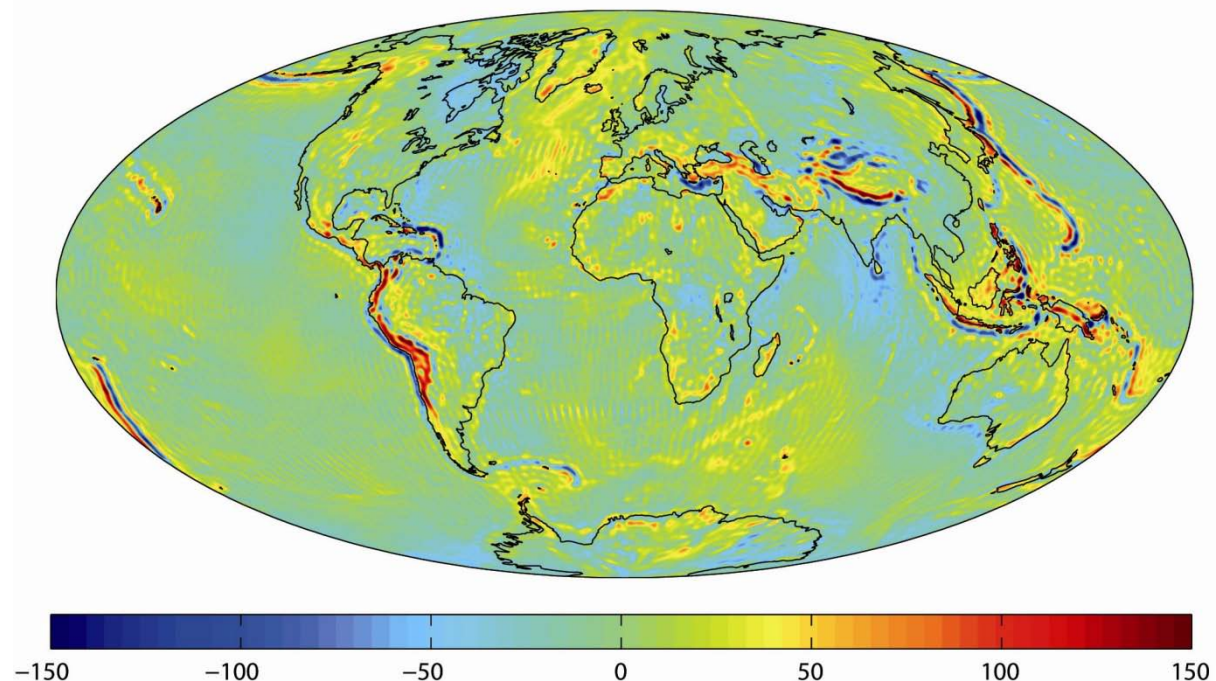
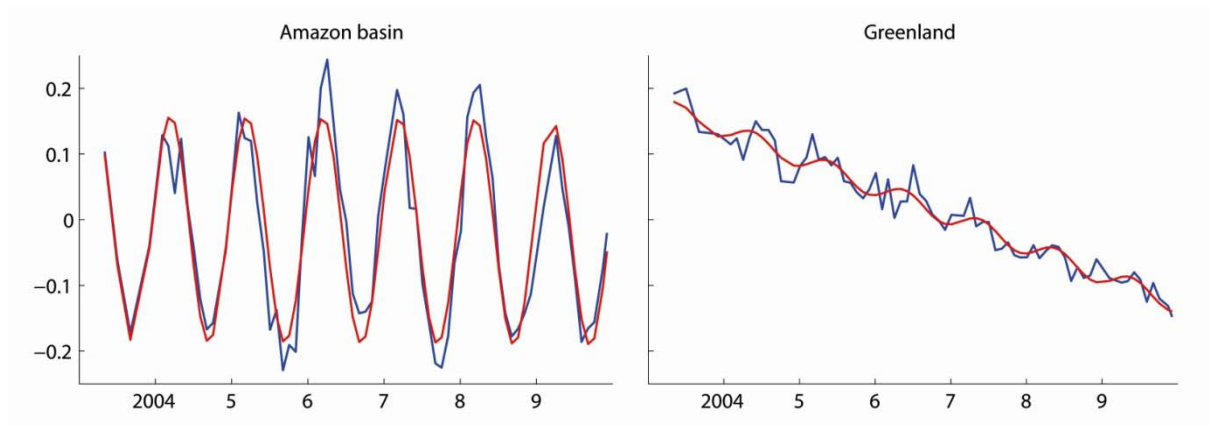


Figure 2.3: Gravity anomalies (in mgal) as derived from AIUB-GRACE03S.

Monthly snapshots are based on a maximum degree and order of 60 of the gravity field. From the time series of monthly solutions secular and periodic time variations are estimated for each spherical harmonic coefficient of the gravity field. Statistical tests reveal significant seasonal variations up to degree 60, but with increasing degree and order the time-variable signal is more and more contaminated by noise. To suppress this noise, sophisticated filtering techniques have to be applied. Figure 2.4 shows variations in gravity in two regions over seven years in terms of equivalent water heights and smoothed by a Gaussian average with a halfwidth radius of 500 km. In Figure 2.4 (left) seasonal variations in the Amazon basin due to the hydrological cycle are the dominating feature. In Figure 2.4 (right) the same kind of signal is shown for inner Greenland. The seasonal variations are superimposed by a clear trend caused by ice mass loss due to global warming process during the past decade.



*Figure 2.4: Temporal variations in the geoid over the Amazon basin (left) and Greenland (right) during seven years, represented by the corresponding thickness of a layer of water (in meter). A model including trend and seasonal variations (red) is fitted to the observed values (blue).*

## Global gravity field determination based on CHAMP-GPS-data

by L. Prange, A. Jäggi and G. Beutler

Astronomical Institute University of Bern

More and more low Earth orbiting satellites are equipped with geodetic GPS receivers for precise orbit determination. The observations of spaceborne GPS receivers have the potential to contribute significantly to the determination of the long wavelength part of the Earth's gravity field. GPS-derived kinematic positions of the CHAMP satellite were used as pseudo observations for global gravity field determination using the Celestial Mechanics Approach (CMA, Beutler et al., 2010a): Apart from the normalized spherical harmonic coefficients of the gravity field model, arc-specific orbit parameters are set up in a so-called generalized orbit determination problem.

The gravity field solution AIUB-CHAMP01S (Prange et al., 2009) is based on one year of CHAMP GPS data. The comparison with other CHAMP-only gravity field models and ground data validations showed that AIUB-CHAMP01S was among the best CHAMP-only models existing in 2007. The suitability of the CMA and of the gravity field determination infrastructure established at the AIUB was thus successfully demonstrated.

The gravity field model AIUB-CHAMP02S was generated from an extended time series of six years (2002-2007) of CHAMP GPS data. Motivated by GNSS model changes, a reprocessing of the GPS orbit and clock products necessary for the kinematic positioning was conducted for the processing time interval. A reprocessed solution based on the same CHAMP GPS data as used for AIUB-CHAMP01S was compared with the latter solution in order to study the impact of the GNSS model changes on gravity field recovery (Prange et al., 2010). It turned out that the change of the GPS antenna phase center variation (PCV) model from relative to absolute has a significant latitude-dependent effect on satellite orbits and derived gravity field models.

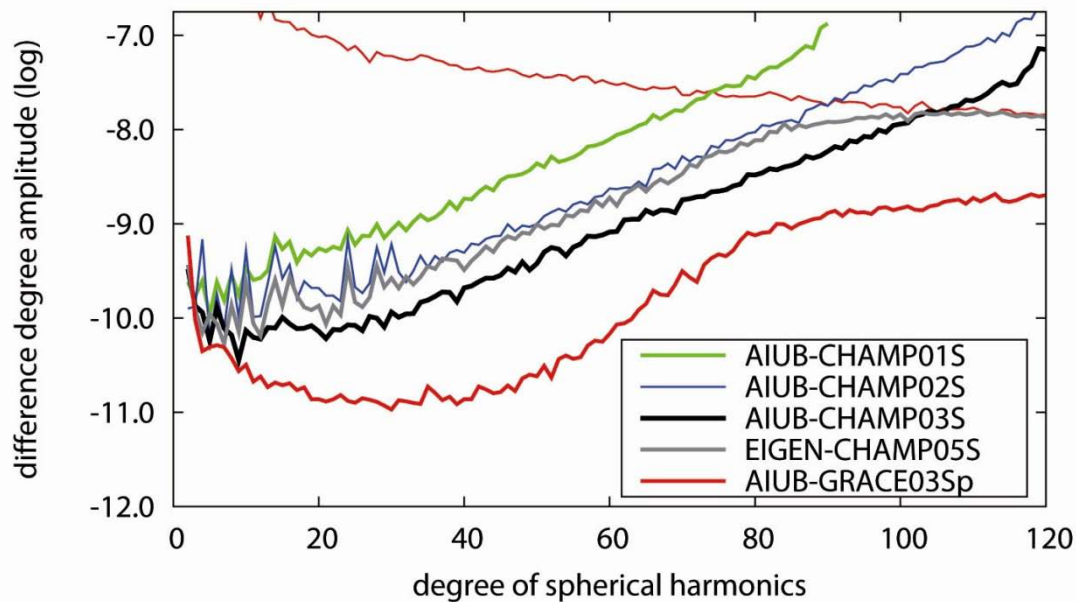


Figure 2.5: Comparison of AIUB-CHAMP01S (created in 2007), AIUB-CHAMP02S (2008), and AIUB-CHAMP03S (2010) with the best other CHAMP-only gravity field model EIGEN-CHAMP05S (2010) and with an AIUB-GRACE solution.

AIUB's latest CHAMP-only model AIUB-CHAMP03S (Prange, 2011) took advantage of several qualitative (empirical CHAMP PCV model (Jäggi et al., 2009a), elevation-dependent observation weighting, consideration of inter-epoch correlations (Jäggi et al., 2010)) and quantitative (extended time series (2002-2009), full data sampling (10 instead of 30 sec)) improvements. High-rate GPS satellite clock corrections were necessary for the analysis. They were taken from the CODE Analysis Center of the IGS for the period 2007-2009 and they were generated particularly for the task of gravity field determination for the period 2002-2006. Internal and external validations show that AIUB-CHAMP03S currently is the best CHAMP-only gravity field model, thus representing the state-of-the-art gravity field recovery using GNSS observations of LEO satellites. The development of the AIUB-CHAMP gravity field models is illustrated by Figure 2.5. The quality of AIUB-CHAMP03S allows it to detect the most prominent seasonal gravity field variations, e.g., in the Amazon river basin (see Figure 2.6), from the monthly contributions to AIUB-CHAMP03S – a result which was not expected from the analysis of CHAMP GPS data.

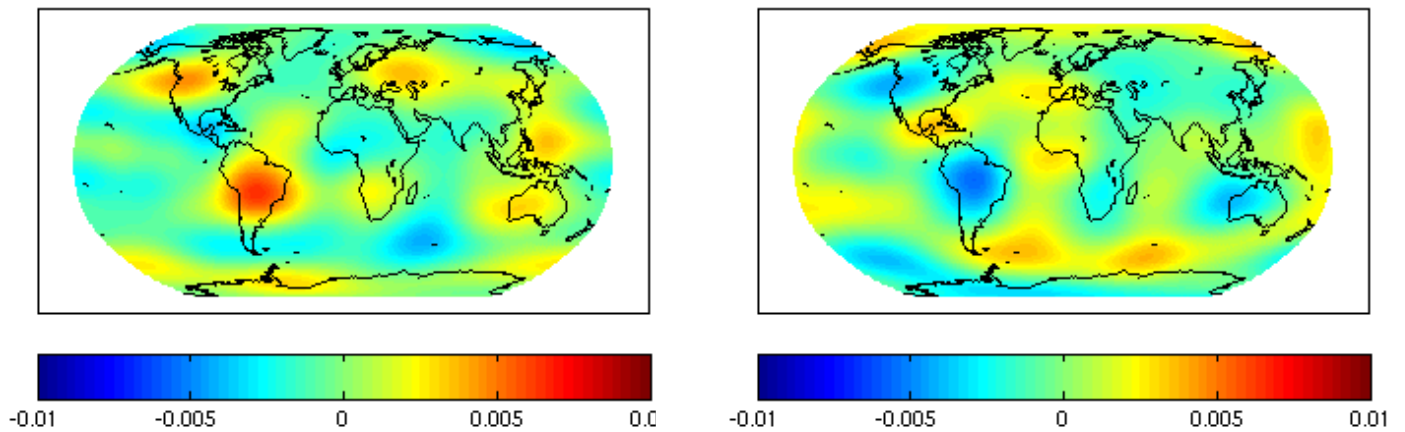


Figure 2.6: Mean seasonal geoid height variations (left: in May, right: in November) derived from the coefficients (up to degree 10) of the monthly contributions to AIUB-CHAMP03S (in m).

## Processing Facility for ESA's GOCE Gravity Field Explorer Mission

by H. Bock, A. Jäggi, U. Meyer, R. Dach and G. Beutler

Astronomical Institute University of Bern

The GOCE (Gravity field and steady-state Ocean Circulation Explorer) satellite is the first core mission of ESA's Earth Explorer programme (Drinkwater et al., 2003) and has been launched on March 17, 2009 from Plesetsk, Russia. Figure 2.7 shows the orbital altitude during the first months of the mission (commissioning phase). Since mid September 2009 the satellite is at an altitude of just 259 km, which is actively maintained by on-board ion thrusters.

The Astronomical Institute of the University of Bern (AIUB) is member of the European GOCE Gravity Consortium (EGG-C), which is responsible for the GOCE Level 1b data processing and Level 2 product generation. This work is integrated in the GOCE High-level Processing Facility (HPF).

AIUB performs precise orbit determination (POD) based on GPS measurements provided by an on-board 12-channel Lagrange receiver. The resulting Precise Science Orbit (PSO) consists of two different orbit types, a reduced-dynamic and a kinematic orbit. The orbit determination for both orbit types is performed in a single processing scheme (Bock et al., 2007 and Visser et al., 2009). The orbit determination process is based on undifferenced GPS measurements. The procedure for generating the PSO is running automatically since October 31, 2009 with a latency of 7-10 days. First GOCE orbit results were presented by Bock et al. (2011b).

The PSO products are validated by independent Satellite Laser Ranging (SLR) measurements. Figure 2.8 shows SLR residuals (mean: 0.97 cm, RMS: 2.29 cm) for the reduced-dynamic GOCE orbits for the time period from April 10 to December 31, 2009. The SLR tracking was rather poor at the beginning of the mission. The number of tracked satellite passes increased considerably with the availability of additional orbit predictions generated by the AIUB since July 21, 2009 (Jäggi et al., 2010).

The remarkable orbit quality can only be achieved when correcting for empirically derived phase center variations (PCVs) of the GOCE GPS antenna (Bock et al., 2011a). It is mainly the cross-track component of the orbit, which benefits from the correction of the PCVs. For the first time SLR data could be used to confirm the significant improvement in the cross-track component of a LEO orbit.

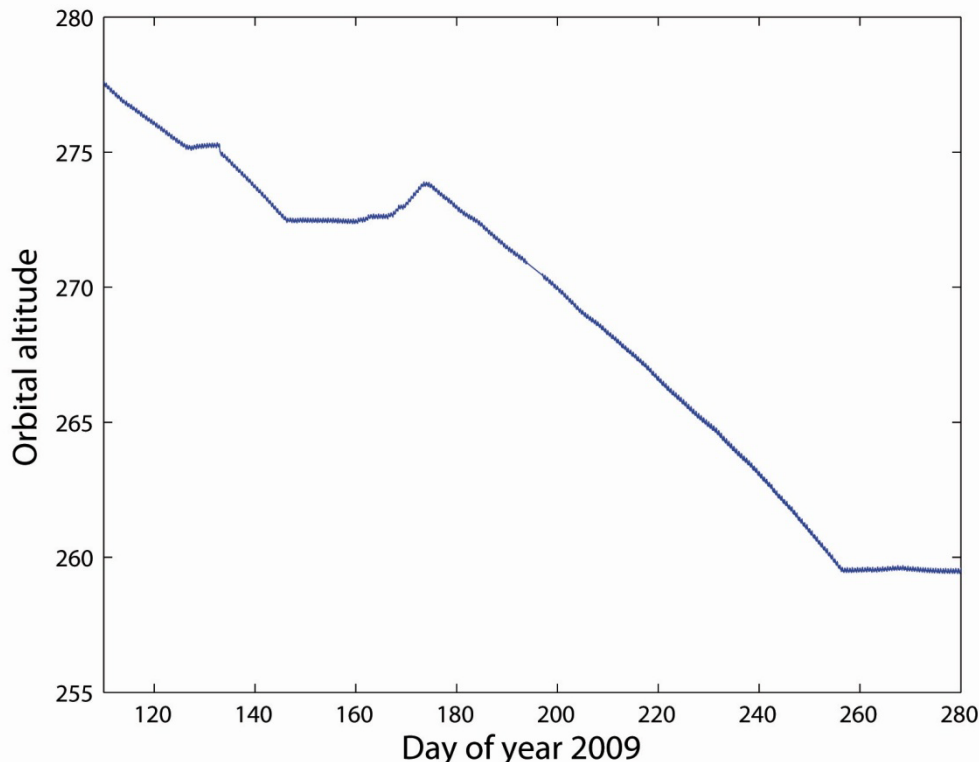


Figure 2.7: Orbital altitude of the GOCE satellite during commissioning phase (Jäggi et al., 2010).

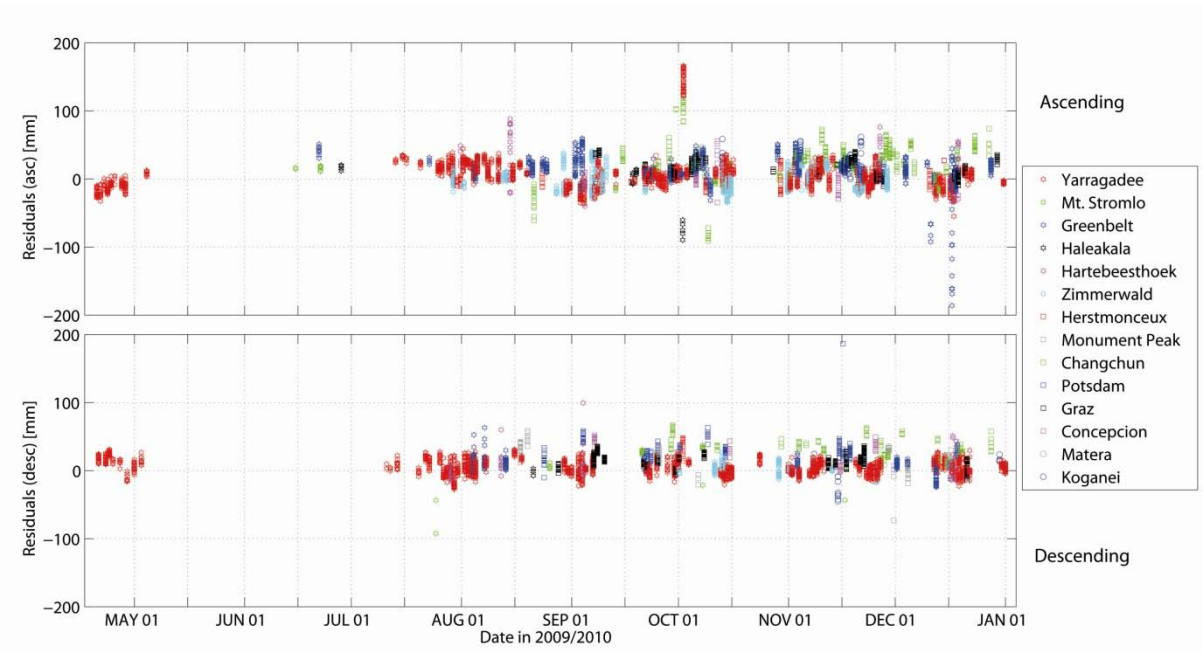


Figure 2.8: SLR validation for reduced-dynamic GOCE orbits from April 10-December 31, 2009.

# Absolute and Relative Gravity Measurements

by U. Marti<sup>1</sup>, H. Baumann<sup>2</sup>, B. Bürki<sup>3</sup> and S. Guillaume<sup>3,4</sup>

<sup>1</sup> Federal Office of Topography, swisstopo

<sup>2</sup> Federal Office of Metrology, METAS

<sup>3</sup> Geodesy and Geodynamics Lab, Institute of Geodesy and Photogrammetry, ETH Zurich

<sup>4</sup> Metrology group, CERN, Geneva

## a) Introduction

The national gravity network SG95 (Schweregrundnetz 1995) was established between 1992 and 1995 by the Geodesy and Geodynamics Lab (GGL) of the ETH Zurich on behalf of the Swiss Geodetic Commission (SGC) and the Swiss Geophysical Commission (SGPC). It was based on absolute measurements on five stations (Zurich, Pratteln, Chur, Lausanne, Monte Ceneri), which have been observed with the JILA-G 6 of the BEV (Vienna) in 1994. This zero-order network was densified by relative measurements on about 110 stations, which formed the first and second order network. Mostly, these relative stations are identical with the principal stations of the national GPS network (LV95). SG95 was connected to the gravity networks of neighbouring countries by a few relative measurements to their nearest absolute stations. The relative observations have been performed with three Lacoste&Romberg G instruments in parallel. The accuracy of the adjusted gravity values of SG95 was in the order of 0.02 mgal. The measurements of SG95 were the contribution of Switzerland to the Unified European Gravity Network (UEGN).

In 2003, the project LSN2004 (Landesschwerenetz 2004) was started to modernize the national gravity Network. In this project, some new absolute stations were established and the existing ones were re-measured with an FG5. These activities were jointly performed by swisstopo and METAS. Additional relative measurements were performed with a SCINTREX-CG5 in order to improve the accuracy and stability of the network. The stations of LSN2004 are mostly the same as the ones in SG95. Only some destroyed or unsuitable stations have been replaced.

## b) Absolute measurements for LSN2004

Since 1999, the Federal Office of Metrology (METAS) owns the only absolute gravimeter in Switzerland. This FG-5 free fall instrument was acquired for their Watt balance experiment (redefinition of the SI-unit 'kilogram') and is principally used in the laboratories of METAS, where about once per month absolute measurements are performed. This instrument participates regularly at the international comparison campaigns. The last of these comparisons were the ICAG 2009 in Sèvres (France) and a regional intercomparison campaign in Walferdange (Luxemburg) in 2008 (EURAMET 1093).

Since 2003, a yearly absolute measurement takes place at the ECGN station in Zimmerwald where a permanent Earth-tide gravimeter is installed as well and regular relative measurements take place. In addition to the measurements in Zimmerwald measurements for LSN2004 are performed on 1-2 additional stations per year. In the last years these were: Andermatt and Zerne in 2008, Lausanne and Zurich in 2009, Andermatt and Monte Ceneri in 2010. The results of these measurements were all published in the AGRAV database of BGI and BKG and are freely accessible. In the future it is foreseen to re-measure as well the remaining absolute stations that have not been occupied since 1994.

## c) Other absolute measurements

In addition to the observations for LSN2004, some other absolute measurements took place in the last years such as at a station in the rock laboratory Mont Terri (2009) and 3 stations at the CERN (2009) for the CLIC project.

A further activity is the re-activation of the calibration line for relative gravimeters in the Jungfrau region, where we have gravity differences of more than 600 mgal over a very short distance. The 2 first stations (Grindelwald and Alpiglen) were observed in 2010. This work will be continued in 2011.

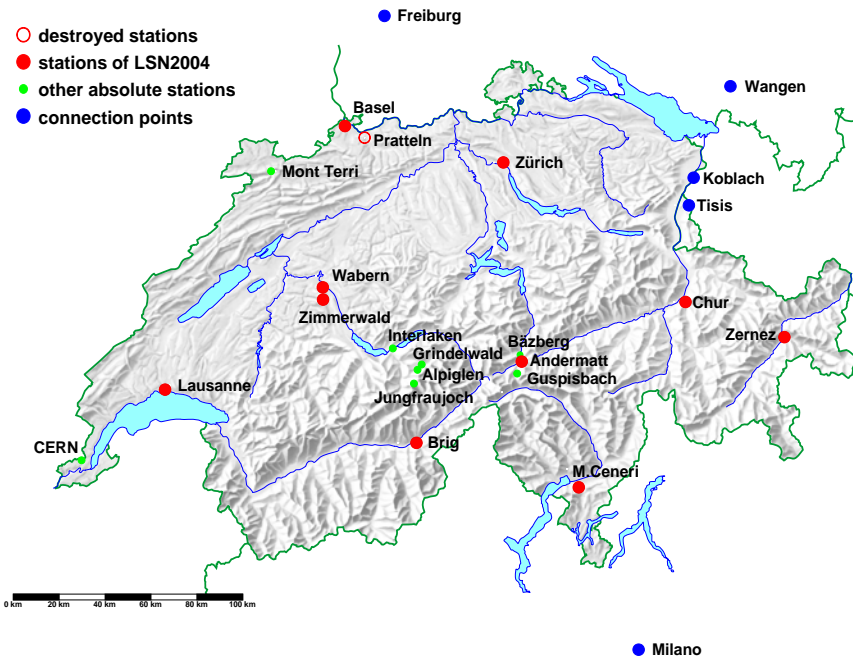


Figure 2.9: Absolute Gravity Stations in and around Switzerland

#### d) Relative measurements

The absolute gravity network (0 order network) is densified by relative measurements (1st and 2nd order network). Until 2007 these measurements have been performed in collaboration between swisstopo and the University of Lausanne in 3 major campaigns (2005, 2006 and 2007). In 2007, swisstopo bought a new Scintrex CG-5 together with ETH Zurich. Unfortunately, this instrument did not work as it should at the beginning. Only since late 2009 it was possible to use it for productive measurements for LSN2004.

It is not foreseen to re-observe all the 2nd order points of SG95. For these stations, without new observations for LSN2004, the original measurements of 1992-1995 are re-processed and treated in a common adjustment with the new measurements. Of course, the accuracy of these points will not be increased in comparison with the results of SG95 and remain in the order of 0.02 mgal.

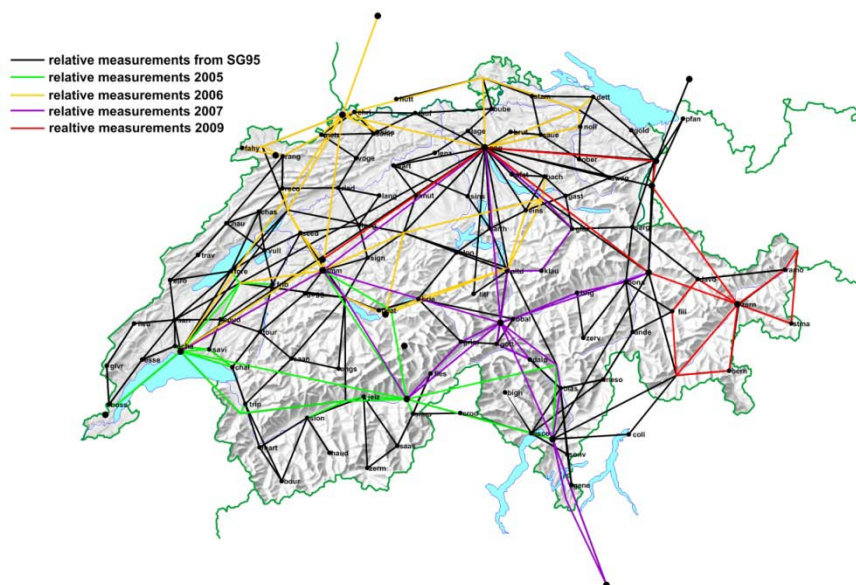


Figure 2.10: Relative Measurements for LSN2004



## Gravity measurements for the Vertical network

by U. Marti and A. Schlatter

Federal Office of Topography, swisstopo

The gravity measurements for the vertical network along the first and second order leveling lines are usually performed in the same year as the leveling measurements. They are used for the calculation of geopotential numbers and orthometric heights and are only performed on a representative selection of all leveling points. For stations without measured gravity, the values are interpolated from the neighboring data on leveling lines or from the gravity data set of the Swiss Geophysical Commission and mass models with an accuracy of better than 1 mgal, which usually is enough for the correction of the leveling data.

Until 2007, a Lacoste&Romberg type G gravimeter was used for these observations. In 2008, ETH Zurich and swisstopo acquired a new Scintrex CG-5 and further observations along the leveling should be performed with this instrument. But because we had big difficulties with this gravimeter until the end of 2009, no further observations could be performed for the vertical network since 2008. The measurements along the leveled lines of 2008 to 2010 (see report in commission 1) have to be caught up in 2011.

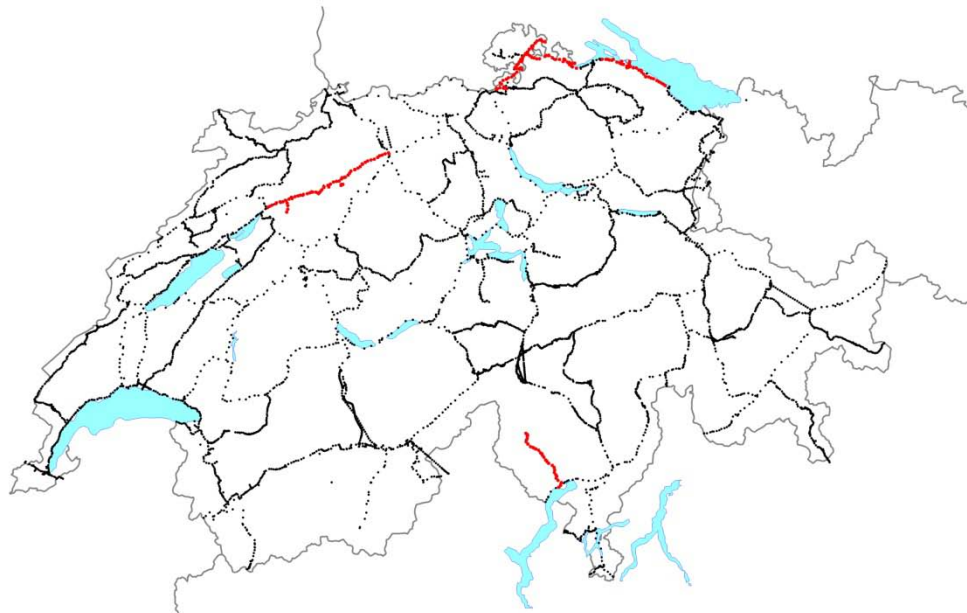


Figure 2.11: Available gravity measurements along the Swiss leveling lines. The red dots indicate the gravity measurements of 2007.

## The Earth Tide Observatory in Zimmerwald

by U. Marti<sup>1</sup> and B. Bürki<sup>2</sup>

<sup>1</sup> Federal Office of Topography, swisstopo

<sup>2</sup> Geodesy and Geodynamics Lab, Institute of Geodesy and Photogrammetry, ETH Zurich

Continuous recording of the Earth tides is necessary for providing accurate corrections for field gravity measurements. The use of the recorded data in conjunction with satellite laser ranging information allows the determination of the elasticity parameters of the Earth's crust (Love's numbers). The measurement system of the observatory of Zimmerwald is composed of a special high-sensitive gravimeter (LaCoste&Romberg ET25) driven by a PC and working at 1 min. sampling interval. This instrument works since 1995 with only a few interruptions.

In February 2007 some minor revisions of the instruments were performed. Especially the data flow was automated and some improvements after power failures were installed. Between February 2007 and November 2009 the ET25 worked very reliably and showed practically no data gaps. This is the longest continuous data series since the first setup of the instrument in 1995.

Unfortunately, in November 2009 the feedback system (MVR) broke down and had to be replaced. This took a long time and caused a lack of data for about 6 months until May 2010. Since then, the instrument works again without any problems.

### Registered Raw Data of the ET25 in Zimmerwald

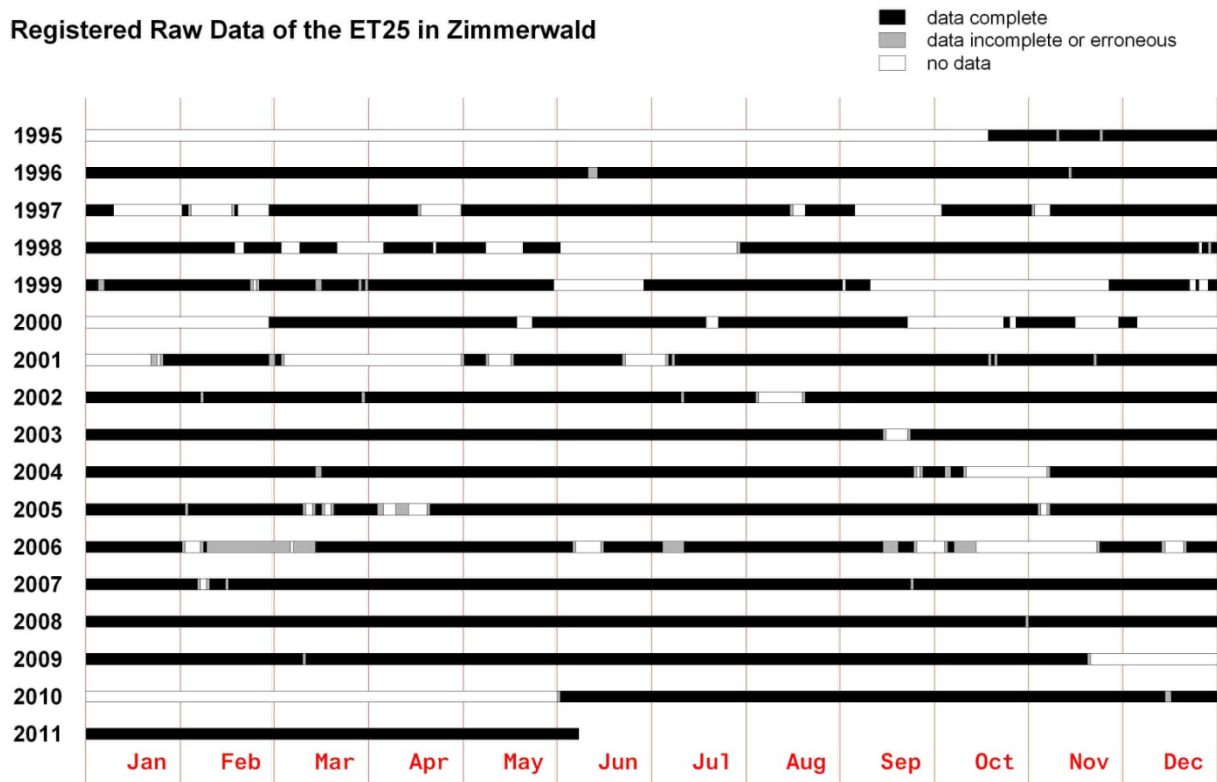


Figure 2.12: Available Earth Tide Data registered in Zimmerwald

## Ultra precise geoid determination for a new generation of future linear collider: A feasibility study at CERN

by S.Guillaume<sup>1,2</sup>, M. Jones<sup>2</sup>, B.Bürki<sup>1</sup> and A. Geiger<sup>1</sup>

<sup>1</sup> Geodesy and Geodynamics Lab, Institute of Geodesy and Photogrammetry, ETH Zurich

<sup>2</sup> Metrology group, CERN, Geneva

The Compact Linear Collider (CLIC) Study is a site independent feasibility study aiming at the development of a realistic technology at an affordable cost for an electron-positron Linear Collider (~ 50 km) in the post-LHC era for Physics up to the multi-TeV centre of mass colliding beam energy range (nominal 3 TeV).

The feasibility issue concerning the CLIC active pre-alignment is to define a reference system and associated sensors over a distance of at least 200m, to allow the alignment of objects within a few micrometers of a straight line. Active pre-alignment (max. 10 micrometers over 200m along a straight line) is a real challenge. One solution studied at CERN is based on the use of Hydrostatic Leveling System (HLS) and Wire Positioning System (WPS) for heights respectively horizontal determinations.

HLS systems have been used for accelerator alignment for many years now. They have the great advantage of providing a vertical reference surface from which certain sensors can measure their distance with a micrometric accuracy. Obviously, HLS are not referred to a straight line but to the instantaneous shape of the water surface in the pipes, and the difficulty lies in determining the form of that surface to the required level of accuracy. Physically this can be formulated as determining the instantaneous equipotential surface of the Earth's gravity field at the level of the water. The primary consequence is that it forces us to determine the instantaneous short wavelength equipotential of the earth's gravity field, at the level of HLS, along the profile where the accelerator is installed. This must be done as a function of time, in Euclidean space, with a relative precision of a few microns over 200 meters.

In the context of feasibility studies of CLIC, an existing tunnel at CERN which has similar properties to the tunnels which are planned was chosen in order to determine an equipotential profile with the best world-wide astro-gravimetric available instrumentation. The tunnel, TZ32, is near and perpendicular to the Jura mountain chain, straight, 800 meters in length, with a diameter of 3 meters at depths between 68 and 88 meters and a tilt of ~1.5 %. In this context, simulations and observations were combined to estimate the spectral properties and the alignment precision which can be expected.

Deflections of the vertical and gravity measurements were carried out every 10 meters along the profile at the Earth's surface directly above the tunnel. Moreover, gravimetric measurements were also observed within the tunnel. They were carried out using the relative gravimeter Scintrex CG-5 linked to three absolute points determined by the Swiss Federal Office of Metrology METAS with the absolute gravimeter FG-5.

The first results show that the expected precision of the determination is possible and opens the possibility of the determination of high precision short-wave length equipotentials. Nevertheless researches in the modelisation and the measurements technique must be improved in order to reduce the time and economic costs of such measurements campaigns. Figures 2.13 to 2.16 focus on some special effects which were investigated in detail.

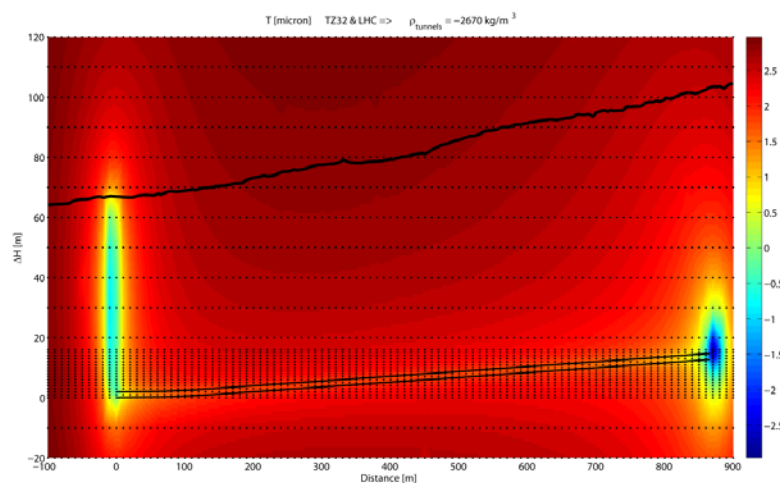


Figure 2.13: Simulation of the effect of mass anomalies due to the tunnels TZ32 and LHC on the gravity potential.

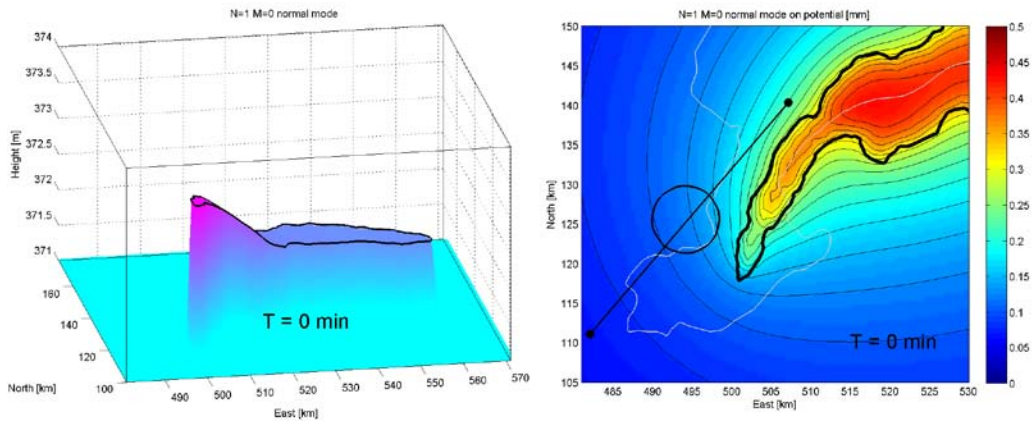


Figure 2.14: Simulation of the effect of the mass anomalies due to “seiches“ on the gravity potential at height = 350 meters.

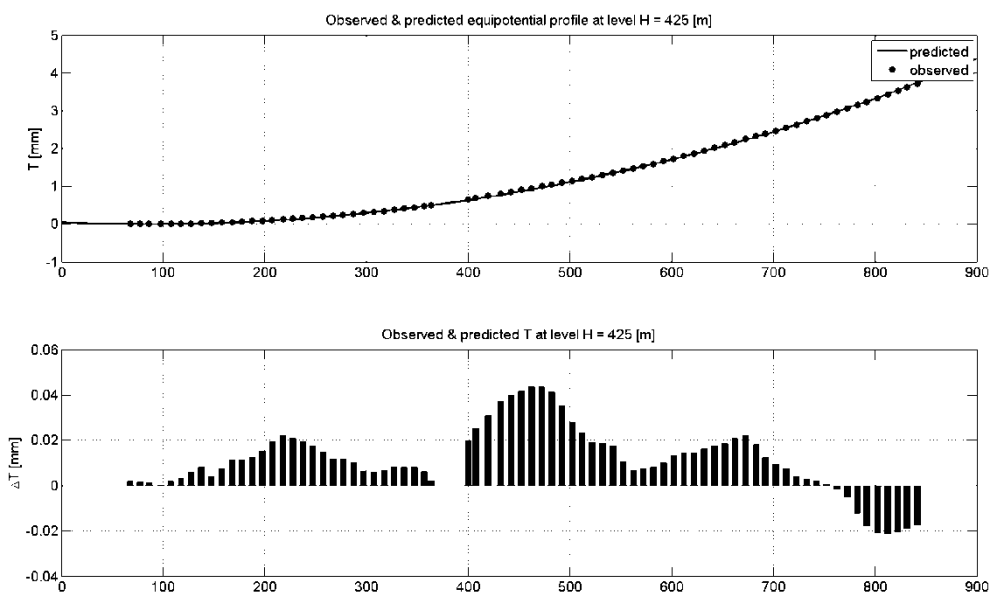


Figure 2.15: Comparisons of the equipotential profiles predicted and observed in the tunnel TZ32.

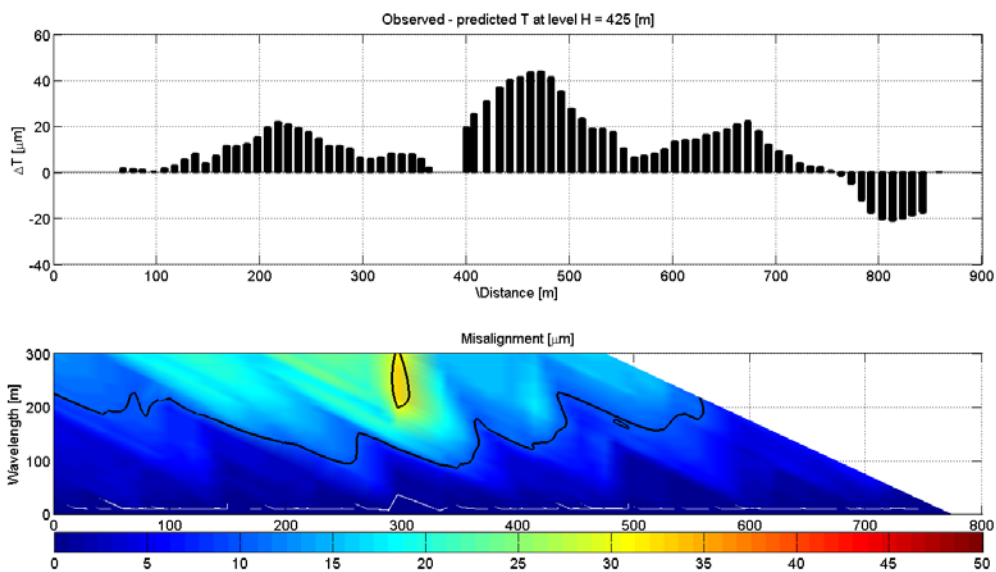


Figure 2.16: Misalignment errors between simulated and measured equipotential profiles in function of wavelengths.

## **GeoHALO: Geoscientific Research with the New German “High Altitude and Long Range Research Aircraft” (HALO)**

by A. Geiger<sup>1</sup>, M. Müller<sup>1</sup>, M. Rothacher<sup>1</sup> and M. Scheinert<sup>2</sup>

<sup>1</sup> *Geodesy and Geodynamics Lab, Institute of Geodesy and Photogrammetry, ETH Zurich*

<sup>2</sup> *Institut für Planetare Geodäsie, TU Dresden*

This project is a joint effort of a geoscientific consortium with the financial and logistic support of the German Research Foundation (DFG), the Helmholtz Association of German Research Centers, the German Aerospace Center and further national and international partners. The consortium under the co-ordination of M. Scheinert (TU Dresden) consists of Institut für Planetare Geodäsie, TU, Dresden, Germany, GFZ, Potsdam, Germany, Institute for Geodesy and Photogrammetry, Swiss Federal Institute of Technology, Zurich, Switzerland, Federal Institute for Geosciences and Natural Resources (BGR), Hannover, Germany, Space Flight Technology Department, German Aerospace Center (DLR), Oberpfaffenhofen, Germany Institut für Hochfrequenztechnik, TU, Hamburg, Germany

A new research aircraft, a modified Gulfstream G550 jet, was handed over to Germany in January 2009. Based at the German Aerospace Center (DLR) in Oberpfaffenhofen this “High Altitude and Long Range Research Aircraft” (HALO) serves as a new platform for atmospheric and geoscientific research.

A consortium of German and Swiss universities and research institutions was formed to utilize HALO for geoscientific applications. Currently, this consortium is working on the relevant equipment to be installed aboard HALO, which shall comprise an entire suite of airborne geophysical-geodetic instrumentation: Two gravity meters, inertial navigation systems, GNSS receivers with zenith, sideward and nadir antennas, magnetometers, and a laser altimeter.

As a first geoscientific HALO mission the GEOHALO mission will be realized in the Eastern Mediterranean. GEOHALO is designed to demonstrate the feasibility and performance of the geophysical-geodetic instrumentation to gain airborne measurements of the potential field quantities (gravimetry and magnetometry), GNSS direct, indirect (reflected) and occultation measurements, and laser distance observations. These airborne measurements shall help to better understand the Hellenic subduction zone and the North-Anatolian fault zone, and to improve the gravity and magnetic fields, which provide important constraints on the lithospheric structure and plate kinematics. In addition, GEOHALO will be utilized to test GNSS remote sensing measurements for altimetry, scatterometry and radio occultation. The Institute of Geodesy and Photogrammetry of ETH Zurich is involved in the subproject of the structural and kinematic modeling of the Aegean based on HALO gravity and magnetic data. Improved knowledge of these properties helps our understanding of earthquake and tsunami hazard associated with the Hellenic subduction zone and the North-Anatolian fault. The knowledge of precise sea level will provide further constraints on the modelling of geodynamic processes.

## **Sea Surface Topography and Marine Geoid by Airborne Laser Altimetry and Shipborne Ultrasound Altimetry**

by P. Limpach, H.-G. Kahle and A. Geiger

*Geodesy and Geodynamics Lab, Institute of Geodesy and Photogrammetry, ETH Zurich*

The aim of this project was to contribute to the improvement of sea level monitoring and to provide local-scale information on the short-wavelength structure of the marine gravity field, by developing enhanced methods for offshore sea surface height (SSH) observations. The methods include airborne laser altimetry, shipborne ultrasound altimetry and GPS-equipped buoys.

Since precise position and attitude of the range sensor are crucial for an accurate SSH computation, instrumental aspects of SSH observations by airborne and shipborne altimetry were analyzed (Limpach, 2010). For this purpose, the survey aircraft and boat were equipped with a multi-antenna GPS array and inertial systems (Figures 2.17 (a) and 2.18 (a)). The SSH was computed from the range data by direct georeferencing (Figure 2.17 (a)). Important aspects are the influences of errors in the differential kinematic GPS positioning and in the attitude determination, as well as the calibration of boresight misalignments. The SSH was reduced to mean sea surface by applying corrections for geophysical effects, including waves, tides, atmospheric pressure and wind forcing (Limpach, 2010).

Several airborne and shipborne SSH surveys were carried out in the Eastern Mediterranean Sea (Limpach, 2010). Dedicated surveys, including deployments of GPS buoys, were performed along Jason-1 radar altimetry ground tracks. Airborne laser altimetry data was acquired along densely spaced flight tracks covering an area of 200 by 200 km around the western part of the island of Crete, Greece, in the vicinity of the Hellenic trench (Figure 2.17 (b)). The objective was the determination of a detailed regional geoid and sea surface topography model in the framework of the GAVDOS project, funded by the European Union. Furthermore, several shipborne campaigns for SSH observations were carried out in the North Aegean Sea, in the vicinity of the North Aegean Trough (Figure 2.18 (b)).

Based on the airborne and shipborne altimetry data, a high-resolution sea surface topography was computed, with an accuracy of better than 10 cm. Geoid undulations were derived from the SSH by subtracting the mean dynamic ocean topography induced by oceanic currents. Around western Crete, the geoid obtained from airborne laser altimetry is characterized by very large gradients, with an average height difference of 20 m along a distance of only 200 km and maximum values of 22 cm/km (Figure 2.17 (b)). These gradients are a clear indication for significant gravity effects caused by the bathymetry and the geodynamic system of the Hellenic trench. In the North Aegean Sea, the geoid obtained from shipborne altimetry shows a distinct depression of 1.5 m, indicating a connection with the bathymetry and the geodynamic features of the North Aegean Trough (Figure 2.18 (b)).

The high resolution and accuracy of the sea surface and geoid heights obtained were verified by comparisons with mean sea surface models from multi-mission satellite radar altimetry, as well as with global and regional geoid models (Limpach, 2010). The reduction of the geoid heights for modeled mass effects of topography, bathymetry, marine sedimentary deposits and crust-mantle boundary revealed pronounced gravity anomalies related to geodynamic processes (see Geoid Modeling in the Aegean Sea in this report).

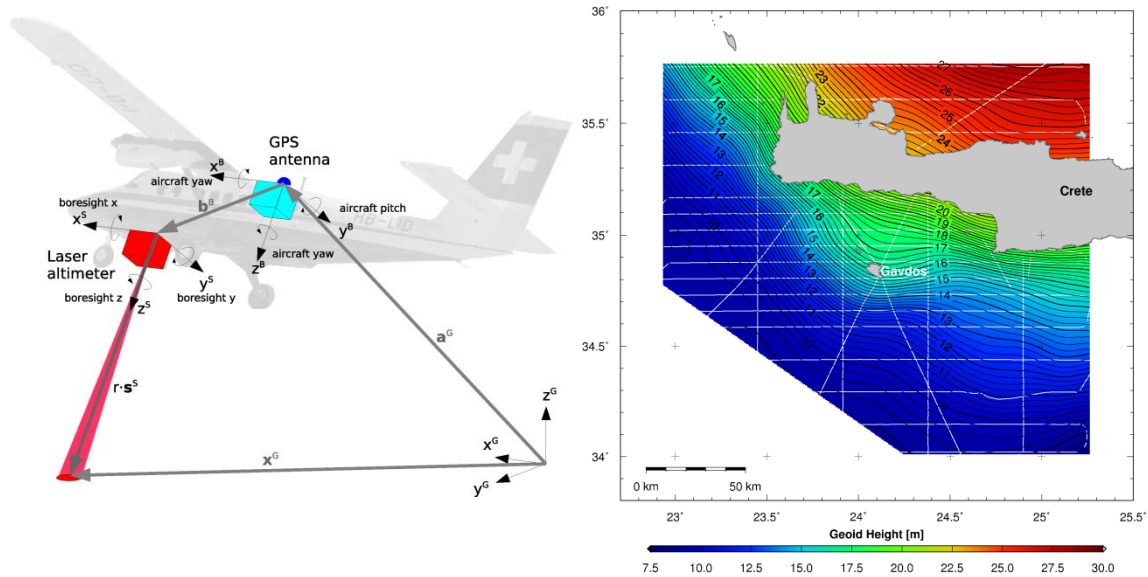


Figure 2.17: (a) Direct georeferencing elements in airborne laser altimetry. (b) Marine geoid heights (with respect to the WGS84 ellipsoid) derived from airborne laser altimetry profiles around Crete. White lines: flight tracks. Contour interval: 0.25 m.

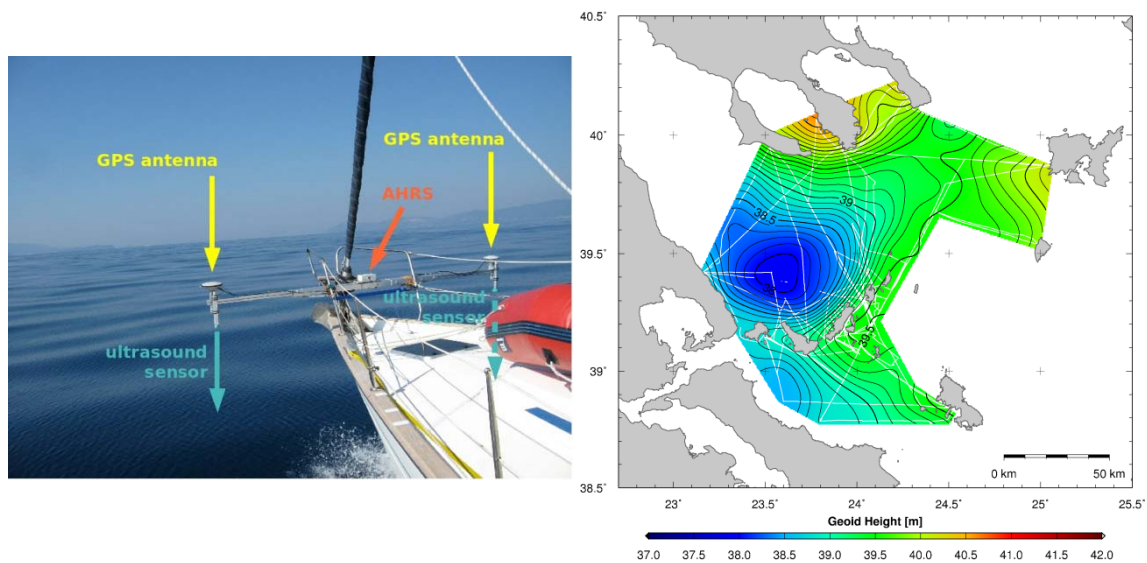


Figure 2.18: (a) Main components of the ultrasound altimetry system mounted at the bow of a sailing yacht, including two ultrasonic distance sensors, two GPS antennas and an inertial AHRS (attitude and heading reference system). (b) Marine geoid heights (with respect to the WGS84 ellipsoid) derived from shipborne ultrasound altimetry profiles in the North Aegean Sea. White lines: ship tracks. Contour interval: 0.1 m.

## Geoid Modeling in the Aegean Sea

by P. Limpach, H.-G. Kahle and A. Geiger

*Geodesy and Geodynamics Lab, Institute of Geodesy and Photogrammetry, ETH Zurich*

In order to allow for a geophysical analysis and interpretation of the airborne and shipborne altimetric geoid solutions in the Aegean Sea (see Sea Surface Topography and Marine Geoid by Airborne Laser Altimetry and Shipborne Ultrasound Altimetry in this report, Figures 2.17 (b) and 2.18 (b)), various mass effects on geoid heights were computed (Limpach, 2010). The effects caused by the above mentioned features were subtracted from the observed geoid heights (Figures 2.19 and 2.20). The residual geoid after mass reduction can be viewed as being caused by unmodeled mass effects. Regional anomalies of the gravity potential are mainly caused by topography, bathymetry, sedimentary deposits, crust-mantle boundary and lithosphere structures like subducting slabs. The mass reduction allows, therefore, to detect anomalous mass distributions possibly caused by geodynamic processes. It was shown that major parts of the geoid can be explained by the mass effects mentioned above. On the other hand, the residual geoid also revealed distinct anomalies which can be related to up to now unrecognized mass distributions.

The region south of Crete is dominated by deep sea water reaching depths of 4000 m and sediment deposits with thicknesses of up to 10 km. The predominant geoid gradients (Figure 2.17 (b)), reaching 0.22 m/km and characterizing the geoid of the entire region, were completely reduced by the modeled mass effects (Figure 2.19). On the other hand, a strong gradient of the mass-reduced residual geoid appears north of Crete. It can, therefore, be concluded that the major up to now unknown geoid anomaly in the area is the relative geoid high north of Crete, rather than the depression south of Crete along the Hellenic trench. The geoid anomaly north of Crete indicates a significant positive mass distribution beyond the northern border of the survey area, possibly linked to the Hellenic subduction zone.

In the North Aegean Sea, it was shown that the predominant geoid low of 1.5 m at the western end of the North Aegean Trough (NAT) (Figure 2.18 (b)) can be explained to a large extent by topographic, bathymetric, and known geologic effects, such as sediments and crust-mantle boundary (Figure 2.20). It is striking, however, that a widely-spread maximum of the residual geoid, reaching 1 m, is encountered north-east of the geoid low. This anomaly indicates the presence of a local mass excess. The geoid anomaly is associated with the northern fault bounding the NAT, which is considered as a major strike-slip boundary, characterized by high seismicity, separating the Anatolia-Aegean plate from Eurasia. It can, therefore, be assumed that the observed anomaly in the residual geoid is caused by an anomalous upwelling of dense material linked to the geodynamic system of the NAT.

With the inversion of the obtained local geoid, models of mass distribution can be further constrained, helping to better understand the dynamics of the Hellenic subduction zone and the westward continuation of the North-Anatolian Fault Zone.



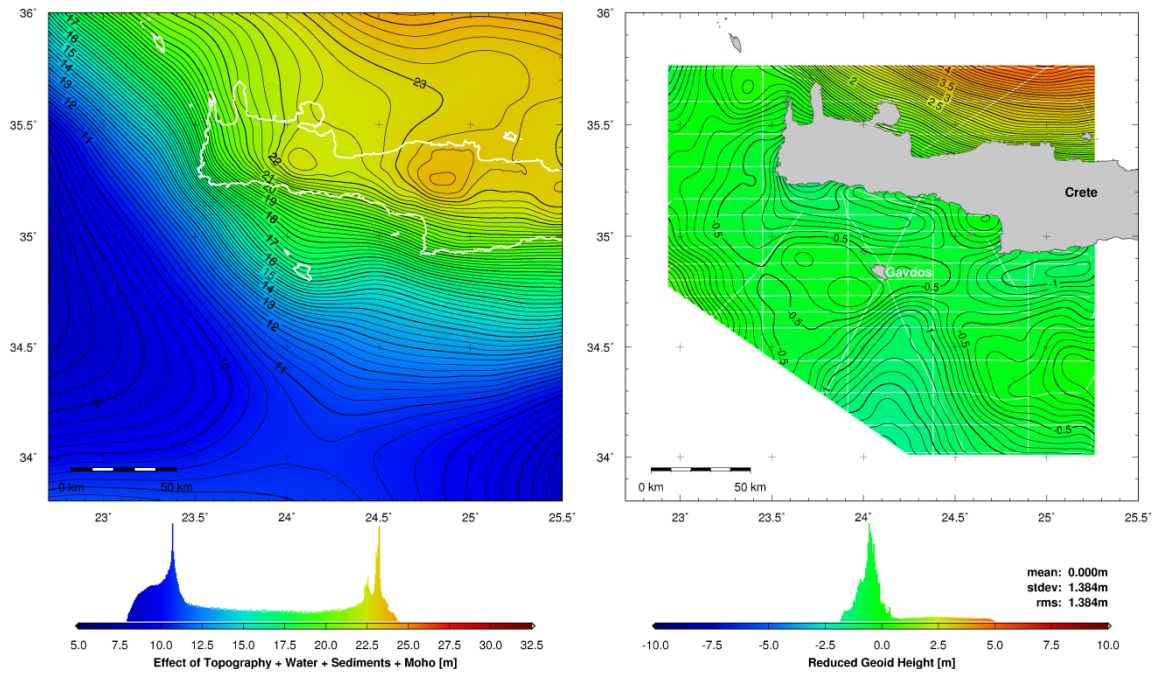


Figure 2.19: (a) Modeled geoid taking into account the mass effects of topography, bathymetry, water, sediments and isostatic Moho depths (contour interval: 0.25 m). A mean offset with respect to the observed geoid heights was added. (b) Residual airborne altimetry geoid reduced for the modeled mass effects (Fig. 2.19a) (contour interval: 0.1 m).

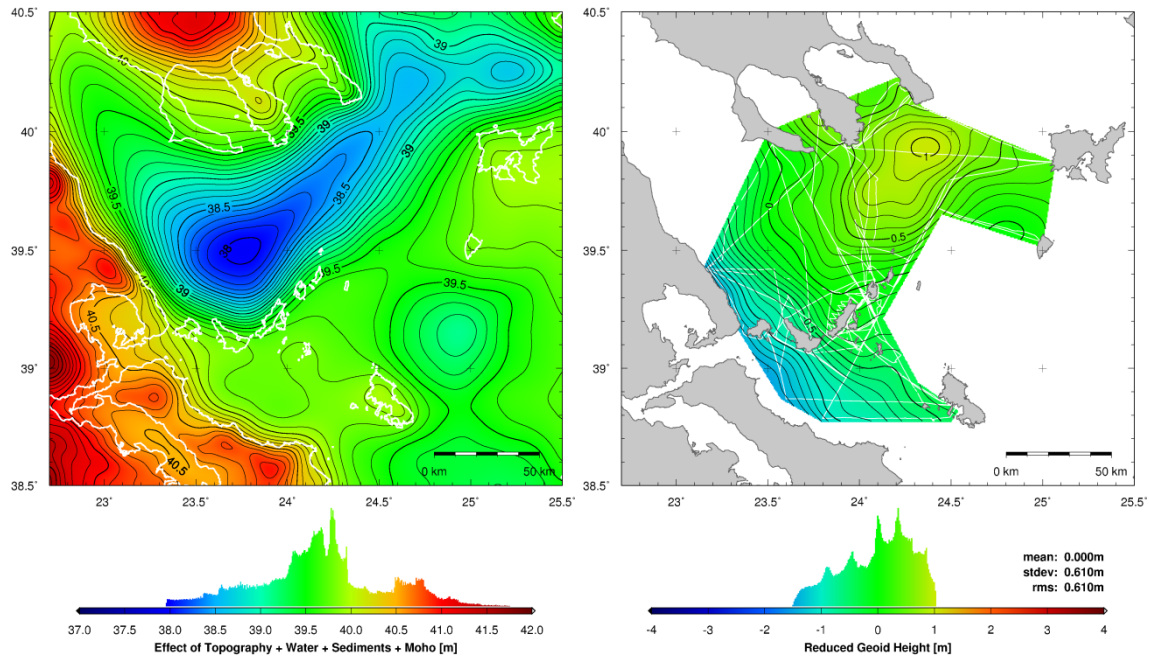


Figure 2.20: (a) Modeled geoid taking into account the mass effects of topography, bathymetry, water, sediments and isostatic Moho depths (contour interval: 0.1 m). A mean offset with respect to the observed geoid heights was added. (b) Residual shipborne altimetry geoid reduced for the modeled mass effects (Fig. 2.20a) (contour interval: 0.1 m).

## Astrogeodetic geoid and isostatic considerations in the North Aegean sea, Greece

by A. E. Somieski, B. Bürki and H.-G. Kahle

Geodesy and Geodynamics Lab, Institute of Geodesy and Photogrammetry, ETH Zurich

The digital zenith camera DIADEM (Digital Astronomical Deflection Measuring System) has been extensively used in measuring campaigns conducted in Switzerland, Portugal and Greece. The campaign in Greece was focused on the North Aegean trough (NAT) which is considered to be a continuation of the seismically active North Anatolian fault zone. In total, 27 deflections of the vertical (DOV) were determined on several islands and along the coastline of the North Aegean sea. The data analysis included the geophysical interpretation as well as the final computation of a local astrogeodetic geoid. The research area has been chosen because of its location in the boundary zone between the Eurasian and Anatolian/Aegean plates. Furthermore, it provides different data sets for comparison and validation, such as gravimetric and altimetric data as well as GPS-derived Sea Surface Heights (SSH) (see contributions by Limpach et al, and Bürki et al, this report).

For the geophysical interpretation, the DOVs have been reduced for mass effects including a digital terrain model, the isostasy model of Airy-Heiskanen and the Moho model of Tsokas and Hansen. The analysis of the isostatic cogeoid revealed a distinct mass excess along the NAT. It supports the assumption of extensional tectonic processes being active in the North Aegean sea. The interpretation of the Moho reduced DOV indicated significant discrepancies of the current Moho model concerning depth and location of local maxima and minima. The respective cogeoid revealed a rising crust-mantle boundary along the NAT.

The final geoid computation has been realized by applying the least-squares collocation method to the residual DOVs in a first step and by restoring the reduced mass effects in a second step. The astrogeodetic geoid and a combined geoid from DOV and SSH clearly reflect the topographic and bathymetric features of the NAT. Especially, the relative mass deficit associated with the deep water of the trough is indicated by a pronounced depression of the geoid. The geoid variations in NS-direction across the NAT amount up to 2.6 m. The combined geoid solution has been compared with available altimetric and gravimetric geoid solutions whereby significant discrepancies of up to 3m have been detected. The new geoid reflects much better the shape and depth distribution of the NAT. The work was performed in cooperation with the Aristotle University of Thessaloniki, Greece. The location of the astro-geodetic stations measured is displayed in Figure 2.21.

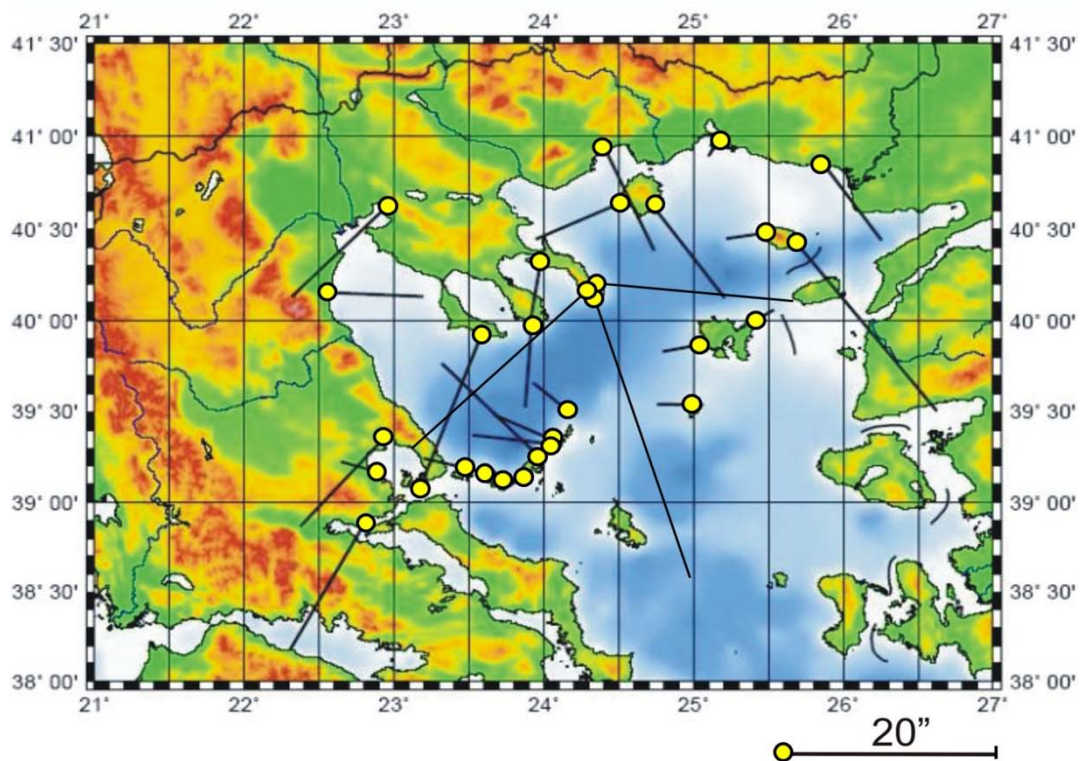


Figure 2.21: Stations with observed deflections of the vertical in the North Aegean Region in Greece.

## Bibliography Commission 2

- Beutler, G., A. Jäggi, L. Mervart, U. Meyer (2010): The celestial mechanics approach: theoretical foundations. *Journal of Geodesy*, vol. 84(10), pp. 605–624, DOI 10.1007/s00190-010-0401-7.
- Beutler, G., A. Jäggi, L. Mervart, U. Meyer (2010a): The celestial mechanics approach: theoretical foundations. *Journal of Geodesy*, vol. 84(10), pp. 605–624, DOI 10.1007/s00190-010-0401-7.
- Beutler, G., A. Jäggi, L. Mervart, U. Meyer (2010b): The celestial mechanics approach: application to data of the GRACE mission. *Journal of Geodesy*, vol. 84(11), pp. 661–681, DOI 10.1007/s00190-010-0402-6.
- Bock, H., A. Jäggi, D. Svehla, G. Beutler, U. Hugentobler, P. Visser (2007): Precise Orbit Determination for the GOCE Satellite Using GPS. *Advances in Space Research*, 39(10), 1638–1647, doi:10.1016/j.asr.2007.02.053.
- Bock, H., A. Jäggi, U. Meyer, R. Dach, G. Beutler (2011a): Impact of GPS antenna phase center variations on precise orbits of the GOCE satellite. *Advances in Space Research*. doi:10.1016/j.asr.2011.01.017.
- Bock, H., A. Jäggi, U. Meyer, P. Visser, J. Van den IJssel, T. Van Helleputte, M. Heinze, U. Hugentobler (2011b): GPS-derived orbits for the GOCE satellite. Submitted to *Journal of Geodesy*.
- Denker, H., J.-P. Barriot, R. Barzaghi, D. Fairhead, R. Forsberg, J. Ihde, A. Kenyeres, U. Marti, M. Sarrailh, I.N. Tziavos (2008): The development of the European Gravimetric Geoid model EGG07. In: Sideris, M. (Ed.), *Observing Our Changing Earth, Proceedings of the IAG General Assembly, Perugia, Italy, July 02–13, 2007*. IAG Symposia Series Vol. 133, 177–186, Springer, Berlin Heidelberg New York.
- Drinkwater, M.R., R. Floberghagen, R. Haagmans, D. Muzi, A. Popescu (2003): GOCE: ESA's first Earth Explorer core mission, *Space Science Reviews*, 108(1–2), 419–432, doi:10.1023/A:1026104216284.
- Geiger, A., A. Schlatter (2010): Von der Potentialtheorie zu den Senkungen am Gotthardpass. *Geomatik Schweiz*, Vol. 108, Issue 12, pp. 628–630, ISSN 1660-4458.
- Hirt, C., W. Featherstone, U. Marti (2010): Combining EGM2008 and SRTM/DTM2006.0 residual terrain model data to improve quasigeoid computations in mountainous areas devoid of gravity data. *Journal of Geodesy* Vol. 84, Nr. 9. September 2010.
- Hirt, C., U. Marti, W. Featherstone, B. Bürki (2010): Assessment of EGM2008 in Europe using accurate astrogeodetic vertical deflections and omission error estimates from SRTM/DTM2006.0 residual terrain model data. *Journal of Geophysical Research* Vol. 115, B10404, doi:10.1029/2009JB007057.
- Jäggi, A., G. Beutler, L. Prange, R. Dach, L. Mervart (2009): Assessment of GPS-only observables for Gravity Field Recovery from GRACE. In *Observing our Changing Earth*, edited by M. Sideris, vol. 133, pp. 113–123, DOI 10.1007/978-3-540-85426-5\_14, Springer ISBN 978-3-540-85425-8.
- Jäggi, A., R. Dach, O. Montenbruck, U. Hugentobler, H. Bock, G. Beutler (2009a): Phase center modeling for LEO GPS receiver antennas and its impact on precise orbit determination. *Journal of Geodesy* 83(12): 1145–1162, DOI 10.1007/s00190-009-0333-2.
- Jäggi, A., H. Bock, L. Prange, U. Meyer, G. Beutler (2010): GPS-only gravity field recovery with GOCE, CHAMP, and GRACE. *Advances in Space Research* 47(6): 1020–1028, DOI: 10.1016/j.asr.2010.11.008.
- Jäggi, A., G. Beutler, L. Mervart (2010a): GRACE Gravity Field Determination Using the Celestial Mechanics Approach – First Results. In *Gravity, Geoid and Earth Observation*, edited by S.V. Mertikas, vol. 135, pp. 177–184, DOI 10.1007/978-3-642-10634-7\_24, Springer ISBN 978-3-642-10633-0.
- Jäggi, A., L. Prange, U. Hugentobler (2010): Impact of covariance information of kinematic positions on orbit reconstruction and gravity field recovery. *Advances in Space Research*, DOI 10.1016/j.asr.2010.12.009.
- Jäggi, A., H. Bock, L. Prange, U. Meyer, G. Beutler (2010b): GPS-only gravity field recovery with GOCE, CHAMP, and GRACE. *Advances in Space Research*, DOI 10.1016/j.asr.2010.11.008.
- Jäggi, A., L. Prange, U. Hugentobler (2011a): Impact of covariance information of kinematic positions on orbit reconstruction and gravity field recovery. *Advances in Space Research*, DOI 10.1016/j.asr.2010.12.009.
- Jäggi, A., G. Beutler, U. Meyer, L. Mervart, L. Prange, R. Dach (2011b): AIUB-GRACE02S – status of GRACE gravity field recovery using the celestial mechanics approach. In *International association of geodesy symposia (in press)*.

- Jäggi, A., H. Bock, R. Floberghagen (2011): GOCE orbit predictions for SLR tracking. *GPS Solutions*, doi:10.1007/s10291-010-0176-6.
- Kenyeres, A., M. Sacher, J. Ihde, H. Denker, U. Marti (2008): EUVN\_DA: Realization of the European Continental GPS/leveling Network. *IAG Symposia Series Vol. 135*, 315-320, Springer, Berlin Heidelberg New York.
- Limpach, P., A. Geiger, H.-G. Kahle (2007): GNSS Applications in Airborne and Seaborne Sea Surface Height Measurements. *Proceedings of the ENC-GNSS 2007, European Navigation Conference, May 2007, Geneva, Switzerland*.
- Limpach, P., A. Geiger, H.-G. Kahle (2007): Sea Surface Topography by GPS Buoys and Airborne Laser Altimetry. *Swiss National Report on the Geodetic Activities in the years 2003 to 2007*, pp. 84-86. Presented to the XXIV. General Assembly of the International Union of Geodesy and Geophysics in Perugia, Italy, July 2007. ISBN 978-3-908440-15-4.
- Limpach, P., A. Geiger, H.-G. Kahle (2007): GNSS Applications in Airborne and Seaborne Sea Surface Height Measurements. *Proceedings of the ION GNSS 2007, 20th International Technical Meeting of the Satellite Division of The Institute of Navigation, September 2007, Fort Worth, Texas*. pp. 2163-2168.
- Limpach, P., A. Somieski, S. Guillaume, B. Bürki, H.-G. Kahle, I. Tziavos (2008): Geoid and sea surface height measurements in the North Aegean Sea. *Proceedings of IAG International Symposium on Gravity, Geoid and Earth Observation GGEO 2008, Chania, Greece*.
- Limpach, P. (2009): Sea surface topography and marine geoid by airborne laser altimetry and shipborne ultrasound altimetry in the Aegean Sea. PhD Thesis Nr. 18225 Eidgenössische Technische Hochschule ETH Zürich. DOI: 10.3929/ethz-a-005876550.
- Limpach, P. (2010): Sea Surface Topography and Marine Geoid by Airborne Laser Altimetry and Shipborne Ultrasound Altimetry. *Geodätisch-geophysikalische Arbeiten in der Schweiz. Volume 80. Schweizerische Geodätische Kommission*. ISBN 978-3-908440-24-6.
- Marti, U., Ph. Richard (2007): Landesschwerenetz (LSN2004): Einrichten der absoluten Schwerestation Basel und Absolutmessungen 2006. *swisstopo-Report 07-11*.
- Marti, U. (2007): Ein neues Modell für das Schweizer Schwerefeld. *Geosciences ACTUEL 1/2007*, Seiten 23-27.
- Marti, U. (2008): The National Gravity Network of Switzerland. Poster presented at the 6th Swiss Geoscience Meeting, Lugano Nov. 22, 2008.
- Marti U., H. Baumann (2010): Absolute Schweremessungen 2007 bis 2010. *swisstopo-Report 10-12. Bundesamt für Landestopografie*.
- Prange, L., A. Jäggi, G. Beutler, R. Dach, L. Mervart (2009): Gravity Field Determination at the AIUB – the Celestial Mechanics Approach. In *Observing our Changing Earth*, edited by M. Sideris, vol. 133, pp. 353-362, DOI 10.1007/978-3-540-85426-5 42, Springer ISBN 978-3-540-85425-8.
- Prange, L., A. Jäggi, R. Dach, H. Bock, G. Beutler, L. Mervart (2010): AIUB-CHAMP02S: The influence of GNSS model changes on gravity field recovery using spaceborne GPS. *Advances in Space Research*, vol.45(2), pp. 215-224, DOI 10.1016/j.asr.2009.09.020.
- Prange, L. (2011): Global Gravity Field Determination Using the GPS Measurements Made Onboard the Low Earth Orbiting Satellite CHAMP. *Geodätisch-physikalische Arbeiten in der Schweiz, Band 81, Schweizerische Geodätische Kommission, Institut für Geodäsie und Photogrammetrie, ETH Zürich*.
- Somieski, A. E. (2008): Astrogeodetic Geoid and Isostatic Considerations in the North Aegean Sea, Greece. *Diss. ETH No. 17790*. doi:10.3929/ethz-a-005710420.
- Visser, P., J. Van den IJssel, T. Van Helleputte, H. Bock, A. Jäggi, G. Beutler, D. Svehla, U. Hugentobler, M. Heinze (2009): Orbit determination for the GOCE satellite. *Advances in Space Research*,43(5), 760-768, doi:10.1016/j.asr.2008.09.016.

### 3 Earth Rotation and Geodynamics

#### CODE Contributions to Earth Rotation Monitoring

by S. Schaer<sup>1</sup>, R. Dach<sup>2</sup>, S. Lutz<sup>2</sup>, M. Meindl<sup>2</sup>, D. Thaller<sup>2</sup> and G. Beutler<sup>2</sup>

<sup>1</sup> Federal Office of Topography, swisstopo

<sup>2</sup> Astronomical Institute University of Bern

The CODE stands for Center of Orbit Determination in Europe - a joint venture of Astronomical Institute, University of Bern, Switzerland, Bundesamt für Landestopographie, swisstopo, Wabern, Switzerland, Bundesamt für Kartographie und Geodäsie, Frankfurt a. Main, Germany, and Institut für Astronomische und Physikalische Geodäsie, Technische Universität München, Germany. CODE is one of the global Analysis Centers (AC) of the International GNSS Service (IGS). The activities of CODE as an IGS AC are described in Dach et al. (2009) or Schaer et al. (2011).

The satellite orbits of Global Navigation Satellite Systems (GNSS) realize a quasi-inertial reference system, so that the analysis of tracking data from the global network of the IGS allows it to estimate Earth rotation parameters (ERPs). As a result x and y positions of the Earth's rotation axis in an Earth-fixed frame (polar motion) and rates thereof as well as excess length of day (LOD) are obtained.

Since April 1994 also daily values for drifts in nutation in longitude and obliquity are estimated at CODE.

Since week 1486 (June 29, 2008) CODE is internally using a 1-hour resolution for polar motion and LOD parameters. The ERPs are represented as a piece-wise linear polygon, so that continuity at the interval boundaries is automatically guaranteed. For the delivery to external sources (e.g., to the IGS via SINEX files) the representation of the parameters is transformed to offset and drift per 1-day interval applying some continuity conditions at the day boundaries. Separate time series are provided directly to the International Earth Rotation and Reference Systems Service (IERS) for further analysis.

Today a time series of more than 17 years is available from CODE. Figure 3.1 shows the Chandler wander of the Earth's rotation axis starting with June 1993. The accuracy of the daily values as compared to other techniques is a few 0.1 mas. Figure 3.2 shows the variations of excess length of day for the time period of more than 17 years.

In the frame work of the reprocessing campaign of the IGS, a time series of ERP based on homogeneous and most up-to-date models has been generated, too (see Lutz et al. 2011).

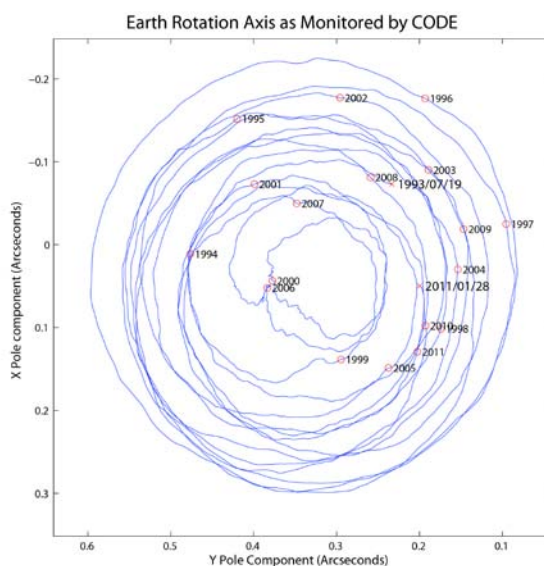


Figure 3.1: Polar motion derived from GNSS observations between July 1993 until January 2011.

CODE Excess Length of Day: 19-07-1993 - 23-01-2011

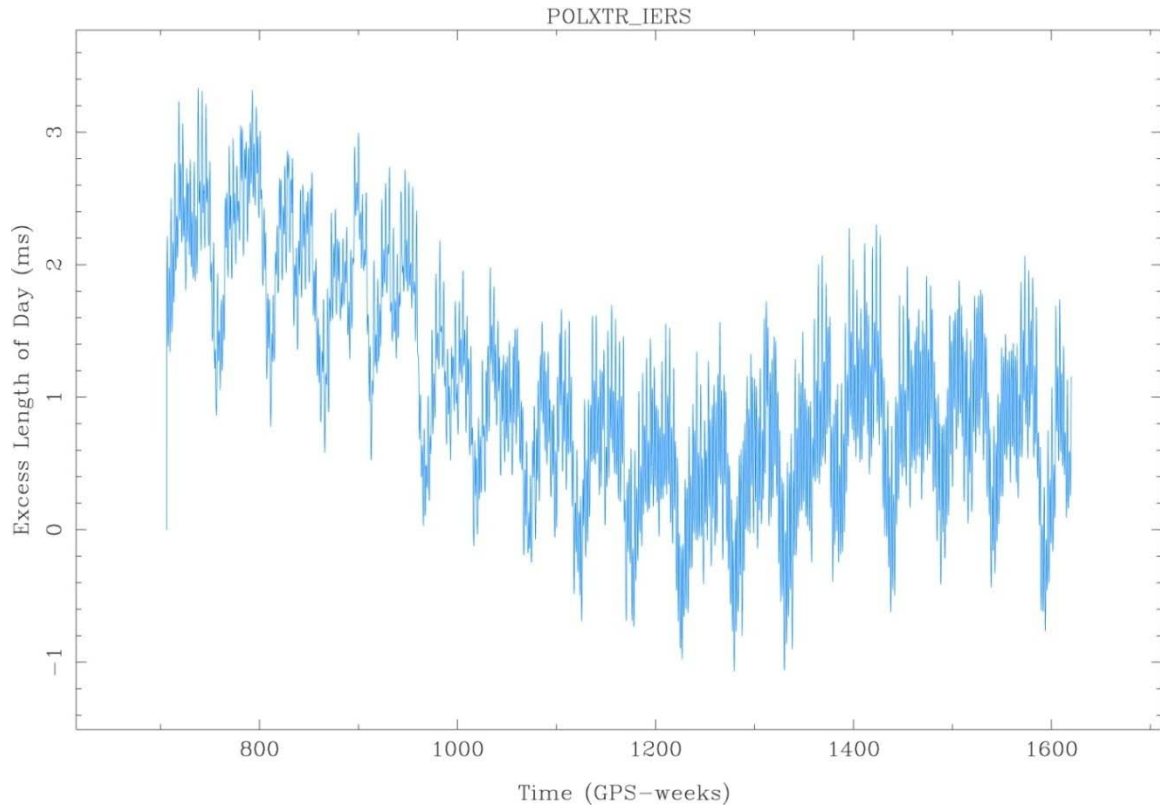


Figure 3.2: Excess length of day derived from GNSS observations between July 1993 until January 2011.

## Subdaily variations in the Earth rotation

by N. Panafidina, M. Rothacher

*Geodesy and Geodynamics Lab, Institute of Geodesy and Photogrammetry, ETH Zurich*

In studies of the Earth rotation two basic reference systems are used: quasi-inertial celestial reference system (ICRS) realized as a set of coordinates of extra-galactic radio sources, and the terrestrial reference system (ITRS) rotating with the Earth and realized as a set of coordinates of stations on the Earth surfaces. The transformation between these systems is done using 5 angles (Figure 3.3): pole coordinates  $x(t)$  and  $y(t)$  bring the pole of ITRS to the Celestial Intermediate Pole (CIP), which is close to the instantaneous Earth rotation axis. The Universal Time (UT1) aligns the rotating ITRS to the inertial space. Two other parameters are corrections to nutation angles given by the theory of precession and nutation. Here we will consider only a set of 3 angles - polar motion ( $x$ ,  $y$ ) and UT1 - which we call Earth rotation parameters (ERP).

Mass redistributions in the system Earth cause variations in Earth rotation, both in the position of the rotational axis (polar motion) and speed of the rotation (UT1). The large-scale annual variation in polar motion, e.g., is caused by a seasonal mass redistribution. On shorter periods the main mass redistribution in the Earth system is caused by the ocean tides. The effect of this phenomenon on Earth rotation has been re-computed from a model for ocean tides, the corresponding model of subdaily variations in Earth rotation (IERS model) comprises ~100 tidal terms in PM and ~70 terms in UT1. Figure 3.4 shows the x-pole coordinate as estimated with 1-hour resolution from GPS observations and as computed from the IERS model. The correlation between the two curves is well seen, while the remaining differences between them should be caused by other effects, such as atmospheric and radiational tides, or non-tidal atmospheric and oceanic angular momenta and atmospheric and oceanic normal modes. Additional variations in ERPs are caused by the triaxiality of the Earth, which leads to a high-frequency nutation of the rotational axis. These nutation terms are not included in the model for precession and nutation. They are taken into account in the terrestrial reference system as a part of polar motion.

In the present study we compute an empirical model of variations in the Earth rotation on tidal frequencies using long time series of Earth rotation parameters (ERPs) with 1 hour resolution obtained from homogeneously re-processed GPS observations over 1994-2007. In order to take into account all the correlations between the parameters amplitudes of variations in the ERPs were set up as additional parameters in daily normal equations. Several tidal models were computed from solutions with different modelling approaches for the GPS orbits in order to identify possible disturbances in the estimated tidal terms introduced by orbital errors.

To test the stability of the tidal terms for different modelling of GPS orbits we computed for each type of orbit model 8 subdaily ERP models, each based on 6 years of data shifted by one year (time period 1994 – 2007), then the RMS values were computed for each tidal term. It was found that the main influence on the estimation of tidal variations in the ERPs has a period of 1 day (2:1 commensurability of orbital revolution and Earth rotation): in case of 1 day arcs the terms with periods very close to 24 hours cannot be reliably estimated, while solutions with 7 days orbital arcs show much better stability of all diurnal tidal terms, the only term with a high RMS is S1, which has a period of exactly 24 hours. This instability of the S1 term can indicate remaining orbit modelling deficiencies, but also some geophysical phenomena like non-tidal atmospheric and oceanic momenta. Tidal terms with periods close to half a sidereal day (~11 hours 58 min) show instability for all types of orbit modelling, since half a sidereal day is the period of revolution of GPS satellites. Figure 3.5 shows as example the RMSs of tidal terms for a solution with 7 days orbital arcs. This instability of the variations with the period of 24 hours makes a geophysical interpretation of the signal very difficult or even impossible. Further investigations of the orbital influences on the estimated tidal terms are therefore needed.

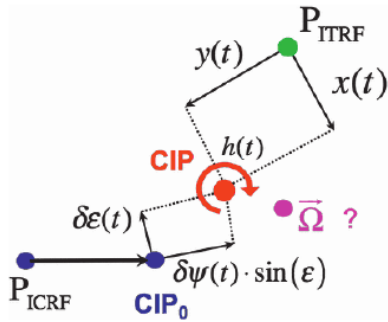


Figure 3.3: Transformation between ITRF and ICRF: pole of ITRF is transformed into an intermediate pole CIP using pole coordinates  $x(t)$  and  $y(t)$ . The rotational angle of the Earth  $h(t)$  is used to align the ITRF to ICRF. The corrections to nutation angles  $\delta\epsilon(t)$  and  $\delta\Psi(t)\cdot\sin(\epsilon)$  bring the CIP to the CIP0 which is given by the theory of precession and nutation

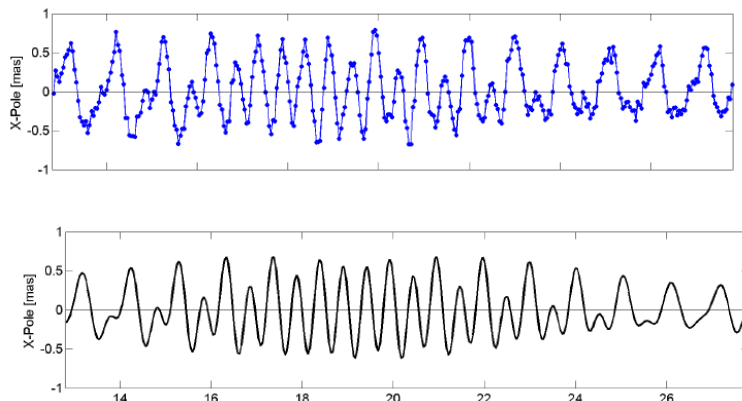


Figure 3.4: X-pole with 1 hour resolution from a GPS solution (up), X-pole computed from a model of variations in Earth rotation induced by the ocean tides (below).

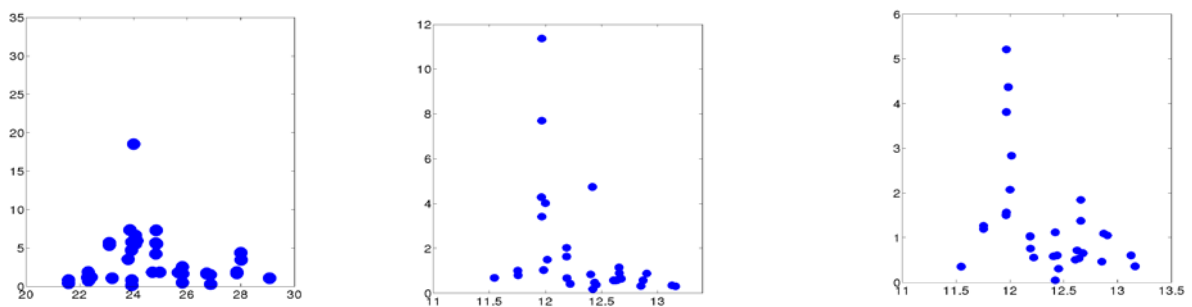


Figure 3.5: RMSs of tidal amplitudes in  $\mu\text{as}$  for GPS subdaily ERP model with 7 days orbital arcs: (a) diurnal prograde polar motion; (b) semidiurnal prograde polar motion; (c) retrograde semidiurnal polar motion. The periods on the x-axis are given in hours.



## Recent Crustal Vertical Movements from levelling and GNSS permanent networks

by E. Brockmann, A. Schlatter

Federal Office of Topography, swisstopo

The analysis of more than 10 years of permanent AGNES and EPN/IGS data allow an estimation of vertical rates for the station coordinates. Additionally, vertical uplift rates can also be estimated using 100 years of repeated levelling for the Swiss levelling benchmarks which were observed at least 3 times. A comparison of both methods, shown in Figure 3.6, impressively shows a general Alpine uplift. Nevertheless, the GNSS-derived vertical rates seem to be significantly higher especially in the northern region of Switzerland.

Due to the fact that the analysis of the Swiss permanent network AGNES is embedded in the European EPN/IGS network, the movements with respect to the stable part of the Eurasian plate can be determined. The results show that Switzerland is rising in average by 1.2 mm/year.

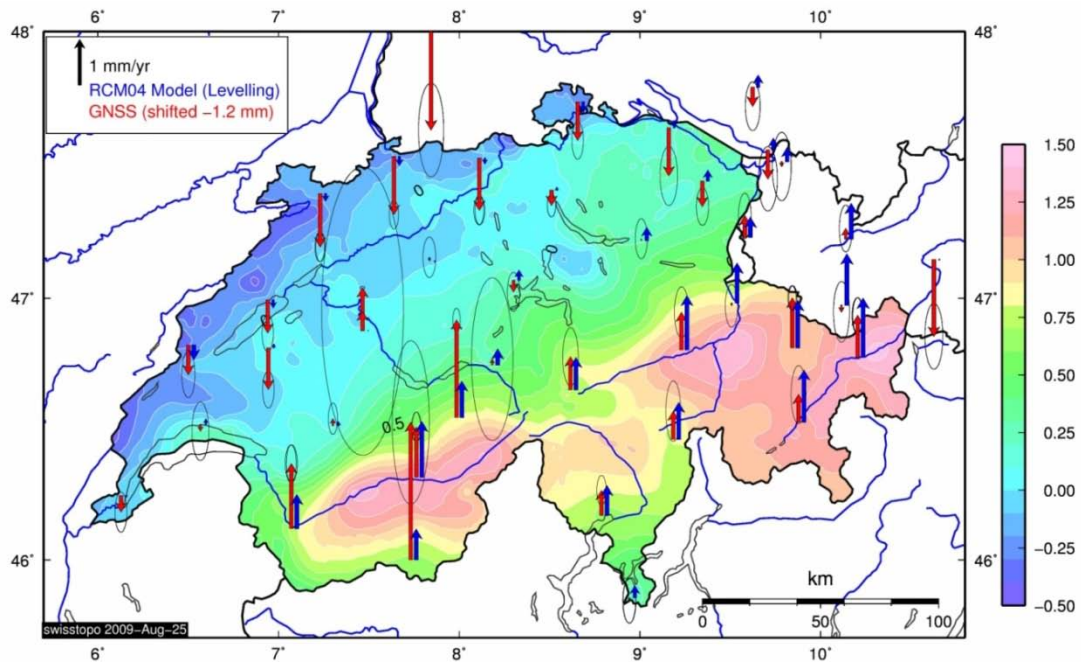


Figure 3.6: Comparison of vertical velocities between GNSS and the levelling-derived model RCM04 expressed in the Swiss system (Aarburg zero vertical velocity). Red arrows indicate GNSS rates, blue arrows indicate RCM04 model values at the AGNES sites. The background contour surface shows the RCM04 model.

## Combined multi-annual GNSS solutions from permanent networks and campaigns

by E. Brockmann

Federal Office of Topography, swisstopo

Using the normal equation stacking method, combined multi-annual combinations are generated based on the permanent networks AGNES und EPN/IGS as well as based on the GPS campaigns between 1988 and 2010.

The time series analysis of the permanent stations is a main element for the long-term monitoring of the stability of the stations and for the Swiss terrestrial reference frame. Differently to this permanent monitoring, the combination based on campaign data allows conclusions with respect to the stability of well monumented stations densifying the permanent network.

Horizontal velocities derived from AGNES for stations with a time series of more than 3 years and from the campaign data for stations covering at least 3 occupations in more than 4 years are given in Figure 3.7.

The estimated horizontal velocities are small. The hypothesis, that there are no movements on the Swiss territory, holds true on a  $1-\sigma$  level of 0.35 mm/year (some obviously locally instable sites included).

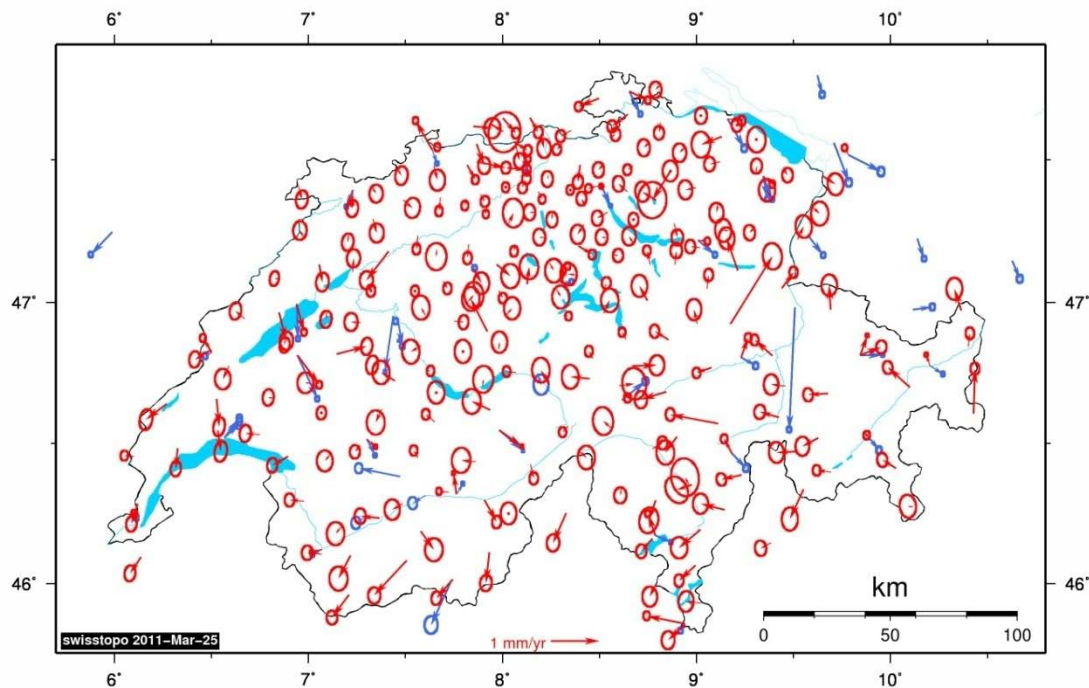


Figure 3.7: Horizontal velocity estimates derived from the permanent network AGNES (in blue) and derived from the campaign data for the LV95 reference points (in red).

## SWISS-4D II: Geodetic analysis of geodynamic deformations in Switzerland

by A. Villiger<sup>1</sup>, A. Geiger<sup>1</sup>, A. Wiget<sup>2</sup> and U. Marti<sup>2</sup>

<sup>1</sup> Geodesy and Geodynamics Lab, Institute of Geodesy and Photogrammetry, ETH Zurich

<sup>2</sup> Federal Office of Topography, swisstopo

The growing demand of very high precision geodetic reference networks necessitates a permanent control of the kinematics of the reference points. The study of the movement of these points allows determining a kinematic deformation model which on the one hand can be used to control and correct the geodetic reference and on the other hand provides utmost important geoscientific insight into tectonic deformation of the crust.

The Federal Office of Topography (swisstopo) established from 1988 on its new national first order GPS based Reference Network LV95 (Landesvermessung 95), and in addition built up an automatic permanent GPS reference network (AGNES) of 34 stations. The LV95 Network has been measured four times whereas AGNES delivers continuous measurements. These two data sets, continuous and episodic, are combined in order to determine velocity and strain fields on the area of Switzerland.

Local deformations have to be kept to a minimum and need to be separated from tectonic deformation rates, which are expected to be relatively small and most likely won't exceed 2mm/a.

Adaptive collocation methods are used for the velocity determination allowing for separation of measured deformation into local signals, reflecting on site influences, and regional signals, assumed to be driven by plate tectonics.

Applying common mode and stacking algorithms to the time-series of the permanent stations of AGNES revealed time correlated signals as well as signals correlated in space. No significant common mode effect is seen in the time-series. However, the stacking algorithms have brought, even though statistically not significant, that almost all sites have some seasonal variations. For the velocity estimation on long time series, these effects are almost filtered out. When using campaign data only, it is crucial to be aware of the time correlations and especially the seasonal effects before interpreting results of velocity determinations.

Further development of the adaptive least-square collocation method, introduced in (Egli et al., 2007) is ongoing. The aim is to devise a truly 3D collocation method which takes into account all cross correlations between all the components of the position vectors. While the tight implementation of the third dimension is still under development, preliminary 2D evaluation has been carried out. The resulting grid of interpolated velocities is displayed in Figure 3.8.

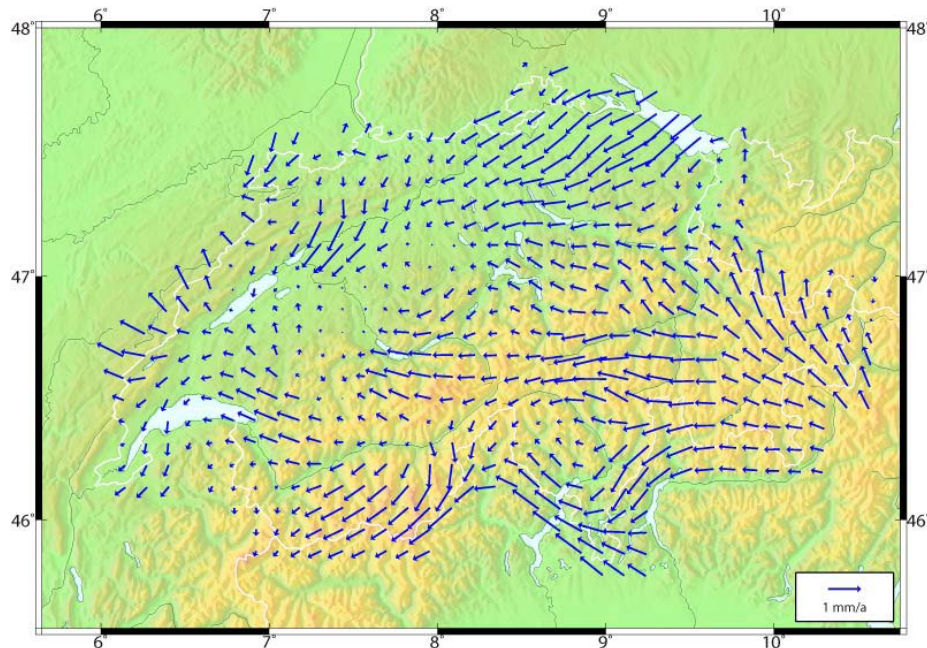


Figure 3.8: Preliminary velocity field derived from CHTRF2004 velocities

## **COGEAR Coupled seismogenic Geohazards in Alpine Regions (COGEAR)**

by A. Geiger<sup>1</sup>, A. Villiger<sup>1</sup> and D. Fäh<sup>2</sup>

<sup>1</sup> *Geodesy and Geodynamics Lab, Institute of Geodesy and Photogrammetry, ETH Zurich*

<sup>2</sup> *Swiss Seismological Service, ETH Zurich*

COGEAR is an interdisciplinary natural hazard project with the goal to investigate the entire hazard chain induced by earthquakes. It includes the tectonic processes and the related variability of seismicity in space and time, earthquake forecasting and the short-term precursors, and the strong ground motion as a result of source and complex path effects. In soils and rock, we will study non-linear wave propagation phenomena and liquefaction as well as the triggering of landslides and avalanches. Here the focus is on the physics of the non-linear processes in relation to topography, geological disposition and slope stability. The consequences are evaluated in terms of hazard scenarios and compound hazards, describing also the interrelation between earthquake-triggered landslides, landslide dam formation, and flooding. The Valais and specifically the area of Visp, as well as the Visper and Matter valleys have been selected as study areas. The tasks include detailed field investigations, the development and application of numerical modelling techniques, and installation of different monitoring systems to test and validate our models. The monitoring systems are for long-term operation and include a continuous GPS and seismic network, a test installation for the observation of earthquake precursors, and two test areas (Visp, St. Niklaus-Randa) to study site-effects and non-linear phenomena. This project will prepare a follow-up risk-related project including the impacts on buildings, infrastructure, ecosystems and society. As a multidisciplinary national program, the scientific and organizational structure underlying this effort combines various disciplines, and strengthens and extends partnerships.

This project forms an integral part of the larger research framework of the Competence Center Environment and Sustainability of the ETH Domain (CCES). Its overall strategic goals are to foster major advancements in research; to establish the CCES partners as international and national focal points for environment and sustainability; to achieve a long-term structuring effect lasting beyond the completion of CCES; to establish a strong wide-ranging education and outreach program; to achieve a visible societal impact with a focus on socio-economic implementation.

As part of the COGEAR project (an interdisciplinary natural hazard project for investigating the hazard induced by earthquakes) the Institute of geodesy and photogrammetry has a collaborative effort and co-operation between scientist in the field of seismology, geology and geodesy, to investigate various aspects of earthquake in the Valais, it includes identification and characterization of active faults, earthquake scaling relationships, ground motion attenuation models, physics-based earthquake modeling and near-source ground motion simulation. Geodetic measurements are performed for deformation estimates and development of a kinematic model of the region. In addition, series of field seismic survey are developed for mapping fault zone faults.

This investigation provides a better understanding of the seismicity and the characteristics of potential destructive earthquakes in the area. It results in the improvement of our capability for ground motion prediction for the assessment of seismic hazard and to mitigate the seismic risk in the area. Furthermore, this study contributes to the evaluation of the critical facilities installed in this area, contributing to improved seismic safety of future and existing structures.

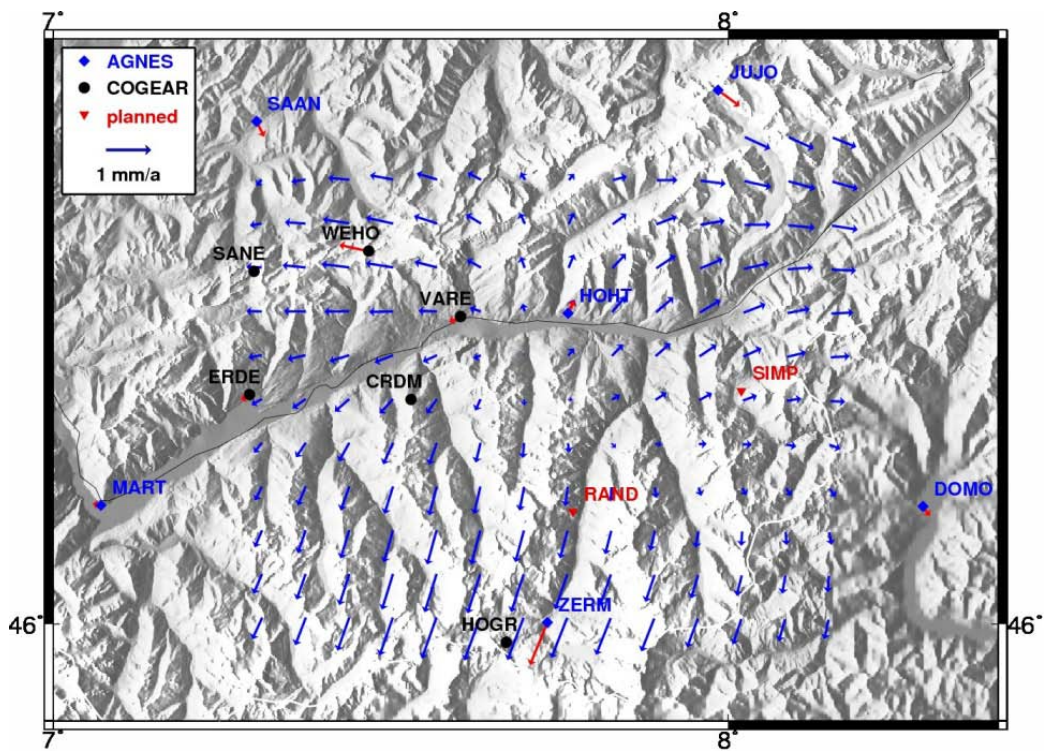


Figure 3.9: Velocity field derived from permanent GNSS stations in the canton Valais (AGNES: swisstopo, COGEAR: CCES-ETHZ)

## **Crustal deformation field in Greece determined from GPS measurements**

*by M.D. Müller, Ch. Hollenstein, A. Geiger and H.-G. Kahle*

*Geodesy and Geodynamics Lab, Institute of Geodesy and Photogrammetry, ETH Zurich*

The Eastern Mediterranean forms the seismically most active region of the Alpine-Mediterranean plate boundary. It is characterized by the collision between the Eurasian, Nubian and Arabian plates. The collision is closely related to continental subduction and formation of the Hellenic trench system. In addition to the relatively slow CCW rotation of the African plate, rapid motion of the Anatolian-Aegean region is encountered, directed towards west-southwest, reaching velocities of up to 35 mm/yr along the Hellenic arc, relative to Eurasia.

Since 1993, GPS measurements have been used to determine crustal deformation in the area of Greece. An extended reoccupation network consisting of about 100 stations has been measured periodically in numerous GPS campaigns since the late eighties, and a continuous GPS network has been operated in the region of the Ionian Sea since 1995. Special efforts were made to obtain consistent results with highest possible accuracies and reliabilities. Data of European IGS and EUREF sites were included in the GPS processing in order to obtain results which are internally consistent with the European kinematic field and to allow for a regional interpretation. The data has been analyzed to derive plate and intraplate deformation, and to study the strain rate field in the deforming zone between the Eurasian and African plates.

The results have been presented in terms of velocities, time series, trajectories of crustal motion and strain rates. Previous geodetic, geological and seismological findings are substantially refined. New important results include a better quantification of N-S extension from northern Greece to the Gulf of Corinth, a refined description of the kinematic field in northwestern Greece in terms of clockwise rotation and a detailed strain rate field in the southeast Aegean sea. Deformation zones to the north and to the south of the North Aegean Trough and in the West Hellenic arc region were studied in detail. Arc-parallel extension of about 19 mm/yr was found along the Hellenic arc.

In addition to transient strain encountered during interseismic periods particular interest was also given to earthquake-related effects. GPS-derived coseismic displacements were investigated for the Ms 6.6 2001 Skyros (Aegean Sea) and Ms 6.2 2003 Lefkada (Ionian Sea) earthquakes. The coseismic effects were investigated in terms of displacement vectors, differences of velocity vectors, and changes of accumulated strain. Furthermore, the GPS results were compared with fault plane solutions and slip models of the corresponding earthquakes. Discontinuous changes of position of about 75 mm were found for the island of Skyros. The 2003 Lefkada earthquake induced coseismic southwestward displacements of up to 72 mm. It is in agreement with the focal mechanism of the mainshock, which caused a dextral strike slip on a northeast striking plane. The cumulative strain after the Lefkada earthquake indicates an increased seismic hazard for the island of Kefalonia, Ionian Sea, Greece. The deformation field in this area is characterized by pronounced dextral shear associated with the Kefalonia fault zone (KFZ).

While the KFZ terminates the subduction of the Hellenic arc, the North Aegean trough is considered to form the western continuation of the North Anatolian fault zone, separating the Anatolian from the Eurasian plate. Most recent GPS and modelling results are presented by Mueller et al. (this report). These are discussed in terms of ongoing deformation processes including dextral faulting and transtension in the North Aegean sea. Furthermore, pronounced gravity anomalies have been found in this region which are attributed to the plate boundary (see Bürki et al., Limpach et al., Somieski et al., this volume).

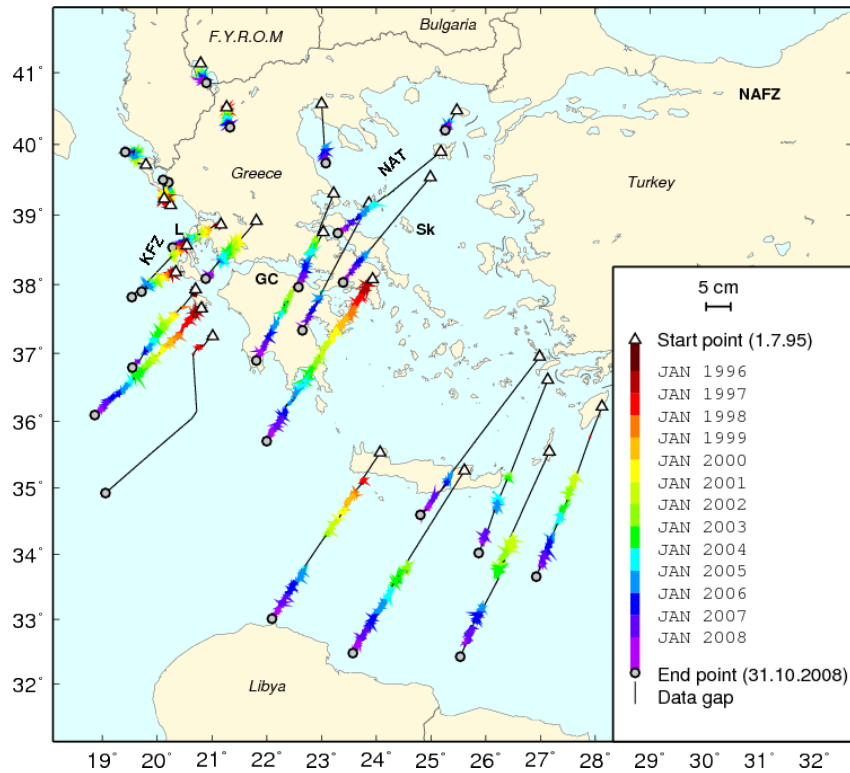


Figure 3.10: Trajectories of crustal motion in Greece for the time period July 1995 to Oct. 2008 based on CGPS measurements (Kahle et al., 2008). GC: Gulf of Corinth, Kfz: Kefalonia fault zone, L: Lefkada, NAFZ: North Anatolian fault zone, NAT: North Aegean trough, Sk: Skyros

## Analysis of long-term GPS observations in Greece and geodynamic implications

by M.D. Müller, A. Geiger and H.-G. Kahle

*Geodesy and Geodynamics Lab, Institute of Geodesy and Photogrammetry, ETH Zurich*

A long-term record of continuous and campaign-type GPS measurements from 1993 to 2009 was compiled in Greece. This data set was homogeneously processed in combination with 72 IGS and EUREF sites located in Europe, North Africa and the Middle East using recently developed processing models. The resulting coordinates were analyzed in order to reduce processing related signals and artifacts. Accurate and reliable rates of crustal motion were calculated, and a detailed kinematic field for Greece was derived. The extension of data records of existing sites and the recent installation of additional continuous and campaign-type GPS sites provide numerous new insights into the present-day kinematic and strain rate fields in Greece (compare Mueller et al., this report).

A special focus was set on the deformation field in the North Aegean domain. This region is characterized by distributed N-S extension and the westward continuation of the North Anatolian fault zone into the Aegean sea. Kinematic block modeling, GPS based strain rate field calculations and Finite Element analyses depict the complex deformation field consisting of NNE-SSW extension and dextral strike-slip. An elementary FE model was set up for the area of the North Aegean domain providing additional insights into ongoing deformation processes in this region (Mueller et al., 2011). The model is kept simple in terms of incorporated faults and rheology. It covers the North Aegean sea, Thessaly, Macedonia and Thrace (Figure 3.11).

The depth of the model amounts to 40 km. Three ENE-WSW to NE-SW trending faults accommodating mainly strike-slip motion were incorporated in the model: The North Aegean trough (NAT), the Skyros-Edremit fault (SEF) and the Psara-Lesvos fault (PLF). The lithosphere was modeled as an elastic material with a Young's modulus of 70 GPa and a Poisson's ratio of 0.25. No fault friction was applied on the contact surfaces as the model is intended to represent a steady-state model. In general, the onset of friction in the FE model would change the energy fractions (strain energy, frictional energy dissipation) and with it the displacements. The application of a friction law requires modeling of a more realistic rheology because the maximum supported shear stress depends largely on pressure and temperature. Crustal heterogeneities and preexisting fault structures are vital features for style and amount of crustal deformation in the North Aegean domain.

Residuals with respect to observed GPS velocities are shown in Figure 3.12 (a). The strain rate field and fault slip rates are depicted in Figure 3.12 (b). The incorporation of strike-slip faults decouples different regions and decreases the strain rates between the faults. Maximum slip rates amounting to 21 mm/yr are calculated on the NAT. Smaller slip rates are concentrated on the southern faults, 10 mm/yr on the Skyros-Edremit fault and 4 mm/yr on the Psaros-Lesvos fault, respectively. The slowly deforming area in northwestern Greece was also identified by applying a kinematic block model.

It can be seen that deformation is confined to distinct areas. Slip rates on the NAT derived with the FE-analysis are concordant with the ones deduced from the locking depth model. The slip rates of the modeled NAT and SEF diminish towards the east because continuous kinematic boundary conditions have been applied. In case of the SEF this effect is of minor importance since right-lateral strike-slip motion is relatively small towards western Anatolia. The model indeed shows that strike-slip motion on the SEF is only to a minor extent due to transferred shear deformation but also caused by the change of direction of velocities, by N-S extension at the eastern border and larger gradients at the western border.

The modeling clearly shows the concentration of strike-slip motion along ENE-WSW to NE-SW trending faults. Pronounced NNE-SSW extension is obtained between Pelion and Chalkidiki. Moreover, residuals with respect to GPS rates point to NNE-SSW extension between Skyros and Agios Efstratios.

Strike-slip characteristics along the NAT were also investigated by the application of a model which is based on a screw dislocation in an elastic half-space (Mueller et al., 2008). Based on this model strike-slip motion diminishes along the NAT from the Ganos fault (22 mm/yr) to the Sporades basin (less than 5 mm/yr). The locking depths vary between 6 and 18 km.

A further elementary FE model was set up to link the slowly deforming South Aegean sea with subduction processes along the central Hellenic trench. The results show that the GPS rates are in good agreement with an uncoupled plate interface. Distinct stress build-up is calculated south of Crete as a consequence of slab geometry and temperature and pressure dependent rheology (Mueller, 2011).



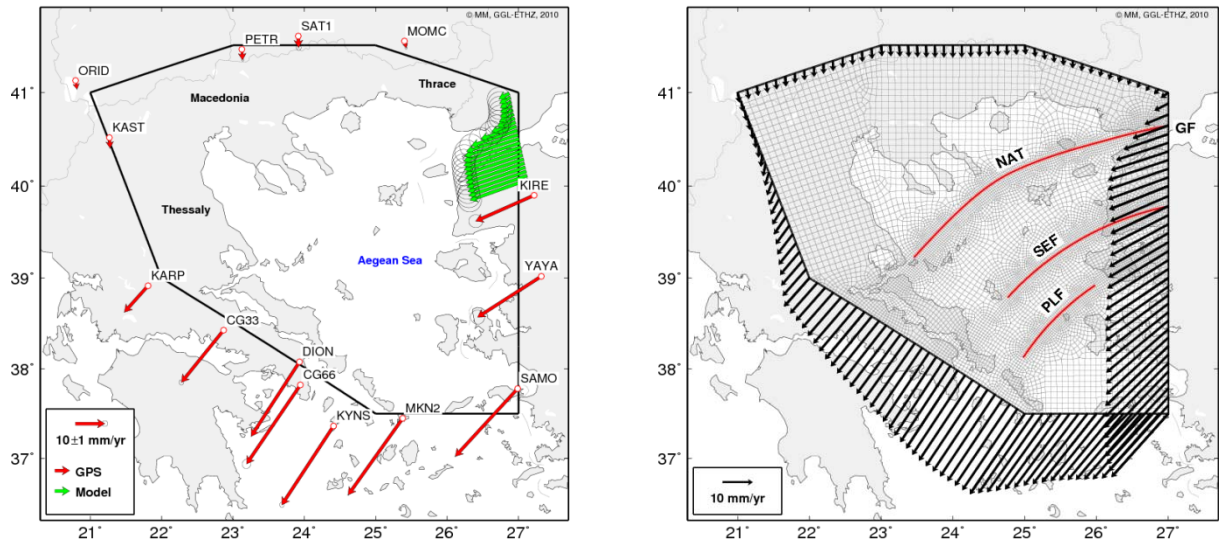


Figure 3.11: (a) Model dimensions (black line) and rates which are used to derive boundary conditions for the FE-model (Mueller et al., 2011). Based on these rates velocities at the model border are predicted using the method of collocation. Red arrows are GPS site velocities. The green arrows correspond largely to the velocity profile derived for the Ganos fault. The rates were transformed to ITRF2005. (b) Kinematic boundary conditions imposed on the nodes located at the border of the FE-model (schematic illustration). The red lines indicate the introduced faults. The light grey lines indicate the mesh of the model. The mesh is finer along the contact surfaces (2.5 km) and coarser in the north and southeast of the model (7 km). NAT: North Aegean trough, GF: Ganos fault, PLF: Psara-Lesvos fault, SEF: Skyros-Edremit fault.

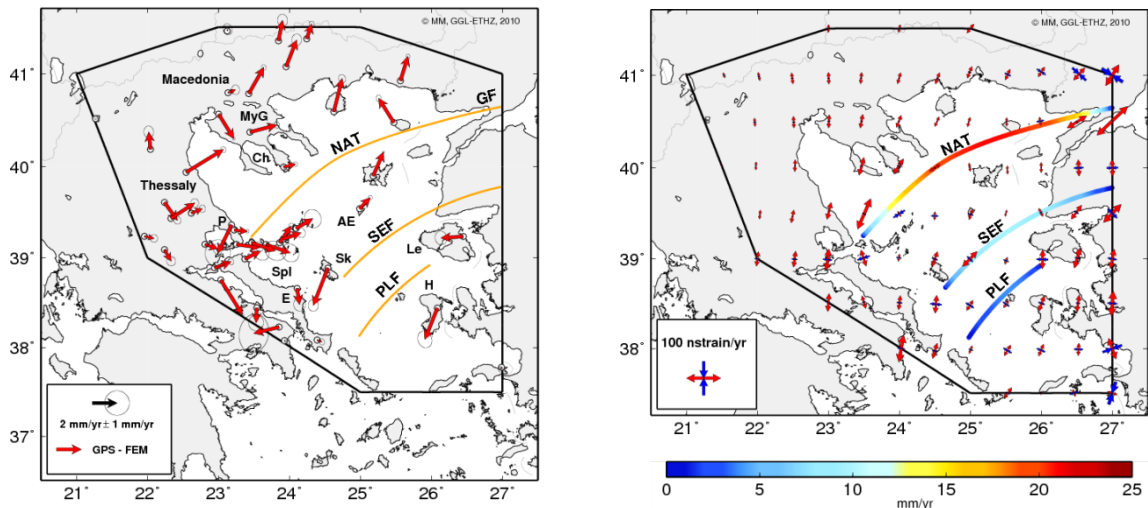


Figure 3.12: Results of FE-modeling. (a) Residuals (GPS rates minus averaged annual FEM displacement rates). The orange lines indicate the introduced faults. (b) Principal strain rate field and fault slip rates corresponding to the indicated colortable (both annual averages). Red arrows denote extension, blue arrows compression. AE: Agios Efstratios, Ch: Chalkidiki, E: Evia, GF: Ganos fault, H: Hios, Le: Lesvos, MyG: Mygdonian Graben, NAT: North Aegean trough, P: Pelion, PLF: Psara-Lesvos fault, SEF: Skyros-Edremit fault, Sk: Skyros, Spl: Sporades islands.

## GNSS Seismology

by S. Häberling and M. Rothacher

*Geodesy and Geodynamics Lab, Institute of Geodesy and Photogrammetry, ETH Zurich*

Earthquakes are globally among the major hazards to human life and infrastructure; additionally, some larger events may trigger a catastrophic tsunami. Fast and reliable quantification of an earthquake is of vital importance for disaster management and early warning systems, not only globally but also for Switzerland. Historically, permanent GPS stations have been operated at 30 seconds or lower sampling rates for studying long-period Earth deformations such as plate tectonics. In recent years the sampling rate has increased up to 100 Hz and considerably improves the observation capabilities for dynamic surface movements during large earthquakes.

The project “High-Rate GNSS for Seismology” funded by the Swiss National Science Foundation is carried out in coordination with the Swiss Seismological Service (SED). The main objective of this project is the thorough investigation of the contribution of GNSS seismology (measuring the dynamic and static displacement with GNSS) to the characterization and quantification of earthquake parameters and, thus, to natural hazards monitoring and early warning systems. For the assessment an end-to-end simulator is developed, where each of the critical steps and all important aspects of the processing can be considered, evaluated and improved. Based on real and virtual earthquakes with specific characteristics, consistent seismograms and ground motions (including static displacements) are numerically generated for station networks with different geometry and density. These waveforms are used to 1) simulate GNSS observations with realistic error sources and to 2) steer and control the motion of a 1D shake table (see Figure 3.13) and a 3D robot carrying a GNSS antenna. The known motion of the shaking table and robot (monitored by a laser interferometer) forms the ground-truth for the movement of the GNSS antenna. The measurements are recorded by our new high-end Javad GNSS receivers at a sampling rate of up to 100 Hz. The processing of these GNSS datasets delivers ground motions that can be compared with those originally generated, in order to assess the quality of the GNSS ground motion recovery. As the final step of the end-to-end simulation, the GNSS-derived ground motions are introduced into a joint inversion with the seismic data. The resulting earthquake characteristics can be compared with the initial earthquake parameters used for the simulation.

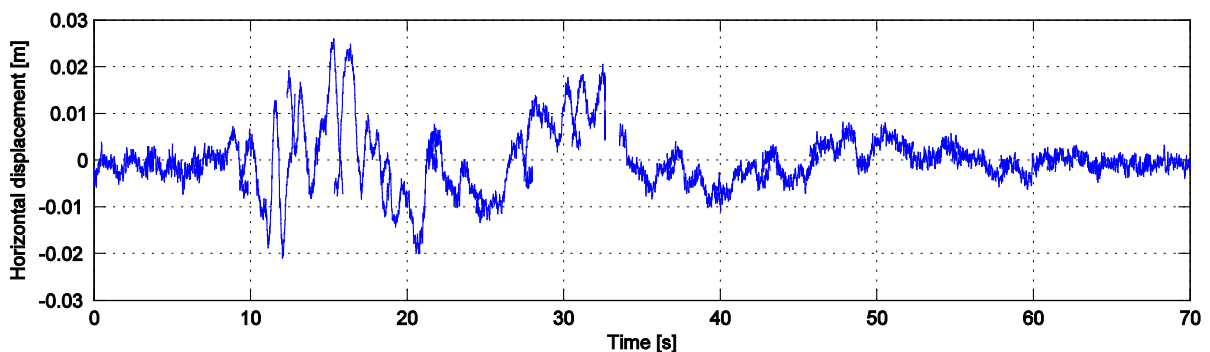


Fig. 3.13: 100 Hz GPS measurements of the downscaled 1995 M6.9 Kobe earthquake generated by a 1D shake table.

## Influence of Atmospheric Pressure Loading on GNSS Analysis

by R. Dach<sup>1</sup>, S. Lutz<sup>1</sup>, J. Böhm<sup>2</sup>, P. Steigenberger<sup>3</sup>

<sup>1</sup>*Astronomical Institute University of Berne*

<sup>2</sup>*Institute of Geodesy and Geophysics, Vienna University of Technology & Gusshausstrasse 27-29, 1040 Wien, Austria*

<sup>3</sup>*Institut für Astronomische und Physikalische Geodäsie, Technische Universität München, Arcisstrasse 21, 80333 München, Germany*

The station coordinates determined by space-geodetic techniques are affected by many effects resulting in geometrical site displacements at different time scales and magnitudes. When analyzing observations of the Global Navigation Satellite Systems (GNSS) it has become widely accepted practice to consider solid Earth tides and ocean tidal loading effects using the latest models for these displacements (e.g., according to McCarthy and Petit 2004), and thus removing the largest effects with magnitudes bigger than a few centimeters.

The repeatability and consistency of time series of weekly station coordinates (e.g., within the International GNSS Service, IGS, Dow et al. 2009) are therefore well below the centimeter level - even for the vertical component (Ferland and Piraszewski, 2009). Several other geophysical effects are currently not taken into account by the IGS for GNSS data processing — even if their expected effects amount to more than one centimeter. Depending on the location of the station such effects are the crustal deformations due to, e.g., atmospheric pressure loading (APL, mainly at inland sites), ocean-induced non-tidal loading (mainly at coastal sites), or continental water mass surface loading in the neighbourhood of the stations.

The reprocessed time series of the CODE Analysis Center (see Lutz et al, 2011) has been used as the basis for a study on the influence of APL on GNSS-derived coordinate time series (CODE: Center for Orbit Determination in Europe, which is a joint venture between the Astronomical Institute of the University of Bern, AIUB, Switzerland, the Swiss Federal Office of Topography, swisstopo, Wabern, Switzerland, the Federal Agency for Cartography and Geodesy, BKG, Frankfurt am Main, Germany, and the Institut für Astronomische und Physikalische Geodäsie at Technische Universität München IAPG/TUM, Munich, Germany).

The study has confirmed that corrections for APL from a geophysical model should directly be applied to the observations instead of an a posteriori correction on the level of weekly coordinate solutions of the space-geodetic services, like the IGS. At first, the repeatability of weekly solutions can be more improved (up to 20% instead of up to 10 to 15%) and secondary, systematic effects in the datum definition may be introduced if the corrections are applied after the processing and the datum definition of the solution (this agrees with the finding from VLBI-analysis published in Böhm et al., 2009).

Correcting for APL directly on observation level has the disadvantage that the model is unrecoverable fixed in the solution. A careful validation of the introduced APL is therefore indispensable. From the practical requirements of an IGS analysis center (operational availability, long and consistent, global series back to at least 1994 for reprocessing purposes) the model from Petrov and Boy, 2004 seems to be best suited.

For validation purpose, scaling factors for the APL corrections from the model have been estimated from 15 years of GPS-data. To confirm the model they are expected to be “one”. On the other hand, to interpret the deviations from the ideal solution in a reasonable way, it is important to consider the magnitude of the variation of the APL effect on the site (the long-term mean effect is absorbed by the station height) because it may vary between more than one centimeter for inland sites and nearly zero at coastal sites. The magnitude of the variations of the APL may be expressed as extracted as the RMS of the APL effect for the particular station taken from the model.

In Figure 3.14 the deviation of the estimated scaling factors for the APL model from “one” is rescaled by the RMS of the APL effect. The dark disks correspond with this setup to a discrepancy of below 1 mm for the vertical and 0.5 mm for the horizontal components between the estimated APL and the APL model itself. They can be seen as a confirmation of the model by the GPS-data analysis. The size of the disk indicates the length of the GPS time series which is an important factor for the uncertainty of the estimated scaling factor. Overall, the APL model of Petrov and Boy, 2004, is confirmed by the GPS-data analysis. It can be considered as a candidate for a direct correction of the observations during the data processing in future.

The study in its full extent including the impact of ignoring the APL corrections on the datum definition in a global network and on obtained satellite orbits has been published in Dach et al., 2011.

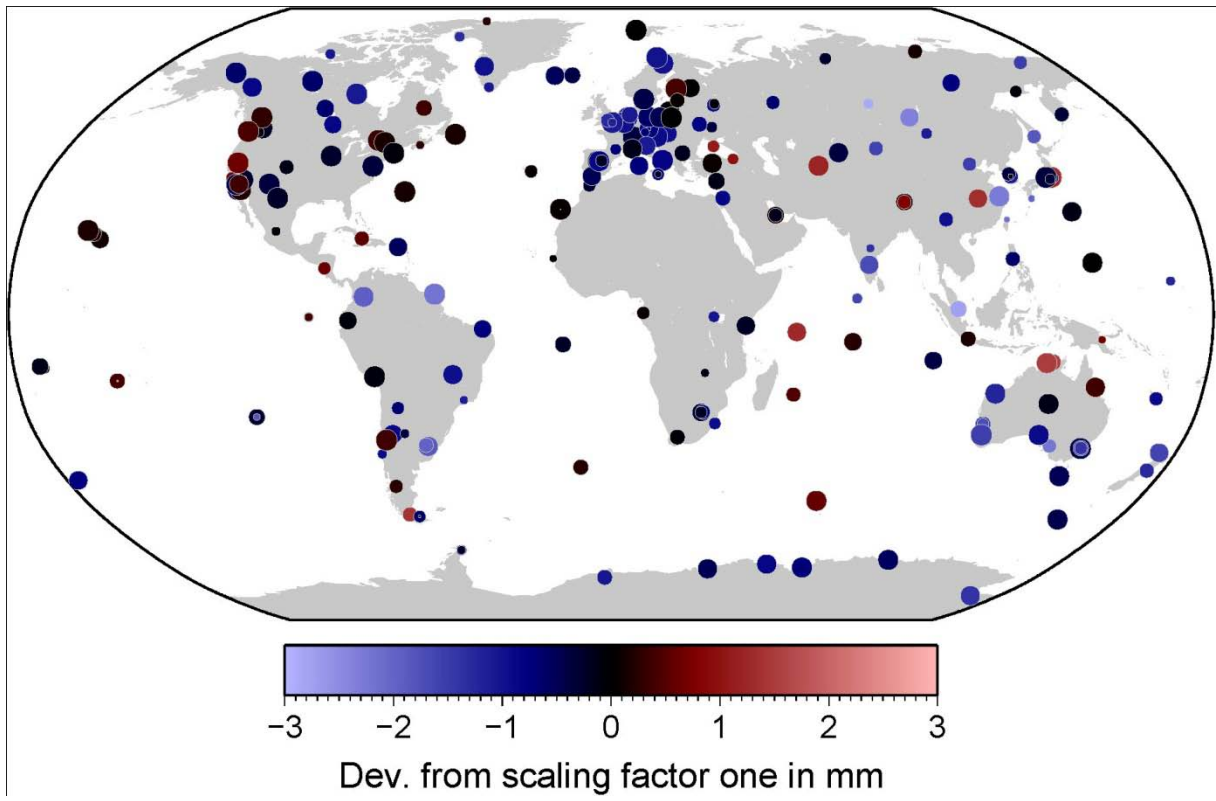


Figure 3.14: Vertical component

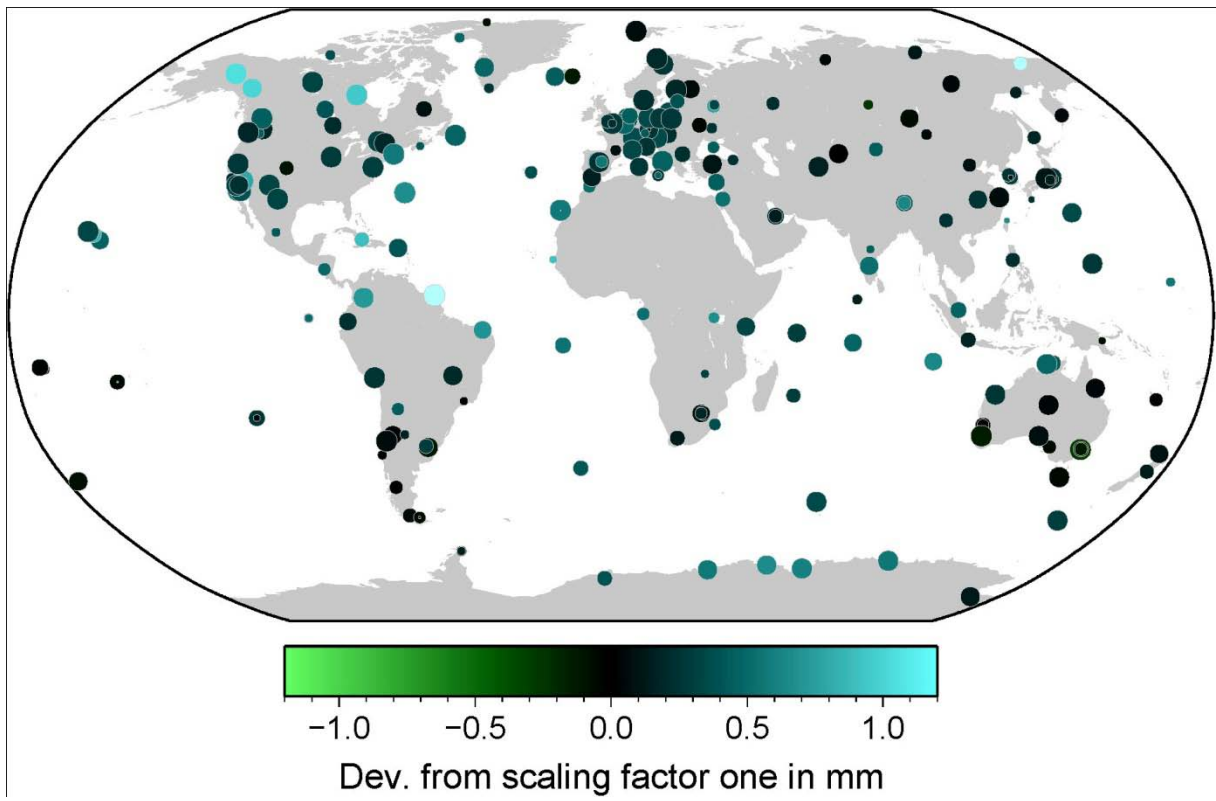


Figure 3.15: North-south component

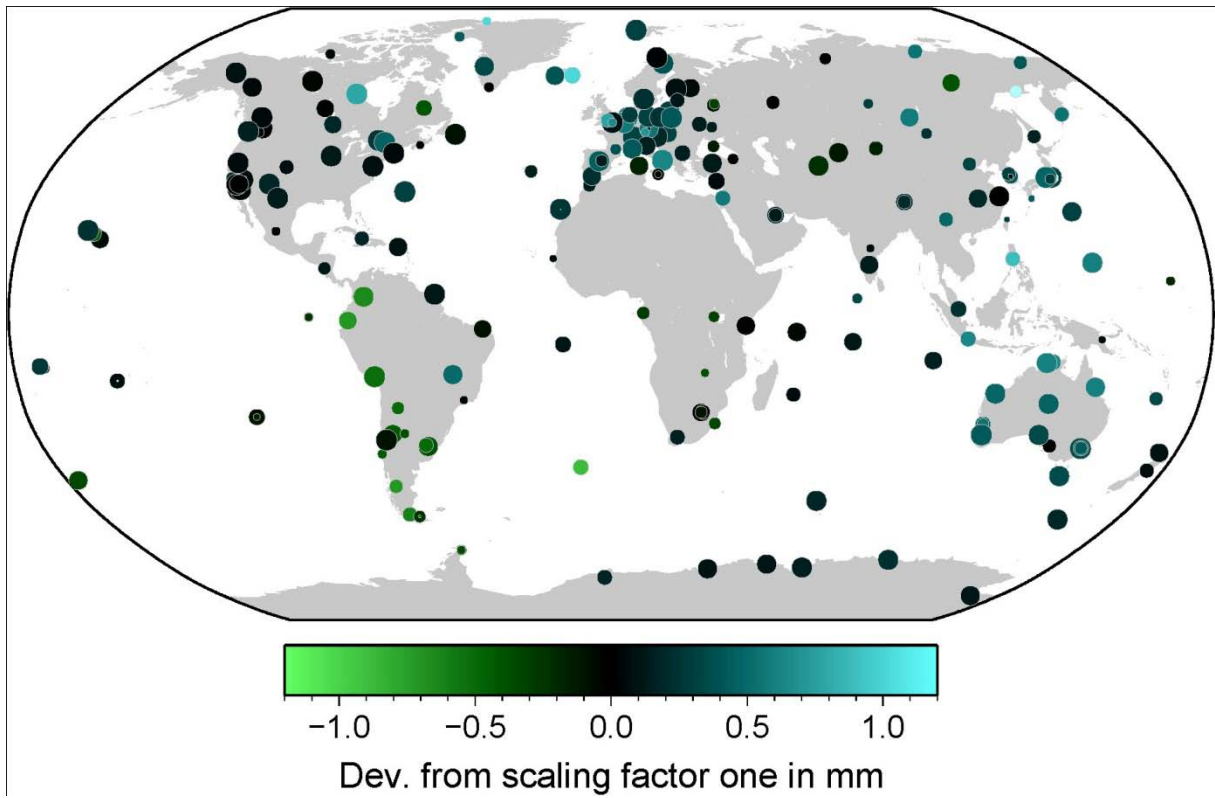


Figure 3.16: East-west component

---

Scaling factors derived from:

○ 15 years of data   ○ 12 years of data   ○ 9 years of data   ○ 6 years of data

Figure 3.17: Deviation of the scaling factors from 1.0 for the APL corrections emerging from the Petrov and Boy (2004) model established by the analysis of 15 years of GNSS data scaled by the size of the APL correction for the station (in units of the RMS of the corrections from the model over 15 years).

## Bibliography Commission 3

- Böhm, J., R. Heinkelmann, P.J. Mendes Cerveira, H. Schuh (2009): Atmospheric loading corrections at the observation level in VLBI analysis. *Journal of Geodesy*, vol. 83(11), pp. 1107-1113, DOI:10.1007/s00190-009-0329-y.
- Brockmann, E., D. Ineichen, U. Marti, S. Schaer, A. Schlatter, A. Villiger (2009): Determination of Tectonic Movements in the Swiss Alps using GNSS and Levelling, In: Kenyon S.C., Pacino M.C., Marti U.J. (Eds), *Geodesy for Planet Earth, Proceedings of the 2009 IAG Symposium*, Buenos Aires, Argentina, August 31 – September 4, 2009.
- Dach, R., E. Brockmann, S. Schaer, G. Beutler, M. Meindl, L. Prange, H. Bock, A. Jäggi, L. Ostini (2009): GNSS Processing at CODE: status report. *Journal of Geodesy* (special Issue: The International GNSS Service (IGS) in a Changing Landscape of Global Navigation Satellite Systems, guest editor C. Rizos), vol. 83(3-4), pp. 353-366, DOI 10.1007/s00190-008-0281-2.
- Dach, R., J. Böhm, S. Lutz, P. Steigenberger, G. Beutler (2011): Evaluation of the impact of atmospheric pressure loading modeling on GNSS data analysis. *Journal of Geodesy*, vol 85(2), pp. 75-91, DOI 10.1007/s00190-010-0417-z.
- Dow, J., R. Neilan, C. Rizos (2009): The International GNSS Service in a changing landscape of Global Navigation Satellite Systems. *Journal of Geodesy*, vol. 83(3-4), pp. 191-198, DOI:10.1007/s00190-008-0300-3.
- Egli, R., A. Geiger, A. Wiget, H.-G. Kahle (2007): A modified least-squares collocation method for the determination of crustal deformation: first results in the Swiss Alps. *Geophysical Journal International* Vol. 168, No. 1, January, 2007 <http://dx.doi.org/10.1111/j.1365-246X.2006.03138.x>.
- Ferland, R., M. Piraszewski (2009): The IGS-combined station coordinates, Earth rotation parameters and apparent geocenter. *Journal of Geodesy*, vol. 83(3-4), pp. 385-392, DOI:10.1007/s00190-008-0295-9.
- Hollenstein, C., A. Geiger, H.-G. Kahle (2007): Crustal deformation field in Greece determined from 10 years of GPS measurements, with special emphasis on time-dependent behavior and the Lefkada 2003 earthquake (solicited). Vol. 09, SRef-ID: 1607-7962/gra/ EGU2007-A-06432. European Geosciences Union (EGU).
- Hollenstein, C., M.D. Müller, A. Geiger, H.-G. Kahle (2008): GPS-derived coseismic displacements associated with the 2001 Skyros and 2003 Lefkada earthquakes in Greece. *Bulletin of the Seismological Society of America*, Vol. 98, No. 1, pp. 149-161, doi: 10.1785/0120060259.
- Hollenstein, C., M.D. Müller, A. Geiger, H.-G. Kahle (2008): Crustal motion and deformation in Greece from a decade of GPS measurements, 1993-2003. *Tectonophysics* 449, pp. 17-40.
- Kahle, H.-G., M.D. Müller, A. Geiger, G. Veis, H. Billiris, D. Paradissis, S. Felekis, D. Galanis (2008): Long-term CGPS measurements (1995-2008) in the Hellenic deformation zone between the Eurasian and African plates. AGU Fall Meeting 2008, San Francisco, USA.
- Lutz, S., P. Steigenberger, R. Dach, S. Schaer, M. Meindl, K. Sosnica (2011): Reprocessing activities at CODE. This volume.
- McCarthy D., G. Petit, eds. (2004): *IERS Conventions (2003)*. IERS technical note 32, Bundesamt für Kartographie und Geodäsie, Frankfurt am Main.
- Mueller, M.D. (2011): Analysis of long-term GPS observations in Greece (1993-2009) and geodynamic implications for the Eastern Mediterranean. Dissertation ETH Zurich.
- Mueller, M.D., A. Geiger, H.-G. Kahle (2008): GPS derived deformation field in Greece. Int. WEGENER conference 2008, Darmstadt, Germany.
- Mueller, M.D., A. Geiger, H.-G. Kahle (2011): GPS derived deformation field in the North Aegean domain and fault related implications. Submitted. *Tectonophysics*.

- Mueller, M.D., A. Geiger, H.-G. Kahle, G. Veis, D. Paradissis, H. Billiris, S. Felekis, J. Galanis (2008): The deformation field in Greece from 13 years of continuous and campaign GPS measurements. *Geophys. Res. Abstr.*, Vol. 10, EGU2008-A-09468. SRef-ID: 1607-7962/gra/ EGU2008-A-09468. European Geosciences Union (EGU).
- Petrov, L., J.P. Boy (2004): Study of the atmospheric pressure loading signal in Very Long Baseline Interferometry observations. *Journal of Geophysical Research*, vol. 109:B03405, DOI:10.1029/2003JB002500.
- Schaer, S., H. Bock, R. Dach, S. Lutz, M. Meindl, E. Orliac, D. Thaller (2011): CODE Contributions to the IGS. This volume.
- Schlatter, A. (2007): Neotektonische Untersuchungen in der Nordschweiz und in Süddeutschland. Kinematische Ausgleichung der Landesnivellementlinien. swisstopo-report 05-45, Bundesamt für Landestopografie, Wabern.
- Schlatter, A. (2009): Rezente Hebungsraten in der Nordschweiz (aus Präzisionsnivellements der Landesvermessung). ENSI Neotektoniksymposium 05.05.09 ETH Zürich. ENSI-AN-6988 öffentlicher Bericht.
- Wiget, A., A. Schlatter, E. Brockmann, D. Ineichen, U. Marti, R. Egli (2007): GPS-Netz NEOTEKTONIK Nordschweiz 2004: Messkampagne im Auftrag der Nagra und Deformationsanalyse 1988 – 1995 – 2004. swisstopo-report 07-03, Bundesamt für Landestopografie, Wabern.
- Wiget, A. (2009): Geodätische Überwachungsnetze in der Schweiz. ENSI Neotektoniksymposium 05.05.09 ETH Zürich. ENSI-AN-6988 öffentlicher Bericht.





## 4 Positioning and Applications

### Real-Time Airborne Mapping

by J. Skaloud, P. Schaer, P. Tomé, Y. Stebler

Ecole Polytechnique Fédérale de Lausanne

The development lead to the conception of an airborne mapping system (Scan2map), whose performance and flexibility is unique world-wide. Earlier version of the system created central activities of a start-up company, while the latter has been transferred as a service to a large international mapping company. The system integrates airborne-laser-scanning, medium format digital camera and navigation sensors and offers real-time mapping with high resolution ( $< 0.1\text{m}$ ) and mapping accuracy ( $1\sigma < 0.1\text{m}$ ). Its setup is ideal for large- or small scale airborne surveying of areas such as open pit mines, gravel pits (for periodic determination of extracted volume), forestry (oblique ALS-mapping collects more information about the canopy), and natural hazards or corridor mapping (power lines, railroads, highways, etc.). Recently, the latest generation of navigation sensors was integrated into the system and a new unit for data synchronization and acquisition was developed.

The algorithmic part of this research focuses on the real-time generation of the laser point cloud from moving platforms. There, the real-time integration of satellite and inertial data was implemented and the integrated trajectory was merged with scanning data via different algorithms developed for this purpose (i.e. fast, approximate, and rigorous). Additionally, two communication technologies suitable for airborne RTK positioning were identified and tested. The real-time generated point cloud was compared to that obtained by post-processing within number of production flights. From that comparison it was concluded that whenever RTK-fixed solution is obtained, and that was 90% of the cases, the respective differences in the laser point-cloud coordinates are not significant for a majority of ALS applications (i.e. smaller than 0.1 m).

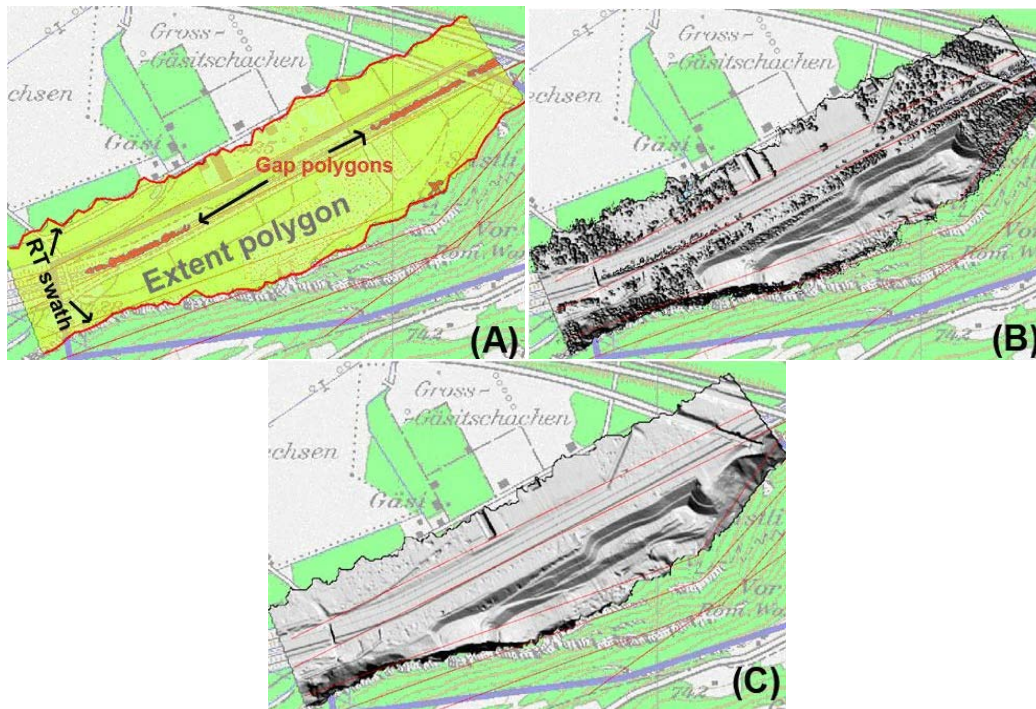


Figure 4.1: Display of different outcomes of the in-flight point-cloud processing: (A) RT swath borders, data extent and gap polygons, (B) DSM hillshade, (C) DTM hillshade.

## Quality Control in Airborne Laser Scanning

by J. Skaloud, P. Schaer, P. Tomé, Y. Stebler, K. Legat

Ecole Polytechnique Fédérale de Lausanne

First part of this research concentrates on the development and implementation of real-time classification algorithms, which are necessary for the production of digital terrain models (DTM) and for the assessment of scanning geometry, which influences the quality of ALS-derived products.

This research area treats time-delayed monitoring of the obtained mapping accuracy. There, a new strategy was developed that allows reliably predicting the quality of differential carrier-phase positioning for cases when transmission of the phase-corrections is not established. Also, a functional model for ALS system errors was developed and optimized for its on-line recovery. Besides the normally considered error sources the model was augmented by the time-delayed estimation of the scanning geometry into the strip-wise quality map. Finally, a technique was conceived that merges the obtained quality indicators established for each laser points with additional information on the scanning density and coverage. The result is a detailed quality-map corresponding to the derived DTM. The technique was optimized for in-flight analyses, but can be applied also in post-mission.

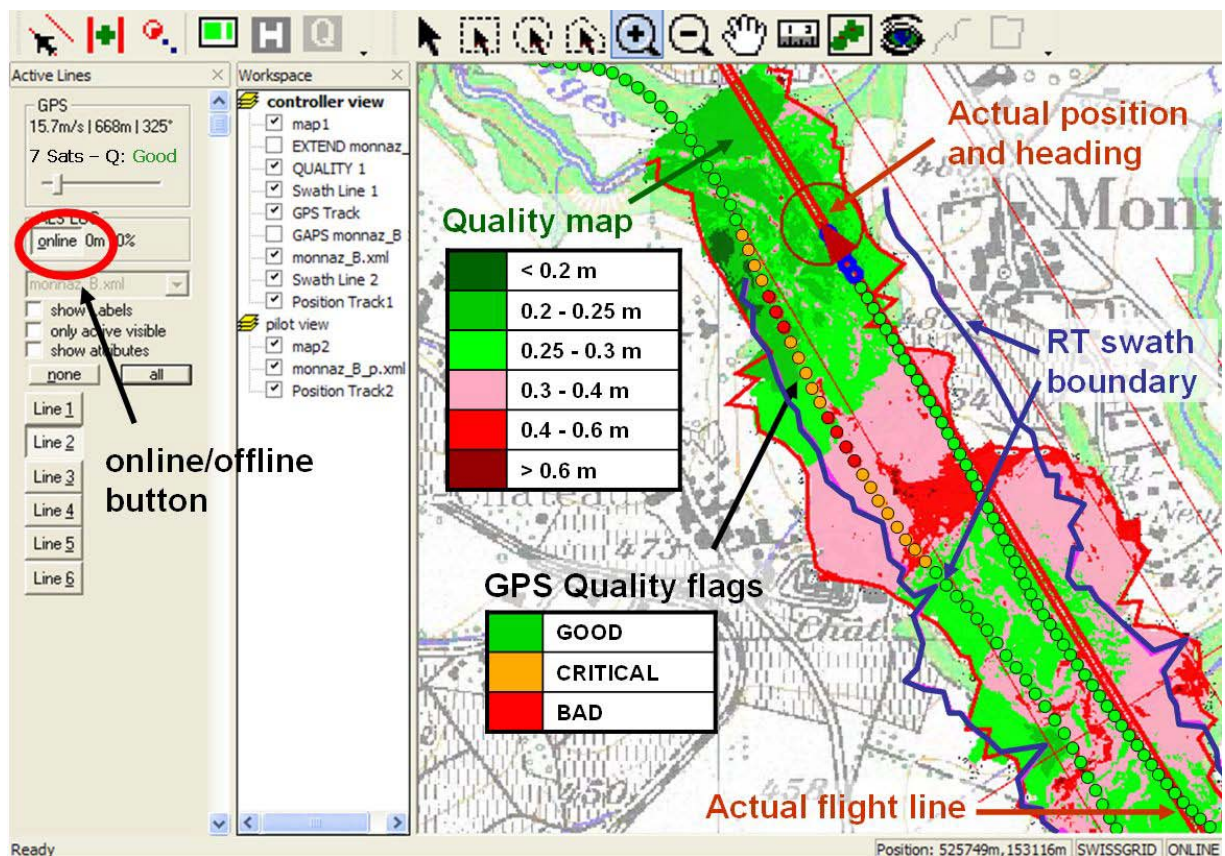


Figure 4.2: Overview of real-time GPS quality monitoring tool.

## Calibration Procedures in Mobile Mapping

by J. Skaloud, P. Schaer, K. Legat

Ecole Polytechnique Fédérale de Lausanne

This research concentrates on the development of algorithms for direct georeferencing and integrated sensor orientation. First, a novel algorithm was derived for the transformation of the sensor's exterior orientation parameters obtained by direct georeferencing (DG) to national reference frames and their subsequent projection for mapping purposes. The emphasis was put on the minimization of distortions arising from the curvature of the Earth and the inevitable length distortion of the map projection.

Second, a new calibration procedure was conceived for medium-format digital cameras when used in direct-georeferencing. This technique minimizes the correlation between the parameters of interior and exterior orientation. The experimental evidence demonstrates its positive influence on the quality of ortho-rectified imagery produced by direct georeferencing (i.e. without bundle adjustment).

Finally, the previously suggested approach for rigorous determination of the bore-sight matrix in Airborne Laser Scanning has been further refined and empirically confirmed on scanners from three leading manufactures. The developed technique is based on expressing the system calibration parameters within the direct-georeferencing equation separately for each target point, and conditioning a group of points to lie on a common surface of a known form.

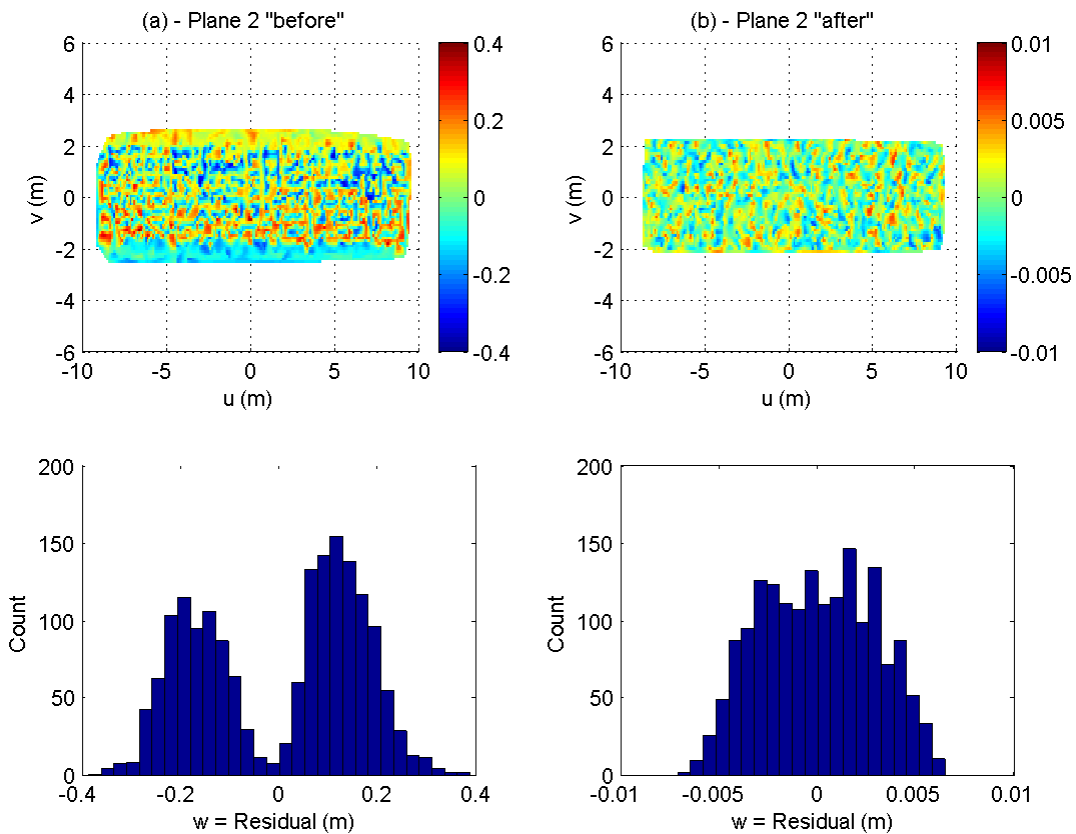


Figure 4.3: The surface plots of the plane-fit residuals in Airborne Laser Scanning with corresponding histograms: (a)-before and (b)-after bore-sight calibration.

## Integrated Sensor Orientation

by J. Skaloud, D. Rouzaud, F. Bayoud

Ecole Polytechnique Fédérale de Lausanne

A previously developed algorithm for vision-aided inertial navigation system has been tested for robotics mobile mapping in outdoor environment.

A new concept was proposed for simultaneous modelling and adjustment of raw inertial, optical and (if available) GNSS observation. This procedure is applicable only in post-mission, however, it allows rigorous and concurrent treatment of dynamic (e.g. inertial) and spatial (e.g. optical) measurements with all spatial-temporal complexity that cannot be expressed in the traditional form of optimal (e.g. Kalman) filtering/smoothing nor the conventional triangulation (i.e. bundle adjustment). The developed theory is for the moment supported only by a simulation scenario from terrestrial mobile mapping where the sections of trajectory lacking GNSS coverage are visited several times. In these parts, the optical observations (ranges and angles) are optimally combined with angular and specific force observations of an IMU through this new approach. The conducted simulations reveal that the parameter estimation via the suggested method is: i) equal to the conventional INS/GNSS integration via optimal smoothing in parts of trajectory when satellites observations are present; ii) largely superior to the optimal smoother when the satellite data are absent and the positioning states derived by inertial coasting are conditioned spatially by optical observations.

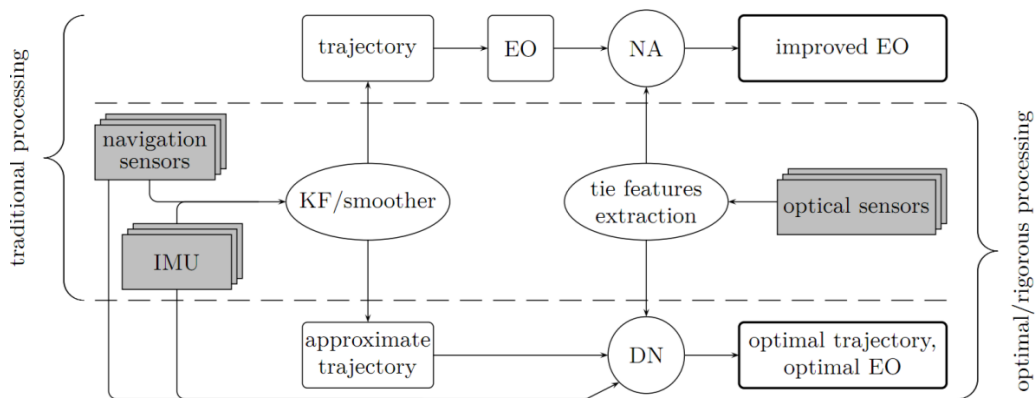


Figure 4.4: Comparison of traditional and proposed integration of navigation and optical sensors in mobile mapping.

## GNSS/MEMS-IMU Integration for Positioning and Orientation

by A. Waegli, J. Skaloud, S. Guerrier, V. Constantin, H. Fournier

*Ecole Polytechnique Fédérale de Lausanne*

This research focuses on the employment of MEMS-IMU's in integrated navigation systems. These low-cost devices are small and lightweight, yet have considerable worse accuracy than the conventional systems used in navigation, kinematics geodesy or mobile mapping. However, a concurrent deployment of number of these devices can potentially improve the quality of trajectory determination in several aspects:

First, the level of noise can be directly estimated thanks to the redundancy of information. This is important as the volatility of observations can vary considerably in these sensors as a function of environmental conditions. When directly observed, the stochastic model in the INS/GNSS integration can be adapted accordingly and continuously.

Second, faulty observations can be detected and isolated prior to the process of integration. For that purpose geometric configurations with n-sensor triads were investigated. It was proofed analytically that in the absence of hardware failures the relative orientation between the triads is irrelevant to system optimality. Several approaches to Fault Detection and Isolation (FDI) are investigated in the context of experiments using reference signals.

Third, the influence of the random errors (uncorrelated and correlated in time) can be suppressed either through direct averaging (i.e. synthetic IMU) or other forms of data processing that are under investigation (i.e. extended or geometrically-constrained IMU).

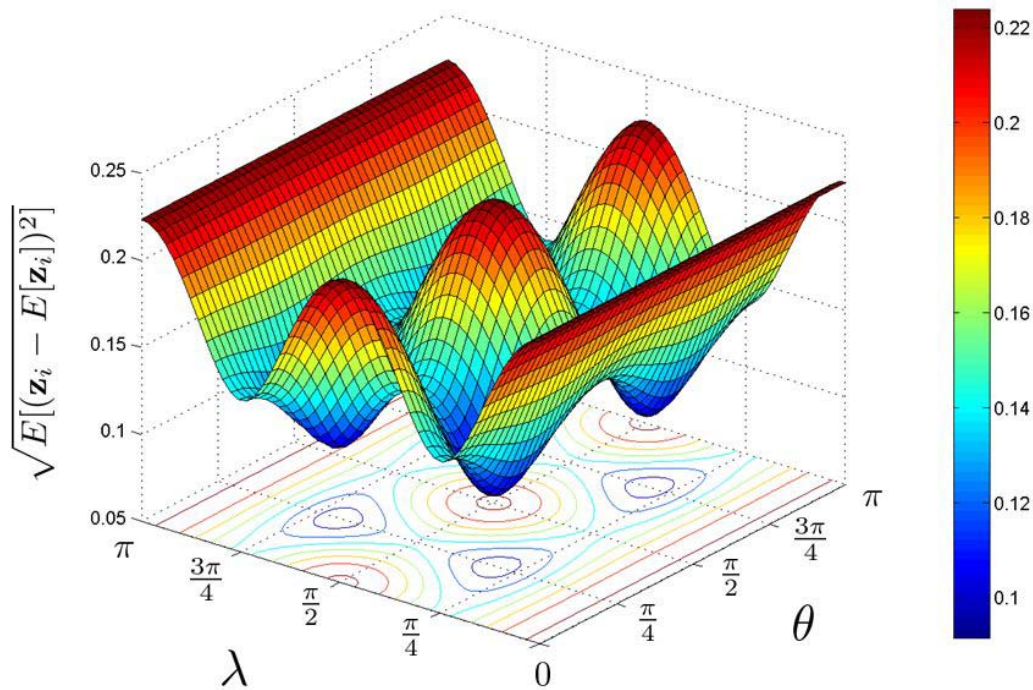


Figure 4.5: Influence of the geometric configuration of a redundant MEMS-IMU system on the controllability of measurements.

## Positioning in dynamic applications

by J. Skaloud, A. Waegli, S. Guerier, P. Tomé

Ecole Polytechnique Fédérale de Lausanne

This research theme deals with trajectory determination in special applications as motor- or winter sports where athletes are exposed to rapid dynamics in surroundings where the reception of satellite signals is intermittent. Furthermore, the ergonomic aspects require employment of small and light-weight devices whenever the sensors are body-worn. Due to these constraints, the reconstruction of the trajectory is based on tightly coupled integration of GNSS and MEMS-inertial MEMS-magnetic observations. The integration methods and performance are evaluated for alpine skiing, where the uninterrupted reconstruction of skier's trajectory opens new possibilities for continuous comparison of athletes' performance throughout the racecourse in terms of position, speed and time. Moreover, when the sensors are rigidly connected to the skis or ski-shoes, other important parameters can be determined with respect to the slope as ski-inclination, side-slipping etc. These parameters are interesting also for moto-sports. There, the ergonomic aspects are less critical and therefore signals from redundant MEMS-IMU configurations can be exploited. In this context, the experimental setups studying concurrent employment of 4 MEMS-IMUs placed on the faces of a tetrahedron shown that the navigation performance can be improved by the factor or two. Other parts of this research concentrated on the development of algorithms for comparing trajectories of different shape with additional parameters (e.g. heart rate, velocities, a motor's revolution, etc.).

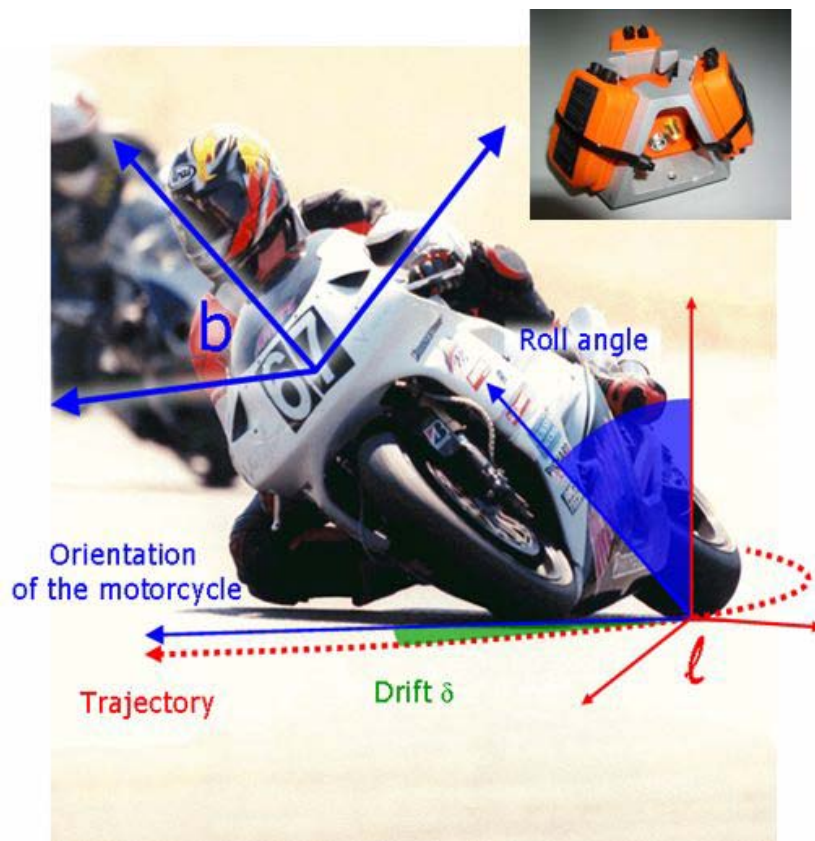


Figure 4.6: Determination of side-slipping of a motorcycle via MEMS-INS/GNSS integration.

## Indoor Positioning and Map Matching

by P.-Y. Gilliéron, B. Merminod, V. Renaudin, P. Tomé, O. Yalak, F. Tappero

Ecole Polytechnique Fédérale de Lausanne

Personal and indoor navigation have grown rapidly with the introduction of ubiquitous computing and new generation of smart phones. Appropriate and accurate positioning is nowadays a central element for many applications and mobile services. However the proper estimation of the user's location remains a challenge. This research domain has mainly focused on the development of concept and algorithms for accurate and reliable positioning in challenging applications (e.g. urban displacement of blind people and guidance of fire-fighters).

In this context, the hybridization of complementary and uncorrelated technologies is necessary for achieving the requirements for a continuous and accurate localization. Some concepts of navigation have been proposed for the improvement of the positioning performance. Most of the investigations are based on the combination of micro-electromechanical systems (MEMS) radio-based systems (e.g. ultra-wideband waves (UWB)) and the use of geographical database. All these technologies provide a large set of raw measurements like accelerations, angular velocities, magnetic field, angles of arrival (AOA), time differences of arrival (TDOA) and also absolute coordinates.

The optimal data fusion relies on filtering techniques (e.g. Extended Kalman Filter (EKF)) complemented with specific motion models. Loose integration and tight integration are considered. One of the most important algorithms is based on the RANSAC paradigm and employs the physical constraints of the pedestrian's walk described by biomechanics. Dedicated map matching algorithms are also developed in order to take into account moving pedestrians within the context of indoor and urban environments.

The validity of the concept has been assessed with indoor experimental results. The tight integration outperforms the loose coupling and enables indoor pedestrian localization with one meter accuracy.

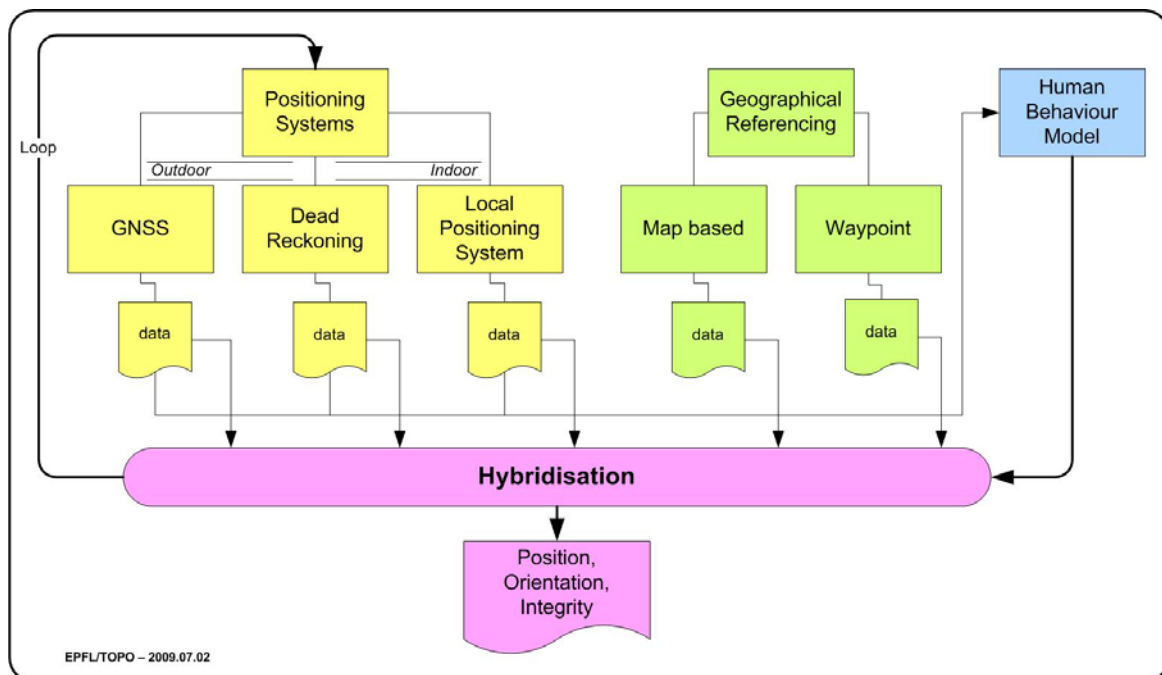


Figure 4.7: Concept of robust positioning system.

## Terrestrial Laser Scanning for Natural Hazards

by J. Wu, P.-Y. Gilliéron, B. Merminod

Ecole Polytechnique Fédérale de Lausanne

An innovative approach is presented for the monitoring of landslides and natural hazards by using laser-scanning technology. This project is mainly focusing on the development of new algorithms for a robust estimation of the terrain deformation. This approach can automatically generate an informative deformation description – so called “deformation map” – providing distinctive characteristics for partial areas, without given *a priori* knowledge. This procedure is entitled as “split/merge” and consists of three major steps – 3D cell splitting, deformation model estimation and deformed areas merging (see Figure 4.8).

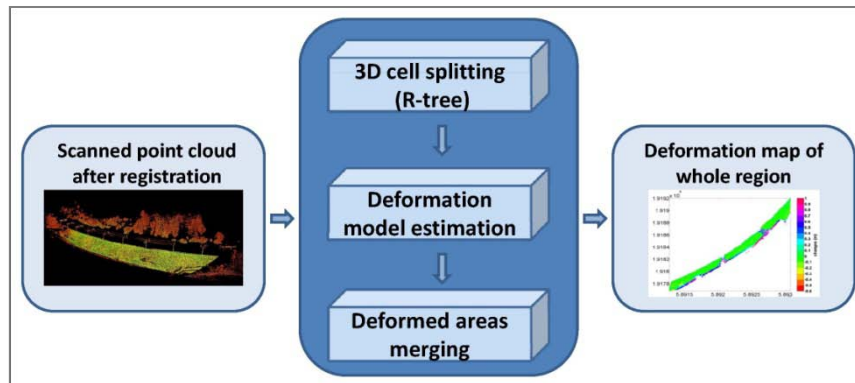


Figure 4.8: System procedure of the deformation map generation.

First, the monitored region is split into 3D uniform cells using a spatial access technique (R-tree), second, deformation parameters of a subset of data are computed for the point clouds in each cell between two epochs by the method of deformation model estimation; third, based on the magnitude of changes in each sub-deformation, all the adjacent and similar parts are merged together by a clustering-based algorithm. Finally the results are presented on a deformation map with the relevant changes of the terrain.

The proposed algorithms have been applied in a real case – a landslide region (about 200 m × 25 m) which had a deep impact on a railway line. This interesting test case has provided practical results for the evaluation of the algorithms. The deformation map of this area (see Figure 4.9) illustrates the vertical displacement derived from this innovative method for the extraction of the deformation parameters of each cell.

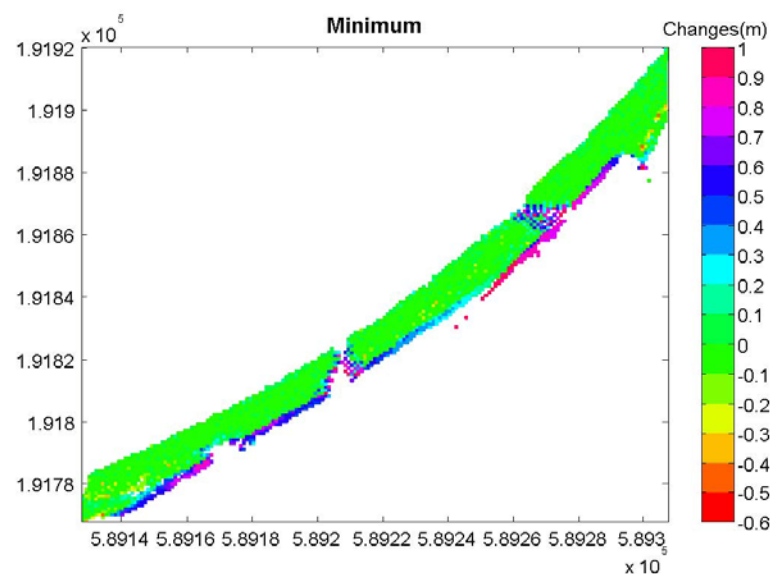


Figure 4.9: Deformation map of the whole slope



## Bernese Software

by R. Dach, H. Bock, U. Hugentobler, A. Jäggi, S. Lutz, M. Meindl, L. Mervart, U. Meyer, E. Orliac, L. Ostini, L. Prange, M. Rothacher, S. Schaer, K. Sosnica, A. Steinbach, D. Thaller, P. Walser, G. Beutler

*Astronomical Institute of the University of Bern*

The Bernese Software (BSW, [Dach et al., 2007]) is at the core of CODE's (Center for Orbit Determination in Europe) activities. CODE is a consortium of four institutions, namely the Astronomical Institute of University of Bern (AIUB, Switzerland), the Swiss Federal Office of Topography (swisstopo, Switzerland), the Bundesamt für Kartographie und Geodäsie (BKG, Germany), and the Institut für Astronomische und Physikalische Geodäsie, Technische Universität München (IAPG/TUM, Germany). CODE is an Analysis Center (AC) of both the International GNSS Service (IGS, GNSS standing for Global Navigation Satellite System) and the European Permanent Network (EPN), and is also an Associated AC of the International Laser Ranging Service (ILRS).

The main goal of the BSW is to provide a high performance and high accuracy reference GNSS post-processing package, integrating the latest commonly adopted recommendations and models (e.g. International Earth Rotation and Reference Systems Conventions), offering the user a maximum of flexibility in customizing processing strategies and options. The BSW comes with a very user friendly interface, but also integrates the so-called Bernese Processing Engine (BPE), a unit for automated processing, especially useful for large network processing and reprocessing efforts. BSW consists of more than 100 programs and of over 1300 modules and subroutines, optimized for speed, is platform independent and is used throughout the world.

There is a big user community of the BSW outside the AIUB with more than 500 institutions all over the world, as shown on Figure 4.10.

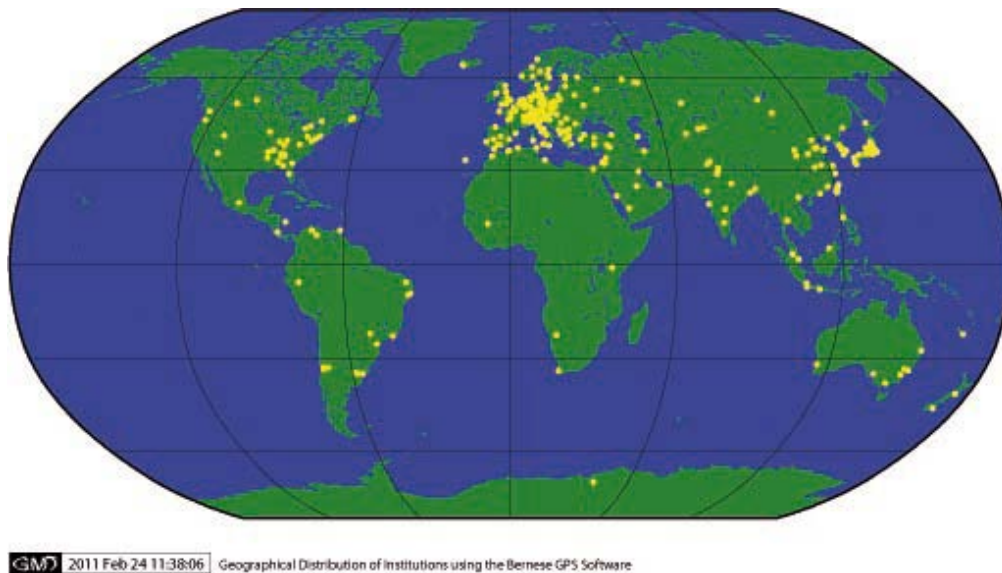


Figure 4.10: Worldwide distribution of the Bernese GPS Software users as of February 2011.

They are still working with version 5.0 of the BSW, but there is an announcement of new version (version 5.2) for the community by the end of 2011. The announcement of the new version with all details is available at <http://www.bernese.unibe.ch/newvers.html>. The most important improvements for version 5.2 with respect to version 5.0 are:

- FODITS: Find Outliers and Discontinuities in Time Series [Ostini et al., 2009]. This tool is dedicated to time series analysis. Time series can be of various types, not only site coordinates.
- An algorithm for GLONASS ambiguity resolution was implemented and validated in CODE routine processing [Schaer et al., 2009].
- Possibility to estimate GLONASS clock corrections [Dach et al., 2010].
- Precise Point Positioning (PPP) now also possible for GLONASS.
- GNSS-specific receiver antenna corrections [Dach et al., 2011]

- Implementation of the new troposphere models: GMF/GPT [Böhm et al., 2006a. Böhm et al., 2006b] and VMF1 [Böhm et al., 2007] for microwave, and Mendes-Pavlis [Mendes and Pavlis, 2004] for SLR data processing.
- Modelling of higher order ionosphere correction terms (2nd, 3rd and ray bending) [Lutz et al., 2010].
- Handling of the quarter cycle L2C shift.
- Update to IERS 2010 Conventions (DE405, OTL-CMC, mean pole, ATL...).
- Geophysical (deformation) models can be introduced as grids and validated by estimating scaling factors [Dach et al., 2011].
- Capability to process SLR-Range data [Thaller et al., 2009].

The above list is far to be exhaustive. A more detailed list of enhancements over the previous version is available from the link given above.

The objective of this new release is to enable the user community to benefit from the latest version developed and used by CODE, but the ultimate, longer-term target, remains a full multi-GNSS version, that can process seamlessly data from any GNSS.

# Multi-GNSS Ambiguity Resolution Algorithms

by S. Schaer<sup>1</sup>, M. Meindl<sup>2</sup>

<sup>1</sup>Swiss Federal Office of Topography swisstopo, Wabern, Switzerland

<sup>2</sup>Astronomical Institute of the University of Bern

We developed three different ambiguity resolution schemes for adequately handling the GPS and GLONASS ambiguity parameters in the “rapid static positioning” mode (where a few minutes or less of data are supposed). We used the well established LAMBDA method for managing the ultimate task of ambiguity resolution to integers. We denoted these LAMBDA-based ambiguity resolution schemes (as illustrated in Figure 4.11) with: “GPS/GLONASS” (without), “mixed-GNSS” (with), and “separate-GNSS” (again without intersystem integer fixing). The scheme of “mixed-GNSS” was added in anticipation of problems due to unjustified, arbitrary integer resolution of intersystem phase biases. It should be emphasized that all these schemes may be easily adapted to schemes coping with dual-frequency, or single-frequency ambiguity parameters from multiple GNSS systems (involving three or more GNSS systems). Concerning our implementation (done into a project version of the Bernese Software), the following aspect is essential: generally all GNSS ambiguity parameters are kept on the level of single (not double) differences. Ambiguity fixing, however, is rigorously done on the level of double differences. The interested reader is referred to [Schaer et al. 2009].

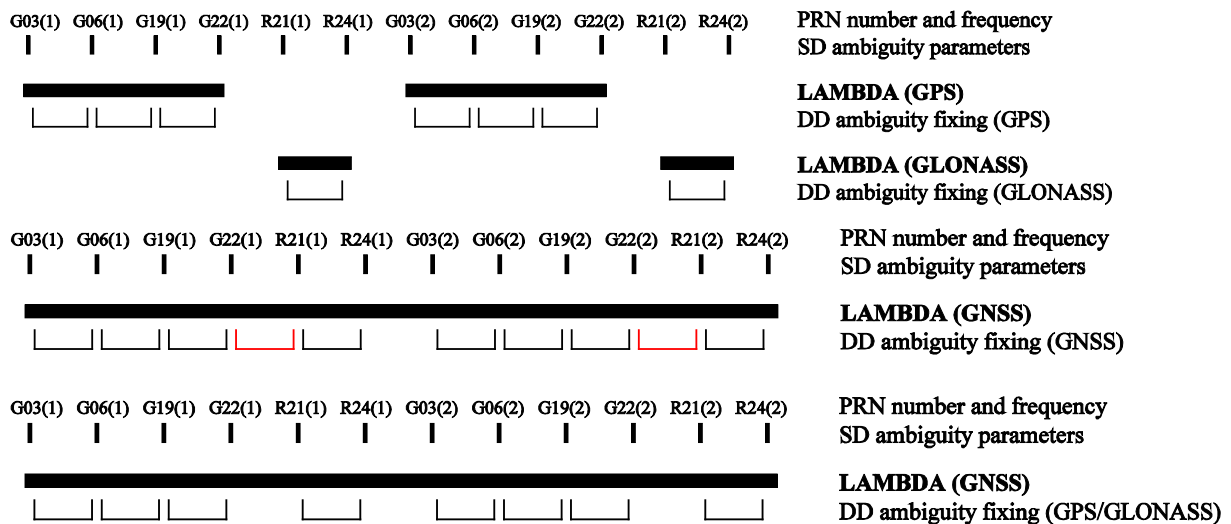


Figure 4.11: Illustration of the implemented “GPS/GLONASS-capable” LAMBDA ambiguity resolution schemes for an assumed observation scenario involving 4 GPS (G) and 2 GLONASS (R) satellites: separate LAMBDA resolution steps for GPS and subsequently GLONASS (top, called “GPS/GLONASS”); common LAMBDA resolution step with (middle, called “mixed-GNSS”) and without (bottom, called “separate-GNSS”) intersystem double-difference ambiguity fixing.

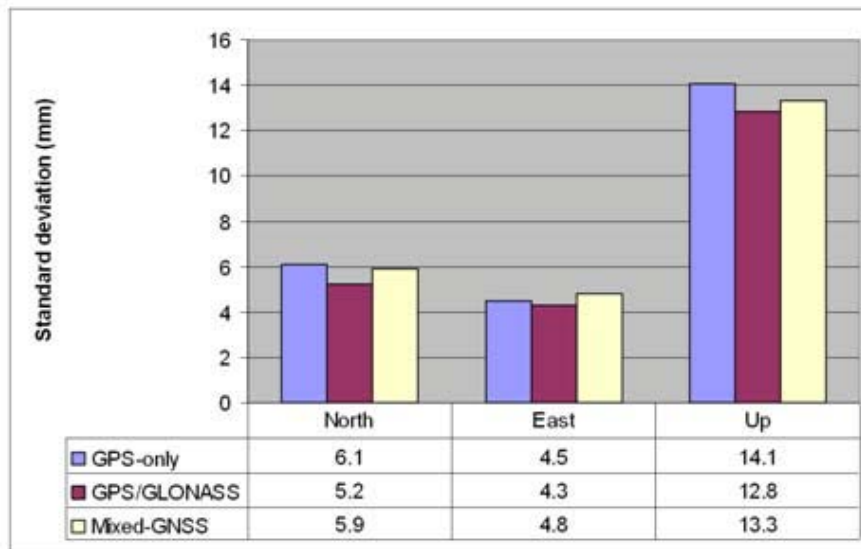


Figure 4.12: Statistics of ZIM2-HUTT baseline vector repeatability results, for September 27, 2008, computed for 288 consecutive five-minute observation spans (using an elevation mask angle of 15°). GPS-only, “GPS/GLONASS,” and “mixed-GNSS” (with intersystem DD ambiguity fixing) results are compared.

The elevation mask angle was used to simulate a gradually increasing restricted satellite visibility. We checked the gathered analysis parameters for each GNSS LAMBDA evaluation (at intervals of 5°) in order to find the maximum elevation mask angle, where a particular GNSS LAMBDA evaluation was just able to provide a correct and adequately accurate baseline vector determination. Figure 4.13 shows that the application “GPS/GLONASS” is in no case inferior to that of GPS-only (the resulting enhancement is always positive or equal to zero). This is more than remarkable.

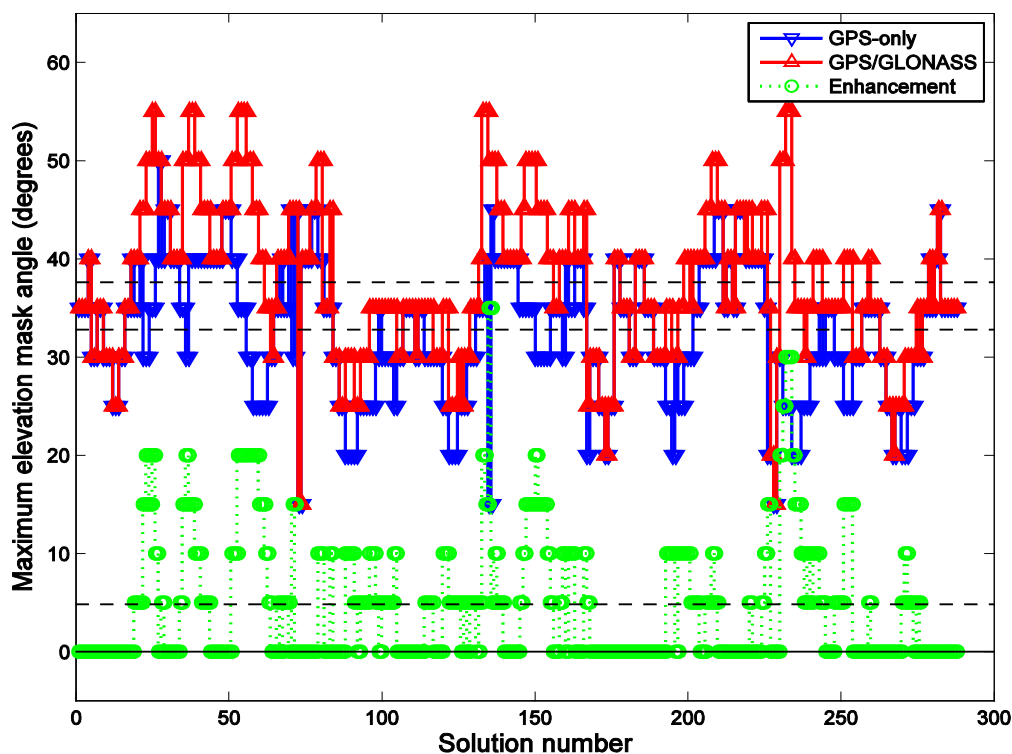


Figure 4.13: Maximum elevation mask angle with successful GPS-only and “GPS/GLONASS” LAMBDA ambiguity resolution, respectively, as determined for the ZIM2-HUTT baseline, for September 27, 2008. Dashed lines indicate daily mean values.

## Analysis and Reassessment of Coordinate Time Series Using FODITS

by *L. Ostini, R. Dach, M. Meindl, U. Hugentobler, S. Schaer, G. Beutler*

*Astronomical Institute of the University of Bern*

The operational processing of data from Global Navigation Satellite Systems (GNSSs) is affected by discontinuities in the resulting time series of products because of model improvements and updates in the processing strategies. Thanks to the computing power available today, it has become possible, to homogeneously reprocess these measurements with the latest processing models (e.g., Steigenberger et al., 2009). One of many other examples is the reprocessing effort of the International GNSS Service (IGS) considering the data starting from 1994. Main products of reprocessed GNSS data are satellite orbits, satellite clock corrections, Earth Rotation Parameters (ERPs), tropospheric Zenith path delay parameters, ionospheric maps, and of course station coordinate parameters, too. As a result of such reprocessing efforts a big number of product time series need to be analyzed asking for an automated tool.

From the analysis experience, however, it is well known that outliers and discontinuities contaminate nearly all position time series even those from homogeneously re-processed solutions. Outliers may be caused by exceptional environmental conditions (e.g., snow accumulation) or anthropogenic effects. Geophysical events, like earthquakes, or simply equipment changes may cause discontinuities in the time series. Unfortunately, there are also outliers and discontinuities in the solution series where the reason is unknown. However, all these events need to be reliably identified to derive accumulated solutions, e.g., for reference frame realization.

For this purpose a new tool has been developed as a component of the Bernese Software (BSW, Dach et al., 2007): Find Outliers and Discontinuities in Time Series (FODITS, Ostini et al., 2008). The result of a cumulative solution (generated, e.g., from a series of normal equation files) is analyzed and reassessed by identifying outliers, discontinuities, velocity changes, and periodic functions in a fully automated way. The results of this tool are prepared to be automatically considered for the next iteration of cumulative solution.

The algorithm of the program FODITS searches the optimal representation of the coordinate time series by adapting a functional model consisting of parameters for discontinuities, outliers, velocity changes, and periodic functions. Epochs of discontinuities (e.g., in case of an equipment change or an earthquake) and velocity changes (e.g., after an earthquake) may be predefined. The corresponding events are tested for their significance. More elements are added to the functional model step-by-step until further components do not significantly improve the representation of the time series anymore.

Figure 4.14 shows the FODITS analysis results for a time series of daily station coordinates from a reprocessing effort for the global IGS-network (generated at CODE, Center for Orbit Determination in Europe). According to the indications in the figure, the analysis of the station REYK identified several significant outliers, an annual signal, two significant (discontinuities due to the) earthquake events (vE1) and (vE3), and two significant (discontinuities due to the) equipment changes (Se1) and (Srae2). Furthermore, in the same figure, we may notice that the earthquake event (ve2) did not induce any significant discontinuity or velocity change, and that the equipment change (sae3) did not induce any significant discontinuity in the time series. For the station WILL, the algorithm revealed two significant discontinuities of unknown reason (D1) and (D2), an annual signal, and several outliers. From both figures --- analysis of REYK and WILL --- we additionally notice how the (colour-coded) standard deviation of the observations improves with the time together with the densification of the GNSS-network and also with the improvement of the receiver and antenna technology.

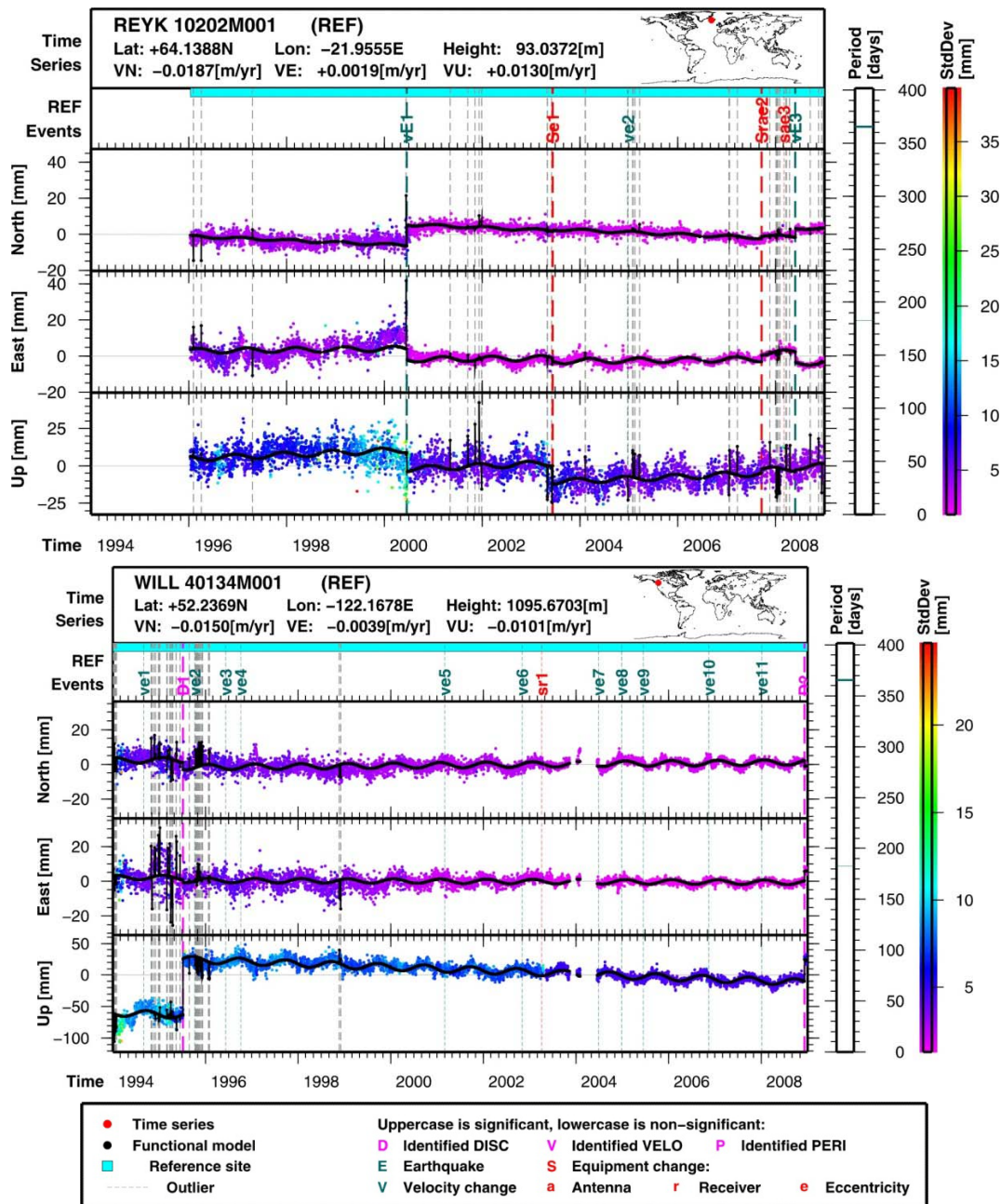


Figure 4.14: FODITS analysis of daily CODE homogeneously reprocessed station coordinate time series.

The global network velocity solutions before (sol-A) and after (sol-B) reassessment of station coordinate time series by the program FODITS are shown in Figure 4.15. A first comparison between the two solutions shows how generally the reassessment of time series corrects large outliers --- for both horizontal and vertical rates --- such as those for stations in South Africa, on the West coast in South America, in Europe, and in Tasmania. In addition, we report that the Root Mean Squares (RMS) of the solution improves from (sol-A) 3.47mm to (sol-B) 1.30mm. This points out that (sol-B) must be better aligned to the underlying TRF than (sol-A). This clearly indicates the improvement of the velocity estimation due to the FODITS analysis identifying events in the coordinate time series.

Analysis and reassessment of station coordinate time series are therefore important steps in reprocessing efforts. Firstly, the analysis allows it to investigate events and signals in the time series. Secondly, the reassessment of position time series allows it to properly align network solutions to underlying TRF frames and to obtain more accurate sets of station positions and velocities.

The (algorithm of the) program FODITS may furthermore be used to analyze other GNSS-derived parameter time series, e.g., kinematic positions, satellite clock corrections, Differential Code Biases (DCBs), etc.

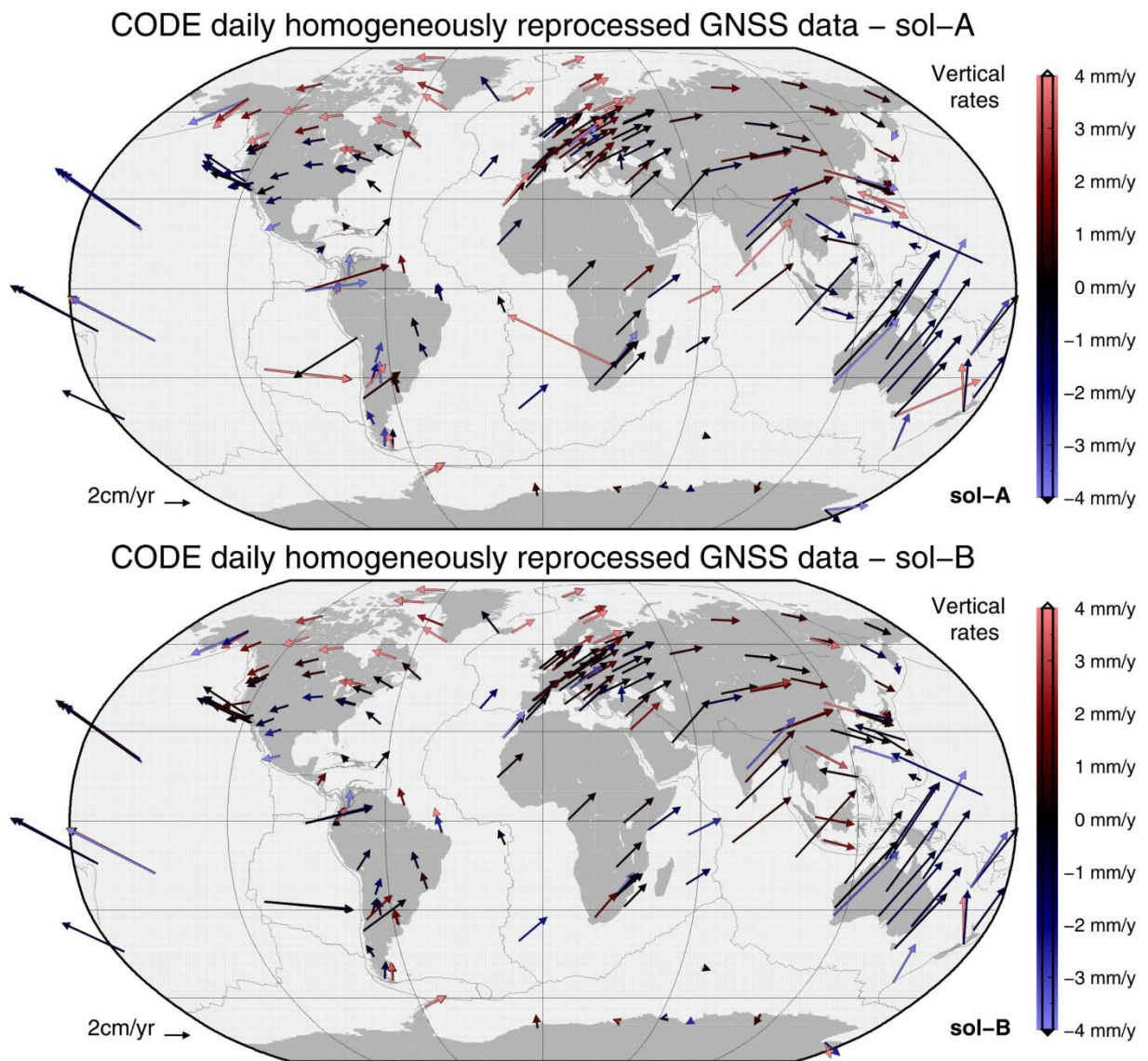


Figure 4.15: Global velocity fields of CODE homogeneously reprocessed GNSS data. (sol-A) before reassessment. (sol-B) after reassessment of position time series by the BSW program FODITS.

## CODE Contribution to Global Ionosphere Monitoring

by S. Schaer<sup>1</sup>, S. Lutz<sup>2</sup>

<sup>1</sup>Swiss Federal Office of Topography Swisstopo, Wabern, Switzerland

<sup>2</sup>Astronomical Institute of the University of Bern

CODE has been extracting information of the total electron content (TEC) from the International GNSS Service (IGS) tracking data since 1995. Since June 1998, related global ionosphere maps (GIM) have been generated in IONEX (Ionosphere Exchange) format and provided to the IGS to support variable applications, e.g., dealing with the ionosphere induced short-term signal variations or the strong horizontal gradients.

In addition to the IONEX product, which is a final product, also corresponding rapid and predicted GIMs are generated at CODE on an operational basis. All GIM products are made available in form of IONEX or as ionosphere files in the internal format of the Bernese Software (Dach et al. 2007). Since July 2000, CODE has additionally been providing RINEX-formatted Klobuchar-style ionosphere coefficients (best fitting CODE's IONEX data).

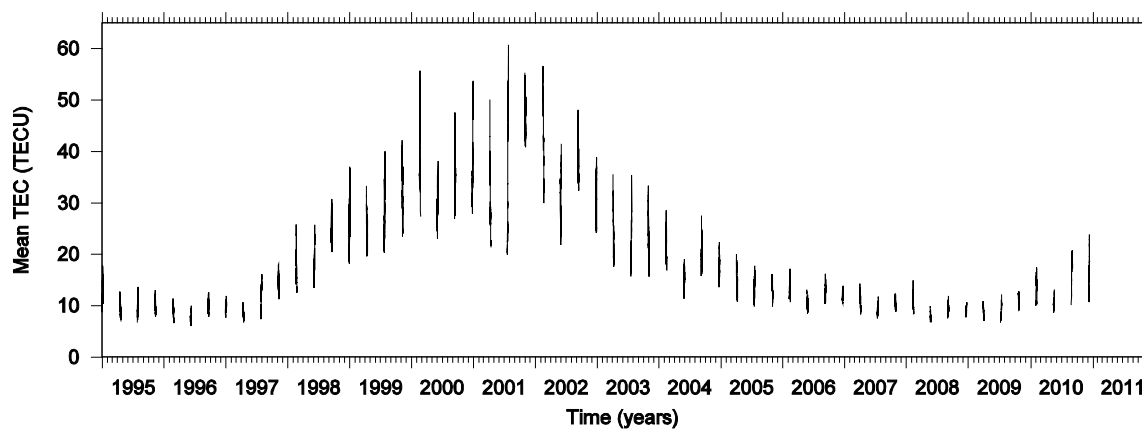


Figure 4.16: The Time series of global mean TEC values extracted from the GIMs produced by CODE covers more than one solar cycle (11-years). Daily averaged mean TEC values, namely the zero-degree coefficients of the spherical harmonic expansion used to represent the global TEC, are shown. Annual and semi-annual variations are visible. The ionospheric signal also includes very pronounced 27-day variations, caused by distinctive groups of sunspots co-rotating with the Sun.

Since the beginning of 2010, CODE has considered not only first-order but also higher-order ionosphere (HOI) and ray bending correction terms for the analysis of space geodetic observations in the operational contributions as well as for a future reanalysis of the data from IGS (Lutz et al. 2009, 2010). It should be mentioned that the previously introduced GIM products are of fundamental importance for computation of these higher-order ionosphere correction terms.

The development version of the Bernese Software was expanded with the ability to assign additional scaling parameters to the second and third order ionosphere term and to the ray bending term. This implementation concept allows switching on and off individually each HOI correction term on normal equation level. Corresponding scaling parameters may be set up globally or even specific to each ground station involved (in order to detect station anomalies and eventually refine HOI correction models). Moreover, the significance of each term may be verified on observation level for different ionosphere conditions.



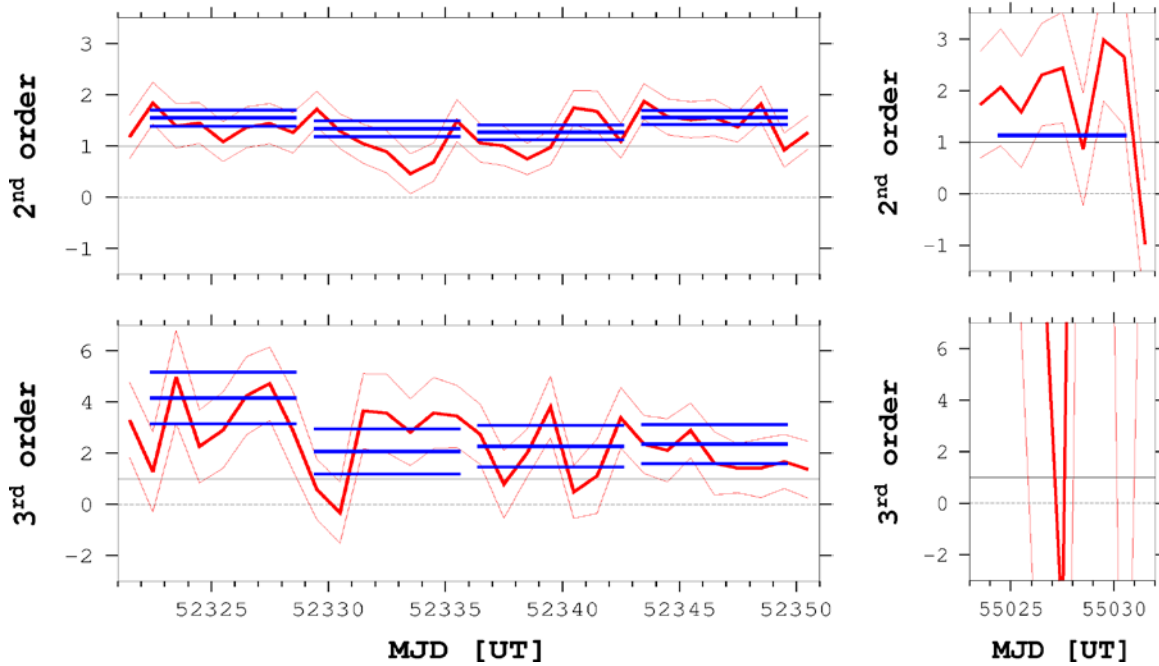


Figure 4.17: Daily (red) and weekly (blue) global scaling factors for the second and third order ionosphere terms are depicted within an interval of their weighted mean RMS covering four weeks with high TEC levels in 2002 (left panels). The situation during one week in July 2009 with low ionosphere activity (right panels) differs completely. The scattering for the daily scaling factors is much more pronounced. This clearly indicates a reduced significance of the HOI corrections for low TEC levels.

In time periods with high ionosphere activity, higher-order ionosphere terms should be considered for global GNSS analysis. In times with low TEC levels, these correction terms are not significant. Depending on station latitude, elevation angle (an elevation mask angle of 3 degrees is used at CODE), and observation epoch, the second order HOI correction term of a single observation may reach few centimeters at extreme cases. Nevertheless, observation corrections due to HOI refraction effects are generally comparably small but the computation of the corresponding correction values is relatively CPU-time consuming. For global analysis, the impact on station positions (and consequently on the reference frame relied on) is of systematic nature and therefore has to be taken into account.

## Geodetic monitoring with 3D adjustment software Trinet+

by P.-H. Cattin, C. Muller

Haute Ecole d'Ingénierie et de Gestion du Canton de Vaud

Nowadays, the geodetic monitoring needs data in three components (East, North, elevation) in order to figure out the internal behaviour as well as global movements of the men's constructions or natural structures. The data acquisition is generally carried out by a combination of GNSS and terrestrial measurements (triangulation, Electronic Distance Measurement, levelling, etc). It is well advised to merge both data in a 3D adjustment model to keep the three dimensional information's. To reach this goal, the Topometric laboratory of the Haute Ecole de Gestion et d'Ingénierie du Canton de Vaud (HEIG-VD) has developed a methodology which consists of using the Swiss GNSS network from Swisstopo and the 3D adjustment software, TRINET+, resulting from a HEIG-VD's project. The first one is linked to the monitoring network and provides a global reference frame. In the monitoring network, the terrestrial measurements provide relative movements. The second one allows to adjust in 3D all the data together, by doing this, the results take into account all the measurements and, the movements are qualified by indicators of accuracy and reliability. Trinet+ allows to analyze those results easier due to his graphical visualization. Several bridges in highways of the Federal Office have been monitored with this methodology. After several campaigns, the global movements are within 5 mm accurate and internal movements are within few millimeter.

In order to confirm, the process, a geodetic monitoring network has been built on the Arenal volcano in Costa Rica, with the collaboration of the volcanology and seismology observatory of Costa Rica. The results have confirmed the ones obtained in Switzerland. Currently, Trinet+ is distributed and used by several geomatic companies.

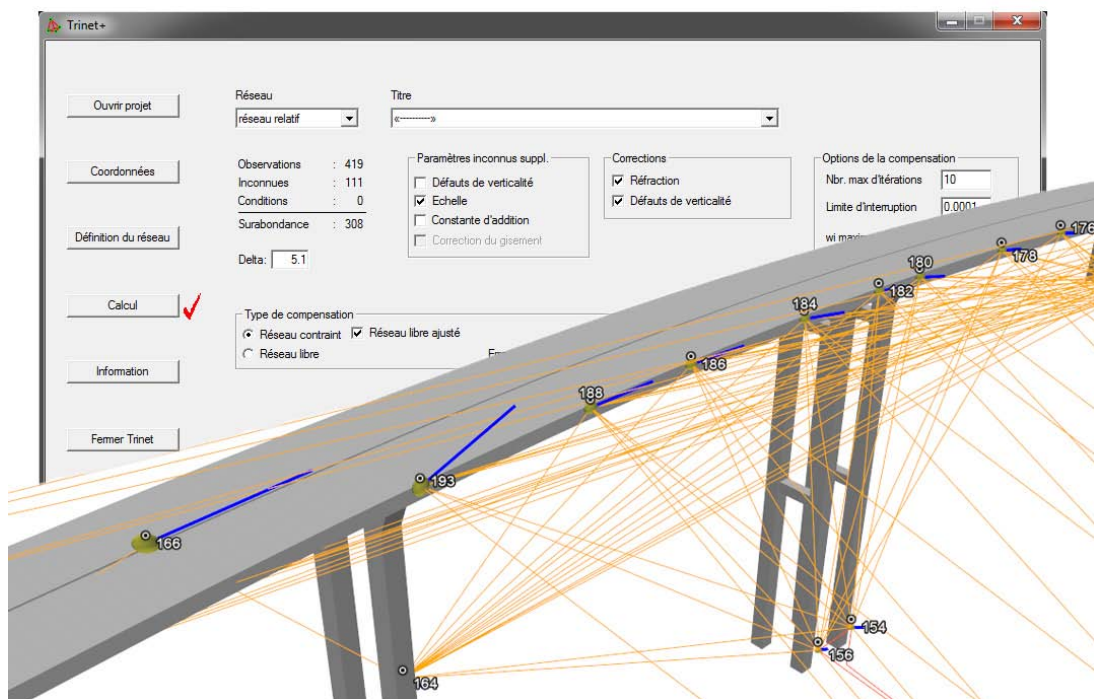


Figure 4.18: Trinet+ and geodetic network

## Near real-time monitoring with low-cost GPS equipments

by P.-H. Cattin, J. Brahier

Haute Ecole d'Ingénierie et de Gestion du Canton de Vaud

The topometric laboratory with the collaboration of MIS institute (Embedded Information Systems) and the REDS (Reconfiguration & Embedded Digital Systems) of the Haute Ecole d'Ingénierie et de Gestion et du canton de Vaud (HEIG-VD) is developing a remote sensor system. This system is made of several low-cost GPS receivers which are able to monitor natural hazard events near real time. Each receiver is composed by one U-blox GPS chip, one Y-Lynx radio module (low energy-consuming) and one battery. It also has a resistant computer; known as base station which is located a few kilometres away from the monitoring site. This system works as follows: first, the base station sends measuring parameters (start and end, frequency of acquisition) to the sensors, second, it receives and stores the GPS raw data (L1 measurements) and finally it transmits this data to a computing center by: Internet, GPRS or Wi-Fi. The automatic post-treatment is carried out by open source software: RTKlib. Then, the results and essential information are published on a webpage.

The Topometric Laboratory is currently testing the whole system on the landslide of La Frasse (Switzerland, VD). Although, these tests are underlining minor weaknesses, the preliminary results are very encouraging because the system is showing that it can detect movements of few centimetres.

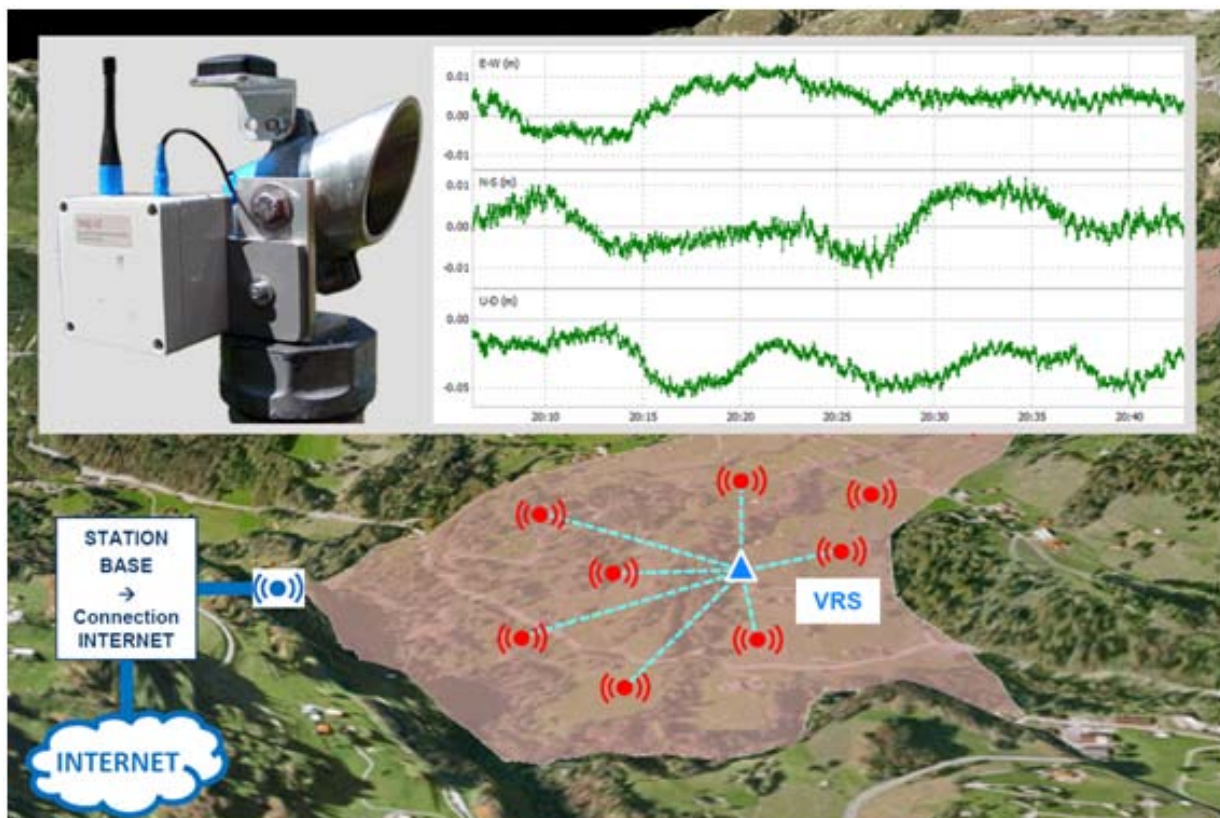


Figure 4.19: Acquisition module and test site

## Points cloud phenomenon: ghosts in the scan

by V. Barras, N. Ferreira, T. Dobers

Haute Ecole d'Ingénierie et de Gestion du Canton de Vaud

Using terrestrial scanner lasers in the field of surveying is extremely interesting. Beyond localized distortions, the results show that specific landmarks no longer have to be indicated in order to obtain modifications in the global form of the object surveyed. The interest becomes even more obvious in eroded areas, where no landmarks can actually be established.

To validate this approach, the first step of our work was to estimate the accuracy and reliability of distances measured by *lasergrammetry*.

Thanks to a battery of tests, we have assessed the quality of distances obtained according to several parameters, such as matter, colour, humidity, direction, or distance. The result of more than 550 scans, performed between 5 and 80m with 3 scanners (SanStation2 and HDS 3000 with TOF, HDS 6100 with phase technology) has shown surprising reactions.

If humidity doesn't bring about any specific reaction, the returns of high intensity (between 99% and 100%) are completely different for both tested pulse lasers. The distances are not correctly appraised and give inaccurate points by more than 2cm on surfaces with a high albedo. A filter applied to the latter measures significantly reduces the noise and makes modeling easier.

Another part of our research was devoted to the detection of bumps and perforations. 3 mm slots are already detectable, even at 80 meters. In this case, the phase laser hardly competes with both pulse instruments above 20 meters. The density and size of the impact do not allow detection of the perforations in the cloud noise.

The conclusions of our work show that it is quite possible to use scanner lasers for surveying activities, especially when expected distortions exceed 5 mm.

A real test was performed on a discharge ramp at the foot of a dam. This high-resistance concrete water slide takes up the huge erosion forces led by alluvia at the time of draining. During the ALTer project, our institute has quantified distortions and highlighted the most eroded areas. Moreover, methods of result modeling for a simplification of the observed 3D phenomena constitute an important part of the on-going work. Solutions integrated into browsers are currently being developed.

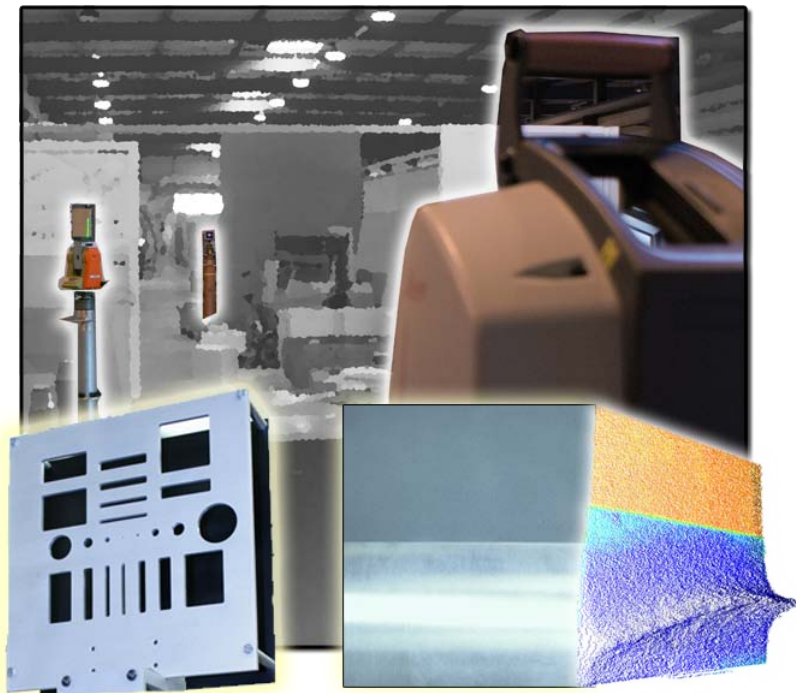


Figure 4.20: Materials and one result of points cloud



## swipos: Lizenzenwachstum

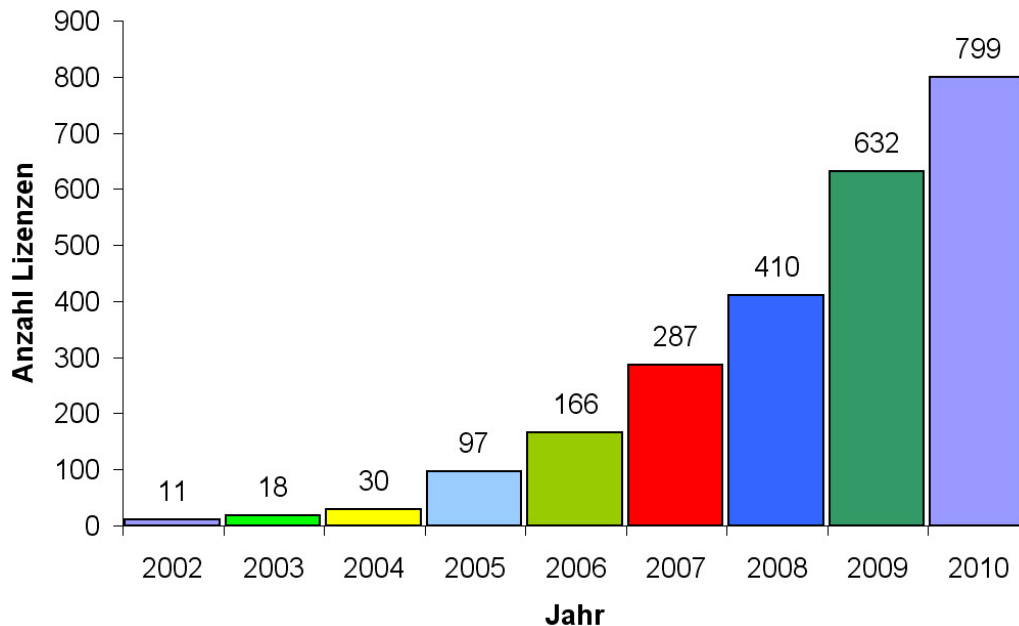


Figure 4.22: Number of swipos licences 2002-2010

In November 2008 some tests on an excavator have been performed (Hardegger, 2008). The main goal of the tests was to demonstrate the feasibility of the machine control using swipos and to assess the achievable accuracy. It has been shown, that the overall accuracy (RTK and the internal calibration of the machine sensors) is about 5 cm. This accuracy is sufficient for some applications like excavation, but for other applications like grading or coating especially the accuracy of the height component is insufficient, here the enhancement with laser is still necessary. At the same time also first applications have been realized in precise farming.



Figure 4.23: Excavator tests

In 2009 the new swipos-INFRA service has been launched for applications in real-time monitoring of infrastructure or landslides. The main idea of the service is to connect local monitoring networks to AGNES by streaming station data to the local network centre. In order to show the feasibility of this concept a monitoring network, consisting of one reference station and two monitoring stations situated in a land slide in the region of Braunwald (GL) and the data of the 6 surrounding AGNES stations have been commonly processed in the real-time monitoring software Trimble Integrity Manager (TIM). Different scenarios of combining the local data with

the reference stations have been studied. The stability of the reference station and the known movements of the land slide of about 2cm/year could be verified (Ulrich et al., 2009).

In order to further improve swipos from a technical and organizational point of view, at the end of 2009 the project swipos-II has been started. After a review and redesign phase (Andrey et al, 2010; Euler, 2010) the four partial projects “infrastructure”, “migration”, “service management” and “new services” have been defined. In 2010 the realization phase started with installation of new communication lines between the AGNES station and the control centre, the elaboration of a concept for a new AGNES/swipos control centre and the procurement of the new software Trimble VRS3Net.

# Control Point Data Service (FPDS)

by M. Burkard

Swiss Federal Office of Topography swisstopo, Wabern, Switzerland

The Control Point Data Service (FPDS) will make available all geodetic control points in a central database, and a part of the information may also be obtained over the Internet. A graphical user interface for revisions and for the administration of the database by the cantonal surveying authorities operates stable since the end of 2006 (Figure 4.24). The central database contains 700 points for category LFP1 (responsibility of swisstopo) and almost 100% or 24'600 points for category LFP2 (on average 0.5 points per km<sup>2</sup>, responsibility of the 26 cantons and the principality of Liechtenstein, status February 2011, not all data are approved). The database of the height control points is completed: 8'600 points of category 1 (HFP1) and 6'900 points of category 2 (HFP2).

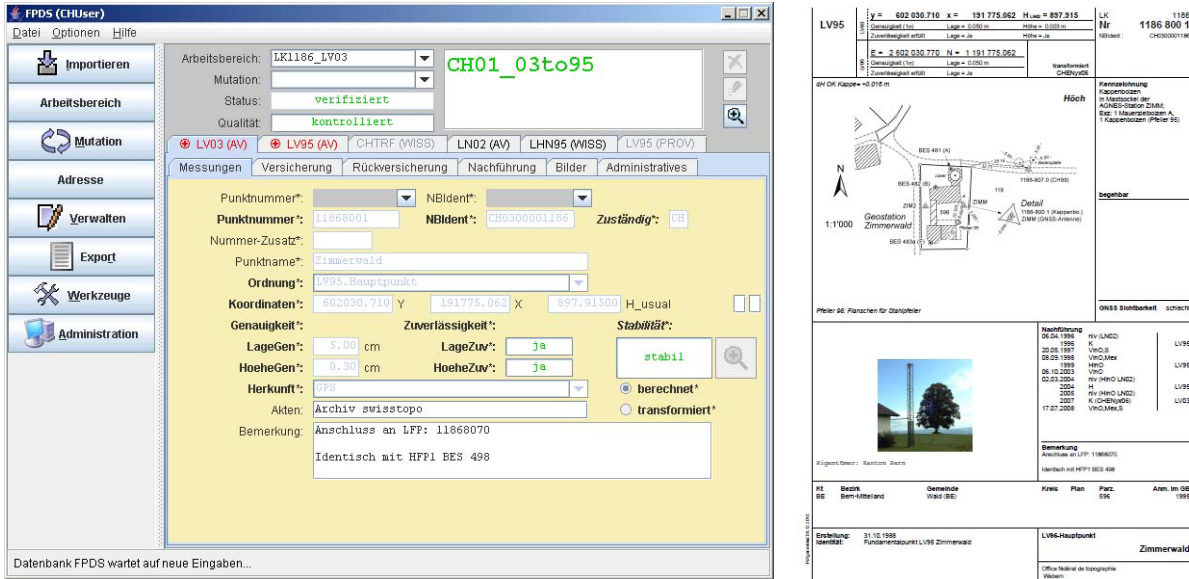


Figure 4.24: User interface for administering the control points in Switzerland (left) and generation of a summary page in pdf file format (right). Example point 1186.800.1 at geostation Zimmerwald.

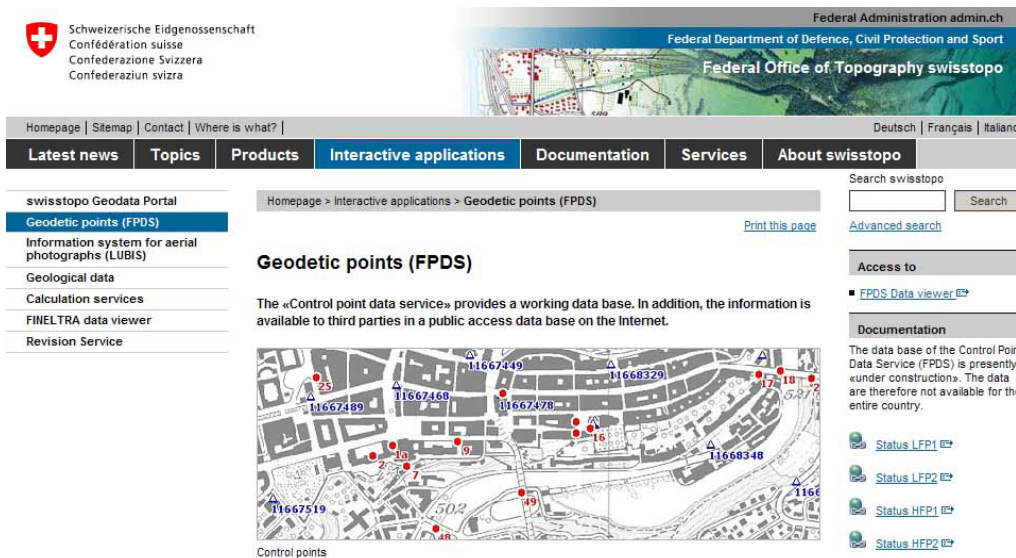


Figure 4.25: Web page design using a content management system (CMS) displaying the FPDS viewer and the current status of the available data of geodetic control points

The public FPDS viewer, which displays the control point information on background maps at different scales on the Internet, has been operational since January 2006 (Figure 4.25). In addition, with different search functions (e.g. by point number, coordinates, city names, etc.), information to the corresponding control points may be accessed.



## GIS System for the National border of Switzerland

by B. Vogel

Swiss Federal Office of Topography, swisstopo

The definition, the realization, the surveying, and the documentation of the Swiss national border is defined on the level of federal law (geoinformation law GeoIG Art. 22, 24 and federal surveying by-law LVV Art. 13). Therefore, this is a task for the Swiss Federal Office of Topography swisstopo. The Swiss national border is a reference data set which is binding for all public authorities. The characteristics of the national border are defined by a commission consisting of the concerned countries and cantons. The maintenance work for the markers of the national border is regulated in different interstate agreements. The description and documentation of the course of the border is part of these agreements.



Figure 4.26: Example of a marker of the Swiss national border

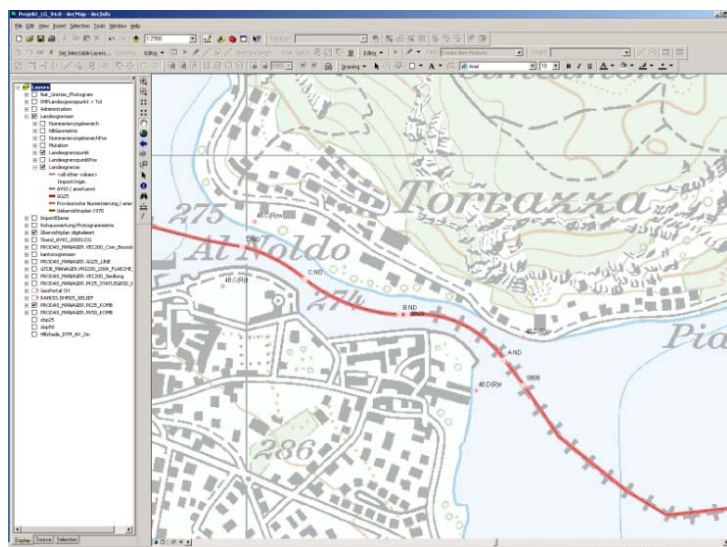


Figure 4.27: Print screen of the GIS for the national border

In future, the Swiss national border is administered by swisstopo using a GIS-system which can easily provide the necessary documentation based on a well defined data model (see Figure 4.27).

In first priority, the complete border is harmonized to enable an interface to the national coordinate reference frame (LV03 or LV95), the European reference frame ETRS89/ETRF93, and the reference frame of the neighbouring countries. This affects the coordinates of the markers as well as the documentation of the borderline. A data checker “CheckService CheckCH“ was developed in order to ensure consistency between national border, border of the cantons, border of the municipalities and the border of private estates.

In second priority, the documentation (protocols, maps) and administration of the notification messages regarding damages of markers will be modernized.

The Swiss border measures in total 1899 km. According to Figure 4.28 it consists of:

- 717 km artificial border (straight line between markers)
- 436 km border along rivers or lakes
- 746 km border along water divides

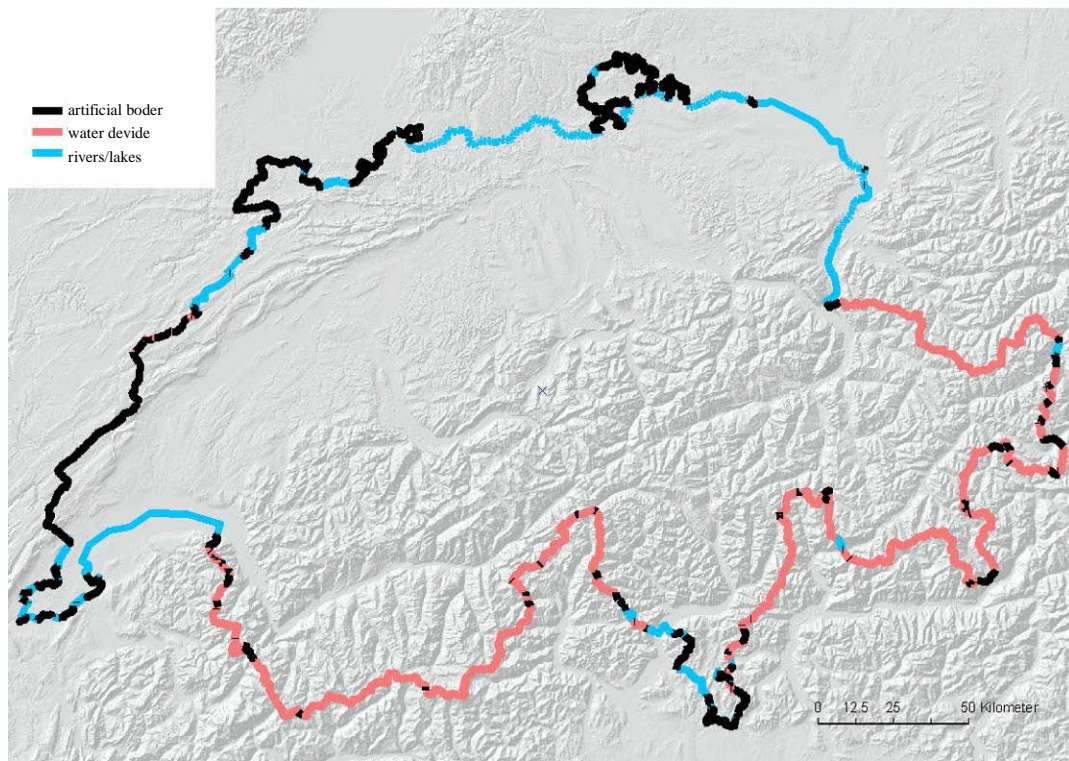


Figure 4.28: The Swiss national border

## Contributions of swisstopo to GNSS Meteorology

by E. Brockmann, D. Ineichen, S. Schaer

Swiss Federal Office of Topography, Swisstopo

Since 1999, swisstopo has been active in different projects covering the area of GNSS meteorology. swisstopo contributed on a routine basis to the European projects COST-716, TOUGH, E-GVAP I + II (with a product availability of more than 98%). Under the umbrella of EUMETNET, estimated troposphere parameters of more than 1500 permanent GNSS sites are provided by 13 analysis centers with an averaged time delay of 1.5 hours (status February 2011; see Figure 4.29).

Due to a memorandum of understanding between EUREF and EUMETNET, signed in 2007, radiosonde data of more than 200 stations can be provided also to the geodetic community. Many of them are closer than 20-30 km to the next GNSS site, allowing comparisons between these collocated sites. Totally 13 sites out of the GNSS sites processed at swisstopo have collocations with radiosonde data. In Switzerland, the so-called super site PAYE is processed by all analysis centers. Comparisons of troposphere parameters are also displayed on swisstopo's monitoring web pages (see Figure 4.30 and 4.31).

Swisstopo supported also the Swiss project GANUWE (finished end of 2010; funded by the Federal Office for the Environment) providing double-difference residuals of its post-processed solutions for GNSS tomography applications. The troposphere parameters are also provided to the STARTWAVE database maintained by the Institute of Applied Physics (IAP) at the University of Berne.

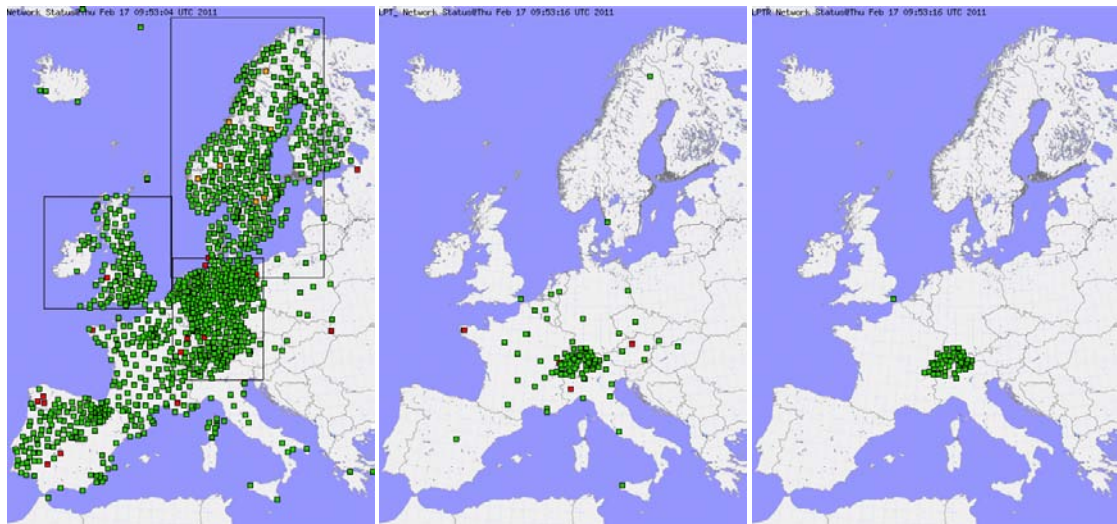


Figure 4.29: GNSS permanent sites processed by all analysis centers (left), processed at swisstopo in near real-time (middle) and processed in real-time (right) on February 17, 2011, 10:00 UTC monitored within the E-GVAP project of EUMETNET

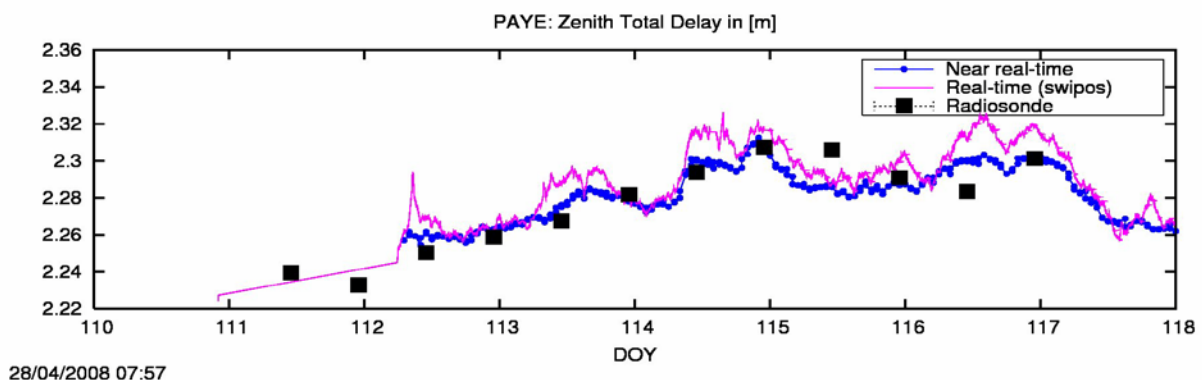
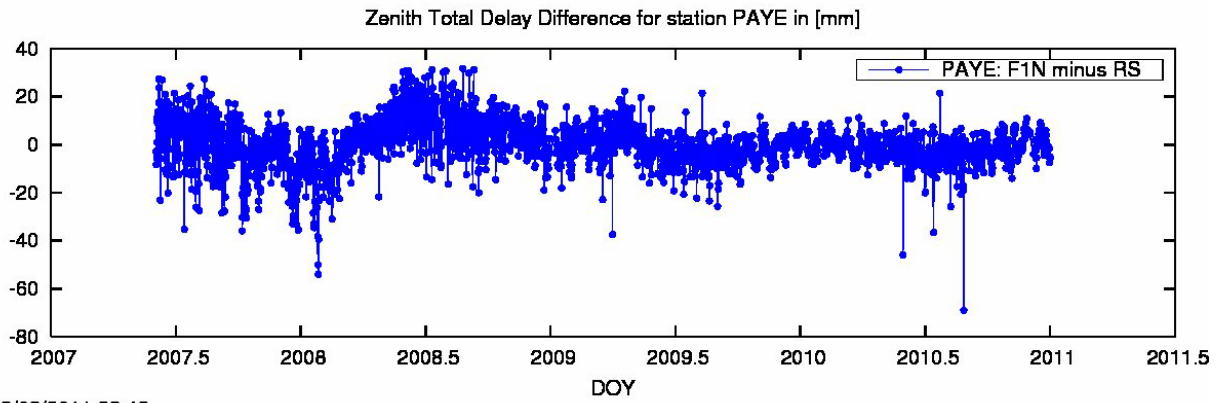


Figure 4.30: Troposphere parameters estimated in near real-time and in real-time compared with troposphere parameters derived from radiosonde data for station PAYE (real-time monitoring April 28, 2008)



13/02/2011 22:42

Figure 4.31: Difference between troposphere parameters estimated from GNSS post-processing and troposphere parameters derived from radiosonde data for station PAYE (long-term monitoring February 2011). A new humidity sensor was used for radiosonde launches after May 2009.

## National Surveying Contributions to the AlpTransit Gotthard Base Tunnel

by A. Wiget, U. Marti, A. Schlatter

Swiss Federal Office of Topography swisstopo, Wabern, Switzerland

On October 15, 2010, the main cut-through of the Gotthard Base Tunnel was achieved, with 57 km the longest, and with a depth of up to 2500 m under the surface also the deepest railroad tunnel in the world.

In the 1990s the Federal Office of Topography swisstopo designed the new national survey of Switzerland, the LV95 (Landesvermessung 1995). Thanks to its country-wide homogenous accuracy of a few centimeters, it also meets the demands of geodetic frameworks required by large engineering projects such as the Gotthard Base Tunnel and the Lötschberg Base Tunnel. Together with the high accuracy requirements for the cut-through of large tunnel networks, there are – especially in the alpine areas – other geodetic characteristics to be taken into consideration such as spatial variations of the gravity field, the kinematics of the upper crust of the Earth as well as the influences of refraction on GPS observations. swisstopo was able to apply various experiences gained in national surveying with GPS, precision levelling and in modelling the gravity field to the project "Gotthard Base Tunnel" (GBT).

With the national geodetic control network LV95, swisstopo had provided a modern, highly precise geodetic reference frame in the mid-1990s. Coordinated with the concept and the observations of the basis network for the GBT and the southern sector "Gotthard South" (Bodio – Lugano), swisstopo established and surveyed additional LV95 control points in 1995. There were now a total of eight LV95 control points available for the AlpTransit network. In addition, further local survey markers were included at each portal and for each intermediate access tunnel, thus making the reference to the (old but still official) national survey LV03 and to cadastral surveying possible. The GPS observations for sectors "Gotthard Base Tunnel" and "Gotthard South" were carried out by the Konsortium Vermessung Gotthard Base Tunnel (VI-GBT) and the Consorzio Geodetico Sud (COGESUD) respectively, each during two days in November 1995 and January 1996. The LV95 control points were occupied permanently during the entire measuring campaign of the basis network GBT in order to position the network optimally. A comparison of the coordinates to those of the GPS national survey network LV95 showed maximum differences (discrepancies from a Helmert transformation) of 5 mm [Haag et al. 1996]. In the course of a repeat measurement in 2005, the differences were also within 2-6 mm [Schätti und Ryf 2007]. The LV95 control points contributed not only to the increase in the accuracy of the network but also to higher reliability, an important component of a tunnel survey.

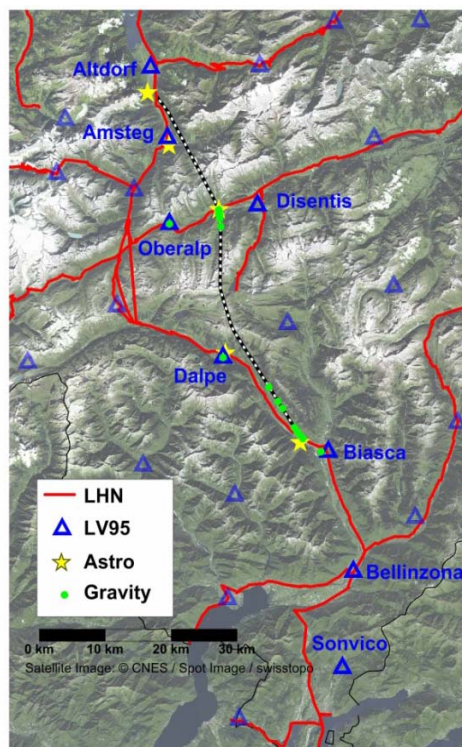


Figure 4.32: Part of LV95 network and vertical network (LHN), gravity and astro points of the base network Gotthard Base Tunnel GBT

Even though the GBT network of 31 points (an extension of approx. 60 km) and the network for the sector "Gotthard South" with 21 points benefited from the highly accurate LV95 network, they were nevertheless transformed and positioned into the LV03 reference frame in order to keep the discrepancies to local coordinates of the portals and access tunnels as small as possible.

The geoid model CHGeo98, which is essentially based on deflections of the vertical and also on GPS levelling data, was used for staking out the GBT. This model, however, is not only a simple reference surface for height determinations but an actual 3D model with which gravity data and deflections of the vertical may be interpolated at any given point beneath and above the earth's surface.

A special investigation [Marti 2002] determined that the mass models from the CHGeo98 would be sufficient for the rigorous tolerances demanded for the construction and cut-through of the GBT and further mass model studies would not be required. In order to determine whether gravity observations would be necessary inside the tunnel or if the extrapolated values for height corrections from the surface to the tunnel section would be sufficient, gravity observations were carried out on a few points around the portals and in the already accessible part of the tunnel in 2005 together with the Institute for Geophysics at the University of Lausanne and compared to the values interpolated from CHGeo98. The resulting maximal discrepancies of less than 3 mgal are negligible for the calculation of orthometric corrections. It was thus established that no systematic gravimetric observations of the GBT would be required and that CHGeo98 provided sufficiently accurate interpolated gravity values [Bürki et al., 2005].

Similar to the procedure for the gravity observations, it was also verified that the values computed from CHGeo98 for the deflections of the vertical and astronomic azimuths were sufficient. This was achieved in summer 2005 through astro-geodetic observations carried out by the Federal Institute of Technology in Zurich and by the Technical University of Hannover around the portals and further access tunnels [Bürki und Guillaume, Geomatik Schweiz 12/2010]. In this investigation the main result again showed that the interpolated values from CHGeo98 were sufficient for the construction of the GBT and that no further observations would be necessary.

The vertical network of the GBT is based on observations of the national levelling network as well as on calculations from the new vertical network LHN95 (Landeshöhennetz 1995) [Schlatter 2007]. This network is in turn based on an orthometric height system and was realized through a kinematic readjustment of all observations made since 1903. In addition to the reduction of influences of the gravity field, tectonic movements (Alpine uplift of up to 1.5 mm/year) are also taken into consideration. For the cut-through of the 57 km long tunnel, only 30 km additional precise levelling observations on the surface were required. They served to connect the portals Erstfeld, Amsteg, Sedrun, Polmengo (Faido) and Bodio (Biasca) to stable markers of the national vertical network LHN. However, further observations extending over several hundred km were carried out for subsidence monitoring, extending the portal networks and for tectonic investigations.

The levelling loop 'mountain pass – vertical shaft – railway tunnel' deserves particular attention. Along the mountain pass one obtains usual levelling heights, which are – without gravity reductions – not consistent with a rigorously defined height system, in the vertical shaft orthometric heights, and in tunnels with only a slight grade, almost exact dynamic heights. Without accounting for the gravity field, the loop closures of even error-free observations are only within decimeters. Together with the unavoidable random observation errors, this leaves a small margin for achieving the demanded cut-through tolerance of 12.5 cm ( $2.5\sigma$ ).

The project management and the VI-GBT nevertheless decided to stay with the official height system for Switzerland (LN02) since the project planning as well as the connecting constructions had already been carried out in this vertical framework. The most important reasons why the official Swiss heights (LN02) differ from orthometric heights by decimeters are [Schlatter und Marti 2005]:

- neither the influence of the gravity field nor the different kinds of heights are taken into account;
- precise levelling observations are still constrained into nodal points whose heights are based on the 'Nivellement de Précision' dating from 1864-91;
- therefore, known recent height changes are also not taken into consideration.
- In order to counteract the disadvantages and shortcomings of LN02, corrections must be applied to the heights during the tunnelling stages, namely:
  - influence of the gravity field in the tunnel (orthometric corrections resp. theoretic loop misclosures);
  - influence of the differences between LHN95 and LN02 (see Table 4.1);
  - influence of the different uplift rates (see Table 4.1), which theoretically exceeds 1 cm only slightly during a construction period of 10-20 years.

Portal	Height	Length GBT	ME LHN95	LHN95 - LN02	LNIV - LN02	Uplift
	[m AMSL]					
Erstfeld	460	0	$\pm 0$ (Ref.)	0 (Ref.)	0 (Ref.)	0.67
Amsteg	510	8	$\pm 3$	0.02	0.01	0.78
Sedrun	1410	21	$\pm 9$	0.13	0.01	0.80
Faido	760	40	$\pm 7$	0.11	0.05	1.25
Biasca	300	57	$\pm 8$	0.11	0.09	1.22

Table 4.1: The accuracy of LHN95, comparison between LHN95, pure levelling heights (LNIV) and LN02 relative to portal Erstfeld as well as vertical uplift with respect to the reference point Aarburg

Based on the available height and density models which were also used for the geoid determination, swisstopo calculated a priori orthometric corrections from the project coordinates for VI-GBT. Figure 4.33 shows the distribution for the cut-through Amsteg  $\leftrightarrow$  Sedrun Nord. It is striking that the vertical shaft has no direct influence; the vertical distance corresponds to an orthometric height difference. If no corrections were applied, the cut-through error would after all still be approx. 3.8 cm.

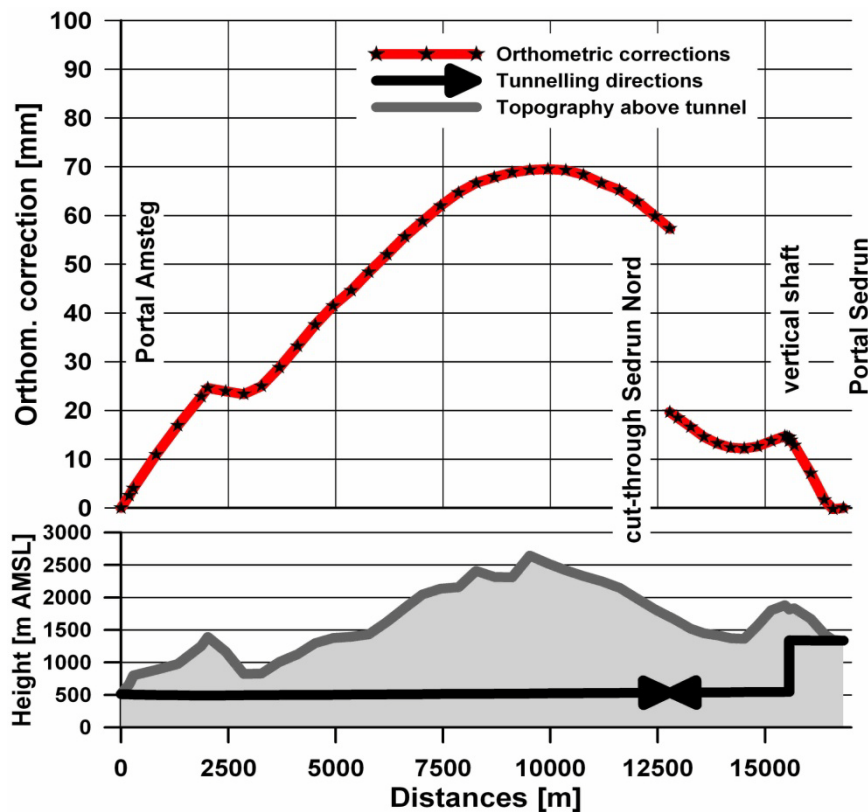


Figure 4.33: A priori orthometric corrections in the tunnel derived from orthometric heights in the portals

## Geodetic Reference System and Break-Through-Results in the Gotthard-Base Tunnel

by R. Stengele, I. Schätti-Stählin

BSF Swissphoto

The 57 km long underground-connection in the Swiss Alps was finally realized with the main break-through in October 2010. In 1995 the survey-consortium "Vermessung Gotthard-Basistunnel" was contracted by the Swiss Railway Company SBB. Four private companies are members of this survey-consortium: Grünenfelder und Partner AG in Domat/Ems, BSF Swissphoto AG in Regensdorf, Studio Meier SA in Minusio, Studio Gisi SA in Lugano.

The Geodetic Networks (horizontal & vertical) have been established in close cooperation with the Federal Office of Topography (swisstopo) resulting in ~ 30 geodetic points within an accuracy of  $1\sigma$  horiz., vert. < 10 mm, covering all five portals of the 57 km long tunnel. The differential accuracy within these networks is <  $10^{-6}$ . All heights have been corrected by influence of ongoing vertical movements of the Alps. The vertical velocities of 0.8 to 1.3 mm per year have been predicted by swisstopo.

All survey work for more than 152 km of tunnels in a period of more than 15 years has been based within these geodetic reference systems. The design of the Geodetic Network underground was a double-polygon, running parallel and separately in two main tunnels in a distance of 40 m. The two polygons have been connected and adjusted after a distance of 1.2 km. Visual length of geodetic measurements underground were limited to 900 m. Gyro-azimuths all 2 to 3 km were used to maximize accuracy and reliability of the underground-network. Local geoid models have been applied to correct geographic azimuths. The design of the geodetic network underground is as follows (see Figure 4.34):

- parallel polygon in two parallel tunnels
- 420 m to 450 m distance between two geodetic points
- connection of two parallel polygons after each 1.2 km
- 1.5 m minimum distance between visual line and tunnel-wall to minimize horizontal refraction
- 900 m maximum distance of measurements underground
- gyro-azimuths each 5 to 7 geodetic points
- measurements of heights by precise levelling

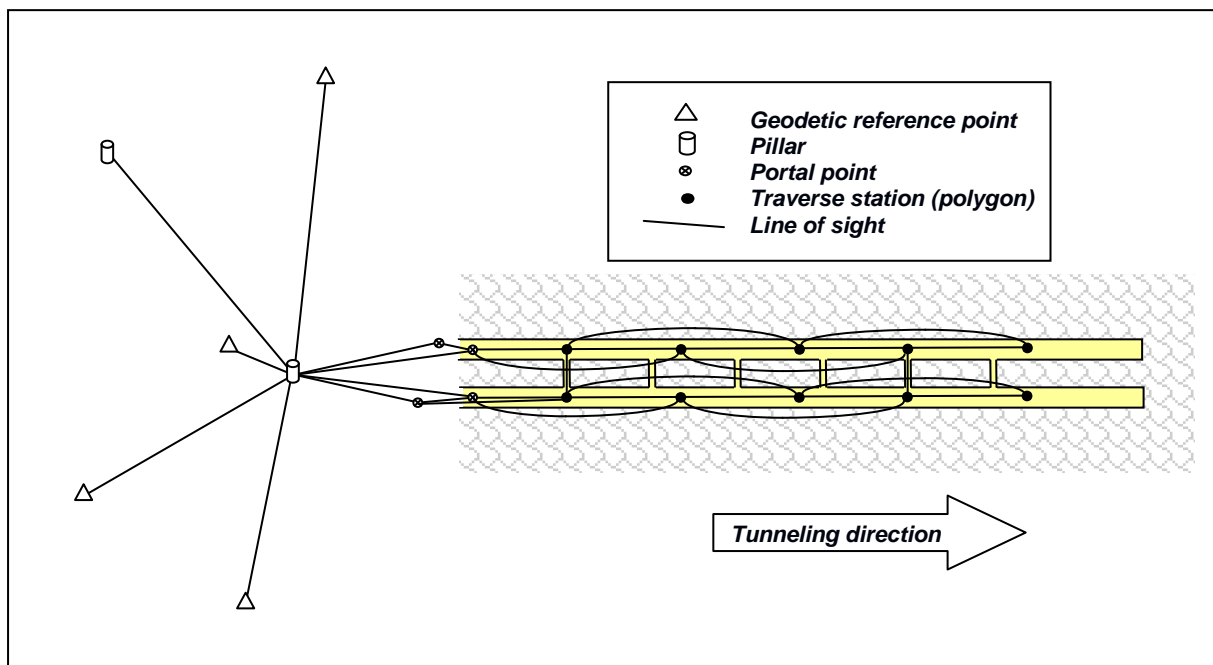


Figure 4.34: Design of Geodetic Network underground

Overall-Network-adjustments with observations > 10 years give a posteriori accuracies ( $1\sigma$ ) for the most important observations as follows: 2.7 cc für horizontal angles, 10.8 cc for gyro-azimuths, 1.6 mm/km für distance-measurements, 0.9 mm/km für precise levelling. Orthometric corrections in the range of > 10 cm have



been applied underground. The break-through-results in five sections of the 57 km long Gotthard-Base Tunnel (see Figure 4.35) are summarized in Table 4.2:

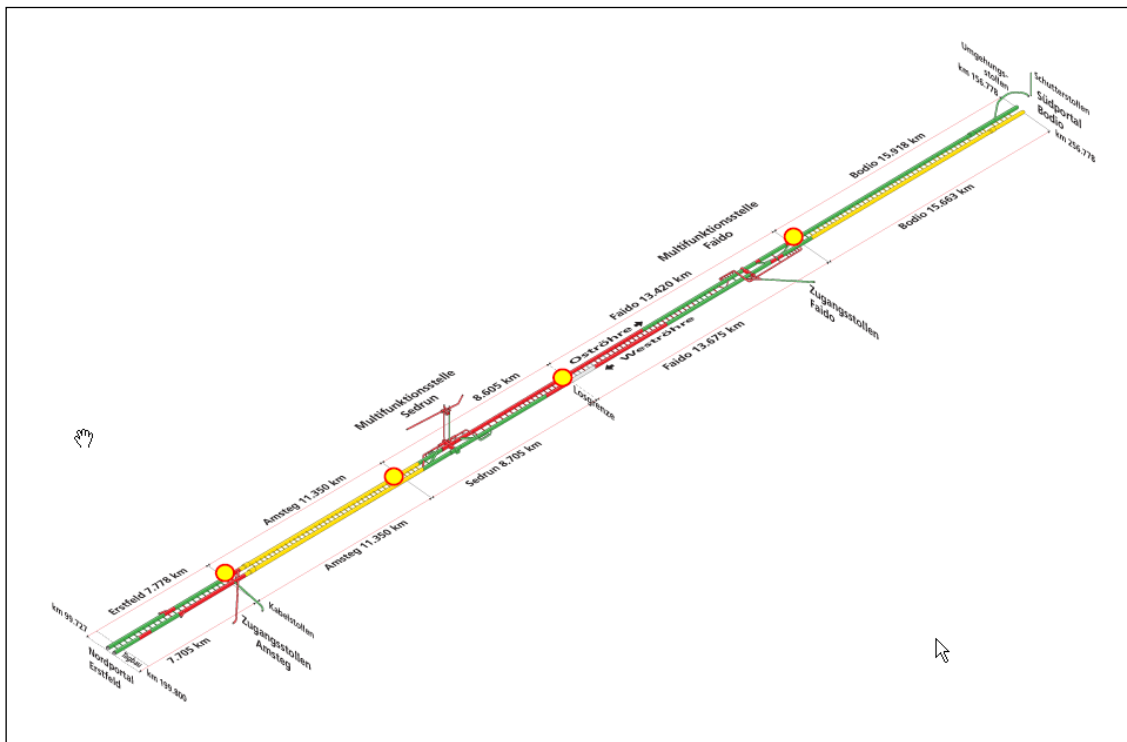


Figure 4.35: Five sections and four break-throughs in the 57 km long Gotthard-Base Tunnel

Date	Section	Length [km]		cross [mm]	long [mm]	vertical [mm]	
22.08.2006	Faido Bodio	4.1	15.7	19.8	92	12	17
14.10.2007	Amsteg Sedrun	13.3	4.0	17.3	137	21	3
16.06.2009	Erstfeld Amsteg	7.8	2.3	10.1	14	33	5
15.10.2010	Sedrun Faido	15.0	8.4	23.4	81	136	11

Table 4.2: Break-through-results

All contractual requirements in accuracy and reliability ( $2.5 \sigma < 25$  cm cross und 12.5 cm vertical) have been fulfilled. From geodetic point of view, two aspects are special highlights:

- 1) The 4 km long section of Sedrun towards Amsteg has to be drilled starting from the bottom of the 800 m vertical shaft in Sedrun. For this purpose, a vertical plumbline to transfer coordinates, height-difference and azimuth has to be measured with maximum accuracy. Different concepts (mechanic plumbline, optical plumbline and inertial sensors) have been used and integrated to a combined solution.

2) The break-through-results in vertical component are exciting "good". Considering

- very long levelling distances with height-differences  $> 1000$  m in the Swiss Alps
- height-measurements in the 800 m vertical shaft Sedrun
- and extensive model-based height-corrections (orthometric corrections, kinematic modelling of vertical movements)

these results are a perfect "proof of concept" for all involved geodesists and surveyors.

## Renaissance of hydro-electric power in Switzerland: Geodetic base networks for new underground pumped storage facility in the Alps

by M. Kistler, E. Brockmann

Swiss Federal Office of Topography, Swisstopo, Wabern, Switzerland

In Switzerland, there are several projects for new water dams with pumped storage facility in the Alps with an investment volume of around a billion Swiss Francs each. These projects need high accurate geodetic base networks as basis for the construction work. swisstopo supported this work in collaboration with companies from the private sector with sensors and measurements – mainly GNSS. The GNSS-analysis is done using the BERNESE Software and using the permanent GNSS network AGNES. This enables a best possible integration of the measured base networks in the official Swiss reference frame LV95.

Baselines of the base network are usually shorter than some kilometres. They are analyzed using L1 observations, whereas for the connection to the permanent sites of the AGNES network (10-30 km baselines) the ionosphere-free linear combination L3 is used. Due to the height extension of more than 2'000m, troposphere parameters need to be estimated. With respect to the datum definition of the network, several options are possible:

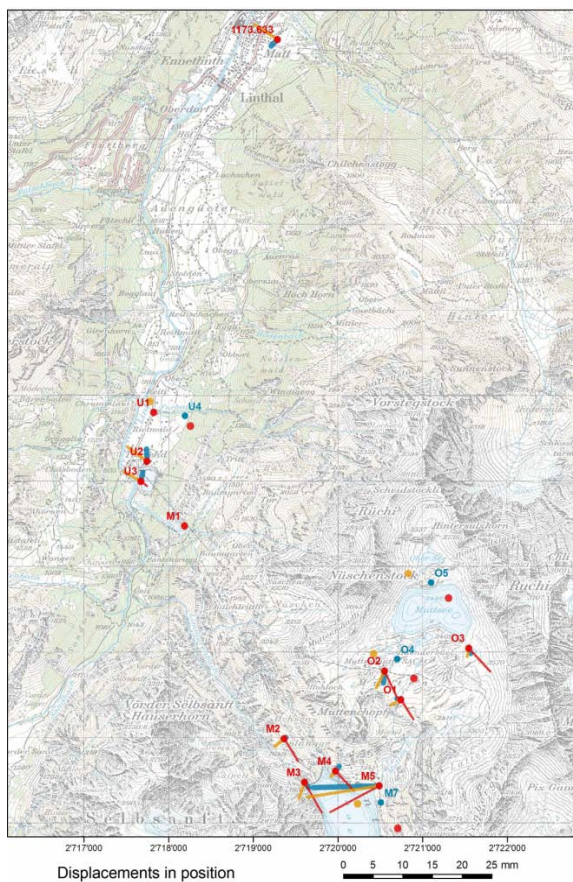


Figure 4.36: Displacements in **position** 2006 – 2009 using different datum definitions (compared to the initial measurements 2006). **Orange**: Alignment to the CORS network of Switzerland, **red** Alignment to a single local point of the national reference frame and **blue**, the final solution aligned to all the existing, stable points of the epoch 2006. On old points (Epoch 2006 - label in red) the displacements are indicated as line. And for new land marks (Epoch 2009 - label in blue) as point. The residuals on the pass points 1173.633, U2, U3, M2, M3, M4, O1 and O2 of the blue solution correspond to the inner accuracy.

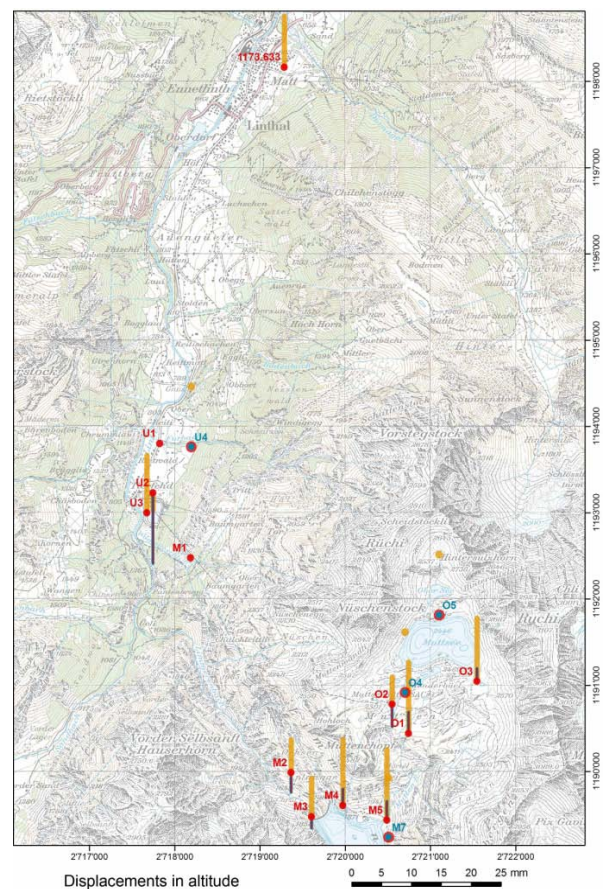


Figure 4.37: Displacements in **height** 2006 – 2009 using different datum definitions (compared to the initial measurements 2006). **Orange**: Alignment to the CORS network of Switzerland, **red** Alignment to a single local point of the national reference frame and **blue**, the final solution aligned to all the existing, stable points of the epoch 2006. The last two variants show the same change in altitude. This indicates a systematic influence of the height transfer using the L3 solution. On old points (Epoch 2006 - label in red) the displacements are indicated as line. And for new land marks (Epoch 2009 - label in blue) as point.

## GBAS Activities

by M. Scaramuzza, P. Truffer

*Skyguide*

A Ground Based Augmentation System, GBAS, enabling instrument precision approaches in category one (Cat-I) weather conditions for aircrafts, is planned to be installed at Zurich International Airport. GBAS is a component of the Global Navigation Satellite System (GNSS) for aviation, consisting of several GNSS reference antennas, receivers, ground processing equipment and a VHF data broadcast.

While in 2005 different countries in the EC initiated the implementation of GBAS, the project was paused in Switzerland because no certified system was available. In the meantime the Federal Aviation Administration (FAA) certified at least one GBAS, so the project was reactivated in the middle of 2010. The first GBAS approach in Switzerland, an ILS look alike approach in CAT-I, is expected by 2015.

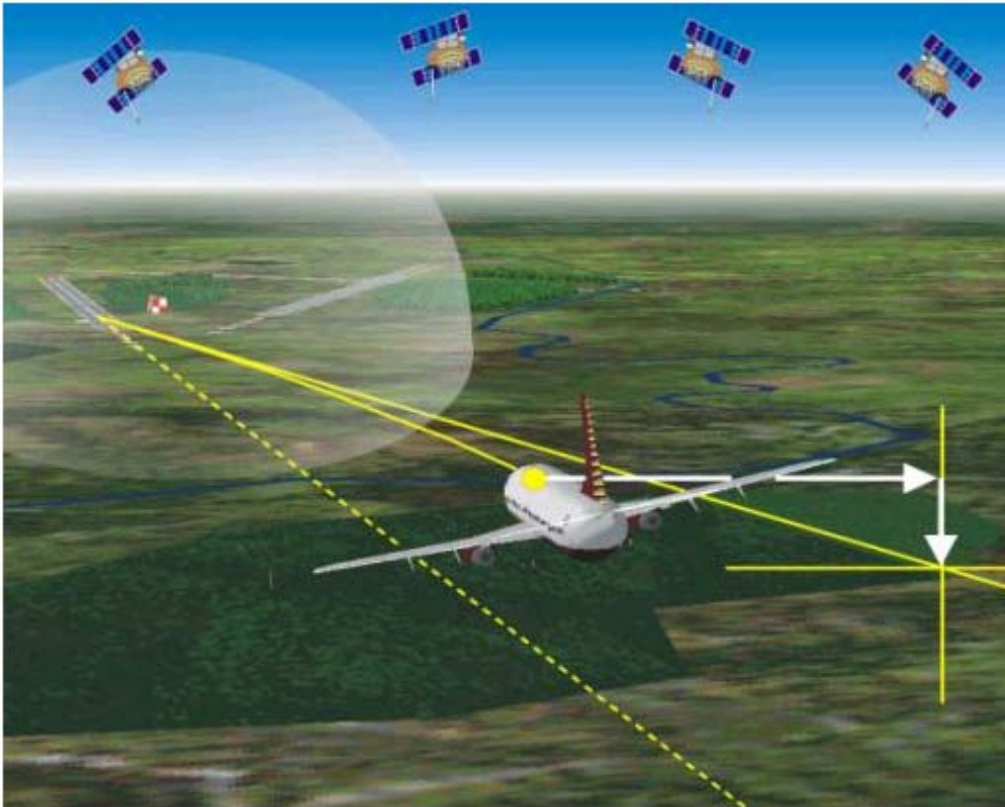


Figure 4.38: GBAS - Ground Based Augmentation System

## GPS performance analysis for ADS-B applications

by M. Troller, P. Truffer, M. Scaramuzza

*Skyguide*

Automatic Dependent Surveillance - Broadcast (ADS-B) is a new surveillance technique for air traffic control. In contrast to radar surveillance, ADS-B uses aircraft's GPS data for surveillance. As the same sensor is used for navigation and surveillance, high requirements for the quality of the data is essential. In cooperation with Eurocontrol, skyguide carried out several GPS performance analyses with an aircraft GPS receiver at the airport of Zurich. In particular, multipath effects have been studied. A relatively undisturbed environment with respect to multipath, a situation near a terminal building, and a location near a taxiway were chosen for data recording. For the multipath analyses, the code minus carrier (CMC) phase measurements of the L1 frequency have been calculated. In the relatively undisturbed environment, observed CMC values were always smaller than 3 m whereas the location near a terminal building showed values of up to 60 m. At the location near a taxiway, multipath effects of taxiing aircrafts have been investigated. However, during the investigations of 33 days, no multipath effects of taxiing aircrafts have been detected and it is, therefore, assumed, that taxiing operations do not degrade the GPS positioning performance.

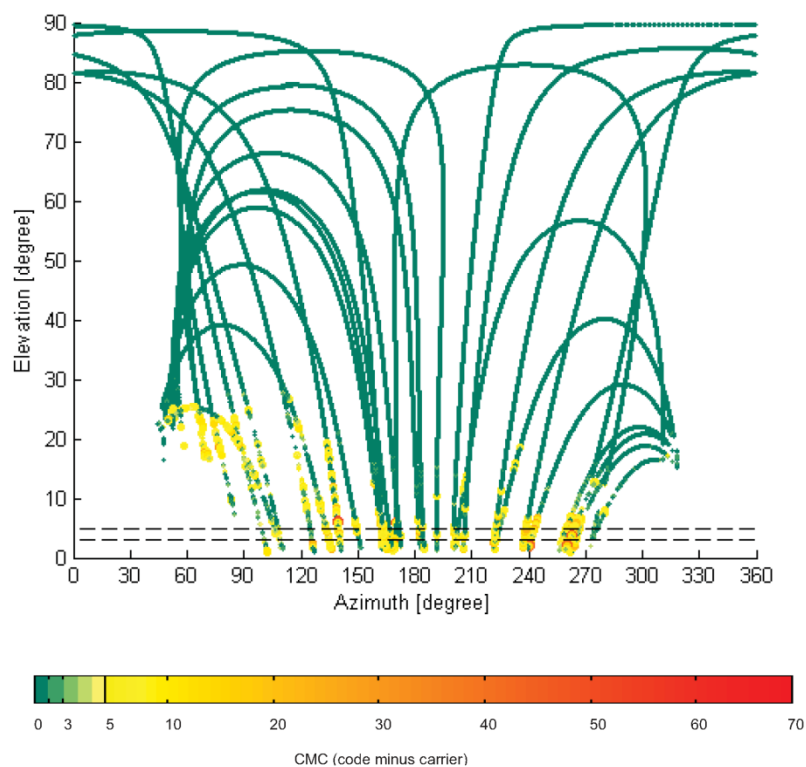


Figure 4.39: Satellite visibility and Code-Minus-Carrier of one day for PRN's 17-32.

## EGNOS for civil aviation applications

by M. Troller, M. Scaramuzza

*Skyguide*

Skyguide is involved in the EGNOS (European Geostationary Navigation Overlay Service) deployment through a service level agreement with the European Satellite Service Provider (ESSP). One of the 34 Ranging and Integrity Monitoring Stations (RIMS) of the EGNOS ground segment is hosted and maintained at Zurich Airport. It monitors constantly the GPS and the EGNOS geostationary satellites and sends its data to a processing centre. EGNOS activities at skyguide also include signal in space validation activities by means of two EGNOS permanent receivers and test flights. These tasks are in coordination with ESA, ESSP, Eurocontrol, other Air Navigation Service Providers (ANSP) and universities. First EGNOS-based approach procedures are planned in Switzerland for autumn 2011.



Figure 4.40: RIMS and WAN racks at Zurich airport



Figure 4.41: One of the two RIMS antenna

# Real-time change of Swiss reference frames with swipos GIS/GEO and RTCM Coordinate Transformation Messages

by B. Sievers, M. Saner

Fachhochschule Nordwestschweiz

Since 2007, RTCM Standard 10403.1 has allowed standardization and optimization of transmission of GNSS RTK corrections between reference stations and rovers by additionally providing so-called transformation messages. In 2009, a bachelor's thesis at the University of Applied Sciences Northwestern Switzerland analyzed whether and in which scope RTCM 10403.1 forms an alternative to the swipos-GIS/GEO real-time positioning service's current method, which uses real-time FINELTRA and HTRANS.

A GNSS positioning service (e.g., swipos GIS / GEO) can centrally manage all necessary information for a change of reference frames within the RTCM transformation messages and transmit them to the GNSS rovers. The transformation messages consist of message types 1021 to 1028 (see Figure 4.40). At regular intervals the rover receives the necessary information (geodetic datum and grid of residuals) to transform its GNSS position within a desired local reference frame.

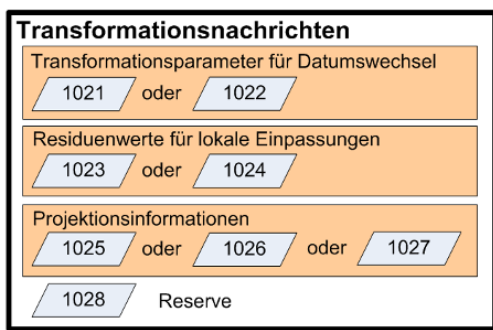


Figure 4.42: Design of transformation message

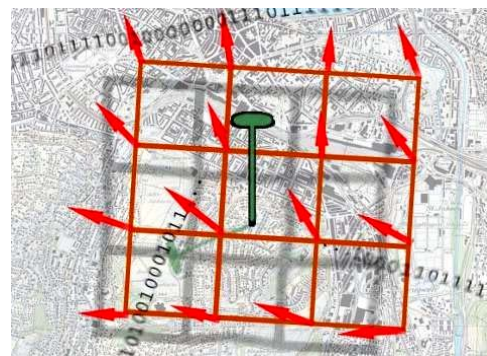


Figure 4.43: Representation of the 16 transmitted residuals (example)

The Swiss Federal Office of Topography (swisstopo, Wabern, Switzerland) currently offers subscribers to its swipos-GIS/GEO positioning service a functioning system for real-time changes of reference frames (see Figure 4.42). These changes are implemented via a specially developed algorithm embedded in the Trimble® GPSNet™ reference station software over a *dynamic link library*. For further processing, the parameters for datum changes have to be saved on the customer's rover.

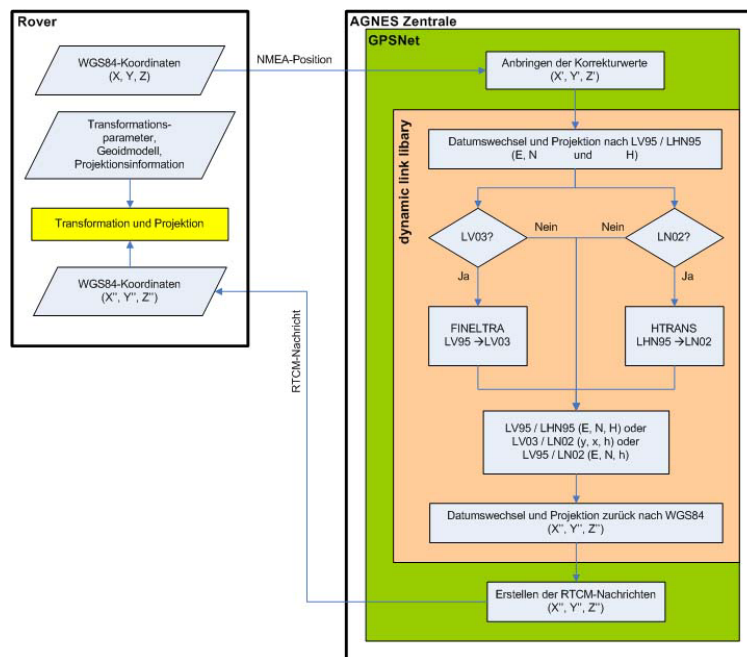


Figure 4.44: Flow chart of a change of reference frames using swipos-GIS/GEO

As an experiment a special generator was activated in the reference station software (see Figure 4.43) to generate transformation messages. The generator now transmitted all information to the rover, so that the rover did not need to save any parameters for the datum and reference frame changes.

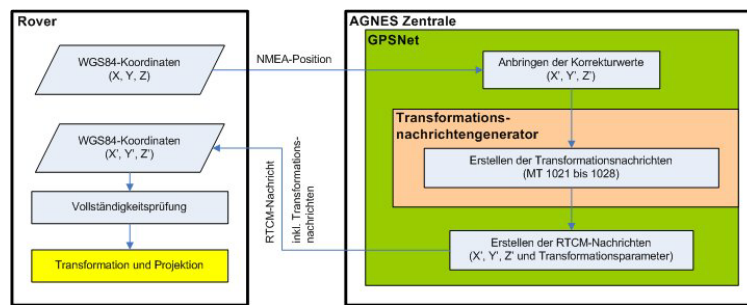


Figure 4.45: Flow chart of a change of reference frames with (RTCM 10403.1, 2009)

Initial trial measurements demonstrated that the application of RTCM 10403.1 (2009) showed very little loss in accuracy compared to the current system. The maximal differences from the current swipos-GIS/GEO solutions were 1.5 cm in horizontal position and 3.0 cm in height. In most cases, such differences were not significant.

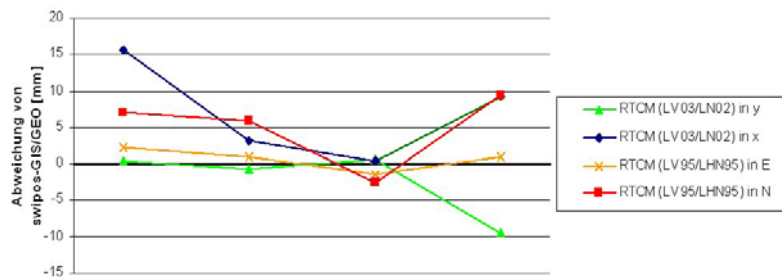


Figure 4.46: Median horizontal deviation of four test points from the reference measurement with swipos-GIS/GEO

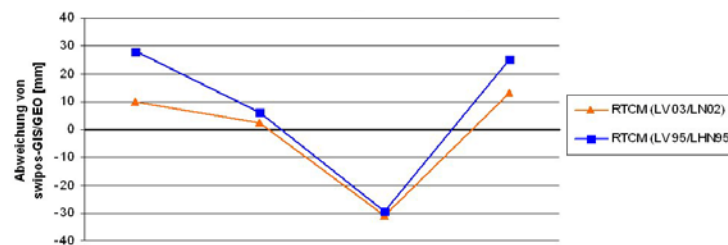


Figure 4.47: Median height deviation of four test points from the reference measurement with swipos-GIS/GEO

The tests with RTCM 10403.1 (2009) hold the potential to replace existing real-time transformations from swipos. The sensor manufacturer should implement RTCM 10403.1 (2009) fully in their measuring instruments and operating software and ensure their mutual compatibility; this would allow a change of system in the software of the swipos positioning service.

#### References:

RTCM 10403.1, (2009). RTCM Standard 10403.1 for Differential GNSS (Global Navigation Satellite Systems) Services - Version 3 + Amendments 1, 2, and 3. Available at: <http://www.rtcn.org>.



## Comparative baseline computation with Bernese GPS Software and Leica Geo Office as well as 3D computation of a slipping region with TRINET+

by B. Sievers, S. Kaiser, M. Schrattner

Fachhochschule Nordwestschweiz

Every year, the Institute of Geomatics Engineering (IVGI) of the University of Applied Sciences Northwestern Switzerland monitors the *Schwanderbärgli* deformation network near Brienz (Canton Bern) with geodetic measurements (GNSS, tachymetry, precision levelling) and evaluates the movements. Since the GNSS observations began, they have been computed using Leica Geo Office software, and adjusted first horizontally, then vertically with LTOP, together with the other measurements. For this report, a bachelor's thesis computed the *Schwanderbärgli* deformation network using Trinet+ and compared the results to those obtained using GNSS.

The Bernese GPS 5.0 Software (Dach et al. 2007) allows flexible computation of GNSS networks according to the most stringent accuracy requirements. Point heights are optimally determined using the surrounding AGNES reference stations, computing troposphere parameters from the GNSS observations and adjusting a combined network (see Figure 4.48).

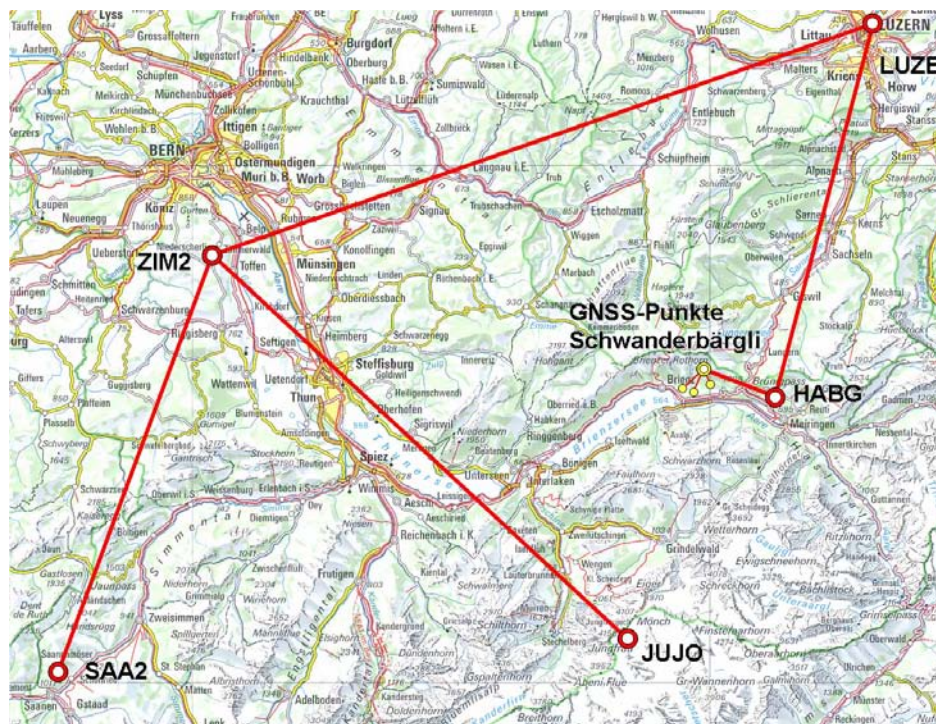


Figure 4.48: Surrounding AGNES stations with the Schwanderbärgli deformation network. LK500 map © swisstopo.

Given suitable evaluation parameters, data from the GNSS sessions can be processed automatically by the Bernese Processing Engine (BPE) (see Figure 4.47). The achieved average accuracy in the ITRF2005 global coordinate reference frame was 1.0 mm North, 0.5 mm East and 2.7 mm in ellipsoidal height. All resulting coordinates were transformed to the Swiss LV95/LHN95 reference frame for further use in Trinet+.

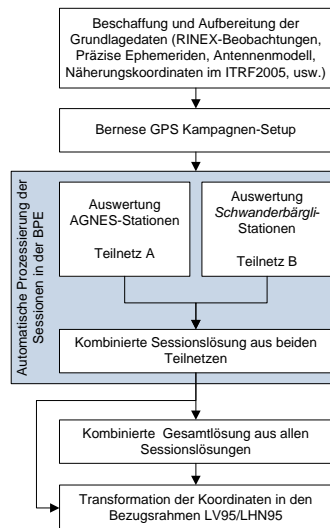


Figure 4.49: Generalized calculation process in Bernese GPS Software

In 2010, as in the previous years, the deformation network was measured in two independent measurement epochs (GNSS baselines, directions, zenith angles, slope distances, levelled height differences). These were named Block 1 and Block 2. The measurements were processed both horizontally and vertically with LGO (Leica Geosystems, 2008) and LTOP (Gubler & Marti 2009), and three-dimensionally with Bernese GPS software and the Trinet+ adjustment software for spatial networks (Guillaume et al. 2009) (see Figure 4.48).

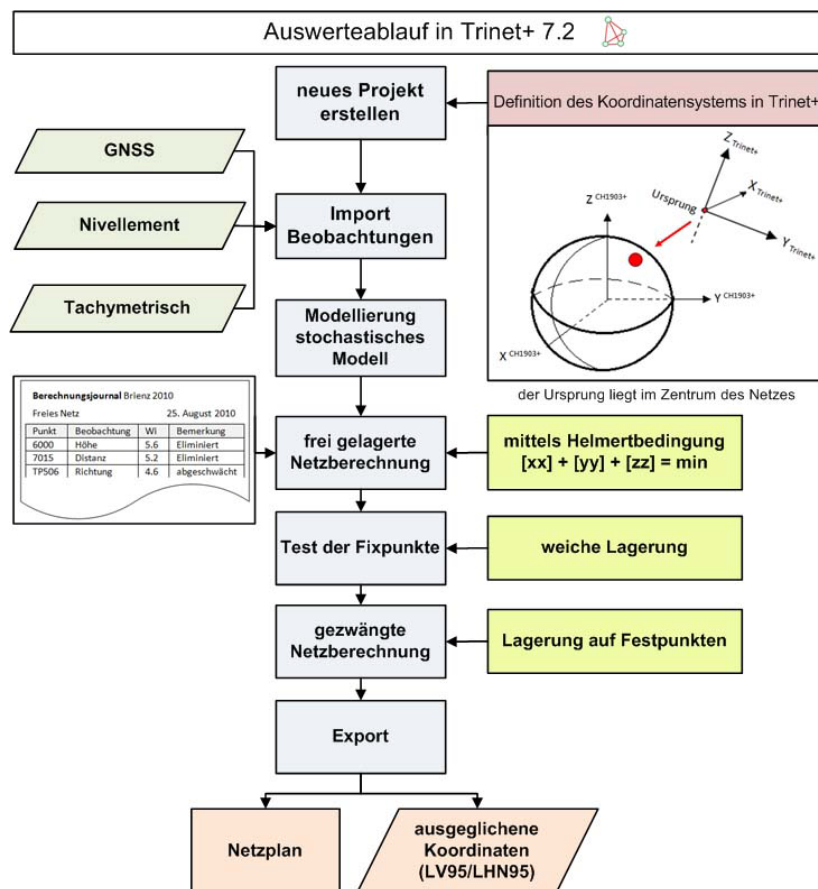


Figure 4.50: Calculation process from project creation to export in Trinet+

The achieved 3D accuracy (Helmert point error) of the new points averaged 2 mm. Comparing the 3D adjustment (Trinet +) with 2D+1D (LTOP) with a similarity transformation led to maximal differences of 9 mm

horizontally and 18 mm vertically. Using the resulting Bernese GPS coordinates increased the achieved point accuracies relative to the GNSS point calculations made using Leica Geo Office 7.0.

The investigations will be continued in the future at IVGI, using both Bernese GPS software and Trinet +.

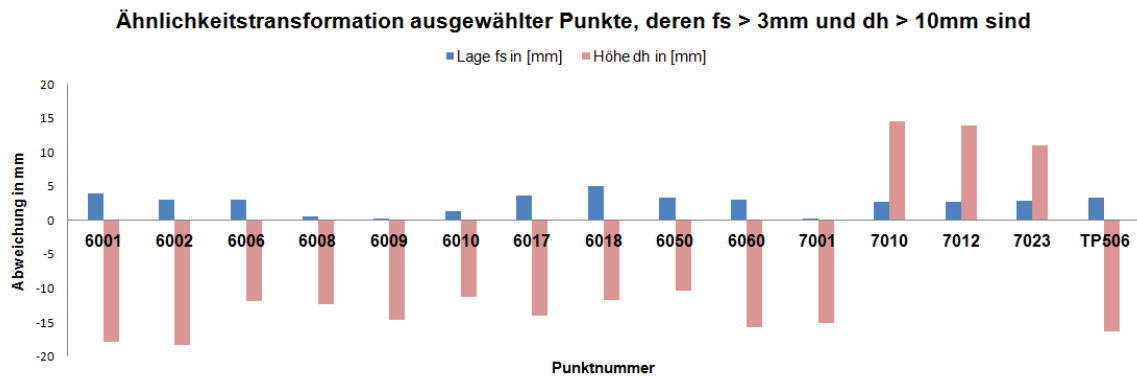


Figure 4.51: Largest residuals between Trinet+ coordinates and arithmetically averaged coordinates from LTOP (Block 1 and Block 2).

## International Conference on Indoor Positioning and Indoor Navigation (IPIN)

by R. Mautz, H. Ingensand

Institute of Geodesy and Photogrammetry, ETH

From September 15-17, 2010 the first International Conference on Indoor Positioning and Indoor Navigation took place at the Swiss Institute of Technology Zurich Science City (ETH). The conference directors Prof. Hilmar Ingensand and Dr. Rainer Mautz from the research group “Geodetic Metrology and Engineering Geodesy” had called for a worldwide know-how transfer in Indoor Positioning to the research community active in this field.

445 researchers, system providers and users from 47 countries answered their call, three times more than had been originally hoped for. 214 extended abstracts had been submitted while 132 full papers had passed the review – now available as the conference proceedings IPIN (2010). 220 presentations were made – ten times more than expected. As a result, up to 6 sessions had to run in parallel with the implication that participants could attend a maximum of 18% of all scheduled presentations. The presentations were organized in 24 technical sessions – each offering an unprecedented focus on a particular technology for indoor positioning. The high number of technical sessions reflected the large diversity of different technologies that can be used to obtain positioning or location information indoors. It was reported that almost any signal/sensor technique can be exploited successfully for this purpose, such as optical, ultrasound, magnetic, ultra-wideband, radio, radar, high sensitive GNSS, RFID and fluorescent light sensors. The accuracy of the systems ranged from high precision instruments used in industrial metrology, such as laser trackers and iGPS, up to room-level indoor navigation based on received signal strengths. A particular group of systems offered pedestrian navigation built on hybrid sensor techniques, such as the integration of inertial navigation and GNSS. One special session was dedicated to foot-mounted navigation, where the short moment of zero-velocity in a step can be exploited.

Due to the diversity of different technological solutions, the field of indoor positioning and navigation is profoundly interdisciplinary. Therefore, the purpose of IPIN was to bring together the experts worldwide in geodesy, informatics, electronics and robotics in order to jointly tackle the challenge of indoor positioning. For the first time, the barrier between the disciplines was breached and researchers and developers with different backgrounds were able to discuss the indoor positioning issue “under one roof”. Many researches admitted that they had not been aware that so many other teams were currently working on the same (or similar) approach until IPIN brought them together.

The geodesists should more intensively apply their expertise in order to, literally, find a position in this emerging research field. However, at IPIN, geodesists were only attracted by high-accuracy sessions such as „Optical Systems“, „Indoor GNSS, Pseudolites“ and their core expertise „Industrial Metrology & Geodetic Systems“. But also the other, less precise methods for localization offer opportunities for geodesy to widen the field of activity by bringing in know-how in adjustment theory, sensor technology and calibration.

As a distinctive feature of IPIN, the organizers had encouraged the attendees to bring along their indoor positioning systems and test their system performance in live demonstrations. In parallel to the oral presentations, 22 different systems were shown in five dedicated demonstration rooms, offering the participants the chance to experience the latest systems in person, see pictures 2-5. The diversity of the systems was enormous, ranging from students’ experimental platforms up to mature solutions offered by companies intended to serve the indoor positioning market.



Figure 4.52: IPIN Logo

What is the market for indoor positioning and indoor navigation? The potential to locate objects and people indoors is a substantial challenge, and is the major bottleneck preventing seamless positioning in all environments. Many indoor positioning applications are waiting for a satisfactory technical solution; including for industrial automation and robotics, asset tracking and logistics, pedestrian navigation in hospitals, homes for

the frail and disabled, and emergency response, in museums, etc., to support ambient assisted living, sensor networks, location based systems/services and many more. Indoor positioning can contribute to our common goal to improve quality of life in urban environments. However, the size of the future market for indoor positioning and navigation is difficult to predict, but is probably enormous.

IPIN has demonstrated that there is no one ideal solution to the indoor positioning problem yet that is reliable, accurate, easily installed and economical. Currently standard navigation systems stop working when the devices enter a building.

The organizers are confident that IPIN has fulfilled its goal by establishing a forum for know-how exchange, thereby boosting research activities that take advantage of synergies between different indoor positioning approaches. In order to further deepen the interdisciplinary collaboration, the scientific committee has chosen to continue IPIN. The second IPIN will take place 21-23 September 2011, in Guimarães, Portugal.

## CLIPS – A Camera and Laser-Based Indoor Positioning System

by S. Tilch, R. Mautz

Institute of Geodesy and Photogrammetry, ETH

The main purpose of CLIPS (Camera and Laser based Indoor Positioning System) is the precise pose estimation of a mobile camera with respect to a laser rig. Since the rig emits laser-beams from a virtual central point, it can be regarded as an inverse camera. Thus, the laser rig can substitute a second camera. Now, the laser beams project bright spots on any surface in an indoor environment. Once the mobile camera has captured these spots, the camera pose can be estimated with respect to the laser rig (Mautz, 2009) (Tilch, 2010).

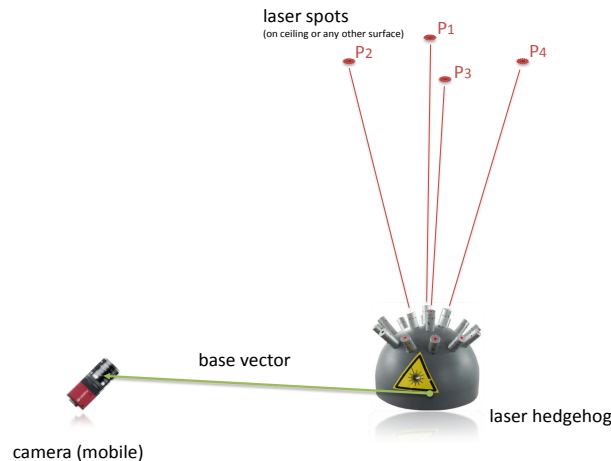


Figure 4.53: Concept of CLIPS

The pose estimation algorithm consists of three fundamental steps. These steps are image processing, camera pose estimation and the introduction of the system scale. First, the digital images have to be processed to assign the laser spots in the images to the corresponding laser beams of the rig. For this purpose, the laser spots are detected and identified in the first image. To speed up the application, subsequent images are processed via a tracking approach that avoids computational expensive laser beam detection.

The second step estimates the camera pose with respect to the laser rig. Subsequent to the point identification of the individual laser beams in the camera image, the relative orientation can be computed. For this task, the 5-point-algorithm proposed by Stewénius (2005) has been implemented. Since the solution of the 5-point-algorithm can consist of up to 10 different possible camera positions, the algorithm is embedded into a RANSAC algorithm. The result (position and orientation of the camera) of the algorithm is decomposed into a translational vector  $b$  and a rotational matrix  $R$  and finally refined by a least-squares optimization.

The final step introduces the system scale. Out of several options for the introduction of the system scale, the simplest option is chosen by directly measuring the distance between the laser hedgehog and the camera using a total station from Leica. The distance measurements are only carried out for the first four camera positions. These distances serve as a scale for the 3D base vectors between the laser rig and the first four camera positions. In addition, the spatial coordinates of the laser points are determined by intersection. Once the 3D positions of the laser spots are known, the relative orientation parameters for further camera positions are determined by spatial resection.

First experiments have shown that the relative orientation of the camera could be correctly determined in all cases and that our new system has the potential to achieve mm-level accuracy or better.

## Glacier Monitoring

by R. Mautz, D.E. Grimm

Institute of Geodesy and Photogrammetry, ETH

The Dirru rock glacier near the village Randa in the alpine valley Mattertal has been object for several monitoring projects. In previous years the rock glacier has been monitored by epochal GPS measurements with an annual frequency. In order to determine the velocity rates more precisely in higher temporal resolution, the rock glacier was monitored by a totalstation for a tentative period of two weeks in summer 2009. 17 prisms were deployed on large boulders within the rock glacier and observed by automated totalstation sightings every 20 minutes. The used instrument was the motorized Leica TPS 1201 totalstation that incorporates the functionality of automated target recognition. Data collection was organized through the monitoring software GeoMos. During the observation period, displacements up to 12 cm were detected (Ober et al. 2009). This corresponds to displacements of 9.3 m per year. However, the annually GPS measurements indicated a mean displacement of 8 m per year. Hence it can be concluded that the velocities of the glacier are higher in June compared to the annual mean. The velocities of the boulders measured near the centerline of the rock glacier were higher compared to those measured near the boundaries.

In addition, a long term monitoring campaign started in summer 2009, where three low-cost single frequency GPS receivers were also deployed.

The GPS data processing is based on differential carrier phase shift determination using Bernese GPS software. Daily station coordinate means, as well as kinematic coordinates with a sampling interval of 5 s are computed. From the data of the low-cost GPS system it was possible to reliably determine velocities in the order of 2 cm/day. Station coordinates were obtained with accuracies (empirical standard deviations) of 0.5 cm for the daily solutions and 1.5 cm for the kinematic solutions.

In order to permit a comparison of the two systems, the GPS antennas and prisms were mounted on the same boulders. As a result, a very good agreement in the velocities of better than 0.1 cm/day was obtained by comparing the filtered GPS Data with the total station solutions (Limpach, Grimm 2009).

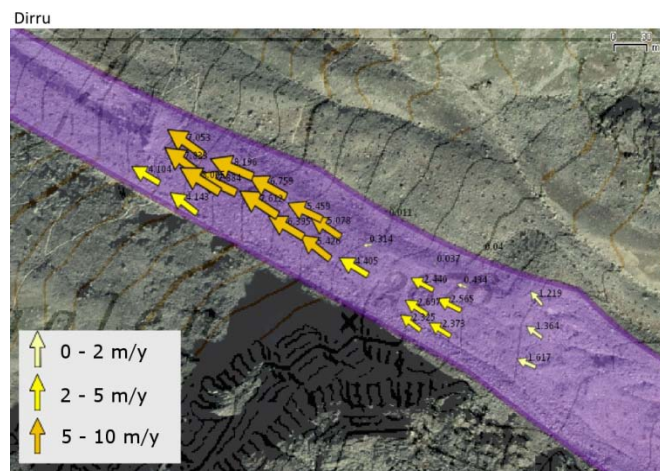


Figure 4.54: Glacier monitoring

Generally, the empirical standard deviations from the measurements of the total station were three times better in the horizontal and five times better in the vertical than those of GPS (Mautz et al. 2010). Lower installation costs and time per point allows deployment of prisms in larger number compared to GPS stations. In addition, the better accuracy qualifies the total station for precise measurements over a short time period (i.e. weeks). On the other hand the GPS system is more appropriate for long term monitoring of some few boulders.

## Streambed Topography Measurement using Range Imaging

by T.K. Kohoutek<sup>1</sup>, M. Nitsche<sup>2</sup>

<sup>1</sup> Institute of Geodesy and Photogrammetry, ETH

<sup>2</sup> Swiss Federal Institute for Forest, Snow and Landscape, WSL

The characterization of streambed topography is crucial to approach problems in fluvial hydraulics, river engineering and geomorphology. In most steep alpine environments measurement apparatus like terrestrial laser scanners or airborne Lidar systems are difficult to successfully apply, because they need free sight, elevated positions and good aerial or road access. In mountain streams this is generally not the case.

The core of our range imaging (RIM) system is a commercial time-of-flight video camera. The camera produces a per-pixel distance measurement using an integrated near-infrared modulated light source and an image sensor that measures the phase-shift between modulated and reflected light at each pixel. If mounted on a lightweight crane vertical above the stream (Figure 4.53), the camera can observe the streambed topography with a 3D resolution of down to 0.5 cm. However, the distance measurements degrade in accuracy under direct sunlight and when strong illumination contrasts occur (Figure 4.54). Additionally turbulent water scattered the light, which led to large variations in the distance image. Flat water surfaces were penetrated by the modulated light and the sub water surface could be measured approximately.

To merge multiple footprints to a single point cloud of the scanned section, the placed control points were used. This allowed the transformation of the local camera coordinates to global coordinates. It is also possible to merge the footprints via a best fit iterative closest point algorithm (ICP). The merged point cloud can then be used to derive a DTM with standard interpolation techniques.

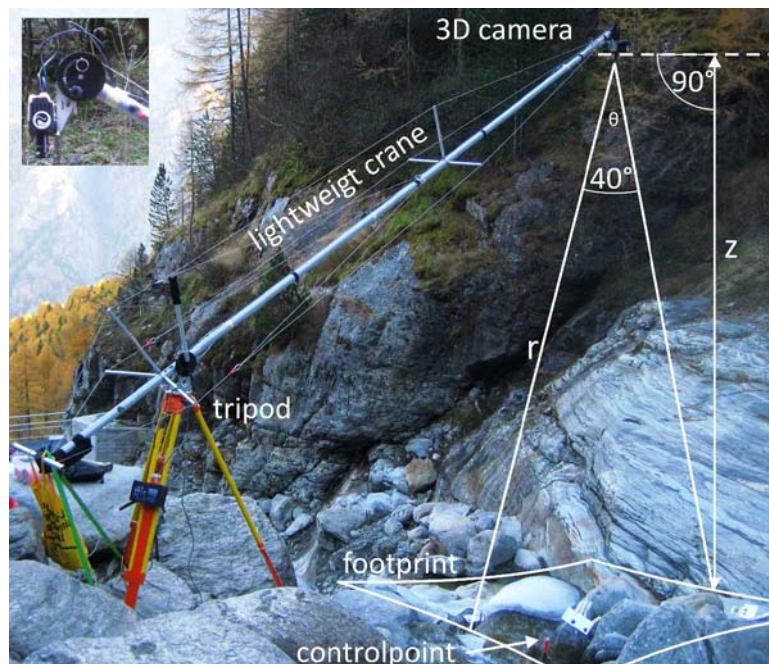


Figure 4.55: Crane with mounted RIM camera over streambed

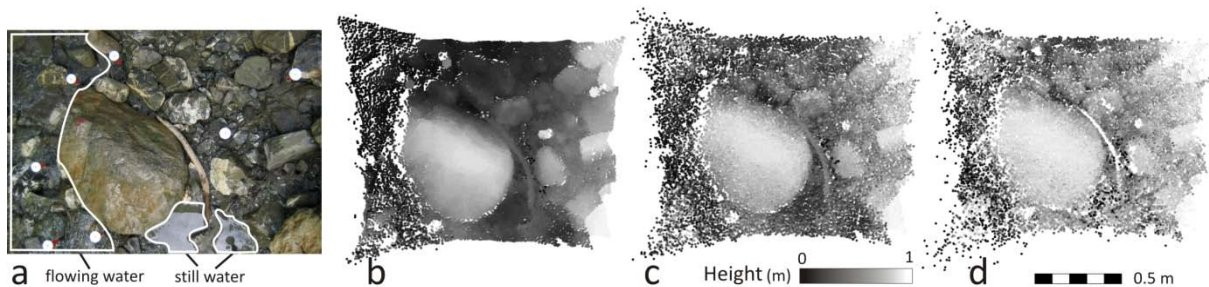


Figure 4.56: Footprint of the RIM camera - a) digital image (standard digital camera), b) range image at night, c) range image at shaded daylight, d) range image at direct sunlight



## Range Imaging for Indoor Positioning

by T.K. Kohoutek, A. Donaubaauer, R. Mautz

Institute of Geodesy and Photogrammetry, ETH

The development of indoor positioning techniques is booming at the moment. For industrial applications such as automation, warehousing and logistics there is a significant demand for systems that have the capability to determine the 3D location of objects in indoor environments without the requirement of physically deployed infrastructure. In particular, tracking of persons in indoor environments has become vital during fire fighting operations, in hospitals and in homes for vulnerable people especially vision impaired or elderly people.

Instead of a locally deployed reference infrastructure (e.g. Wi-Fi hot spots) inside buildings, the method relies on a digital spatio-semantic interior building model, based on the CityGML scheme (Figure 4.55) and a range imaging (RIM) point cloud. The method based on RIM belongs to the optical map-based indoor positioning systems. In contrast to traditional optical sensors, the range image does not reflect the brightness of the objects in the scene, but the distance of these objects to the range imaging camera. The expected 3D position accuracy for objects seen by a RIM camera (in terms of a  $1-\sigma$  standard deviation) is 1 cm for distances of 2 m and 1 dm for distances of 10 m. The largest error budget contributes the low-accuracy distance measurement. According to the manufacturer MESA® Imaging the ranging accuracy of the current model SR4000 is 1.5 cm for objects in 8 m distance at a level of reflectivity of 100%. Range Imaging can be particularly used for the purpose of indoor positioning, because in contrast to the other photogrammetric methods, range imaging can exploit semantic 3D geoinformation models. The reference points for the transformation are the corners of the room, vertices of doors, windows and other fixed installation or furniture. Figure 4.58 shows the comparison between an observed 3D point cloud from the range imaging sensor and a form primitive of a data base model.

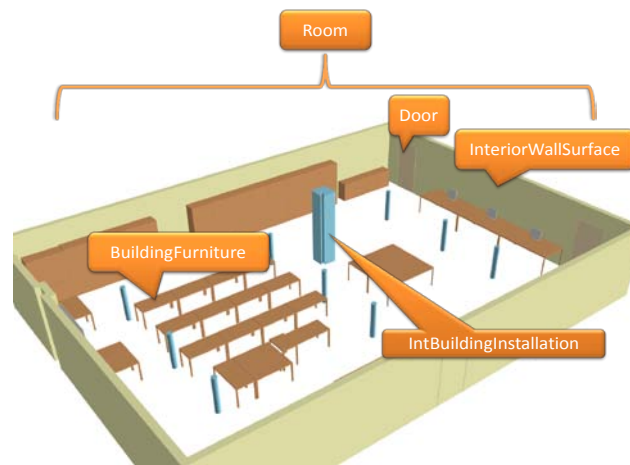


Figure 4.57: ETH Zurich lecture room in CityGML

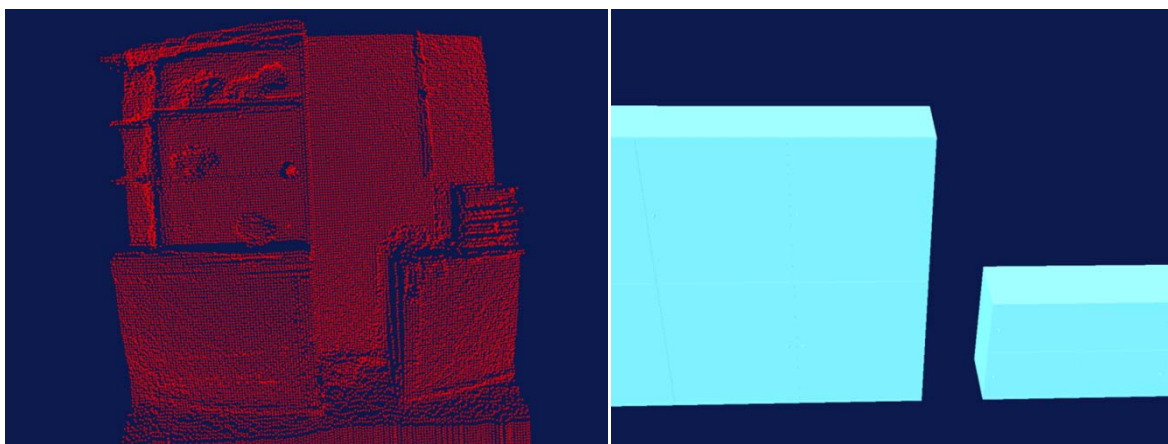


Figure 4.58: Object comparison between a range image (left) and form primitives from data base (right)

## Sensor Fusion for Digital Elevation and Object Modelling in Rome

by T.K. Kohoutek, P. Theiler

Institute of Geodesy and Photogrammetry, ETH

During the autumn in 2007 and 2008, as well as in spring 2010, several measurement campaigns of ETH Zurich – IGP in collaboration with the German Archaeological Institute (DAI) Rome have been achieved in the city center of Rome, Italy. The goal of those measurements has been the preparation of a digital elevation model of the Domus Aurea and detailed object models of historical buildings. To reference the heights of the measured points, additional measurements around and in the Colosseum (Figure 4.57) as well as in the Ludus Magnus (The Great Gladiatorial Training School), Forum Romanum and surrounding territory have been done.



Figure 4.59: Measurement points at Domus Aurea

The Domus Aurea is placed at the Colle Oppio in the north-east of the Colosseum and encompasses 0.5-1 km<sup>2</sup>. The Ludus Magnus is placed east from the Colosseum towards the Colle Celio. The measurements were mostly done using satellite navigation systems (GNSS) but also total stations and laser scanner. The DAI is very interested in the point heights to conclude the surface of the Colle Oppio in the ancient epochs when the “Golden House” of Nero and the Baths of Trajan were built. A coordinate transformation was calculated to combine the measurements from different local systems. In a further step the measured point coordinates had to be associated with previous measurement data of the DAI at the Pantheon. Therefore a static measurement of eight hours with GNSS (GPS and GLONASS) was done to combine both net in a post processing. During several student these different elevation (Figure 4.58), slope and aspect models of the terrain have been realized.



Figure 4.60: DEM of Domus Aurea overlaid with constructions of several epochs



Figure 4.61: Colored laser scan in the Forum Romanum

## Unmanned aerial vehicle in cadastral applications

by Henri Eisenbeiss, Madeleine Manyoky, Pascal Theiler

Institute of Geodesy and Photogrammetry, ETH

Due to the increasing demand on updating 3D data and 3D cadaster data as data base for various GIS and mapping applications, there is a need for fast and efficient surveying methods, which combine the data acquisition with additional information such as images, orthoimages, 3D-models of buildings and infrastructure, and elevation models.

Nowadays, in cadastral surveying measurement instruments like tachymeters and GNSS receivers are applied. These instruments are highly developed with respect to accuracy and performance for surveying tasks. However, these sensors normally only allow the mapping of points and lines.

In contrast to the traditional surveying methods, photogrammetry is used for mapping and up-dating of maps and orthoimages of large areas. However, normally due to the flight height and the image resolution, aerial images have less ground resolution and limited use in cadastral surveying.

In the last years the developments for robotic systems were fast-paced in a way that autonomous flying unmanned aerial vehicle (UAV) could be used as photogrammetric data acquisition platform for large-scale areas. These UAV systems are typically equipped with different sensors for navigation and positioning of the system and mapping sensors such as still-video cameras, LiDAR systems and so forth.

In our first studies we applied this technique in two test areas, where typical mapping tasks were simulated. The first test area Krattigen is located in a country side in the Canton of Berne. This site is a typical parcel of land in a mountainous area in Switzerland. The second test area is located at the Science City Campus Hoenggerberg, ETH Zurich (see Figure 4.60). This test area represents a typical suburban area in Switzerland.

Both sites were documented with tachymetry and UAV. The tachymetric method was applied as it would be normally used for a real cadastral surveying task. All individual steps of the workflow including data acquisition, data cleansing and the plan development were completed for both test areas. The method UAV consists of flight planning, image acquisition, image orientation, stereoscopic measurements of the object structures and the plan development.

The results of the image orientation shows that the limiting factors are camera calibration, image quality and definition of the ground control points (natural or artificial control points) in the image space. However, it was possible to fulfil the accuracy requirements for cadastral surveying. Furthermore, the results show that both methods obtain comparable results with respect to accuracy, completeness and expenditure time. Thus, the UAV method could be used as a supplement to the standard surveying methods, while additional data such as overview images and orthoimages could be derivated from the acquired images (see Figure 4.62).



Figure 4.62: Left: Overview image of the test area Campus Science City Hoenggerberg. Right: Map of the test area generated from UAV images.

## Positioning methods of Unmanned Aerial Vehicles (UAVs)

by Henri Eisenbeiss

Institute of Geodesy and Photogrammetry, ETH

The precise reconstruction of the 3D-trajectory of mini-UAVs in real time can be determined with several geodetic measurement methods. Normally, UAVs have GNSS, INS, compass and barometer sensors on-board for the determination of their position and orientation. Due to the limitation of the payload, the low-cost sensors mounted on the system have light weight and less accuracy. Thus, we are focusing on the evaluation and improvement of the accuracy of the navigation data.

The following sensors can be used as internal and external sensors for the positioning and orientation of the UAV system (see Figure 4.61):

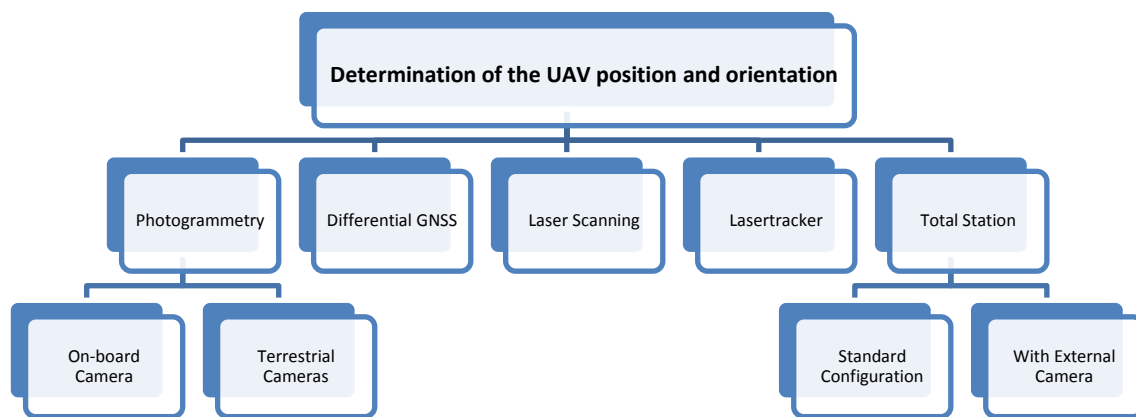


Figure 4.63: Overview of tracking sensor for the positioning and orientation of the UAV system.

In order to achieve real-time 3D-measurement data with accuracy better than 1 cm and high temporal resolution ( $\geq 5$  Hz), so far only tracking of total stations has been investigated successfully (Eisenbeiss et al. 2009). This kind of technology is particularly well suited for applications, which require millimeter accuracy in planimetry and height for object distances up to 300 m, which is a normal distance of an UAV image strip. The polar coordinate measurement system determines, using the 3D-distance as well as the horizontal and vertical angle, the XYZ-position of a moving  $360^\circ$  prism with respect to a certain time stamp. In the last years, the main manufacturers of geodetic measurement systems worked on the optimization of kinematic observations of total stations. GNSS, Lasertracker and LiDAR-Systems, however, do not meet the requirements for this particular task. Additionally, the tracking of the helicopter using high speed cameras could be applied in small areas, while for larger areas, due to the limitation of the field of view of the camera, a new construction for the automatic target tracking is necessary. Thus, for a first test we decided to use the available tracking tachymeter.

Considering the influence of different parameters like:

- the maximum tracking speed,
- the precision of the  $360^\circ$ -prism,
- the dynamic behavior of the integrated two-axes tilt sensor,
- the synchronization of the angle and distance measurements, as well as the latency and dead times, and
- the behavior of the target tracking,

it is possible to achieve an absolute accuracy of a few millimeters. This is not particularly required for the analysis of the flight trajectory of image data acquisition. However, the potential accuracy would help to analyze the flight trajectory of an UAV with an implemented LiDAR or range camera system in future work. The observed flight trajectories of autonomous flights of UAVs were compared to the planned trajectory and the trajectory generated from the navigation data of the UAV.

In future work we will focus on the determination of the orientation data using total stations in combination with terrestrial cameras. Thus, the UAV platform will be additionally equipped with reference marks, such as infrared diode, which can be observed from the total station and from the terrestrial camera.

## **GNSS Orientation Finding**

*by D.E. Grimm*

*Institute of Geodesy and Photogrammetry, ETH*

The knowledge of a geodetic measuring system's orientation is often of particular importance. Nevertheless, satellite based positioning systems (GNSS) work at a first glance without orientation; GNSS does not need any orientation, nor does it deliver any orientation information.

There is no need for orientation of the antenna when obtaining the coordinates, apart from minor influences such as antenna phase centre offsets. However, if GNSS is used for stake out for instance, orientation information is required. And there are several more applications that require orientation in addition to the position. Some application areas are navigation, guidance for construction machines and farming equipment, initial orientation for surveying tasks and pedestrian navigation. In navigation the moving direction (heading) is required to provide further route information. In pedestrian navigation orientation information is very advantageous. Knowing the viewing direction of a pedestrian enables a navigation device to give proper directives and help the user to find his way or his point of interest.

The objective of this research project is to augment GNSS receivers with a possibility to determine the orientation of the antenna. The orientation of the antenna is determined, without moving the antenna or using auxiliary sensor like compass or gyro.

The antenna orientation is realized by using the information of the satellite constellation. By knowing the antennas position and the satellite's positions, the satellites can be used as directional references. To use this information, the direction of arrival (DOA) of the satellite signals has to be known. The main task of this work is to determine the direction of arrival. As this is not directly measurable, a detectable base quantity has to be found.

The signal to noise ratio serves as such a base quantity. The signal to noise ratio of each satellite's signal is mainly dependent of the actual satellite constellation, but remains stable for several minutes. A specific, partial attenuation of the antenna can now influence the measured signal to noise ratio of some received satellites. The signal intensity decreases when the attenuating material is placed between the antenna and the satellite. By rotating this material around the antenna, a geometrical relation can be effected. By analyzing the signal to noise ratio in respect of the rotating attenuation, the direction of arrival of the satellites can be located.

With the help of adequate analysis tools, the orientation of the antenna can be calculated with a standard deviation of about 3 degrees.

## GPS-Tomography and Assimilation in Numerical Weather Models (GANUWE)

by D. Perler, A. Geiger

Institute of Geodesy and Photogrammetry, ETH Zurich

GPS tomography allows to estimate the distribution of water vapor in the troposphere. The goal of the project GANUWE is to develop a GPS tomography software providing 4D water vapor fields for assimilation in numerical weather prediction models. In the project, a tomography software based on the Kalman Filter approach using new voxel parameterization techniques was implemented. The software was validated with synthetic tests and within a long-term study using GPS observations from the Swiss permanent network AGNES (Perler et al. 2011). In addition, the impact of new global navigation satellite systems (GNSS) and additional receiver stations on the accuracy was investigated.

Sensitivity analyses are carried out for two extensions of the measurement setup: (a) use of the upcoming GNSS Galileo, and (b) augmentation of the number of receiver stations. An accuracy measure was computed each hour with a total simulation duration of 24 hours (see Perler et al. 2010). Figure 4.62 shows the stations of the GPS network AGNES (black squares) and the synoptic network ANETZ (black triangles). The red lines indicate the floor plan of the grid used in the experiment. Figure 4.63 shows the accuracy for different measurement configurations. The use of the additional satellite navigation system Galileo increases the accuracy by about 10-15%. The main effect is, however, a more consistent accuracy over time. This is clearly visible in combination with a dense network (blue vs. purple line in Figure 4.65).

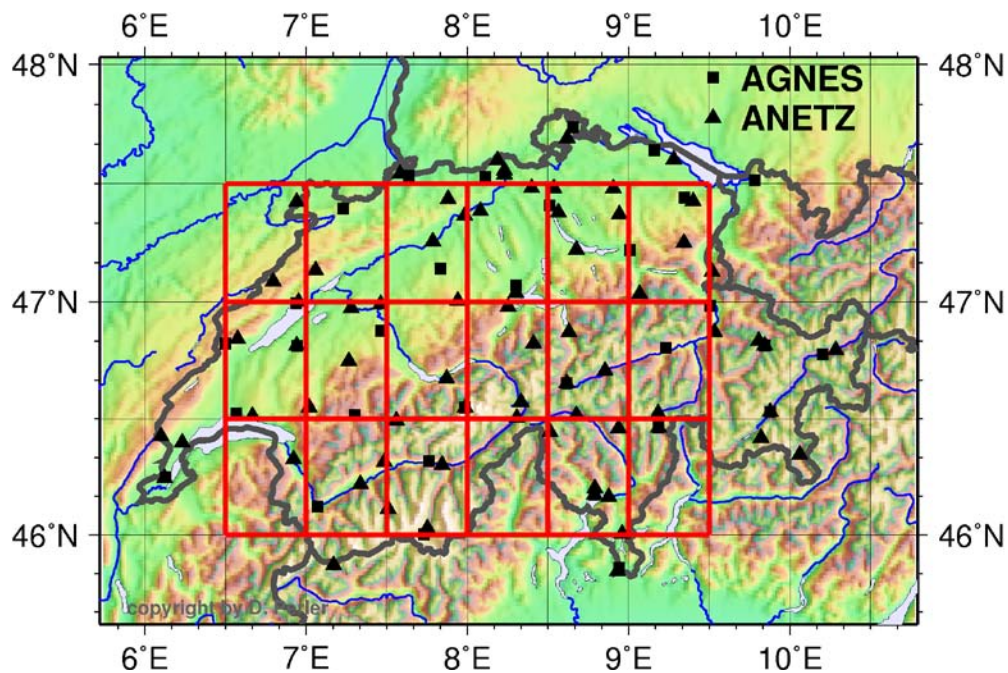


Figure 4.64: GPS network AGNES (black squares, swisstopo) and the synoptic network ANETZ (black triangles). red lines: used voxel grid.

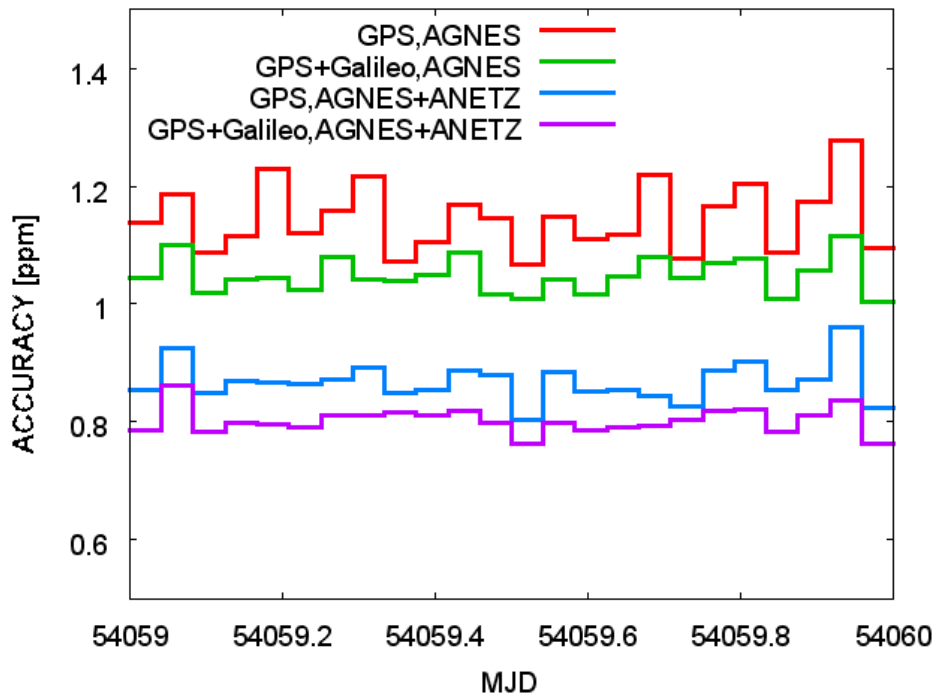


Figure 4.65: Accuracy of tomographic solutions. Adding system Galileo increases the accuracy by about 10-15%. Addition of a dense receiver network (ANETZ)(blue and purple lines).

The use of the supplementary network ANETZ (providing about 60 additional stations) increases the accuracy by about 25%. Further investigations have shown that additional receiver stations have a larger impact on the accuracy than additional satellites. Figure 4.63 also shows that the increase of the accuracies achieved by additional receiver stations and satellites is cumulative. This suggests that equipping new stations with multi-GNSS capable receivers will strongly improve the quality of tomographic results.

## Geodetic contribution to the process understanding and prediction of hydrological extremes and complex hazards (APUNCH)

Fabian Hurter, Alain Geiger

Institute of Geodesy and Photogrammetry, ETH Zurich

APUNCH is an interdisciplinary project, supported by the Competence Center Environment and Sustainability of the ETH Domain (CCES), that investigates the process chain from heavy rainfall to hydrological hazard on catchment scale, specifically in the Matter- and Saastal of the canton Valais. The aim of understanding the process chain is to improve predictions of hydrological parameters and flood risk mitigation.

Predicting the amount, timing, and location of heavy precipitation is still a very demanding task. However, it is a prerequisite to take appropriate short time measures to mitigate flood risks from mountain rivers. The classical approach using radar images to predict precipitation fields some hours ahead is still superior to the forecast from numerical weather prediction models. This is mostly due to inadequate initial conditions of the numerical weather model with respect to the atmospheric water vapour distribution. Water vapour fields determined from GNSS systems complement the off-ground measurements of atmospheric water vapour, as shown by various studies around the world. The Geodesy and Geodynamics Lab at ETH Zürich contributes to the APUNCH project with its expertise in GNSS meteorology.

Since water vapor in the atmosphere slows down RF electromagnetic waves, hence causes path delays in measurements of GNSS receivers, the integrated water vapor along the ray-path from satellite to receiver can be determined. Deploying a receiver network allows the 3D retrieval of the atmospheric water vapor using a tomographic algorithm. To study the evolution of water vapor fields with respect to precipitation, high resolution in space and time are needed. This requires a very dense and carefully designed station network. During a field campaign in summer 2010, such a network was set up in the Zermatt region on an area covering approximately 100 square kilometers (Figure 4.64). It included 33 geodetic GNSS receivers and 4 half-permanently installed low-cost 1-frequency receivers. For validation purposes, 25 radiosondes were launched within the measuring period.

In collaboration with the hydrology group of ETHZ (Prof. P. Burlando), we also have access to rain gauge measurements along a terrestrial profile in the Zermatt region. The rain gauge measurements and radar measurements from MeteoSwiss will be compared to the water vapor fields from GNSS. This is used to study the devolution of rain events in an alpine region and to better understand correlations between the rain and the water vapor field. With the combination of GNSS measurements with radar and rain gauge data, the goal is to make a step forward in the combination of weather data for better precipitation forecasts.

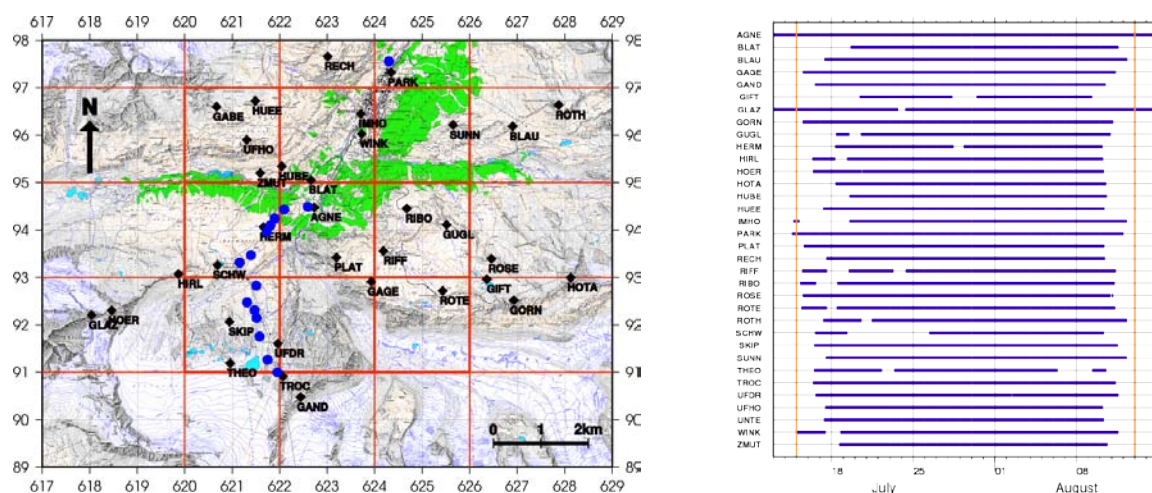


Figure 4.66: Map on the left shows the Zermatt region with the geodetic GNSS receiver network deployed during the summer campaign 2010 (swiss grid coordinates in kilometers). Blue dots denote the rain gauge transect set up by the hydrology group of Prof. P. Burlando. Red lines that overlay the map indicate the model grid for the tomographic reconstruction of the atmospheric water vapor from GNSS measurements. Time plot on the right shows the stations' activity. Station AGNE belongs to the Automatic Geodetic Network Switzerland (AGNES). All other stations were installed for the duration of the campaign. Red vertical lines mark start and end of campaign.



## **X-Sense: Monitoring Alpine Mass Movements at Multiple Scales**

*by P. Limpach, F. Neyer, A. Geiger*

*Institute of Geodesy and Photogrammetry, ETH Zurich*

Global climate change dramatically influences mountain areas like the European Alps. As a consequence, destructive geological processes can be triggered or intensified and the stability of slopes are influenced, leading to possible landslides. The interaction between these complex processes is poorly understood. The research work within the X-Sense project considers the above aspects with the following aims: (a) Development of wireless technology for environmental sensing under extreme meteorological and mechanical conditions. (b) Integration of various sensing dimensions (such as pressure, humidity, crevice movements, high precision deformation and movements) in terms of sensing and processing hardware, software and sensor fusion algorithms. (c) Extension of the spatial scope from local (microscopic) measurements to large scale information based on satellite radar remote sensing as well as fusion of the resulting information to achieve an unparalleled degree of precision in space and time. (d) Usage of this new measurement technology for advanced applications in science and society: geophysical research and early warning against landslides and rockfall.

The X-Sense project is funded by the Swiss National Science Foundation program Nano-Tera. X-Sense is a collaborative project between the Computer Engineering and Networks Lab of ETH Zurich, the Geodesy and Geodynamics Lab (GGL) of ETH Zurich, the Department of Geography of the University of Zurich, the Federal Office for the Environment (FOEN), and the company Gamma Remote Sensing.

In a pre-project to X-Sense, the GGL is operating a test network for GPS monitoring on Dirru rockglacier in the Matternal (Swiss Alps) since June 2009 (Figure 4.67 (a)), with financial support of FOEN. The goal of the test network is to investigate the potential of low-cost GPS receivers for a precise monitoring of slope instabilities in mountain areas. A permanent GPS monitoring should allow to validate displacement velocities detected by InSAR, strengthen the understanding of processes linked to permafrost-related slope instabilities, and improve existing monitoring and early-warning systems. The test network consists of three permanent GPS stations (Figure 4.67 (a)): a reference station placed within a stable area and two stations on the rockglacier. All stations are equipped with low-cost L1 GPS receivers and powered by solar panels (Figure 4.67 (b)). The GPS data processing is based on differential carrier phase techniques. Daily station coordinates as well as kinematic coordinates with sampling intervals of 5 to 30 s are computed at cm-level accuracy. The time series of 17 months of GPS data shows the capability of the low-cost system to reliably observe station velocities in the order of 1.0 to 2.5 cm/day (Figures 4.67 (c) and 4.67 (d)). Also, seasonal velocity variations in the order of 0.5 cm/day were detected, as well as inter-annual variations of the velocity pattern of the rockglacier. Investigations are in progress to assess the correlation between the observed surface velocities and meteorological data.

The GPS monitoring system is enhanced by additional developments that are carried out in the course of the X-Sense project. These include improvements in on-site hardware installation, data communication, and parameter estimation schemes. Since winter 2010/2011, the test network is being augmented with more GPS stations, partly including on line data transmission.

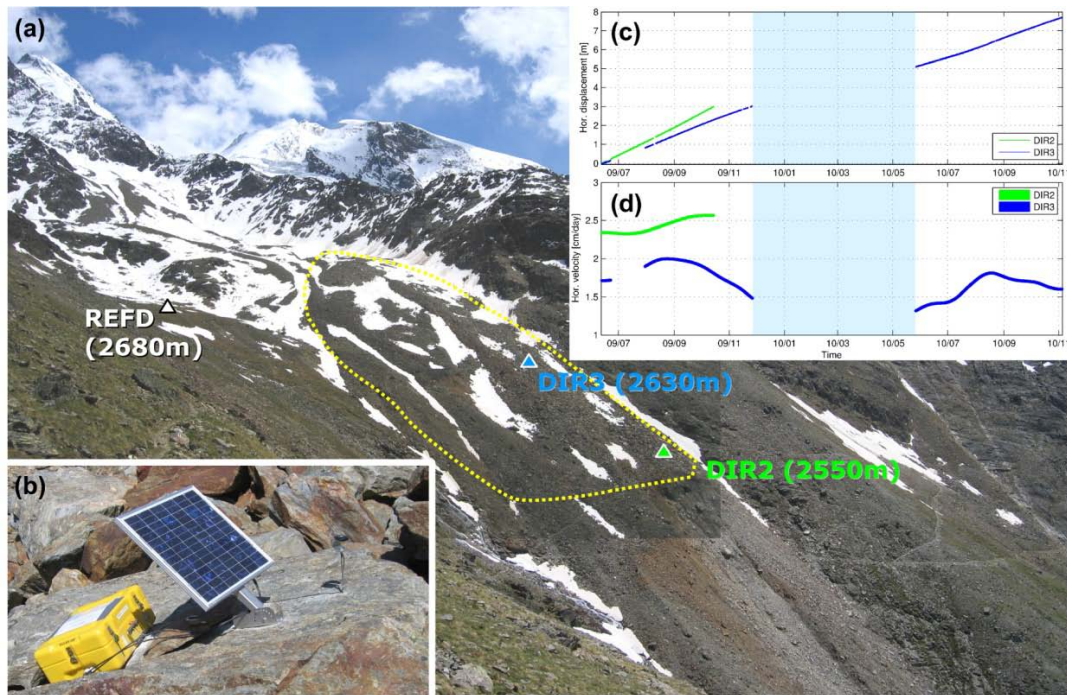


Figure 4.67: (a) GPS test-network on Dirru rockglacier (yellow area), with three permanent GPS stations (REFD: reference; DIR2 and DIR3: stations on rockglacier). (b) GPS station DIR2. (c) Horizontal displacements of GPS stations DIR2 (green) and DIR3 (blue) from June 2009 to Nov. 2010 (17 months). (d) Horizontal velocities of DIR2 and DIR3. The operation of DIR2 had to be stopped in Oct. 2009, due to its critical position at the front of the rockglacier. Blue background: data gap caused by snow cover.

## GPS-Gyro

by S. Häberling, A. Geiger

Institute of Geodesy and Photogrammetry, ETH Zurich

To this day, the satellite-based navigation systems such as the Global Positioning System (GPS) have been mainly used for positioning applications. 3D rotations or attitude rates are commonly determined by the straight forward application of multi-antenna systems. An additional method to retrieve 3D rotation angles from measurements with a single GPS antenna in real-time has been devised. The information about the angular velocities and the full 3D rotation in addition to the position would enlarge the applicability of GPS in machine control and air navigation.

The method takes advantage of the properties of the circularly polarized electromagnetic waves that are transmitted by the GPS satellites. The rotation of the receiver antenna relative to the satellite antenna generates a phase shift called “phase wind-up” (Figure 4.66). Depending on the type of rotation and on the elevation angle of the incoming signal this phase shift, measured from different satellites, allows the description of the full 3D antenna rotation.

For the detection of small angular velocities in GPS raw data it is necessary to build the geometry free linear combination L4 to eliminate perturbations on carrier phase. The detection algorithm is based on the prediction of that L4 signal by appropriate filter methodologies. The computation with multiple prediction lengths was demonstrated by real observations with a dual frequency receiver at an acquisition rate of 10 Hz. The results indicate that minimal rotational velocities of 3-3.5 °/s are significantly (99%) detected depending on time of day (e.g. ionosphere) and satellite constellation. The algorithm developed for the determination of the full 3D rotation generates stable solutions. This was verified by simulations and real measurements (Figure 4.67).

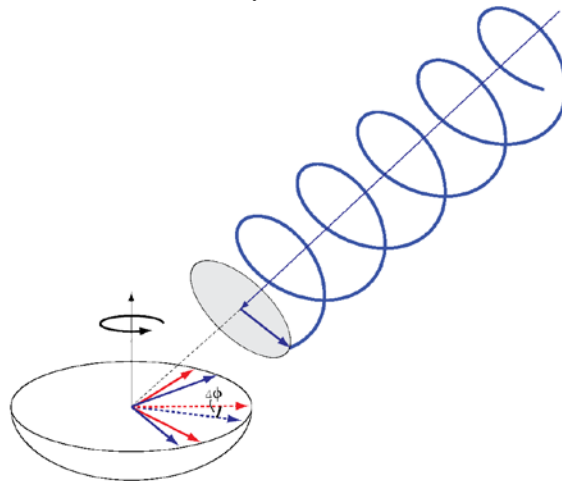


Figure 4.68: A simplified schematic illustration of an incoming circularly polarized electromagnetic wave. Due to the rotation of the GPS antenna (blue to red) an angle (phase shift  $\Delta\phi$ ) occurs between the two dipole vectors (dashed). They can be described as a projection from the polarization plane (grey) onto the antenna plane.



Figure 4.69: Measurement setup with the rotation simulator and the mounted GPS antenna.

## Geodetic aspects of GNSS assisted approach and landing, Radar surveillance and multilateration

by M. Manyoky, C. Iosifescu, A. Villiger, St. Rutzer, A. Geiger

Geodesy and Geodynamics Lab, Institute of Geodesy and Photogrammetry, ETH Zurich

In different studies geodetic know-how has been applied to air navigational problems. The most important questions concern the civil usability of GNSS for approach and landing where guidance is one of the most challenging applications for satellite-based navigation.

The regulations in aeronautic navigation currently permit GNSS supported approaches in the following cases: non-precision approach and approach with vertical guidance. In discussion is also Cat I, precision approach. The special approach and landing procedures created for GNSS require usually backup by conventional navigation facilities.

Theoretical analyses and simulations show that the number of visible satellites as well as the constellation can become critical during a curved approach trajectory. The situation, as shown theoretically, can be improved by using additional GNSS, like GLONASS and the future European Galileo.

Integrity is one of the most important requirements for aviation to be fulfilled also by GNSS. One of the studies carried out focuses on the Receiver Autonomous Integrity Monitoring (RAIM) algorithms, which are included in the category of Aircraft Based Augmentation System, and perform a consistency check, inside the GNSS receiver, in order to alert the user immediately in case of a system failure. Based on the initial definition of RAIM, the impact of the exclusion of some satellites on the position has been investigated. The generated Stanford plots show that the positions tend to cluster together and outliers emerged only by intentionally introducing measurement errors, thus demonstrating the stability of the systems.

Integrity risk is defined as the probability that the Navigation System Error (NSE) exceeds either the Horizontal or Vertical Alert Limits (HAL and VAL) and the navigation system alert is silent beyond the time-to-alarm. On the other hand, continuity risk is defined as the probability that the navigation system alarm will drop during the operation (precision approach in this case). These are competing constraints on the system; integrity failures shall not lead to Hazardously Misleading Information (HMI) favouring a small alert limit but continuity failures lead to False alarms favouring a large alert limit.

The availability emphasizes the operational economy of the navigation system. It is computed as the fraction of time the GNSS augmentation system is providing position fixes to the specified level of accuracy, integrity and continuity.

The true error must not exceed the protection level by more than a certain probability. If the computed protection level exceeds the corresponding alert limit then the alarm is activated and the operation cannot proceed. If the operation has already begun this condition is a continuity breach and a missed approach procedure is initiated. Otherwise the system is declared unavailable for that epoch.

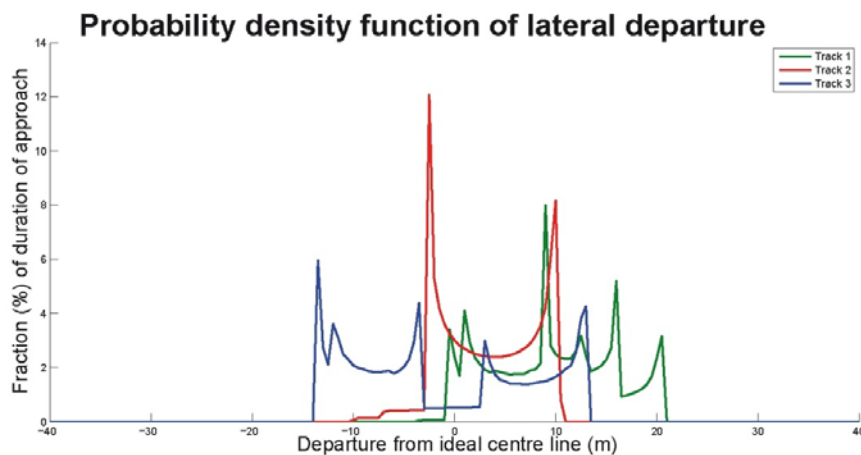


Figure 4.70: Probability density function of lateral departure (fraction (%) of duration of approach). Example of three different tracks. It is clearly seen, that departures during an individual approach are by far from a normal distribution.

Investigation on the statistics of approaches has been carried out revealing the non-Gaussian distribution of the departure from ideal approach trajectory of a single aircraft (Figure 4.68). Therefore, statistical calculation based on a few aircraft trajectories has to be reviewed for the correct use of the appropriate error distribution.

Multilateration is a ground based system to position aircrafts. Distances from several ground stations to the aircraft are measured. Knowing the co-ordinates of the stations the position of the aircraft can then be calculated by a resection of several known distances. Additionally calibration constants might be determined at the same time by well known geodetic techniques. Discussions are still in course to use multilateration as back-up systems for other navigational installations, eg. GNSS.

The increasing traffic density (Figure 4.69) especially in the Swiss airspace makes high demands also on surveillance and collision hazard mitigation. To this end investigations have been carried out to geometrically determine hot spots concerning collision hazard. The analysis was based on one month of track data.

### Aircraft Positions (24 hours)

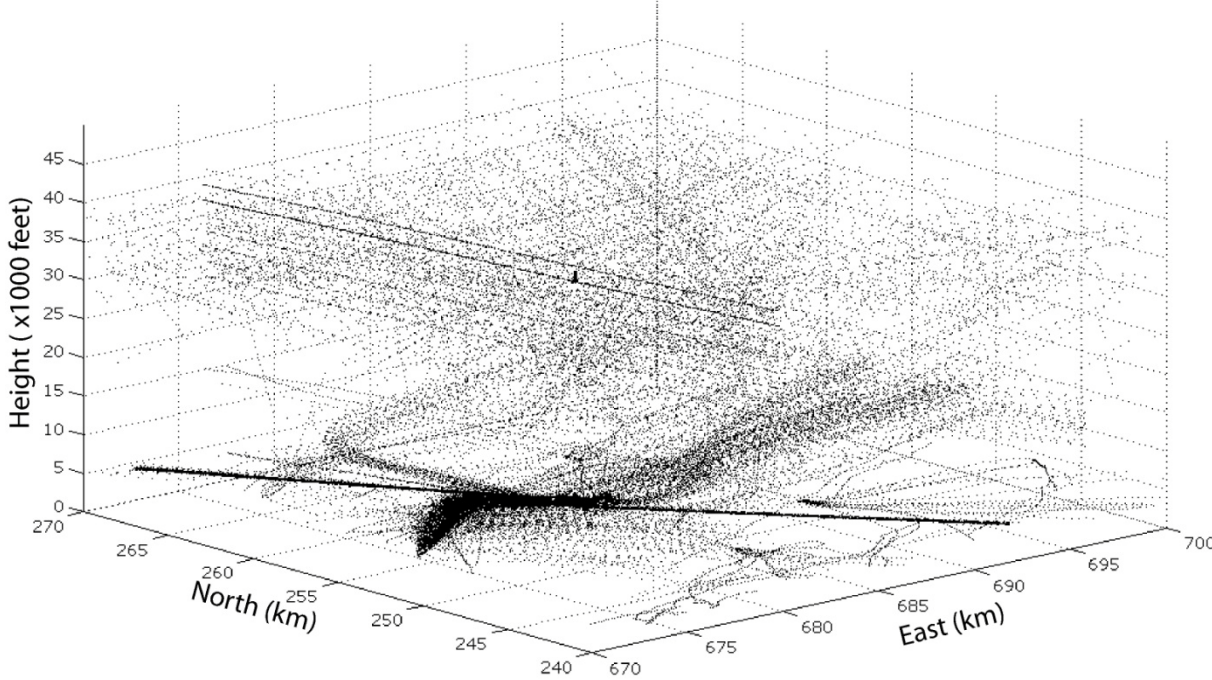


Figure 4.71: Aircraft positions (24 hours) in the airspace above Zurich airport (30 km X 30 km x 35000 ft). The figure illustrates the complexity of the surveillance task in dense traffic areas.

## **Analysis and corrections of non-hydrostatic effects on GNSS observations and antenna errors for accurate GPS and Galileo IWV estimates**

by F. Scirè Scappuzzo<sup>1</sup>, B. Bürki<sup>2</sup>, A. Geiger<sup>2</sup>, H.-G. Kahle<sup>2</sup>

<sup>1</sup> *Physical Sciences Inc. (PSI), Andover, MA, USA*

<sup>2</sup> *Institute of Geodesy and Photogrammetry, ETH Zürich*

Ground-based GNSS receivers provide highly valuable information on integrated water vapor (IWV). Several feasibility studies have demonstrated the practicability of this method. Meteorological institutes assimilate these data in numerical weather prediction models. The IWV is derived from a model based on atmospheric variables, GNSS zenith delays and zenith hydrostatic delay (ZHD) estimates. Investigations were carried out to study these effects in high mountainous areas, such as the Jungfrauoch, Switzerland, located at an altitude of 3'600 m.a.s.l. It is affected by high winds associated with non-hydrostatic conditions. Corresponding corrections to the classical GPS estimates have to be applied in order to achieve utmost possible accuracies. The core of the research work was devoted to develop models of the ZHD which include non-hydrostatic effects caused by orographic uplifting of air masses.

Achievements included the estimation of IWV from signal delays and their mathematical modelling. Specific validation studies were performed which resulted in the confirmation of the need for non-hydrostatic corrections. A model was developed for the estimation of the deviation of the pressure from hydrostatic equilibrium, and its effect on GNSS corrections was implemented. The correction model was applied to real field data sampled at station Jungfrauoch, Switzerland. This GPS site located at high altitude is important because it is used as reference for altitude corrections for the IWV estimates of the Swiss national GPS network. Additional field data were acquired from Mt. Washington, and other US mountainous sites, which are exposed to extreme wind conditions characterized by strong vertical accelerations of air masses.

The validation was achieved by comparing IWV estimates, with and without non-hydrostatic corrections with radiometer based estimates at Jungfrauoch. Although the radiometer data were sparse it was shown that the correction model works best for the case of passage of high winds over narrow mountain ridges. This was also confirmed using a statistical analysis of meteorological data. It was demonstrated how the non-hydrostatic model developed can be integrated into better IWV GNSS estimates at high-altitude stations exposed to severe weather conditions. The algorithms developed are a useful tool for correcting non-hydrostatic effects in an environment where other data are not available or are not applicable.

During the studies it emerged that the performance of the GNSS receiving antenna was as important as the non-hydrostatic effect. An effort was, therefore, also focused on the enhancement of the GNSS antenna design. Major topics of concern were the mitigation of multipath, antenna phase center stability and radome effects. Furthermore, future satellite signals in a broad bandwidth, such as emitted from GALILEO, were considered. The characteristics of GNSS receiving antennas and the principles of ground planes were analyzed in detail with the aim to optimize the classical choke ring ground plane. A new wideband low-multipath antenna was developed by considering the propagation of surface waves rather than cutting them off. The novel antenna prototype was successfully fabricated and tested. The bulk of his work was performed in the frame of the external ETH PhD thesis of Dr. F. Scirè Scappuzzo. Cooperating partner was the Department of Geography and Environment, University of Boston, USA.

## Geodetic Project Course 2008 in Greece

by B. Bürki, H.-G. Kahle, S. Guillaume, Ph. Kehl, M. Müller

*Institute of Geodesy and Photogrammetry, ETH Zürich*

At the end of their studies graduate students at the Department of Civil, Environmental and Geomatic Engineering of ETH Zurich attend the Geodetic Project Course (GPC). The general goal is to carry out project planning, perform practical field work, data processing at their own initiative and get practice in team work. The GPC 2008 has been organized in the region of the North Aegean sea, Greece, between the peninsula Halkidiki und the chain of the Northern Sporades Islands.

The most striking topographic feature in this region is the Holy Mountain Athos (Agios Athos, Figure 4.70) located at the south-eastern tip of Halkidiki. It belongs to the self-governed monastic state Athos. Its offering a most spectacular view over the northern part of the North Aegean Sea. Since the mountain rises directly from the sea it was obvious to tie the relief of the equipotential surface directly to sea level. In this respect the main target was the de-termination of the equipotential surface at sea level (geoid).



*Figure 4.72: The Holy Mountain ATHOS (2033 m above sea level) located at the southern tip of the Halkidiki peninsula in the Northern Aegean Sea (Greece).*

### Methods applied

Different measuring scenarios were applied in the context of the GPC 08 to determine the geoid:

- Determination of the direction of the local plumb line, expressed in deflections of the vertical by means of astrogeodetic measurements to the stars.
- Assessment of the geoid changes between the north-west and the south-east borders of the island of Alonissos by a trigonometric 3-dimensional height profile crossing the northern part of Alonissos. For this purpose, a precise geodetic height traverse based on high-precision reciprocal vertical angle- and distance measurements was measured. The total stations used for this purpose were equipped with the measurement system DAEDALUS which enables high-precision reciprocal vertical angle measurements (see contribution Bürki et al., this volume).
- GPS observations at several islands as well as on board of a yacht equipped with several GNSS receivers and ultrasound sensors (see report Sea Surface, Limpach et al., this volume).

The deflections of the vertical were measured by means of two different systems:

High-precision Digital Astronomical Deflection Measuring System (DIADEM). This equipment is shown in Figure 4.71. It consists of a camera which is taking images in zenith direction in two opposite orientations. With this system the astronomical latitude and longitude are determined with an accuracy of about 0.1 arcsecs. Due to the heavy weight of this instrument (about 100 kg in total), its use is restricted to stations which are accessible by car.



Figure 4.73: The zenith camera system DIADEM near the Monastery Agios Pavlos (Athos). Prior to the observations to the stars, the geodetic coordinates are determined with a GNSS receiver (visible on top of the camera).

The second system takes advantage of light weight which offers easy transportability. In order to perform measurements also on top of Holy Mountain Athos, two systems DAEDALUS have been transported (Figure 4.73) to this station at a height of 2033 m a.s.l. These systems consist of a total station and a small CCD camera which can be clipped on to the telescope instead of the eyepiece enabling fully automated digital observations of stars (Figure 4.74). The method applied is very close to the well known method of equal heights. As with DIADEM, the outputs of DAEDALUS are the astronomic latitude  $\Phi$  and longitude  $\Lambda$  of the station.

The deflections of the vertical are obtained by determining the differences between astronomic latitude and longitude ( $\Phi$ ,  $\Lambda$ ) and the corresponding parameters ( $\varphi$ ,  $\lambda$ ) referring to the ellipsoid.



Figure 4.74: Transport of the material to Holy Mount Athos (left). The buildings in the background belong to the Monastery Agios Pavlos (Saint Paul). TCA1800 Total station with DAEDALUS system mounted (right).





Figure 4.75: Students with two DAEDALUS systems preparing the measurement on top of Mount Athos.

The shape of the geoid finally was computed using the approach of astronomic levelling. The successful measurements clearly revealed that the gravitational attraction of the mountain corresponds to a relative geoid high reaching 62 cm (Figure 4.75). The lateral gradient of the geoid slope reached up to 12 cm/km seaward of the Holy Mountain Athos.

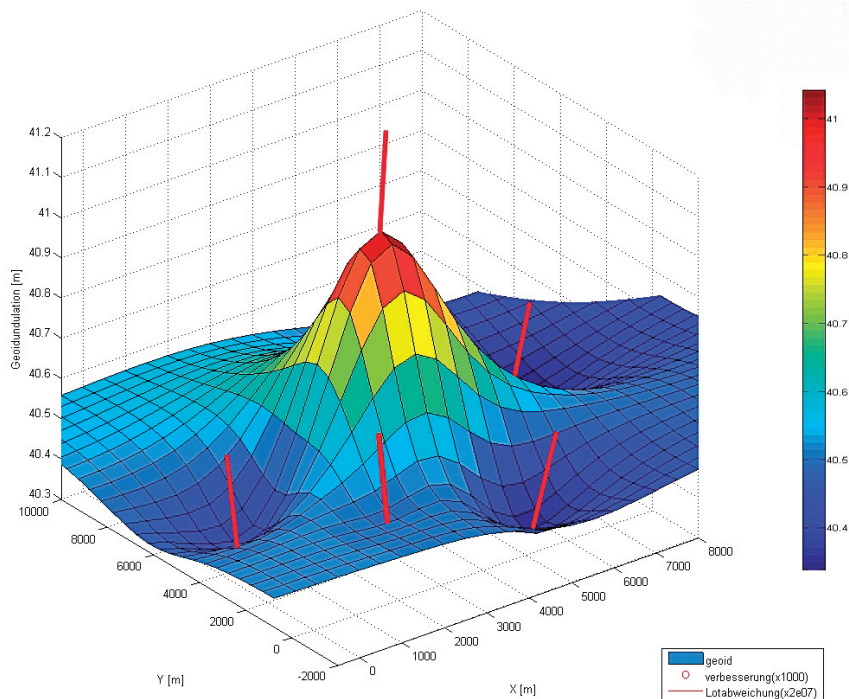


Figure 4.76: The shape of the geoid in the the area of Mount Athos. The gravitational attraction rises the geoid by 62 cm. The red lines indicate the direction of the local plumb line (normal to the geoid).

Relatively large gradients of the geoid were also detected at the north-west coast of the island of Alonissos (Northern Sporades, Greece) (inset A in Figure 4.76) reaching up to 9 cm/km. Steep fault zones in the earth's

crust, deep basins and corresponding sedimentary fillings are likely the reason for the slant sea surface encountered offshore Alonissos. The measurement system developed by Ph. Limpach (GGL) consists of five geodetic GPS receivers and two ultrasonic ranging sensors, which were installed on a yacht (compare Sea Surface, Limpach et al., this report). The instantaneous sea surface, corrected for tides, barometric pressure and other dynamic effects, allows for the determination of a sea surface height that corresponds to the geoid. This method reveals local inhomogeneities in coastal areas, which cannot be detected by satellite radar altimetry. The North Aegean Trough is of particular interest because of its seismotectonic activity. Its dynamics can be further studied by incorporating the sea surface topography as additional modelling constraints.

The GPC08 contributed substantially to the regional geoid determination in the Northern Aegean Sea. This area of research activities conducted by the Geodesy and Geodynamics Lab is displayed in Figure 4.77.

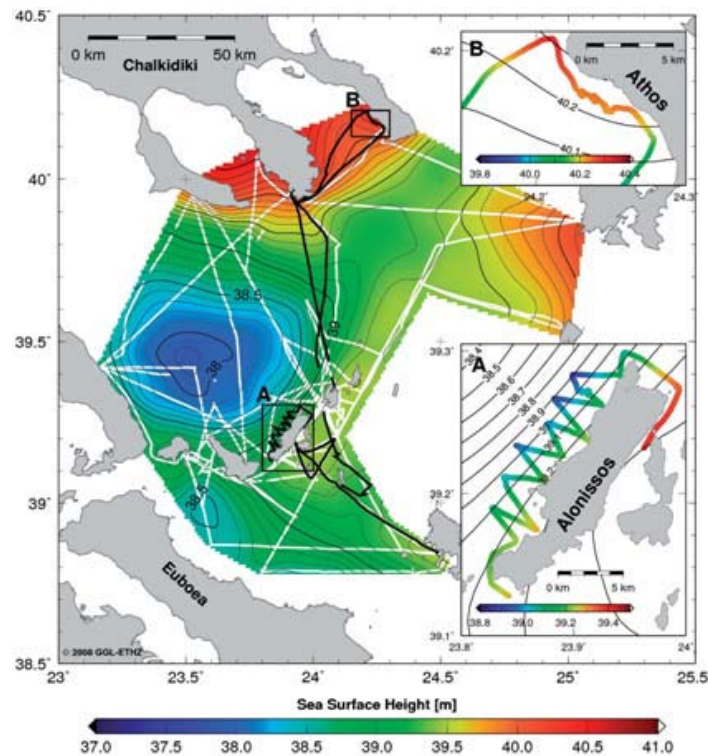


Figure 4.77: Sea surface topography in the Northern Sporades, referred to the WGS 84 ellipsoid. Black tracks were measured during the Geodetic Project Course 2008. White tracks originate from previous campaigns (compare Sea Surface, Limpach et al., this report). The insets A and B show color coded sea level profiles for Alonissos and Athos, respectively.

Participating students: J. Bertsch, S. Büttler, C. Feuer, C. Forrer, F. Gigon, S. Haeberling, R. Loop, D. Näpflin, K. Troxler, P. Wirz, R. Wolf

We would like to express our sincere thanks to our colleagues from the Aristotle University of Thessaloniki (Prof. I. Tziavos, Dr. C. Tokmakidis) and to the Authorities of the Independent Monastic State Athos. Particular thanks are addressed to the Abbots of the monastery Agios Pavlos and Megistis Lavras for their hospitality.

## Geodetic Project Course 2010 at CERN

by S. Guillaume<sup>1,2</sup> and B. Bürki<sup>1</sup>

<sup>1</sup>Institute of Geodesy and Photogrammetry, ETH Zürich

<sup>2</sup>Surveying Section at CERN

The traditional three-weeks Geodetic Project Course (GPC) organized by the Institute of Geodesy and Photogrammetry was exceptionally realized at CERN (Organisation Européenne pour la Recherche Nucléaire) in the section of surveying in the group of Accelerators and Beam Physics. Six geomatic master's-level students had the opportunity to work on two different projects which are directly related to current research projects at CERN.

The first task was the determination of a new astro-geodetic geoid in the region of the world famous particle physics experiment, the Large-Hadron Collider (LHC). Astronomical deflections of the vertical were successfully measured and processed with the Digital Astronomical Deflection Measuring System (DIADEM) with an accuracy of 0.1 arc seconds. The astro-geoid was then computed using appropriate mass models (remove-restore technique) and the residual field was interpolated and predicted with least-square collocation based on a 3<sup>rd</sup> order Markov covariance model. This new geoid can be considered with a sub-centimetric precision.

The second project was related to the feasibility study of the new electron-positron linear collider projected at CERN, the Compact Linear Collider (CLIC). The aim was to validate the use of the system DAEDALUS, developed at GGL, in terms of precision and automation for the determination of the three-dimensional positions of ceramic spheres fixed on accelerator facilities. The system DAEDALUS consists of a combination of a total station with a CCD camera and appropriate software in order to carry out highly accurate angular observations automatically without human intervention. A micro-geodetic network formed by angular observations measured from several stations and interferometric distances were processed in the three-dimensional software Trinet+ in order to estimate coordinates and statistical indicators. These positions were compared with a Coordinate Measuring Machine (precision better than 1 micron) and shows that spheres placed on objects of 1 to 2 meter length can be measured with a precision better than 10 microns which opens up to DAEDALUS the field of industrial metrology. For more details on the DAEDALUS system comparison: (Bürki et al, this report).

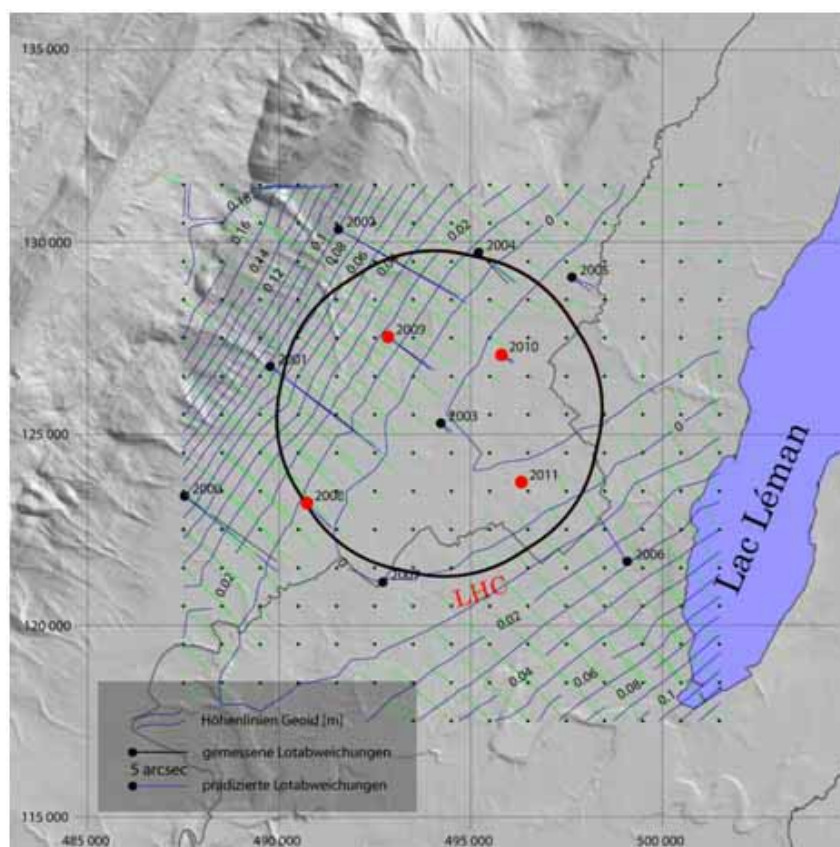


Figure 4.78: Observed and predicted deflections of the vertical and geoid undulations in a local geodetic datum.

## Determination of Atmospheric Water Vapor Abundance using Solar Lunar Spectrometry

by St. Münch<sup>1,2</sup>, B. Bürki<sup>1</sup>, M. Rothacher<sup>1</sup>, H.-G. Kahle<sup>1</sup>, P. Sorber<sup>1</sup>, H. Becker-Ross<sup>2</sup>, St. Florek<sup>2</sup>, M. Okruss<sup>2</sup>, R. Tischendorf<sup>2</sup>

<sup>1</sup>Institute of Geodesy and Photogrammetry, ETH Zurich

<sup>2</sup>Leibniz-Institute of Analytical Sciences (ISAS), Berlin

Atmospherical water vapor plays a crucial role in the understanding of global climate change, as it contributes most to the atmospheric greenhouse effect. Its role in positive feedback effects (warming leads to stronger vaporization and thus higher water vapor concentrations) and negative feedback effects (increased humidity leads to forming of clouds which act as sunlight reflectors) is still not sufficiently understood. In the field of satellite geodesy water vapor also plays a significant role. The nonobservance of the influence of water vapor on the signal propagation leads to systematic errors. Several measurement techniques operating with microwave signals are affected, such as GNSS, Satellite Altimetry or VLBI (Very Long Baseline Interferometry).

Differential Optical Absorption Spectrometry (DOAS), either used with artificial light sources or natural radiation sources like the sun, has been a powerful instrument for the determination of trace gas concentrations in open atmosphere for many decades. The high resolution solar spectrometers SAMOS and GEMOSS, jointly developed by the Geodesy and Geodynamics Lab (ETH Zürich) and the Leibniz-Institute of Analytical Sciences (ISAS), have proved that DOAS is also feasible for the remote determination of total water column values with high temporal resolution and very high precision. The fact that the measurement instruments are auto-calibrated shows its potential as a validating method for other instrumental approaches such as Water Vapor Radiometry (WVR) or GPS Meteorology. SOLUSAR (Solar Lunar Spectrometer for Atmospheric Research) is the third instrument in line and is developed by ETHZ, ISAS and GFZ Potsdam (Figure 4.79). It primarily operates in a very narrow wavelength band in the near-infrared (790 nm - 802 nm) which has proven to be very well suited for the analysis of water vapor absorption lines. The instrument which is far more compact than the predecessor instruments has the possibility though to obtain adjacent wavelength regions as well. An improved light conductance paired with a high sensitivity CCD sensor should provide the possibility to measure sun light reflected by the moon which has intensities 5 to 6 magnitudes lower than direct sun light. Thus the operation time could be prolonged to night times and low sunlight situations (overcast sky).

The retrieved spectra are analyzed in real-time using advanced processing algorithms to instantly provide water vapor values with even improved accuracy.

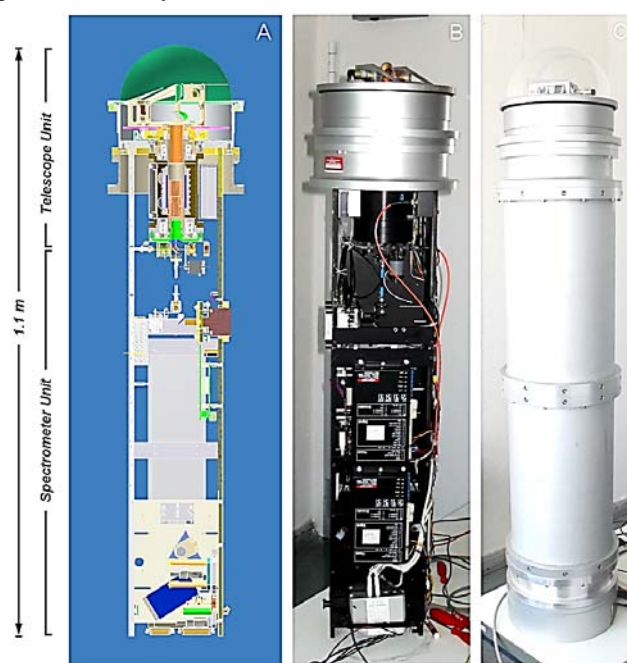


Figure 4.79: (A) Mechanical and Optical Layout of the “Solar Lunar Spectrometer for Atmospheric Research” consisting of a Tracking Telescope and the actual spectrometer.

(B) Unclosed Spectrometer with integrated control electronics.

(C) Spectrometer mounted in its robust and hermetically sealed aluminum casing.

# DAEDALUS: A Versatile Digital Clip-on Measuring System for Total Stations

by B. Bürki, S. Guillaume, P. Sorber, H.-P. Oesch

Institute of Geodesy and Photogrammetry, ETH Zurich

DAEDALUS designates a measuring system which was designed and developed at the Geodesy and Geodynamics Lab (GGL) at ETH Zurich primarily for automated on-line astro-geodetic measurements. It consists of a small CCD camera which can easily be clipped on a Total Station instead of the ordinary eye-piece, a pluggable front lens, a low-cost GNSS receiver for timing purposes, and dedicated software for steering, imaging and on-line processing. The system enables new possibilities for fully automated high-precision digital angle measurements, unaffected by human interference, both in outdoor as well as in indoor applications. The software DAEDALUS is capable to perform optical target recognition by using various image processing algorithms like least-squares template matching, circle recognition or center of mass operators. Although DAEDALUS was initially designed for astro-geodetic use, the results obtained reveal new and unexpected possibilities in other disciplines such as automated terrestrial and engineering surveying, deformation, vibration, and frequency analysis, and photographic documentation. For applications where event timing is needed, high-precision time-tagged measurements are possible by means of a GNSS receiver, equipped with an external antenna for indoor applications. In connection with the telescope of a total station, calibrated CCD sensors are capable to determine the horizontal and vertical angle readings for directions to stars and other targets by means of image processing and appropriate transformations. Up to now, the system has been applied with TCA 1800, TCA 2003 and TDA 5005 Total Stations from Leica Geosystems to demonstrate new and still unexploited possibilities of this new technique.

## 1. System Description

The basic mechanical principle of DAEDALUS was the constraint that no mechanical changes at the total station are allowed. Therefore the CCD camera has to be fixed at the telescope instead of the ordinary eyepiece by means of an appropriate mechanical interface. Although the camera dimensions are very small, the camera as out-of-the-box mounted at the telescope prevents measurements at elevation angles above about 45 degrees. In order to overcome this mechanical constraint, the camera was converted in a way that the initially stacked electronic prints are separated and mounted in two flat stacks as shown in Figure 4.79.

A CCD camera model Guppy F-080C from Allied Vision Technologies (AVT) was chosen for this application. One essential feature for the choice of this camera was the possibility to trigger the shutter by means of external software-driven pulses. In connection with a small GNSS receiver this system allows to control exposure start and exposure time precisely. Its CCD sensor is equipped with 1024 x 768 pixels with a size of 4.65 by 4.65 microns. The camera is capable to transfer up to 30 full frames per second by means of a firewire 1394a interface.



Figure 4.80: Transformed CCD camera and the mechanical Leica interface (aluminum plate, left picture). The right picture shows the camera mounted on a TCA 1800. This flat layout allows to measure in zenith direction.

The optical system gives a resolution of approximately 4 arcsec/pixel. Under the realistic assumption that it is possible to extract objects with a precision of 1/10 pixel or better, the potential of angular measurements of the best Total Stations on the market ( $0.5'' = 0.15 \text{ mgon}$ ) can be fully exploited.

## 2. Optical Target Recognition (OTR)

Three different algorithms of optical target recognition using image processing are implemented in DAEDALUS:

- 1) Center of mass (well suited for symmetric lights, such as e.g. stars, lamps, leds).
- 2) Template least-squares matching (suited for objects with sufficient contrast either in daylight or arbitrarily illuminated objects in nighttime).
- 3) Circle matching (applied for special targets such as illuminated ceramic spheres in industrial applications).

### 3. Practical Applications

#### 3.1 Micro-triangulation for industrial metrology

Optical micro-triangulation is a new and powerful technique for measuring 3D objects very precisely without touching them. The basic principle is to measure horizontal directions and zenith angles of well defined targets from at least two different locations in order to determine a micro geodetic network by means of three-dimensional intersections. Dedicated experiments were carried out in the context of the Geodetic Project Course 2010 at the European Organisation for Nuclear Research (CERN) in Geneva with graduate students in geomatics and planning of ETH Zurich (see also contribution GPC 2010 by Guillaume et al.).

For micro-triangulation purposes, the measurement of an object with ultra precisely known reference benchmarks of ceramic material was chosen. The calibration bench (size 0.6 x 0.2 m, see Figures 4.80 (a) and (b)), as applied for wire positioning sensors (WPS) calibration at CERN served as test object. The spatial coordinates of the reference benchmarks were measured with a coordinate measuring machine (CMM) at a precision level of 1 micron. To eliminate instrumental errors, the DAEDALUS measurements using two TDA 5005 instruments from Leica equipped with DAEDALUS were carried out in two faces. The small white spheres were observed from four stations distributed around the object. The network scale was fixed by measuring a baseline between two sphere positions whose separation distance was determined at a precision level of 1 micron by means of a laser interferometer.

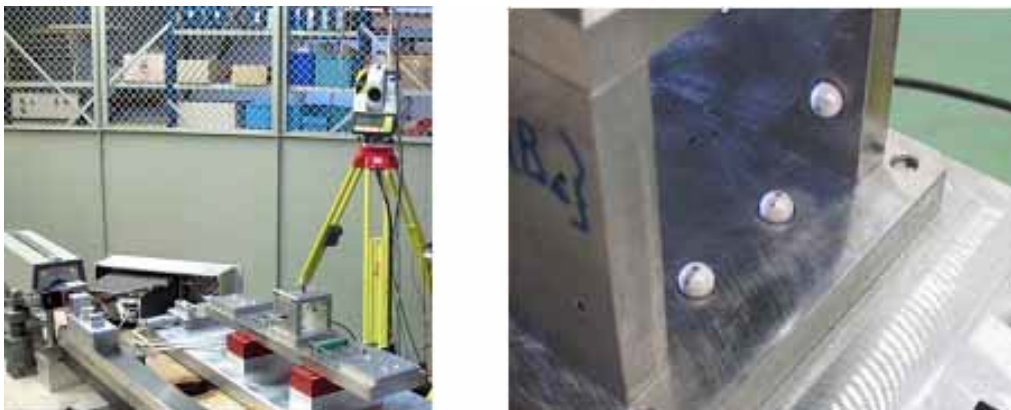


*Figure 4.81: Total Station TDA 5005 from Leica equipped with DAEDALUS during the measurements of the ceramic spheres of the calibration bench (left). The HP-interferometer was used as scale reference for the micro-triangulation. The right picture shows a close-up of the ceramic spheres at the calibration bench which define the reference frame for calibration of Wire Positioning Sensors at CERN.*

The comparison of 3D coordinates measured with DAEDALUS and CMM using a 3D Helmert transformation show that a fully automatic micro-triangulation with OTR is conceivable at an accuracy level of about 5 microns for objects with a size in the order of 1-3 meter.

#### 3.2 Real-time deformation and vibration analysis

This application demonstrates the potential of OTR for measuring real-time high-frequency deformations and vibrations. The aim was to determine the response of a steel bridge, crossing the river Rhone, exited by the passage of trucks (see Figure 4.81). The methodology of this outdoor application can be easily imagined and adapted for similar indoor tasks. The measurements were planned and carried out by the University of Applied Sciences at Yverdon-les-Bains, Switzerland.

The measurements were carried out with a Leica TCA 2003 equipped with DAEDALUS. The target was a standard torch (see Figure 4.81) fixed in the middle of the bridge where significant movements are expected. The distance separating the Total Station to the lamp was 40 meters. The robust tracking of the torch light has been achieved during daylight by setting the CCD exposure time to a few milliseconds and by applying an adapted threshold for the background subtraction.

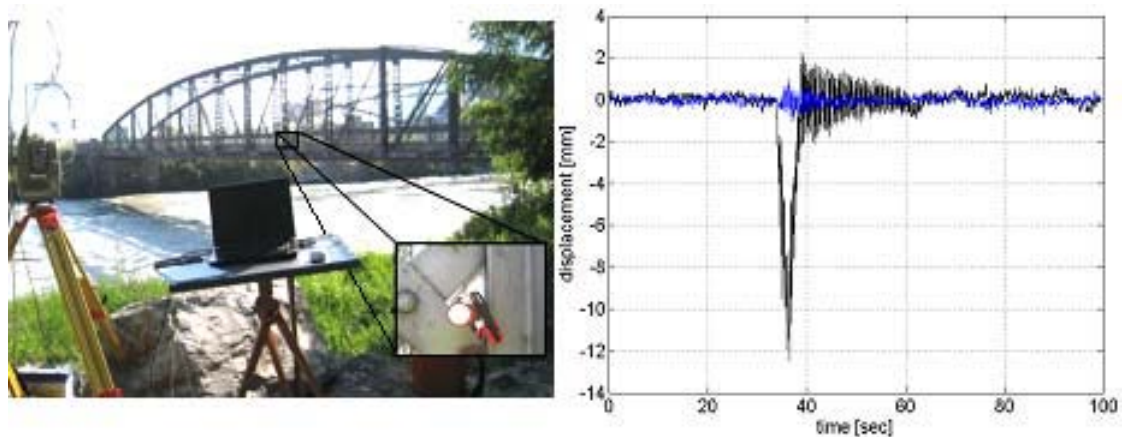


Figure 4.82: Steel bridge crossing the Rhone River in the Canton Wallis in South-Western Switzerland (left). At the left a DAEDALUS system measures high-frequency displacements (15 Hz) to a torch fixed in the middle of the bridge. Vertical (black) and lateral (blue) displacements of the bridge observed with DAEDALUS during the passage of a truck (right).

The vertical movements of the bridge can be interpreted in two parts, the main deformation due to the charge applied by the truck and the damped oscillation at the eigenfrequency. Figure 4.82 shows the spectral decomposition of the vertical oscillating part by Fast Fourier Transform (FFT).

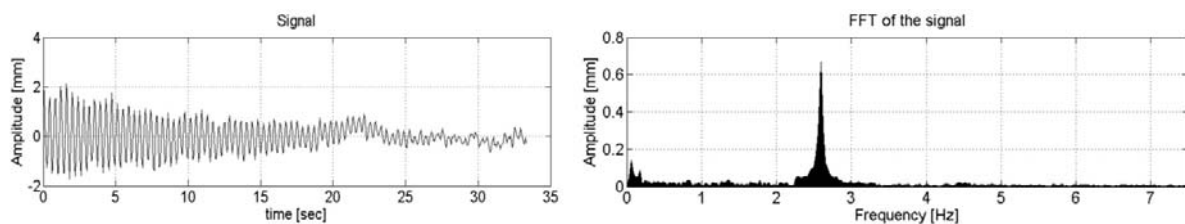


Figure 4.83: Oscillation of the bridge (left) and its spectral decomposition after the passage of a truck. The dominant (eigen)-frequency at 2.59 Hz can be detected clearly in the right graph.

### 3.3 Refraction monitoring by simultaneous reciprocal vertical angle measurements

In this application, two Leica TCA 1800 Total Stations, equipped with DAEDALUS systems and two TCRP 1201 systems were used in parallel set-ups with the aim to measure the refraction and its changes in the lowest layer of the atmosphere. The measurements were performed continuously during 16 hours across the Elbe River, about 80 km North of Hamburg, Northern Germany. The method consisted of reciprocal observations of vertical angles at two stations simultaneously.

In order to perform these measurements, an electronic print with four power diodes were fixed around the objective of each Total Station and used as targets in order to satisfy optimally the reciprocity condition (see Figures 4.83 and 4.84). The observations are perfectly synchronized since the CCD camera can be triggered and synchronized accurately to UTC by a time signal provided by a small GPS receiver. In this way the simultaneity of the measurements was realized easily and independently from the distance between the stations and any communication support. The stations were located at both sides of the Elbe River, 2.3 km apart. The measurements were carried out in first and second telescope positions in order to eliminate the impact of a possible index error. After processing, two time series are of main interest. The time series of the refraction factor  $\kappa$  and the height difference (see Figure 4.84) which, in theory, should remain time-independent. This would be the case only if the refractive field would be symmetric and, as a consequence, the variation of  $\kappa$  would be eliminated completely.

In parallel, identical measurements were carried out by means of two Leica TCRP 1201 Total Stations and retroreflective prisms using ATR in order to verify and validate the reliability of the results obtained. Although the distance observed was longer than the instrumental specifications, the stations worked well. However, it is interesting to see that the instruments stopped working after 10 pm. thus producing data gaps in the time series of

ATR measurements until 6 a.m. This is most likely due to the fact that ATR failed to measure over such a long distance (2.3 km) under turbulent and highly refractive atmospheric conditions.



Figure 4.84: Leica TCA 1800 Total Station equipped with DAEDALUS and additional four power diodes symmetrically arranged around the telescope. Two total stations equipped this way enable centered reciprocal vertical angle measurements.

Although the theoretically most accurate observation and processing method was applied, the height difference observed varies between 0.90 m and 1.14 m. This result clearly shows that the hypothesis of symmetric propagation conditions cannot be validated from sunrise until two o'clock in the consecutive morning. Moreover, the time series of the processed refraction index  $\kappa$  revealed large variations reaching values up to nearly +1.0 thus fundamentally and significantly differing from the nominal value of +0.13 (see. Figure 4.85). Under sunny conditions, even significantly larger fluctuations and peaks values of  $\kappa$  (up to values of  $\kappa = 16!$ ) were observed in the context of an accompanying refraction experiment over grassland ground near Hamburg.

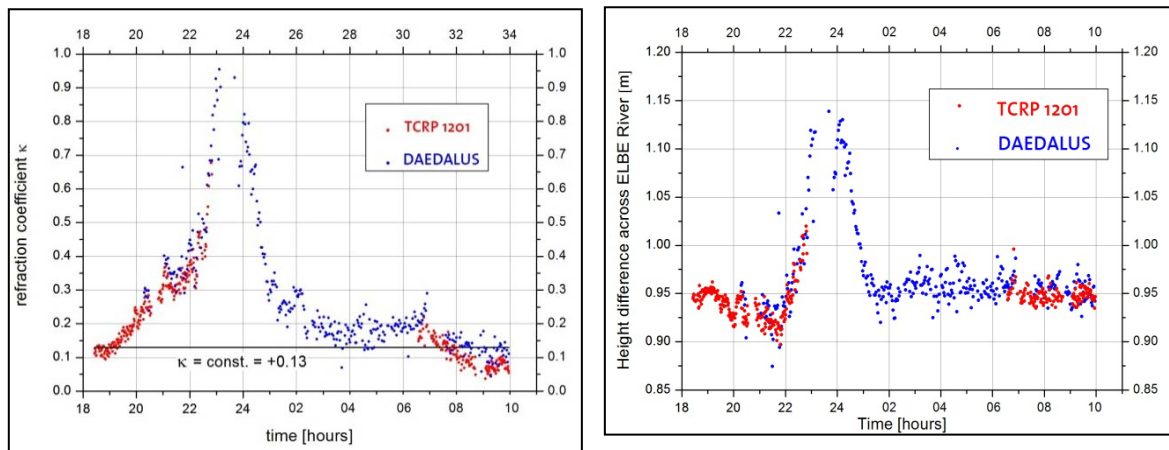


Figure 4.85: Evolution of the refraction coefficient  $\kappa$  observed by reciprocal vertical angle measurements across the Elbe River (left). Height difference observed (right). The series show a significant non-symmetric behavior of the refractive index from sunset until two o'clock a.m.

### 3.4 Astro-geodetic measurements

As described in the second chapter the initial application promoting the development of DAEDALUS was its use in the frame of astro-geodetic measurements. Mainly deflections of the vertical and astronomic azimuths are in the prime focus of this discipline. Results obtained at ETH Zurich revealed accuracies for astronomic latitude and longitude on the order of 0.2 to 0.3 arcsec which is appropriate for local geoid determination.



## Automotive RTK Precision Positioning Approach

by Hans-Jürgen Euler

inPosition GMBH

The typical route guidance is often considered as the only automotive application. Nevertheless, the traffic scenarios become more complex and the positioning needs for vehicles in these scenarios are getting more demanding. These demands are stretching significantly beyond the capabilities of today's single-system, single-frequency GNSS receivers. Within the European 7<sup>th</sup> framework programs the project GAMMA-A (GNSS Supervisory Authority grant agreement no° 248198; [GAMMA-A 2010]) is a triple-frequency mass-market receiver development for automotive applications ([Wasle et al 2010]). GAMMA-A is reaching out to meet these challenging demands. Among the removal of the first order ionospheric refraction effects, the second respectively third frequency available opens also the opportunity to increase positioning accuracy by applying real time kinematic (RTK) algorithms with fast integer ambiguity resolution.

In general RTK approaches are well established for surveying and controlled machine automation environments without challenging obstruction scenarios with frequent signal interruptions. All these approaches do not fit for use in automotive applications.

Typical RTK solutions are targeting high-accuracy position in the sub-centimeter range. In contrast the mass-market is currently focused on single-frequency range solutions with meter type positioning at best. Therefore, decimeter positions are already providing tremendous improvement for most demanding mass-market applications. Target specifications for an automotive RTK application have been defined with a target position accuracy of around 10 cm within 10 seconds of complete acquisition of a sufficient number of satellites. These target numbers are less challenging with respect to the position quality, but the initialization time is significantly shorter than in typical RTK.

The RTK positioning is only one element of the processing chain. These target specifications are the basis for requirements on observation accuracy such as pseudoranges and phase range observations. Initial target values for pseudorange and phase range observations have been established through first simulations. An initial setup outlined with the proposed algorithms for initialization of the so-called widelane ambiguities which shall be the basis for the automotive RTK positioning. Even though that the overall positioning accuracy requirement has been reduced for an automotive RTK application to around decimeter accuracy, the requirements especially on phase range observations are still challenging. The influences caused by the atmosphere have to be removed by suitable information from reference station networks rather than individual stations.

In the last years, a method emerged for precise real-time positioning. The so-called state-space-representation (SSR) is already discussed for distribution based on RTCM messages ([Stürze et al 2008], [Schmitz 2010]). The concept of state-space representation models the different bias and supplies the representation model of these biases. The advantage is that these biases are changing generally slower than the satellite geometry. Therefore, an SSR will be more tolerant for latency and missing epochs in the information dissemination. This tolerance makes SRR a sort of a candidate solution for cases with less reliable communication such as the car environment.

During the research a prototype software based on filters using a widelaning technique for integer ambiguity resolution has been implemented (see for further details [Euler 2010]). In order to test the behavior of these filters test data has been generated including frequent randomly distributed cycle slips. The cycle slips were introduced into the data stream for the moving station only. Every satellite was simulated to experience a cycle slip based on a randomly generated number.

Figure 4.86 shows the coordinate deviations in presence of ionospheric residuals and frequent cycle slips. The signals used for widelaning are E1 and E5a. For the one hour data interval 1750 cycle slips are present. In average every 2 seconds a cycle slip occurs on one of the satellites. Assuming an average number of 11 tracked satellites, in average about every 23 seconds the signal to a specific satellite has been interrupted. There are a few gaps in the positioning when the number of satellites with sufficiently converged filters drops below 4 or the associated position dilution of precision (PDOP) does not allow proper positioning. The graph shows only positions with a PDOP of 10 or less. The percentage of epochs with positions available is about 86.5%. The PDOP is marked through magenta dots and relates to the axis on the right.

[Euler 2010] outlines this approach for precise positioning based on carrier phase observations in more detail. The integer ambiguity resolution through widelanes in conjunction with the distribution of so-called state-space-representation of external error corrections provides a feasible approach. The requirements of continuous carrier phases and uninterrupted communication links are circumvented. Therefore, especially for the harsh automotive environment it provides a way of relatively fast initializations with respectable accuracies at least in the low sub-

meter range when the odds are strong. With less contaminated observation data the approach can deliver decimeter accuracy positions.

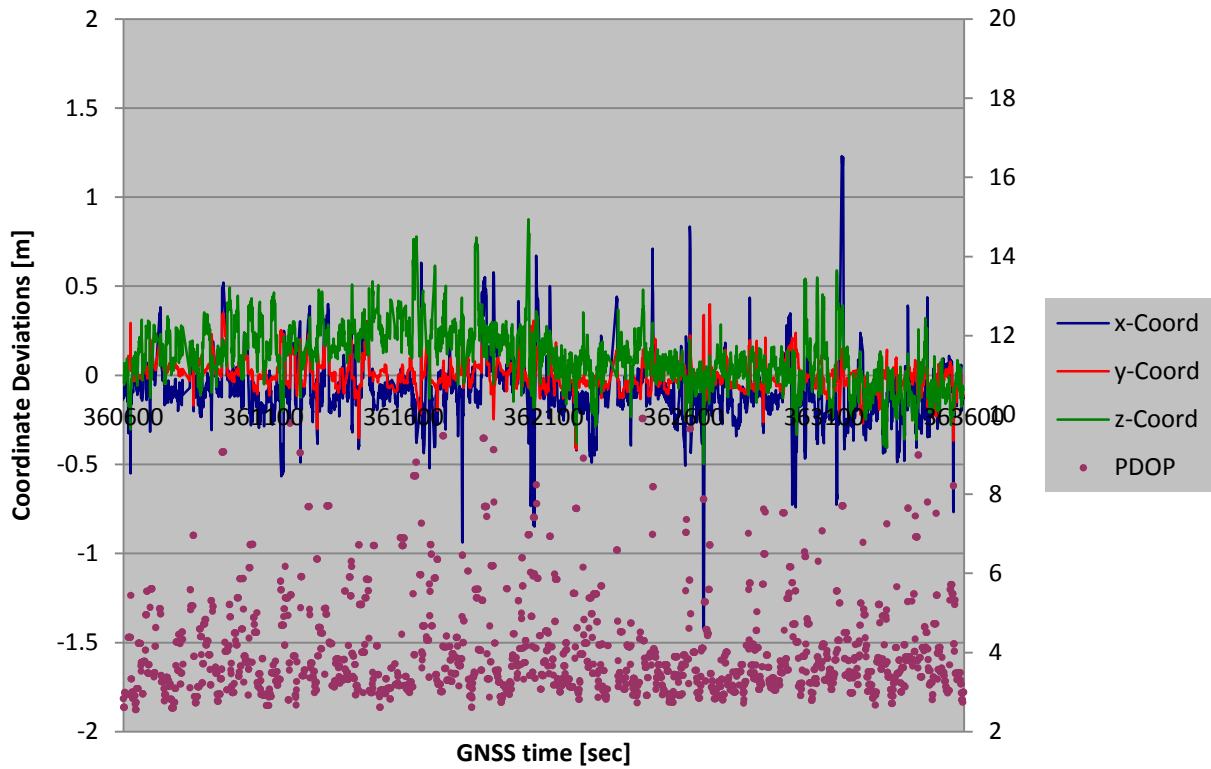


Figure 4.86: Coordinate Deviations for Dataset D09 with Simulated Cycle Slips (E1/E5a)

References:

<http://www.gamma-project.info/gammaa/index.html>

## First Galileo Data Processing

by C. Rösli and M. Rothacher

Institute of Geodesy and Photogrammetry, ETH Zürich

Recently a few JAVAD GNSS receivers were purchased at the Geodesy and Geodynamics Lab (GGL) with the goal to collect a set of Galileo data from the first two Galileo test satellites, namely GIOVE-A (launched on December 28, 2005) and GIOVE-B (launched on April 27, 2008) and to see, whether the E1 and E5a frequency signals can be processed and analysed. Two JAVAD SigmaS-G3T receivers with GrAnt-G3T antennas were set up on a pillar and on a tripod, forming a baseline of less than 5 meters. Data were recorded for a few days in October, November and December 2009. The measurements were then processed with a version of the Bernese GPS Software that had been modified for Galileo data processing by Drazen Svehla and Markus Hinze at TU Munich.

In a first step, the code observations were processed using only the orbits and satellite clocks available in the navigation messages transmitted by the GIOVE satellites. The navigation messages were usable for GIOVE-B during the time of the measurements. GIOVE-A did not transmit useful information, however, during this period. The processing of the GIOVE-B data initially also presented some problems, because the satellite clock offsets in the navigation messages were not correctly updated from one set to the next. This shows that the GIOVE satellites are still test satellites and are not intended for operational use yet.

In a second step, precise orbits estimated by the group of Urs Hugentobler at TU Munich were used. The GIOVE satellites could be used to compute a code-based solution that gives consistent results (on the code noise level) for Galileo and GPS. This is documented in Figure 4.87 showing the residuals of the combined GPS/Galileo code solution for October 22, 2009. GIOVE-A (orange) is observed for only a short time and agrees less with the GPS satellites. However, GIOVE-B (red) shows no systematic deviation and fits almost perfectly into the GPS solution. The jumps in the residual time series of the individual satellites are caused by the changing satellite scenario. Offsets between the satellites are mainly due to differential code biases. The offset estimated between the GPS and Galileo time systems using code measurements are given in Figure 4.88. They are quite consistent for the two stations and the two different days.

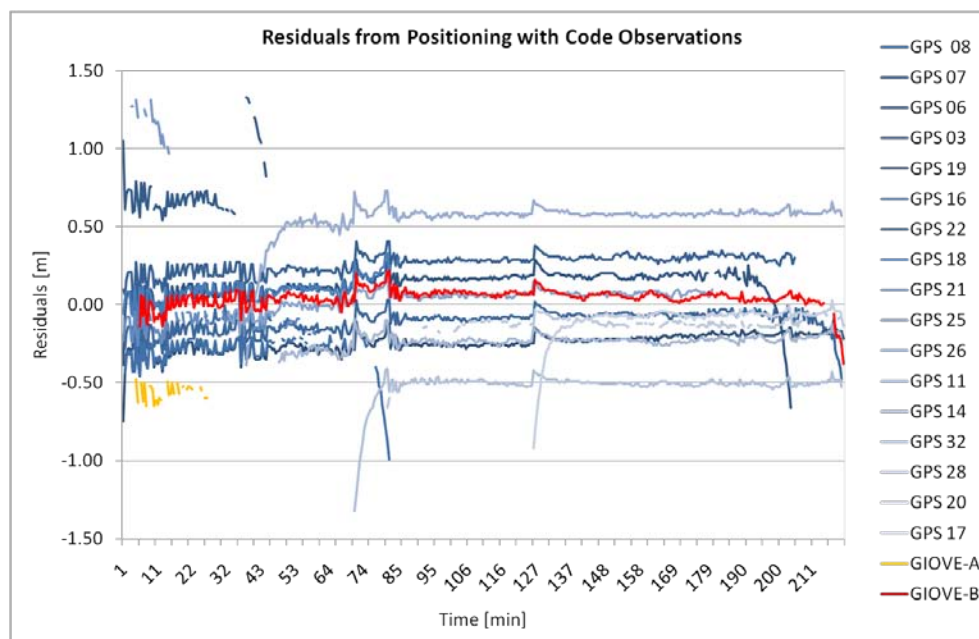


Figure 4.87: Residuals of the code measurements after estimating one set of the station coordinates over the entire observation time interval (October 22, 2009). Offsets between satellites are mainly the result of differential code biases.

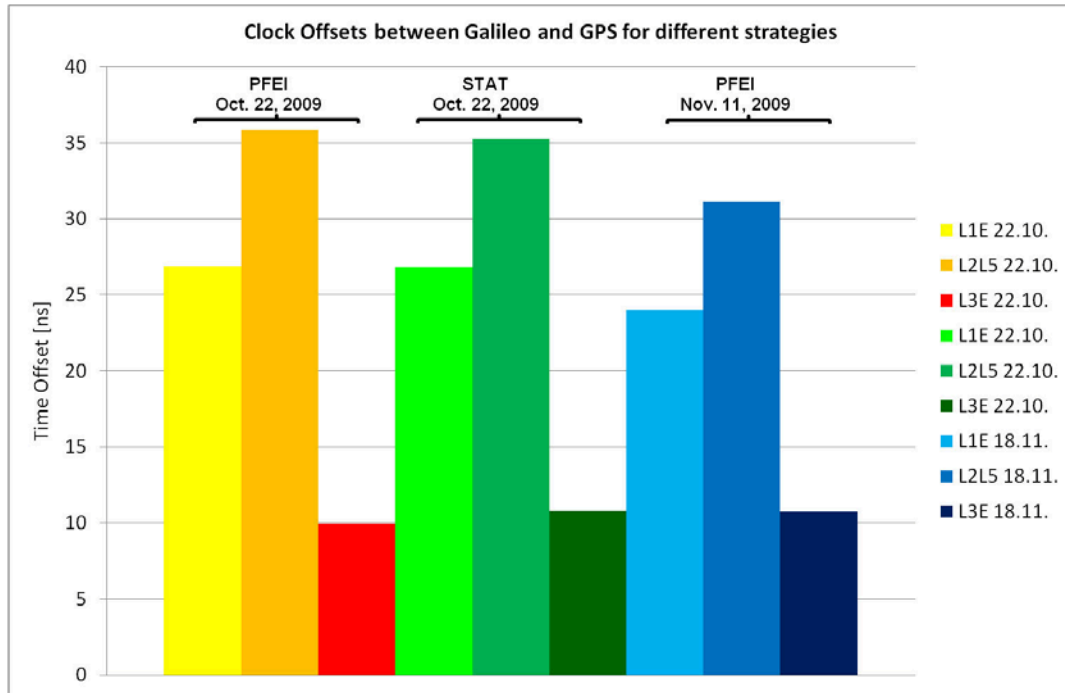


Figure 4.88: Offsets estimated between the GPS and Galileo time systems using code measurements from two stations and two different days (October 22 and November 18, 2009).

Only few data sets were collected and analysed so far. The availability of the Galileo signals is rather unpredictable due to the testing character of the two satellites. However, the potential of having two independent but compatible systems is already emerging. The results are promising for future positioning with Galileo and GPS.

## Bibliography Commission 4

- Andrey, D., Ch. Misslin, U. Wild (2010): Review und Redesign von AGNES/swipos: Konzeptstudie zur technischen Weiterentwicklung. swisstopo-Report 09-06, Bundesamt für Landestopografie, Wabern.
- Bayoud, F., J. Skaloud (2008): Vision-aided inertial navigation system for robotic mobile mapping. *Journal of Applied Geodesy* 2 (2008), 39-52.
- Böhm, J., B. Werl, H. Schuh (2006b): Troposphere mapping functions for GPS and very long baseline interferometry from European Centre for Medium-Range Weather Forecasts operational analysis data. *Journal of Geophysical Research* 111:B02406. doi:10.1029/2005JB003629.
- Böhm, J., R. Heinkelmann, H. Schuh (2007): Short note: a global model of pressure and temperature for geodetic applications. *Journal of Geodesy* 81(10):679–683. doi:10.1007/s00190-007-0135-3.
- Böhm, J., A. Niell, P. Tregoning, H. Schuh (2006a): Global Mapping Function (GMF): a new empirical mapping function based on numerical weather model data. *Geophysical Research Letters*, 33:L07304. doi:10.1029/2005GL025546.
- Bürki, B., M. Ganz, Ch. Hirt, U. Marti, A. Müller, P.V. Radogna, A. Schlatter, A. Wiget (2005): Astrogeodätische und gravimetrische Zusatzmessungen für den Gotthard-Basistunnel. swisstopo-Report 05-34, Bundesamt für Landestopografie, Wabern.
- Bürki, B., S. Guillaume (2010): Astrogeodätische Lotabweichungs- und Azimutmessungen für AlpTransit. *Geomatik Schweiz* 12/2010, p. 620-627.
- Bürki, B., S. Guillaume (2010): „DAEDALUS: A versatile usable digital clip-on measuring system for Total Stations“. Proc. 2010 International Conference on Indoor Positioning and Indoor Navigation (IPIN), 15-17 September 2010, Zürich, Switzerland. 10 pp.
- Bürki, B., S. Guillaume, P. Sorber, H.-P. Oesch (2010): DAEDALUS: A Versatile Usable Digital Clip-on Measuring System for Total Stations, International Conference on Indoor Positioning and Indoor Navigation IPIN, 2010.
- Carosio, A., O. Reis (1996): Geodetic Methods and Mathematical Methods for the Establishment of New Trans-Alpine Transportation Routes, Bericht IGP No. 206, ETH Zürich.
- Constantin, V., A. Waegli, J. Skaloud (2008): Le filtre de Kalman unscented - outil performant en géodésie cinématique, *Géomatique Suisse*, Vol. 1/2008, pp. 12-17.
- Dach, R., J. Böhm, S. Lutz, P. Steigenberger, G. Beutler (2011): Evaluation of the impact of atmospheric pressure loading modeling on GNSS data analysis. *Journal of Geodesy*, vol. 85(2), pp. 75-91, doi:10.1007/s00190-010-0417-z.
- Dach, R., U. Hugentobler, P. Fridez, M. Meindl (2007): Bernese GPS Software Version 5.0, Bern: Astronomical Institute, University of Bern. Available at: <http://www.bernese.unibe.ch/> [Accessed February 3, 2011].
- Dach, R., U. Hugentobler, P. Fridez, M. Meindl eds. (2007): Bernese GPS Software, Version 5.0. Astronomical Institute, University of Bern.
- Dach, R., S. Schaer, H. Bock, S. Lutz, G. Beutler (2010): CODE's New Combined GPS/GLONASS Clock Product. IGS Workshop 2010, Newcastle upon Tyne, England, 28 June - 2 July, 2010.
- Dach, R., R. Schmid, M. Schmitz, D. Thaller, S. Schaer, S. Lutz, P. Steigenberger, G. Wübbena, G. Beutler (2011): Improved antenna phase center models for GLONASS. *GPS Solutions*, vol. 15(1), pp. 49-65, doi:10.1007/s10291-010-0169-5.
- Eisenbeiss, H., W. Stempfhuber, M. Kolb (2009): Genauigkeitsanalyse der 3D-Trajektorie von Mini-UAVs. In: *Zukunft mit Tradition "29. Wissenschaftlich-Technische Jahrestagung der DGPF"*, Ed.: Seyfert, E., Publikationen der Deutschen Gesellschaft für Photogrammetrie, Fernerkundung und Geoinformation (DGPF) e.V., Potsdam, 407-417.
- Euler, H.-J. (2010): Zukunftsanalyse zu AGNES/swipos Diensten. swisstopo-Report 09-06a, Bundesamt für Landestopografie, Wabern.
- Euler, H.-J. (2010): Novel Precision Positioning Approach for Automotive Applications based on RTK, Galileo Receiver for Mass Market Applications in the Automotive Area, Proceedings of the European Navigation Conference - ENC GNSS 2010, Braunschweig, 19-21 October.

- Fournier, H., J. Skaloud, A. Waegli (2009): The use of wavelet transform for an automated initialization in GPS/MEMS-IMU integration. In Proceedings of the 13th IAIN World Congress, volume 1, pages 27-30, Stockholm, Sweden.
- Geiger, A., M. Scaramuzza, H. Wipf (2008): Führung, Ortung, Positionierung, Lecture Notes, Aeronautics, HSW, pp. 350.
- Geiger, A. (2009): Dynamische Positionierung, Lecture Notes, Institute of Geodesy and Photogrammetry, ETHZ, pp. 160.
- Geiger, A. (2009): Navigation, Lecture Notes, Institute of Geodesy and Photogrammetry, ETHZ, pp. 244.
- Geiger, A., S. Guillaume, F. Forrer (2009): G-MoDe Detection of Small and Rapid Movements by a Single GPS Carrier Phase Receiver, The VII Hotine-Marussi Symposium Roma, 2009.
- Geiger, A., A. Schlatter (2010): Von der Potentialtheorie zu den Senkungen am Gotthardpass. Geomatik Schweiz 12/2010, Seiten 628-629.
- Gilliéron, P., et al. (2008): La navigation pédestre dans l'espace public: évaluation des besoins et esquisses de solutions. 2008: Lausanne.
- Gubler, E., U. Marti (2009): LTOP, Wabern: Bundesamt für Landestopografie swisstopo. Available at: <http://www.swisstopo.admin.ch/internet/swisstopo/de/home/products/software/products/ltop.html> [Accessed February 3, 2011].
- Guerrier, S., A. Waegli, J. Skaloud, M.P. Victoria-Feser (2010): IEEE Transactions on Aerospace and Electronic Systems, accepted for publication.
- Guillaume, S., B. Bürki (2008): "DAEDALUS, an Astro-Geodetic On-Line Observation System, User Manual V1.0, Institute of Geodesy and Photogrammetry, ETH Zürich.
- Guillaume, S., A. Geiger (2007): Real-Time Small Movement Detection with a Single GPS Carrier Phase Receiver, Proc. ENC-GNSS'07: European Navigation Conference, 29-31 May 2007, Geneva, Switzerland, p. 506-516.
- Guillaume, S., A. Geiger, F. Forrer (2009): G-MoDe Detection of Small and Rapid Movements by a Single GPS Carrier Phase Receiver, The VII Hotine-Marussi Symposium Roma.
- Guillaume, S., C. Muller, P. Cattin (2009): TRINET+ - Logiciel de Compensation de Reseaux 3D, HEIG-VD, Yverdon-les-Bains: HEIG-VD.
- Haag R., A. Ryf, R. Stengele (1996): Grundlagennetze für extrem lange Tunnel am Beispiel des Gotthard-Basistunnels. Ingenieurvermessung 1996, Graz.
- Häberling, S., A. Geiger (2010): Determination of attitude change by a single GPS antenna, in Proceedings of 2nd International Conference on Machine Control & Guidance, March 9-11, Bonn, Germany pp. 149-150.
- Hardegger, Th. (2008): 3D-Baggersteuerung mit swipos-GIS/GEO: Machbarkeitsstudie (WK Th. Hardegger, 10.-28. November 2008). swisstopo-Report 08-32, Bundesamt für Landestopografie, Wabern.
- Hirt, C., U. Feldmann-Westendorff, V. Böder, B. Bürki, S. Guillaume, R. Heyen, T. Stelkens-Kobsch, H. Sternberg (2008): "Präzise Höhen- und Schwerfeldbestimmungen an Stromübergängen und Meerengen", Geoinformation in der Küstenzone, Hafen City Universität Hamburg, 08.-09.10.2008 (Hrsg. K.-P. Traub, J. Kohlus and T. Lüllwitz), Points Verlag, Norden Halstad, pp. 59-72.
- Hirt, C., S. Guillaume, A. Wisbar, B. Bürki, H. Sternberg (2010): "Monitoring of the Refraction Coefficient in the Lower Atmosphere using a Controlled Setup of Simultaneous Reciprocal Vertical Angle Measurements". J. Geophys. Res., 115, D21102, doi:10.1029/2010JD014067.
- Hirt, C., S. Guillaume, A. Wisbar, B. Bürki, H. Sternberg (2010): Monitoring of the refraction coefficient in the lower atmosphere using a controlled setup of simultaneous reciprocal vertical angle measurements, Journal of Geophysical Research, vol. 115, d21102, 14 pp.
- Hurter, F., D. Perler, A. Geiger (2010): Monitoring atmospheric water vapor in the Zermatt region with GNSS in Abstract Volume 8th Swiss Geoscience Meeting, 19.-20. November, 2010, Fribourg, Switzerland.
- Hurter, F., D. Perler, A. Geiger (2010): Using GNSS receivers to monitor atmospheric water vapor in Zermatt in Symposium Posters CCES-Latsis Symposium, 15.-17. November, 2010, ETH Zuerich, Switzerland.
- Mautz, R., M. Kunz, H. Ingensand (eds.) (2010): IPIN. Proceedings of the 2010 International Conference on Indoor Positioning and Indoor Navigation (IPIN), ISBN: 978-1-4244-5864-6, IEEE Xplore, 974 p.

- Jehle, M., D. Perler, D. Small, A. Schubert, E. Meier (2008): Estimation of Atmospheric Path Delays in TerraSAR-X Data using Models vs. Measurements. *Sensors* 8 (12), 8479{8491.
- Jones, M., J. Boerez, S. Guillaume, J. Hinderer, B. Bürki (2010): Latest Results from the CLIC Geodetic Studies, 11th International Workshop on Accelerator Alignment IWAA.
- Kahlmann T., F. Remondino, S. Guillaume (2007): Range imaging technology: new developments and applications for people identification and tracking, IS&T/SPIE Symposium on Electronic Imaging 2007 in San Jose, CA USA, Vol.6491.
- Kehl, Ph., J. Staehelin, A. Geiger, H.-G. Kahle (2007): Dynamic Monitoring of Air Pollutants in Zürich (Switzerland) using a Streetcar as Measuring Platform. Abstracts of the 6<sup>th</sup> International Conference on Urban Air Quality, Cyprus, University of Hertfordshire, vol. 6.
- Kehl, Ph. (2009): GPS Based Dynamic Monitoring of Air Pollutants in the City of Zurich. Philippe Kehl, Geodätisch-geophysikalische Arbeiten in der Schweiz, Swiss Geodetic Commission, Vol 78. 156 p.
- Lichti, D., J. Skaloud, P. Schaer (2008): On the calibration strategy of medium format cameras for direct georeferencing. International Calibration and Orientation Workshop EuroCOW 2008, Castelldefels, Spain, 30.1-1.2. 2008.
- Limpach, P. (2009): Rock glacier monitoring with low-cost GPS receivers. Glacier Hazard Workshop 2009 Vienna, Glacier Hazards, Permafrost Hazards and GLOFs in Mountain Areas: Processes, Assessment, Prevention, Mitigation. Vienna, Austria. 10–13 November 2009.
- Limpach, P., D.E. Grimm (2009): Rock glacier monitoring with low-cost GPS receivers. Abstract Volume 7<sup>th</sup> Swiss Geoscience Meeting, November 2009, Neuchatel, Switzerland.
- Lutz, S., S. Schaer, M. Meindl, R. Dach, P. Steigenberger (2009): Higher-order ionosphere modeling for CODE's next reprocessing activities. AGU 2009 Fall Meeting, San Francisco, CA, USA, December 14-18, 2009.
- Lutz, S., S. Schaer, M. Meindl, R. Dach, P. Steigenberger (2010): Higher-Order Ionosphere Modeling for CODE's Next Reprocessing Activities. IGS Workshop 2010, Newcastle upon Tyne, England, 28 June-2 July, 2010.
- Lutz, S., M. Troller, A. Geiger, H.-G. Kahle (2007): Data processing and requirements for high-resolution GPS tomography. *Geophysical Research Abstracts*, vol. 9. ISSN: 1029-7006, EGU2007-A-09033.
- Lutz, S., M. Troller, A. Geiger, H.-G. Kahle (2007): High-resolution GPS tomography in the mountainous Canton of Valais, Switzerland. *Geophysical Research Abstracts*, vol. 9, ISSN: 1029-7006, EGU2007-A-09142
- Lutz, S. (2009): High-resolution GPS tomography in view of hydrological hazard assessment. Geodätisch-geophysikalische Arbeiten in der Schweiz, Swiss Geodetic Commission, Vol 76. 202 p.
- Lutz, S., M. Troller, D. Perler, A. Geiger, H.-G. Kahle (2010): Better Weather Prediction Using GPS, *GPS-World*, Vol. 21, No. 7. 40-47.
- Marti, U. (2002): Alptransit Gotthard Basistunnel: Schwerefeldstudie. Technischer Bericht 01-36; Bundesamt für Landestopographie, Wabern.
- Mautz, R. (2009): "Camera and Laser Indoor Positioning System (CLIPS)". Proposal to the Swiss National Science Foundation, (unpublished).
- Mautz, R., D. Grimm, P. Limpach, S. Tilch, A. Geiger (2010): Bestimmung der Fließgeschwindigkeiten von Blockgletschern. *Geomatik Schweiz*, Vol. 108, Issue 6, pp. 264-268, ISSN 1660-4458.
- Mendes, V. B., E.C. Pavlis (2004): High-accuracy zenith delay prediction at optical wavelengths. *Geophys. Res. Lett.*, 31, L14602, doi:10.1029/2004GL020308.
- Misslin, Ch., U. Wild (2009): Antennenheizung für AGNES-Stationen: Dokumentation der Tests in Wabern und San Bernardino. Report 09-03, swisstopo, CH-3084 Wabern.

- Ober, C., G. Flury, H. Püschel, M. Dreier, M. Brügger, P. Theiler, S. Tilch (2009): Blockgletscher – Monitoring. Bericht des Geodätischen Projektkurses in Randa, Institut für Geodäsie und Photogrammetrie, ETH Zürich.
- Ostini, L., R. Dach, M. Meindl, S. Schaer, U. Hugentobler (2008): FODITS: A New Tool of the Bernese GPS Software to Analyze Time Series. EUREF 2008 Symposium, Brussels, Belgium, June 18-21, 2008.
- Ostini, L., R. Dach, M. Meindl, S. Schaer, U. Hugentobler (2009): FODITS: A New Tool of the Bernese GPS Software to Analyze Time Series. In Proceedings of EUREF 2008 Symposium, Brussels, Belgium, June 18-21, 2008.
- Perler, D., A. Geiger, D. Leuenberger, E. Brockmann, H.-G. Kahle (2008): Impact of GNSS Network Design on Water Vapour Tomography. In 6th Swiss Geoscience Meeting: Lugano, 21st-23rd Novembre 2008: Abstract Volume, Canobbio, pp. 141. University of Applied Sciences of Southern Switzerland, Institute of Earth Sciences.
- Perler, D., A. Geiger, D. Leuenberger, E. Brockmann, H.-G. Kahle, M. Rothacher (2009): A new parameterized fully ellipsoidal 3D-filtered tomographic approach for GNSS water vapor retrieval. Geophysical Research Abstracts, EGU General Assembly 2009, Vienna.
- Perler, D., A. Geiger, F. Hurter (2011): 4D GPS water vapor tomography: New parameterized approaches. Journal of Geodesy 2011.
- Pittet, S., V. Renaudin, B. Merminod, M. Kasser (2008): UWB and MEMS Based Indoor Navigation, Journal of Navigation, 61, 396-384 (2008).
- Pottiaux, E., E. Brockmann, W. Soehne, C. Bruyninx (2008): The EUREF - EUMETNET Collaboration: First Experiences and Potential Benefits. In: Ihde, J. and H. Hornik (Eds): Subcommission for the European Reference Frame (EUREF), Brussels, 2008, EUREF Publication No 18, also published in Bulletin of Geodesy and Geomatics (BGG) edited by F. Sanso (in prep).
- Renaudin, V., O. Yalak, Ph. Tomé, B. Merminod (2007): Indoor Navigation of Emergency Agents, European Journal of Navigation, 5, 36-45 (2007).
- Renaudin, V., O. Yalak, Ph. Tomé, B. Merminod (2007): Inertial and RFID sensors for Indoor navigation in case of emergency intervention, In Proceedings of TimeNav 2007, Geneva, 29 May - 1 June.
- Renaudin, V., B. Merminod, M. Kasser (2008): Optimal Data Fusion for Pedestrian Navigation based on UWB and MEMS, in PLANS 2008. 2008, Monterey, California (USA).
- Renaudin, V. (2009): Hybridation MEMS/UWB pour la navigation pédestre intra-muros. 2009. Thèse EPFL 4429.
- Renaudin-Schouler, V., P.-Y. Gilliéron (2011): Personal Robust Navigation in Challenging Applications. Journal of Navigation, 2011. 64(02): p. 235-249.
- Scaramuzza, M., A. Geiger (2007): Multilateration, internal report to skyguide.
- Schaer, P., J. Skaloud, S. Landtwing, K. Legat (2007): Accuracy Estimation for Laser Point Cloud Including Scanning Geometry. The 5<sup>th</sup> International Symposium on Mobile Mapping Technology, Padua, Italy, May 29-31.
- Schaer, P., J. Skaloud, P. Tome (2008): Towards in-flight quality assessment of airborne laser scanning. ISPRS XXI Congress, Beijing, China, July 3-11.
- Schaer, P., J. Skaloud, Y. Stebler, P. Tomé, R. Stengele (2009): Airborne LiDAR in-flight accuracy estimation. GPS World, 20(8):37-41, 2009.
- Schaer, S., E. Brockmann, M. Meindl (2009). Dach, R., U. Hugentobler, P. Fridez, M. Meindl, eds. (2007): Bernese GPS Software, version 5.0, Astronomical Institute of the University of Bern, February, 2007.
- Schätti I., A. Ryf (2004): Hochpräzise Lotung im Schacht Sedrun des Gotthard-Basistunnels. XVI. Internationaler Kurs für Ingenieurvermessung, Zürich.
- Schätti, I., A. Ryf (2007): AlpTransit Gotthard-Basistunnel: Grundlagenvermessung, letzte Kontrollen vor dem ersten Durchlag. Ingenieurvermessung 2007, Graz.
- Schätti I., A. Ryf (2007): AlpTransit Gotthard-Basistunnel: Grundlagenvermessung, letzte Kontrollen vor dem ersten Durchschlag. XV. Internationaler Kurs für Ingenieurvermessung, Graz.
- Schlatter, A., U. Marti (2005): Höhentransformation zwischen LHN95 und den Gebrauchshöhen LN02. Geomatik Schweiz 8/2005, p. 450 – 453.



- Schlatter, A. (2007): Das neue Landeshöhennetz der Schweiz. Geodätisch-geophysikalische Arbeiten in der Schweiz, Band 72. Schweizerische Geodätische Kommission 2007.
- Schlatter, A., B. Mattli (2009): BLS-AlpTransit: Lötschberg-Basistunnel: Präzisionsnivellement 2006 durch den Basistunnel als Ergänzung zum Landeshöhennetz und als Grundlage für die Bauwerksüberwachung. swisstopo-report 07/12, Bundesamt für Landestopografie, Wabern.
- Schmitz, M. (2010): State Space Technology - Principle, RTCM Standardization and Examples, GNSS-reference networks - QUO VADIS Seventh ALLSAT Open, June 17, Hannover.
- Schneider D., U. Marti, A. Wiget (1996): Die neue Landesvermessung der Schweiz LV95 als Grundlage für die Vermessung der neuen Eisenbahn-Alpentransversen 'AlpTransit'. Ingenieurvermessung 1996, Graz.
- Scirè Scappuzzo, F. (2009): "Analysis and corrections of non-hydrostatic effects on GNSS observations and antenna errors for accurate GPS and Galileo IWV estimates", Dissertation. ETH Zürich No. 18289.
- Skaloud, J., P. Schaer (2007): Towards Automated LiDAR Bore-sight Self-calibration. The 5<sup>th</sup> International Symposium on Mobile Mapping Technology, Padua, Italy, May 29-31.
- Skaloud, J., K. Legat (2008): Theory and Reality of Direct Georeferencing in National Coordinates, ISPRS Journal of Photogrammetry and Remote Sensing, 63: 272-282.
- Skaloud, J., Schaer, P., Stebler, Y., Tomé, P. (2009). Real-time registration of airborne laser data with sub-decimeter accuracy, Journal of Photogrammetry and Remote Sensing 65(2), 208-217, 2009.
- Skaloud, J., D. Lichti, G. Vosselman (ed.), Maas, H.-G. (ed.) (2010). Calibration, In: Airborne and Terrestrial Laser Scanning, 2010, p. 83-133, Whittles Publishing, ISBN: 978-1-904445-87-6.
- Skaloud, J., P. Schaer (2010): Optimizing Computational Performance for Real-Time Mapping with Airborne Laser Scanning. In: The International Archives of the Photogrammetry, Remote Sensing and Spatial Information Sciences, volume 38. p 9.
- Skaloud, J., D. Rouzaud (2011): Rigorous integration of inertial navigation with optical sensors by dynamic network, NAVIGATION: Journal of the Institute of Navigation, special issue, accepted for publication.
- Steigenberger, P., M. Rothacher, R. Dietrich, M. Fritsche, A. Rülke, S. Vey (2009): Reprocessing of a global GPS network; Journal of Geophysical Research, Vol. 111, Nr. B5, EID B05402, American Geophysical Union, ISSN 0148-0227, DOI: 10.1029/2005JB003747, 2006.
- Stewénius, H. (2005). "Gröbner Basis Methods for Minimal Problems in Computer Vision", Ph.D. thesis, Centre for Mathematical Sciences, Lund Institute of Technology.
- Stürze, A., W. Söhne, G. Weber, L. Mervart (2008): Real-Time GNSS - Modellierung im Zustandsraum (State Space), FGS Workshop, Wettzell, 16 –18. Juli.
- Tappero, F. (2009): Low-cost optical-based indoor tracking device for detection and mitigation of NLOS effects, in Eurosensors XXIII. 2009: Lausanne (Switzerland). p. 497-500.
- Tappero, F., B. Merminod (2009): Image-based indoor tracking device for detection and mitigation of NLOS effects. Sensors and Actuators A: Physical, 2009.
- Tilch, S. (2010): "Entwicklung eines optischen Innenraum-Positionierungssystems", Master Thesis, Institute of Geodesy and Photogrammetry, ETH Zurich.
- Tomé, P., et al. (2008): Improving pedestrian dynamics modelling using fuzzy logic, in PED2008 Conference in pedestrian navigation. 2008: Wuppertal (Germany).
- Troller M., D. Leuenberger, E. Brockmann, A. Geiger, H.-G. Kahle (2007): GPS-Tomography: Results and Analyses of the Operational Determination of Humidity Profiles over Switzerland. Geophysical Research Abstracts, vol. 9.
- Troller, M., A. Geiger, D. Perler, H.-G. Kahle, D. Leuenberger, E. Brockmann (2007): GPS-Tomography for Meteorology: Impact on operational weather forecast, Proc. ION GNSS 2007., Sept. 25–28, 2007, Fort Worth, USA, p. 2861-2869.
- Troller, M., D. Leuenberger, E. Brockmann, A. Geiger, H.-G. Kahle (2007): Impact of GPS-Tomography on Operational Weather Forecast: Determination of the 3D Distribution of Humidity, Proc. ENC-GNSS'07: European Navigation Conference, 29 - 31 May 2007, Geneva, Switzerland, p. 174-179.

- Troller, M., D. Leuenberger, E. Brockmann, A. Geiger, H.-G. Kahle (2007): Use of CGPS Network to determine Tropospheric Vapor of NWP Models: Selection Studies and Results of a One Year Investigation with Radiosondes. *Journal of Geophysical Research*, June 2007.
- Ulrich, D., D. Andrey (2009): Real-time Monitoring mit swipos: Dokumentation der Versuche mit Trimble Integrity Manager (TIM) am Beispiel des GPS-Überwachungsnetzes Braunwald. swisstopo-report 09-05, Bundesamt für Landestopografie, Wabern.
- Waegli, A., Guerrier, S., Skaloud, J. (2008). Redundant MEMS-IMU Integrated with GPS for Performance Assessment in Motorsports, PLANS 2008, Joined Symposium of IEEE and ION on Position Location and Navigation, Monterey, California, USA, May 5-8.
- Waegli, A., A. Schorderet, C. Prongue, J. Skaloud (2008): Accurate trajectory and orientation of a motorcycle derived from low-cost satellite and inertial measurement systems. In *Engineering of Sport 7*, Vol 1, 223-230. Springer Verlag Paris.
- Waegli, A., J. Skaloud (2007): Assessment of GPS/MEMS-IMU Navigation Performance in Ski Racing, European Navigation Congress ENC-GNSS, Geneva, Switzerland. May 29 – June 1.
- Waegli, A., J. Skaloud (2007): Turning Point: Trajectory Analysis for Skiers. *Inside GNSS*, Spring: 24-34.
- Waegli, A., J. Skaloud, P. Tome (2007): Assessment of the integration strategy between body-worn MEMS sensors with application to sports, ION-GNSS, Fort Worth, Texas, September 25-28.
- Waegli, A., J. Skaloud, S. Guerrier, M.E. Parés (2010): Noise reduction and estimation in multiple micro-electro-mechanical inertial systems. In: *Measurement Science and Technology*, 21, 065201-065212, 2010.
- Wasle, E, Ph. Berglez, J. Seybold, H.-J. Euler, M. Overbeck, G. Rohmer, A. Kahmann (2010): Galileo Receiver for Mass Market Applications in the Automotive Area, Proceedings of the European Navigation Conference - ENC GNSS 2010, Braunschweig, 19-21 October.
- Wiget, A. (2007): BLS-AlpTransit: Lötschberg-Basistunnel: Übersicht über die Grundlagenvermessung und weitere Beiträge des Bundesamtes für Landestopografie zur Vermessung des Lötschberg-Basistunnels. swisstopo-report 07-09, Bundesamt für Landestopografie, Wabern.
- Wiget A., U. Marti, A. Schlatter (2010): Beiträge der Landesvermessung zum AlpTransit Gotthard-Basistunnel. *Geomatik Schweiz* 12/2010, Seiten 575-581.
- Wild, U., D. Andrey, E. Brockmann, D. Ineichen, St. Schaer (2007): Improvements for the Swiss Positioning Service (swipos) due to GLONASS. Paper presented at TimeNav07, Geneva, 2007.
- Wild, U., E. Brockmann, S. Grünig (2008): AGNESII / GLONASS: Projektantrag, Reporting und Schlussbericht. swisstopo-Report 08-13, Bundesamt für Landestopografie, Wabern.
- Wild, U. (2010): AGNES/swipos: Integration von real-time Stationen aus Frankreich / Italien: Konzept und Beschaffung SW-Lizenzen. swisstopo-Report 08-33, Bundesamt für Landestopografie, Wabern.
- Wu J., P.-Y. Gilliéron, B. Merminod (2010): An integrated methodology for change detection via terrestrial laserscanning: case study of the landslide in Flamatt. In 8<sup>th</sup> Swiss Geoscience Meeting, Fribourg Switzerland, November 19-20.
- Wu J., P.-Y. Gilliéron B. Merminod (2011): A Split/Merge approach for landslide monitoring via Terrestrial Laser Scanning. In Conference of Earth Observation of Global Changes (EOGC), Munich, Germany, April 13-15.
- Wu J., B. Merminod (2010): A split/merge approach for change detection via terrestrial LIDAR. In Workshop on Remote Sensing Methods for Change Detection and Process Modeling, Cologne, Germany, November 18-19.
- Wüthrich, Th., A. Wiget (2008): Beitrag zur Konstruktion der Landesgrenze Deutschland – Schweiz im Untersee nach der Methode der “einmittenden Kreise” gestützt auf digitalisierte Uferlinien der Bodensee-Tiefenvermessung 1985-1990. swisstopo-report 08-09, Bundesamt für Landestopografie, Wabern.